1958

Rotation capacity requirements for beams and frames of structural steel, Ph.D. Dissertation, Lehigh University, (1958)

G. C. Driscoll Jr.

ROTATION CAPACITY REQUIREMENTS FOR BEAMS AND FRAMES OF STRUCTURAL STEEL

by

George C. Driscoll, Jr.

A DISSERTATION

Presented to the Graduate Faculty
of Lehigh University
in Candidacy for the Degree of
Doctor of Philosophy

Lehigh University
1957

Approved and recommended for acceptance as a dissertation in partial fulfillment of the requirements for the degree of Doctor of Philosophy.

_____ Date

_____ Professor in Charge

Accepted _____ Date

Special committee directing the doctoral work of Mr. George C. Driscoll, Jr.

_____ Chairman

_____

_____

_____

ACKNOWLEDGEMENTS

The author wishes to express his appreciation for the helpful suggestions and criticisms made by several of the research personnel at Fritz Engineering Laboratory during the development and preparation of the work presented in this dissertation. Dr. Robert L. Ketter was especially helpful in lending the full use of his calculations on the plastic design of multi-span frames. Le Wu Lu checked the theoretical derivations and carried out many of the numerical calculations for the resulting curves.

The supervision, encouragement, and critical review of this work by Dr. Lynn S. Beedle, Professor in charge of the dissertation, are sincerely appreciated.

The analytical work described in this report is part of a project on "Welded Continuous Frames and Their Components being carried out under the direction of Lynn S. Beedle. The project is sponsored jointly by the Welding Research Council and the U.S. Navy Department under an agreement with the Institute of Research of Lehigh University. Funds are supplied by the American Institute of Steel Construction, American Iron and Steel Institute, Office of Naval Research, Bureau of Ships, and the Bureau of Yards and Docks. The work was done at Fritz Engineering Laboratory of which Professor William J. Eney is Director.

TABLE OF CONTENTS

A B S T R A C T

Plastic analysis of steel structures depends on the ability of the members to form plastic hinges and to redistribute moments. In order for redistribution of moment to take place, certain plastic hinges must sustain their plastic moment through some angle of rotation. The amount of rotation required may affect the stability of the structure and, therefore, may affect the geometry of the structural shapes selected and the spacing of lateral bracing. The ability of a structural member to rotate the required amount in order to redistribute the necessary moments and form a mechanism is defined as the "rotation capacity". The angle of rotation during which a yielded segment of beam must sustain its plastic moment value is termed the "hinge angle".

This dissertation deals with a method of calculating the approximate hinge angle through which a member must be able to rotate to form a mechanism. The method of solution is based on the assumption that the complete bending moment diagram for a structure can be obtained from a routine plastic analysis. The method is based on the further assumption that, when a structure has reached ultimate load and formed a mechanism, the length of the yielded zones at each plastic hinge is zero. This makes it possible to calculate rotations, slopes and deflections by methods of the theory of elasticity, accounting for the plastic hinges simply by changing the boundary conditions to allow for the

necessary freedom to rotate. In this dissertation, the method used to calculate rotations, slopes, and deflections is an adaptation of the classical elastic slope-deflection method.

The problem of calculating the required rotation capacity of a structure is examined in three steps:

1) Calculation of the ultimate load and ultimate moment diagram.

2) Location of the first and last plastic hinges to be formed in the structure.

3) Calculation of deflection and rotation by using the slope-deflection equations and considering boundary conditions appropriate for a structure in the plastic range.

The study is aimed at the determination of the rotation capacity of multi-span gabled frames. However, the theory is developed in simple stages and covers a three-span continuous beam and single-span portal frames as the basic steps in the method are illustrated. The new work of the dissertation is primarily concerned with steps (2) and (3) of the above method. Multi-span frames are solved by separating the frames into single span elements called subassemblages. Then the results of the rotation calculations for single-span frames

are used to advantage. Special treatment is given to finding the location of the last plastic hinge in multi-span frames. In treating this problem, the concept of a self-supporting subassemblage containing the last plastic hinge and non-self-supporting subassemblages, which rely on adjacent spans for part of their support, is introduced. An interesting discovery in the study of multi-span gabled frames was that it was possible, under certain cases of loading, to form mechanisms in which the roof deflects upwards causing negative work to be done by the roof loads.

Using the results of the theoretical studies, some typical structures are designed as illustrations and their required rotation capacity is compared with the actual rotation measured in some experimental tests.

1. INTRODUCTION

Recent developments in the plastic analysis of steel frames and their component parts have presented a more rational basis on which to design welded continuous structures. Methods based on these developments give promise of economies to be gained by taking advantage of the reserve of strength of structural steel beyond the elastic limit, by using simple methods of analysis, and by assuring a uniform factor of safety against failure for all structures.[1]

Plastic analysis supplements the classic elastic theory by utilizing knowledge of the behavior of structural steel beyond the elastic limit. It is known that the same property of ductility which allows deformation without additional load of a tension or compression member, will also allow a flexural member, stressed to a limiting moment (designated as the plastic hinge moment) to bend or rotate without additional moment. The ability of a plastic hinge to maintain a constant moment while rotating through a finite angle allows a structure or member to transfer additional increasing load to other less-stressed portions of the structure until sufficient plastic hinges have formed to cause the structure or a portion thereof to become a mechanism. These two properties are known as the plastification of cross section and redistribution of moment. While plastification of cross section and redistribution of moment are the two primary factors involved in the plastic analysis of structures, certain other factors affect plastic behavior, and at times can govern the plastic analysis or design. Axial

compressive forces and shear forces combined with bending moment tend to reduce the plastic hinge moment of a given structural member. However, axial loads less than 15% of the compressive yield load of a member, as are most common in rigid portal frames, reduce the plastic hinge moment only a small amount and may be neglected.[1] The usual shear forces in a normal balanced design are also small enough so that the plastic moment is not seriously reduced. When the shear forces are large, they occur in a section of steep moment gradient which generally allows strain hardening to produce a counteracting effect.[4]

The presence of residual stresses due to cooling, welding or cold bending tends to reduce the yield load of a structure. In a compression member, the maximum load is also reduced; but in a member subjected to bending only, the predicted plastic hinge moment is usually achieved.[20]

The factors just mentioned affect the magnitude of the plastic hinge moment but have little influence on the ability of the member to absorb plastic rotations. Other factors may affect not only the plastic hinge moments but also the ability of the section to rotate thus modifying the redistribution of moment. These other factors are brittle fracture, local buckling and lateral buckling. In structures which have thus far been investigated, brittle fracture has not proved to be of concern because careful welding procedures and inspection, and the use of satisfactory materials for the temperatures encountered prevented brittle behavior.[5] The occurence of premature local buckling can be prevented by selecting shapes of the proper geometric proportions.[8,9] Lateral buckling also may be prevented by

providing proper bracing to the members.[19] It is evident, then, that proper attention must be paid to the possibility of brittle fracture, local buckling, and lateral buckling to assure sufficient strain or rotation to permit redistribution of moment.

There is no single answer as to how much strain or rotation of a plastic hinge is required to allow a mechanism to form. The attainment of strain hardening has arbitrarily been selected as a criterion in the previously mentioned studies on local and lateral buckling. The ability of a plastic hinge to rotate at or near the maximum moment has been defined as rotation capacity.[18]

This paper will present methods for calculating the rotation capacity required to allow a mechanism to form in a structure and will give results for some specific cases. The object of the study is actually two-fold--one aim is to discover methods of calculating the rotations which must be sustained for the calculated maximum load to be attained. The second aim is to determine if some maximum amount of required rotation capacity may be specified for given geometrical and loading conditions which will not be exceeded in any structure so that a design rule may be set up eliminating the necessity of calculating the required rotations. The latter goal is desirable because the calculation of deflections and rotations for even the simplest of structures is tedious and to be avoided if at all possible.

Essentially the problem of calculating the required rotation

capacity is one of calculating the deformation at ultimate load. This problem may be examined as if it were broken into three distinct steps:

(1) Calculation of the ultimate load and ultimate moment diagram.

(2) Location of the first and last plastic hinges to be formed in the structure.

(3) Calculation of deflection and rotation by solving the differential equation for the curvature of bending members considering boundary conditions appropriate for a structure in the plastic range.

This study is primarily aimed at the determination of the required rotation of multi-span gabled frames. However, the development of the theory is carried out in several stages, using examples of simpler structures to illustrate the progress at each stage. Thus, the methods of defining limits of types of mechanisms and location of first and last plastic hinges, as well as simple calculations of hinge angles, are first shown for a three-span continuous beam. Then, a study of single-span portal frames is carried out to indicate the method of handling problems involving structures with sidesway. The solution of problems of multi-span frames is accomplished by separating them into subassemblages. The concept of self-supporting and non-self supporting subassemblages is introduced with the problem of flat-roofed multi-span frames. An additional type of mechanism, designated as a "reverse" mechanism, is studied in the final phase concerning multi-span gabled frames.

2. PHYSICAL SIGNIFICANCE OF ROTATIONS

Before making actual calculations of the rotations of structures, it may be helpful to visualize the behavior of a structure in forming a mechanism under the action of steadily increasing proportional loads.

The illustrative example, to be used in this chapter is a three-span beam case as shown in Fig.2.1. For the present, suppose that a mechanism would form in the main span with the first plastic hinge at the interior supports. (Fig 2.2)

The actual moment-curvature behavior of a typical wide-flange shape such as might be used for this beam is shown diagrammatically in Fig 2.3. This curve shows the elastic range, the initial inelastic region (showing the effect of residual stresses), the gradual transition from yielding in the flanges to the complete plastic hinge, and finally the strain-hardening range. This curve and the factors that affect it have been fully discussed in literature on the subject of plastic behavior.[1]

For the purpose of simplifying calculations, assumptions of behavior in an idealized manner will be used in this development. The material in the beam will be assumed as a ductile material having the idealized stress-strain curve shown in Fig 2.4, i.e., strain-hardening and the upper yield point will be neglected. As a further assumption, the M-Ø curve will be used in the idealized form shown in Fig 2.5. In

addition to assuming an idealized stress-strain curve, this curve neglects residual stresses and the gradual transition from elastic to fully plastic behavior.

In the first phase of the formation of a mechanism, the complete beam would be elastic. The deflected shape of the beam would be a fully continuous smooth curve. The shape of the elastic curve over support B would be as shown in Fig 2.6a. Note that the slope at the support is the same in each span. The load-deflection curve for the beam in this first phase would be as shown diagramatically by curve I in Fig 2.7 and 2.8. Increasing the loads until the maximum moment at B reached M_p would cause a plastic hinge to form at that point. In this condition, the curvature $\emptyset$ of point B would not be uniquely determined by the moment. The curvature could be the equivalent of point A in Fig 2.5, in which case the beam would look like Fig 2.6a at the joint, or the curvature could be the equivalent of any other point on line AB in Fig 2.5. Then the beam would have a discontinuity at the joint as in Fig 2.6b. In a case like this, the slope at the joint is not the same in each span. Since the amount of discontinuity is not uniquely determined by the moment at the hinge, it must be governed by the behavior of other parts of the structure.

Because the three-span beam is an indeterminate structure, formation of the first plastic hinge would not create a mechanism. However, the formation of this plastic hinge would introduce a "known" moment into the picture, thereby removing the indeterminacy. (Because

of symmetry, plastic hinges would form at the two inter supports simultaneously.) At this stage, the remainder of the length of the beam would still be bent in smooth curves, and the three spans could be considered as separate simple beams loaded as shown in Fig 2.9. Except for local conditions caused by yielding at the supports, these spans would be piecewise continuous and satisfy the conditions which permit the slope and deflection to be calculated by standard elastic methods. Therefore, the end slopes at the interior supports could be calculated and the angle of discontinuity determined.

On increasing the loads proportionally, the changes in moments in the three spans would be those of simple beams, because the end moments M_p would remain constant. This is the phase of loading in which redistribution of moment takes place. The load-deflection curve due to this increment of loading would be as shown diagrammatically by curve II in Fig 2.7 and 2.8. Eventually, the center of the main span would have its moment increased to M_p. Then the curvature $\emptyset$ at that point would be undefined as in the case of the first hinge. However, at the precise instant the moment reached M_p, the M-$\emptyset$ relationship would be the equivalent of point A in Fig 2.5. This stage in the behavior of a structure is very important because it is the last stage at which a solution may be obtained for the slopes and deflections of the structure. It is also the stage at which the ultimate load of the structure has been reached. Considering the deflected shape of the beam at this same stage, it is

apparent that the three spans would still be bent in smooth curves between the supports and that the spans would satisfy the conditions which allow slope and deflection to be calculated by elastic methods. This would permit the calculation of the "hinge angle" which is the main objective of this study. This critical hinge angle is the angle through which the first plastic hinge must rotate up to the instant that the last plastic hinge just begins to form. The importance of this angle is evident when it is realized that if the computed value cannot be reached, the structure may not be able to carry the predicted ultimate load on which plastic analysis is based.

Although a structure plastically designed would not be required to deform further after formation of the last plastic hinge, consideration of its behavior in this range is worthwhile because it sheds some light on the virtual displacement method of determining ultimate load.

Up to the instant that the last plastic hinge forms in the middle of the main span, the curve of the beam would be smooth as in Fig 2.10a. This is the boundary condition which makes possible the determination of slope and deflection of the beam. Once the last hinge has formed, its rotation could increase without addition of load and a hinge angle would be evident as shown in Fig 2.10b by the angle H_E. It would not be possible to calculate the hinge angles since the structure would now be overdeterminate and subject to an infinite number of solutions for deflection and hinge rotation.

At this point it may be well to distinguish between the "slope angles" and the "hinge angles" which have been discussed above and the "mechanism angles" which are used to determine the ultimate load of structures by the virtual displacement method.

The angles such as θ_{BC} and θ_{EB} shown in Fig 2.6 and 2.10 are slopes to the "elastic" curve of the structure. The hinge angles such as H_B (Fig 2.6b) are the differences in adjacent slopes at a point where a discontinuity has occurred due to formation of a plastic hinge. These slopes and angles have unique values up to the ultimate load.

In contrast, the mechanism angles (also designated as functions of θ, but without subscript) are imaginary rotations of complete segments of members resulting from imaginary controlled displacements of structures already at their ultimate load. Because the external loads and internal moments remain constant during these virtual displacements, internal and external work may be expressed simply as a function of load, M_p, geometry of the structure, and θ. Equating internal and external work from these expressions gives a value for load in terms of M_p and geometry of the structure with θ cancelling completely.

The physical picture of these angles will be shown with the aid of Fig 2.11. Fig 2.11a shows a typical method of describing the mechanism of the beam for the purpose of writing the virtual work equation. The beam, already at maximum load, has been subjected to a virtual displacement, Δ, causing virtual rotations θ at the interior

supports, and 2 θ at the center plastic hinge. (Loads have been omitted to allow the angles to be seen more clearly.) In Fig 2.11b is seen an enlarged view of the portion BE of the beam just before the virtual displacement was effected. The bent shape of all members is piecewise continuous between hinges. Because bending moments will remain constant throughout any subsequent displacement, the shape of each of these pieces will remain constant. This is just as if they were rigid curved links connecting the hinges at each end. Shown in Fig 2.11b are the vertical deflection δ due to bending and the hinge angle H_B. In the condition indicated by the drawing, the beam would just be reaching maximum load and H_B would be the hinge angle in order that the beam reach this value. Fig 2.11c shows the beam after the virtual displacement, Δ, has taken place. The corresponding rotation of rigid link BE amounts to the virtual angle θ, and the added rotation at joint E is 2 θ.

The mechanism angles caused by the virtual displacement Δ are θ at joint B and 2 θ at joint E. These are superimposed on the hinge angles which were H_B at joint B and zero at joint E. Of course, for the purpose of the virtual work equations, the virtual displacements are assumed to approach zero in order that they won't constitute a change in the geometry of the structure.

The same picture holds true for any other structure such as a portal frame. With the formation of each plastic hinge, a discontinuity appears in the deflected shape of the member. However, there are unique

solutions for deflection and rotation up to the point at which the last plastic hinge reaches its maximum moment. This is the condition for which hinge angles are to be calculated. Deformation beyond this point is mechanism action and rotations and deflections can no longer be calculated.

3. FUNDAMENTAL EQUATIONS FOR CALCULATION OF ROTATIONS AND DEFLECTIONS AT MAXIMUM LOAD

Calculations of the deflections and rotations of flexural members at maximum load is accomplished by integration, with appropriate boundary conditions, of the differential equation:

$$\frac{d^2y}{dx^2} = \emptyset \qquad \ldots(3.1)$$

where y = deflection from original straight line of member

x = distance along member

$\emptyset$ = curvature of member, a function of moment

Since $\emptyset$ is a function of moment and since the moment is a function of x, $\emptyset$ may be expressed as a function of x.

Next the question arises of the form of $\emptyset$ for use in this equation. $\emptyset$ could conceivably be used in a form which would represent the actual shape of the M-$\emptyset$ curve and could also include the effect of residual stresses and strain hardening. (Fig 2.3). However, this would require the use of tedious calculation procedures and probably give answers which are not particularly more significant than those which can be derived using simplifying assumptions.[12] For the purpose of obtaining quickly a qualitative over-all picture of the rotation capacity problem, the assumption of the idealized M-$\emptyset$ curve as shown in Fig 2.5 will be made. By using this assumption, the function of $\emptyset$ along a member and between plastic hinges may be represented as M/EI just as in elastic analysis. This

neglects only the area between the solid line and the dotted line and may be shown to have a small effect.[12]

By assuming $\emptyset$ equal to M/EI it is possible to use all of the conventional methods for calculating deflections which use orderly procedures or evaluated integrals of the M/EI curve in the form of formulas and thus simplify mathematical operations. These methods include moment-area, conjugate beam, virtual work and slope-deflection. The choice of method is generally governed by individual preference as to an orderly form for calculations or an easily remembered sign convention.[1,17]

In the following solutions, slope-deflection equations will be used in the following form:

$$\theta_N = \theta'_N + R_{NF} + \frac{\ell}{3EI}\left[M_{NF} - \frac{1}{2} M_{FN}\right] \qquad \ldots(3.2)$$

θ_N = Slope of near end of member

θ'_N = Slope of near end of similarly loaded member when simply supported $= \pm \frac{w\ell^3}{24EI}$ for uniformly-distributed load

R_{NF} = Rotation of a chord between ends of member

= Deflection of one end of a member with respect to the other divided by the distance between them = δ/ℓ

ℓ = Length of member or portion of member

M_{NF} = Moment at near end of member

M_{FN} = Moment at far end of member

Any of the sign conventions convenient for slope deflection may

be used. The convention used here is that slope angles are defined as positive when the rotations are clockwise, and end moments are defined as positive when acting in the clockwise sense.

θ with appropriate subscript is used to represent the slope on both sides of a hinge location. H, the hinge angle, is used to represent the difference in slope at a plastic hinge when the maximum load is first reached. See Fig 2.6.

Once the bending moments for a structure are known, the slope-deflection equations are used by writing an equation similar to (3.2) for each end of each member. The unknowns in these equations will be the θ and R terms (θ' is known for each segment). Additional equations will be needed to solve the problem. These will be obtained by considering the boundary conditions for the particular structure as will be shown in the following chapters.

4. REQUIRED ROTATION OF A THREE - SPAN CONTINUOUS BEAM

Most of the principles used in the solution of rotation capacity problems can be illustrated by the relatively simple example of a three-span continuous beam. In the following sections it will be shown that "domains", in which each of the several possible mechanisms for a given structure will occur, can be determined by equating expressions for the plastic hinge moments. Domains in which each possible plastic hinge is first to form can be determined by equating the expressions for the elastic moments at possible plastic hinges. The method of using slope-deflection equations with boundary conditions appropriate for structures in the plastic range to calculate hinge angles will also be shown.

4.1 POSSIBLE MECHANISMS, DOMAINS, AND REQUIRED PLASTIC MOMENTS

A number of available methods of analysis use the properties of plastification of cross section and redistribution of moment as a basis for calculating the ultimate loads of structures.[1,15,16] An important advantage of these methods of plastic analysis over methods of elastic analysis is the elimination of the solution of large numbers of simultaneous equations in the analysis of highly indeterminate structures. Instead, orderly procedures may be used to calculate the ultimate loads consistent with various assumed mechanisms. Each such load constitutes an upper bound for the maximum load of the structure. At the same time, any assumed set of loads and redundants which satisfy

equilibrium without the plastic hinge moment being exceeded at any point in the structure constitutes a lower bound for the true maximum load of the structure. The exact maximum load is indicated when an upper bound and a lower bound prove to be equal.

Consider the three-span continuous beam shown in Fig 4.1. The main span has a length L and is flanked by two side spans of length βL. A uniformly distributed load w pounds per foot is applied to the main span, and a load of α w pounds per foot to the side spans. The cross section and material are constant throughout.

Since the relative loads and span lengths are undetermined as stated, the mode of failure cannot be uniquely defined. It is possible for a mechanism to form either in the center span or in the side spans.

If a mechanism is to form in the center span, plastic hinges will form at interior supports B & C and at the center of the main span. For this case, an elementary calculation will give as the expression relating the plastic hinge moment of the beam and the maximum load:

$$M_p = \frac{wL^2}{16} \qquad \ldots(4.1)$$

If a mechanism is to form in the side span, plastic hinges will form at the interior supports B & C and at an intermediate point in each side span where the moment is maximum. The distance from the exterior support to each of these hinges will be some fraction ζ of the side span length βL, i.e. $\zeta\beta L$. The plastic hinge moment in this case

is given by the expression:

$$M_p = \alpha\, \beta^2\, \frac{wL^2}{2}\, \frac{\zeta(1-\zeta)}{(1+\zeta)}$$

where $\zeta = \sqrt{2} - 1 = 0.4142$

then $M_p = \frac{1}{11.66}\, \alpha\, \beta^2\, wL^2$ ...(4.2)

For a given beam section, side span length and side span loading, the mechanism which would require the greater value of M_p will form. A special condition is that in which both mechanisms occur simultaneously. For this case, both expressions for M_p must be equal. By combining equations (4.1) and (4.2) an expression for the values of α and β for which both mechanisms can form is obtained.

$$\alpha\beta^2 = \frac{1}{8}\, \frac{(1+\zeta)}{\zeta(1-\zeta)} \qquad \ldots(4.3)$$

By substituting for ζ its value 0.4142, this equation reduces to:

$$\alpha\beta^2 = 0.728 \qquad \ldots(4.4)$$

This curve is plotted in Fig 4.2.

The unshaded area of Fig 4.2 contains all values of α and β for which the mechanism will form in the main span with a plastic hinge moment given by equation (4.1). The shaded area contains the values of α and β for which the mechanism will form simultaneously in the two side spans, and the plastic hinge moment will be given by Eq. (4.2).

4.2 LOCATION OF LAST PLASTIC HINGE

As was stated earlier, the boundary conditions used in calculating deflection and rotation in the plastic range depend on the location of the last plastic hinge. One way of determining the location of the last plastic hinge is to calculate step-by-step the load versus moment behavior of the structure starting with an elastic solution.

In the case of the three-span beam, one step is sufficient because only two hinges are necessary to form a mechanism (because of symmetry the two hinges at the interior supports count as one hinge). Thus, locating the first hinge by an elastic solution gives the location of the last hinge by elimination.

From an elastic analysis of the beam, the following moments at various sections may be obtained:

Maximum Moment in Main Span

$$M_E = \frac{wL^2}{4}\left[\frac{1}{2} - \frac{\alpha\beta^2 + 1}{2\beta + 3}\right] \qquad \ldots(4.5)$$

Moment at Interior Supports

$$M_B = \frac{wL^2}{4}\left[\frac{\alpha\beta^3 + 1}{2\beta + 3}\right] \qquad \ldots(4.6)$$

Maximum Moment in Side Span

$$M_F = \frac{wL^2}{32\alpha\beta^2}\left[\frac{3\alpha\beta^3 + 6\alpha\beta^2 - 1}{2\beta + 3}\right]^2 \qquad \ldots(4.7)$$

For a given loading and span length, one of these moments will prove to be the largest and, therefore, the first plastic hinge would occur at that location. For each possible mechanism the magnitude of the

moments should be compared at the two sections at which hinges form. Thus, for the main span mechanism, the question of interest is whether or not M_B is greater than M_E. For the side span mechanism, M_B and M_F should be compared.

When M_B and M_E are equated, the resulting expression in α and β gives the boundary between the regions where the first plastic hinge forms at B and where the first hinge forms at E.

$$\frac{\beta + 1.5}{\alpha \beta^3 + 1} = 2 \qquad \ldots(4.8)$$

This curve is plotted as the lower curve in Fig 4.3. The region below the curve designates the values of α and β for which the maximum elastic moment is at the center of the main span E. The region above the curve designates α and β for maximum elastic moment at the interior supports B.

Similarly, equating M_B and M_F results in an equation separating the regions for maximum elastic moment at B and at F.

$$\frac{(3\alpha\beta^3 + 6\alpha\beta^2 - 1)^2}{\alpha \beta^2(2\beta + 3)(\alpha\beta^3 + 1)} = 8 \qquad \ldots(4.9)$$

This curve is plotted as the upper curve in Fig 4.3. Within the region enclosed by this upper curve, the maximum elastic moment occurs at F. Below the curve the maximum elastic moment occurs at point B.

As an approximation consistent with the assumptions made in Chapter 2, the limiting value of the elastic moment may be considered as the plastic hinge moment. Thus, the three areas in Fig 4.3 indicate

the values of α and β for which each of the three possible plastic hinges are the first to form.

By superimposing Fig 4.2 on Fig 4.3, a single chart (Fig 4.4) is obtained which indicates both the type of mechanism and the location of the first plastic hinge. This information by elimination also gives the location of the last plastic hinge, providing all the information needed to deduce boundary conditions.

The method used in this case for the determination of the order of formation of plastic hinges is the simplest form of the step-by-step method. However, for a highly indeterminate structure, the step-by-step method would require a complete elastic solution of the structure for each plastic hinge that forms.

Fortunately there exists a method of calculation which uses only the maximum load moment diagram to determine the last plastic hinge.[15,1] This method consists of assuming any given plastic hinge to be the last to form and making a deflection calculation based on this assumption. This calculation is repeated with as many "last plastic hinge" assumptions as there are uncertainties as to its true location. The true last plastic hinge corresponds to the greatest calculated deflection. This second method is most valuable in the study of multi-span rigid frames.

4.3 DERIVATION OF EQUATIONS FOR HINGE ANGLES

Using the findings of sections 4.1, and 4.2, it may be

determined that there exist four possible cases of mechanism and order of formation of plastic hinges for the three-span continuous beam. Diagrams of these cases are shown in Fig 4.5. The hinge angle at the first plastic hinge together with sketches singling out the boundary conditions and unknowns for each case are given in Fig 4.6. Using these conditions, the hinge angle will be calculated for each case.

Case I. Main Span Mechanism--First Hinge at Midspan

For this case the plastic hinge moment is

$$M_p = \frac{wL^2}{16} \qquad \ldots(4.10)$$

The boundary conditions are indicated in Fig 4.6. Slope-deflection equations are to be written for lengths AB and BE with continuity assumed at joint B, the last plastic hinge. In span AB, the rotation at B is calculated as the end rotation of a uniformly loaded simple beam A-B with a moment M_p applied at end B. From Eq (3.2),

$$\theta_{BA} = -\frac{(\alpha w)(\beta L)^3}{24EI} + \frac{\beta L}{3EI}\left[M_p - \frac{1}{2}(0)\right] \qquad \ldots(4.11)$$

In semi-span BE, the end slope at B is:

$$\theta_{BE} = \frac{wL^3}{24(8)EI} + R_{BE} + \frac{\frac{L}{2}}{3EI}\left[-M_p + \frac{1}{2}M_p\right] \qquad \ldots(4.12)$$

Since $\theta_{BE} = \theta_{BA}$

$$R_{BE} = \frac{wL^3}{24EI}\left[-\alpha\beta^3 - \frac{1}{8}\right] + \frac{M_pL}{3EI}\left[\beta + \frac{1}{4}\right] \qquad \ldots(4.13)$$

The end slope of member EB at E is:

$$\theta_{EB} = \frac{-wL^3}{24(8)EI} + R_{BE} + \frac{\frac{L}{2}}{3EI}\left[-M_p + \frac{1}{2}M_p\right] \qquad \ldots(4.14)$$

Substituting for R_{BE}:

$$\theta_{EB} = \frac{wL^3}{24EI}\left[-\frac{1}{4} - \alpha\beta^3\right] + \frac{M_pL}{3EI}\beta \qquad \ldots(4.15)$$

By symmetry, the hinge angle, H_E, is twice θ_{EB}

$$H_E = \frac{wL^3}{24EI}\left[-\frac{1}{2} - 2\alpha\beta^3\right] + \frac{2}{3}\frac{M_pL}{EI}\beta \qquad \ldots(4.16)$$

By use of equation (4.10) this equation may be expressed either in terms of M_p or w. Thus

$$H_E = \frac{wL^3}{48EI}(2\beta - 1 - 4\alpha\beta^3)$$

$$= \frac{M_pL}{3EI}(2\beta - 1 - 4\alpha\beta^3) \qquad \ldots(4.17)$$

Equation (4.17) may also be written in the form

$$\frac{H_E}{\phi_pL} = \frac{2}{3}\beta - \frac{1}{3} - \frac{4}{3}\alpha\beta^3 \qquad \ldots(4.18)$$

where

$$\phi_p = \frac{M_p}{EI} = \frac{wL^2}{16EI} \qquad \ldots(4.19)$$

Equation (4.18) is plotted in non-dimensional form as a family of curves in Fig 4.7b. Values of α and β for which Equation (4.18) is applicable are limited by the appropriate domain in Fig 4.4. As plotted in Fig 4.7b, all values of α and β satisfy this requirement.

Case II. Main Span Mechanism--First Hinge at Support B

Because the final mechanism is the same as Case I, the plastic

hinge moment is

$$M_p = \frac{wL^2}{16} \quad . \qquad \ldots(4.19)$$

The critical angle is the hinge angle at interior support B. This is obtained by calculating the end slope of the simple beam AB with end moment M_p as for Case I and also calculating the end slope of simple beam BC with two end moments M_p (Fig 4.6, Case II). The hinge angle is then the difference in slopes.

$$\theta_{BA} = \frac{wL^3}{48EI}\left[\beta - 2\alpha\beta^3\right] = \frac{M_pL}{3EI}\left[\beta - 2\alpha\beta^3\right] \qquad \ldots(4.20)$$

$$\theta_{BC} = \frac{1}{96}\frac{wL^3}{EI} = \frac{1}{6}\frac{M_pL}{EI} \qquad \ldots(4.21)$$

$$H_B = \theta_{BC} - \theta_{BA} \qquad \ldots(4.22)$$

$$H_B = \frac{wL^3}{96EI}\left[4\alpha\beta^3 - 2\beta + 1\right]$$

$$= \frac{M_pL}{EI}\left[\frac{2}{3}\alpha\beta^3 - \frac{1}{3}\beta + \frac{1}{6}\right] \qquad \ldots(4.23)$$

The non-dimensional form of this equation is:

$$\frac{H_B}{\theta_{pL}} = \frac{2}{3}\alpha\beta^3 - \frac{1}{3}\beta + \frac{1}{6} \qquad \ldots(4.24)$$

This equation is plotted as a family of curves in Fig 4.7a. The values as plotted are consistent with the limits imposed on α and β for the main span mechanism with first hinge at the support (Fig 4.4).

Case III. Side Span Mechanism--First Hinge at Support B

When the mechanism forms in the outer span, one hinge forms at

the interior support and one forms at point F whose distance from the outer support A is 0.4142βL. The required plastic moment value is given by

$$M_p = \frac{1}{11.66}\,\alpha\beta^2\,wL^2 \qquad \ldots(4.25)$$

The controlling boundary condition in this case is that the beam remains continuous at point F until the mechanism has formed.

The hinge angle at B may be calculated from the end slopes of two simple beams having the given moment diagrams.

$$\theta_{BA} = -\frac{\alpha\beta^3 wL^3}{24EI} + \frac{M_p\beta L}{3EI} \qquad \ldots(4.26)$$

$$\theta_{BC} = \frac{wL^3}{24EI} - \frac{M_p L}{2EI} \qquad \ldots(4.27)$$

$$H_B = \frac{M_p L}{6EI}\left[\,0.915\beta - 3 + \frac{2.915}{\alpha\beta^2}\right] \qquad \ldots(4.28)$$

In non-dimensional form, the equation for H_B is:

$$\frac{H_B}{\phi_p L} = 0.1524\beta - \frac{1}{2} + \frac{0.486}{\alpha\beta^2} \qquad \ldots(4.29)$$

where

$$\phi_p = \frac{M_p}{EI} = \frac{\alpha\beta^2 wL^2}{11.66EI} \qquad \ldots(4.30)$$

This case is plotted in Fig 4.8a.

Case IV. Side Span Mechanism--First Hinge in Span at Section F

In this case, the first hinge forms in the side span. Span BF

is analyzed as an overhanging cantilever extending from simple span BC. Span Af is a simple span supported at one end by the original end support and at the other end by the cantilever span BF. The controlling boundary condition is continuity at point B, the position of the last plastic hinge.

The hinge angle for this case is:

$$\frac{H_F}{\theta_p L} = 0.368\beta - 1.207 + \frac{1.173}{\alpha\beta^2} \qquad \ldots(4.31)$$

This is plotted in Fig 4.8b. Since equation (4.31) is negative for all values of α and β for which it applies, the absolute value is plotted.

4.4 ILLUSTRATIVE EXAMPLES

Before proceeding with further theoretical development, it may be worthwhile to solve a numerical example to illustrate the use of the charts.

Given:	Three equal spans, L = 30 ft. Main span maximum load, 2k/ft. Side span maximum load, 1k/ft.
Find:	Rolled shape for the beam. Hinge angle required to develop all necessary plastic hinges.

From the given data, $\alpha = 0.5$

$\beta = 1.0$

Entering Fig 4.4, it is found that this beam will form a main span mechanism with the first hinge at the supports.

Since $M_p = \frac{wL^2}{16}$

then $Z = \frac{M_p}{\sigma y} = \frac{wL^2}{16\sigma_y}$ ...(4.1)

$= \frac{2 \times 30 \times 12 \times 30}{16 \times 33} = 40.8 \text{ in.}^3$ ...(4.32)

A 14 WF 30 has a plastic section modulus of 47.1 in.^{3} and is the most economical section strong enough for this load. Fig 4.7a gives the hinge angle for a main span mechanism with first hinge at the interior support. For $\alpha = 0.5$ and $\beta = 1.0$

$$\frac{H_B}{\phi_p L} = 0.166 \quad \text{...(4.33)}$$

Then $\phi_p = \frac{M_p}{EI} = \frac{\sigma y Z}{EI}$

$= \frac{33 \times 47.1}{30 \times 10^3 \times 289.6} = 0.000179 \text{ rad/in.}$ ...(4.34)

Substituting in Eq. (4.33) for ϕ_p and L,

$H_B = 0.166 \times 0.000179 \times 360 = 0.0107$ rad.

$H_B = 0.61$ degrees

Therefore, a hinge angle of 0.61 degrees is required at the support to form a mechanism in a 14 WF 30 beam continuous over three 30 ft. spans and loaded with a side span load equal to half the intensity of the main span load.

b. Examples of Extreme Cases

In practical design cases, the side span load intensity would rarely be more than the main span load, and because there must be some

dead load, the side-span load also would rarely be less than 25% of the main span load. If α is assumed to be bounded by these limits, $1.0 > \alpha > 0.25$, and Figs 4.7 and 4.8 are searched for the greatest possible hinge angles, the following results are obtained:

Greatest Hinge Angle at Support:

($\alpha = 0.25$, $\beta = 1.70$)

$$H_B = 0.425\ \phi_p L \qquad \ldots(4.35)$$

Greatest Hinge Angle in Side Span Beam:

($\alpha = 1.0$, $\beta = 1.85$)

$$H_F = 0.186\ \phi_p L \qquad \ldots(4.36)$$

Greatest Hinge Angle in Main Span Beam

($\alpha = 0.25$ $\beta = 0.82$)

$$H_E = 0.030\ \phi_p L \qquad \ldots(4.37)$$

Again taking the case of a 30-ft. main span and a 14 WF 30, the maximum possible hinge angles are:

$H_B = 0.0274$ radians $= 1.57$ degrees

$H_F = 0.0120$ radians $= 0.69$ degrees

$H_E = 0.00193$ radians $= 0.11$ degrees

Thus, a much greater hinge angle is required if the first hinge is to form at a support than is required if the first hinge is to form at some intermediate location in a beam.

4.5 COMPARISON WITH EXPERIMENTAL RESULT

Data is available on the hinge rotation of a 14 WF 30 member tested in a corner connection test.[5] In this test, the moment gradient was nearly the same as it would be in the critical portion of a three-span continuous beam with $\alpha = 0.25$ and $\beta = 1.70$ (Fig 4.9). At the same time, the member was subjected to an axial component of load. The hinge rotation measured over a 10 inch length was 0.0281 radians. This is greater than the value of 0.0274 radians which would be required for the most severe case in the above example. Other sizes and shapes of test members have exhibited the same or better rotation characteristics. It thus appears that structural members should not have difficulty in developing the needed hinge angles at the supports of three-span continuous beams.

4.6 SUMMARY OF STUDY OF THREE-SPAN BEAM

The following summarizes the results of the calculations made for the three-span beam.

(1) Expressing the plastic hinge moments in general terms for each type of possible mechanism in a given structure, and equating the expressions, results in an equation separating the domains in which each type of mechanism will form. (Eq (4.4)) (Fig 4.2).

(2) Equating expressions for the elastic moments at each possible plastic hinge location, results in a set of equations separating

the domains in which each plastic hinge is first to form. (Eq (4.8) & (4.9)). (Fig 4.3).

(3) Combining the graphs for type of mechanism and location of the first plastic hinge gives a graph indicating four possible combinations of mechanism and first plastic hinge (Fig 4.4).

(4) Expressions were developed for the hinge angle, H, for the four possible failure modes by using slope-deflection equations. These are presented in Eqs (4.18), (4.24), (4.29), and (4.31), and in curve form in Figs 4.7 and 4.8.

(5) The extreme values of possible hinge angles were determined and are given in Eq (4.35), (4.36) and (4.37).

(6) For a specific extreme example of a three-span beam using a 14 WF 30 with a 30 ft. main span, the hinge angle required was 0.0274 radians. The result of a corner connection test, using a 14 WF 30 and having a moment diagram almost the same as the beam in the example was able to absorb a hinge rotation of 0.0281 radians. This was experimental evidence that the hinge angle requirements for three-span beams are not too severe to be met by rolled shapes. Since corner connections fabricated from other rolled shapes exhibited as good or better behavior it can be concluded that rolled shapes, in general, will exhibit satisfactory rotation capacity characteristics for three-span beams.

5. REQUIRED ROTATION OF SINGLE-SPAN FRAMES WITH PINNED BASES

The slope-deflection method of calculating hinge angles will now be applied to single-span portal frames. The added factor of sidesway is introduced into the problem of rotation capacity.

Ketter[10] has presented equations and charts which permit the rapid design of single and multiple span frames. This work will be referred to in order to obtain the required plastic moment for the various possible mechanisms. The same system of notation will be followed closely in the development of hinge angle equations.

5.1 MECHANISMS, DOMAINS, AND PLASTIC MOMENT VALUES

Consider the typical gabled portal frame with pinned bases shown in Fig. 5.1. The frame has a span L, a column-height of aL and a roof rise bL. The special case of a flat roofed frame is obtained when b equals zero. Rolled structural shapes of constant cross section are assumed. A uniformly distributed vertical load of w pounds per foot is applied to the entire roof. The effect of all horizontal forces is represented by a load P equal to AwL/2a applied at the top of the windward column.

The possible mechanisms which determine the maximum load of this frame are a sidesway or panel mechanism (Fig. 5.2a) and a general composite mechanism (Fig. 5.2b).

For the panel mechanism, the relationship between plastic moment and ultimate load is:[10]

$$\frac{M_p}{wL^2} = \frac{A}{4} \qquad \ldots(5.1)$$

The maximum load-moment expression for the composite mechanism is:[10]

$$\frac{M_p}{wL^2} = \frac{1}{4}\left[\frac{(1-\alpha)(A+\alpha)}{1+\frac{b}{a}\alpha}\right]$$

where

$$\alpha = \frac{1}{\frac{b}{a}}\left[\sqrt{1 - \frac{b}{a}\left[A\left(1+\frac{b}{a}\right) - 1\right]} - 1\right] \quad \text{for } \frac{b}{a} > 0$$

or

$$\alpha = \frac{1-A}{2} \qquad \text{for } \frac{b}{a} = 0 \qquad \ldots(5.2)$$

As was shown in the case of a three-span beam, equating these two equations will give an expression defining values of b, a, and A for which both of the mechanisms will form simultaneously. The expression will also indicate the boundary between the regions where the two mechanisms predominate, or

$$A = \frac{1}{1+\frac{b}{a}} \qquad \ldots(5.3)$$

This equation is plotted as a family of curves in Fig. (5.3). A separate curve relating side load and column height is given for each value of the roof rise factor, b, from 0 to 1.0. If at a given column height, the side load factor A falls below the appropriate curve, the composite mechanism will form. For values of the side load factor above the curve,

a panel mechanism will form.

5.2 LOCATION OF FIRST AND LAST PLASTIC HINGES

Since the structure under consideration is indeterminate to the first degree, two hinges will be sufficient to form a mechanism. Determination of the location of the first plastic hinge by means of an elastic solution will then give the location of the last plastic hinge by elimination.

Plastic hinges are shown in Fig. 5.2 to exist only at the two knees, C and E, and in the windward rafter at F. An elastic solution will give the following values for the moments at these points.

Moment at Windward Knee

$$M_C = \frac{wL^2}{8}\left[\, A(F+J) \;-\; G \,\right] \qquad \ldots(5.4)$$

Moment at Lee Knee

$$M_E = -\frac{wL^2}{8}\left[AF + G\right] \qquad \ldots(5.5)$$

Maximum Moment in Windward Rafter

$$M_F = \frac{wL^2}{8}\left[1 + 2A + A^2 + \frac{b}{a}F(A^2 - A) - AF + \frac{b}{a}GA - \frac{b}{a}G - G + \frac{1}{4}\frac{b^2}{a^2}(G + AF)^2\right] \qquad \ldots(5.6)$$

In the above equations a plus (+) sign designates a moment which causes tension on the inside of the frame. The functions F, G, J, and N are given by:

$$F = \left[\frac{\frac{16a}{\sqrt{1+4b^2}} + 24 + 12\frac{b}{a}}{N} \right]$$

$$G = \left[\frac{8 + 5\frac{b}{a}}{N} \right]$$

$$J = \left[24\,\frac{b}{a} + 16\,\frac{b^2}{a^2} \right]$$

$$N = \left[\frac{8a}{\sqrt{1+4b^2}} + 12 + 12\frac{b}{a} + 4\,\frac{b^2}{a^2} \right] \qquad \ldots(5.7)$$

Equations (5.4 through (5.7) are derived from superposition of two cases given in Ref. 7. The substitutions F, G, J, and N have been made to reduce the bulk of the equations, and the load parameter A has been added.

Because hinge E is common to both mechanisms, the problem of location of first plastic hinge reduces to finding when M_C and M_F equal M_E.

By equating M_C and $-M_E$ and making the substitutions in Eq. (5.7), the following boundary between first plastic hinge at E or at C is obtained:

$$A = \frac{8 + 5\frac{b}{a}}{12\frac{b}{a} + 8\frac{b^2}{a^2}} \quad \text{for } b > 0 \qquad \ldots(5.8)$$

When b=0, the first hinge cannot occur at C.

Another limit on the first hinge at E is the occurrence of an equal or greater elastic moment at F. The boundary for this case is obtained by equating M_F and $-M_E$.

$$0 = A^2 \left(1+\frac{b}{a} F + \frac{1}{4}\frac{b^2}{a^2} F^2\right) + A \left(2 - \frac{b}{a} F - 2F + \frac{b}{a} G + \frac{1}{2}\frac{b^2}{a^2} FG\right)$$

$$+ \left(1 - \frac{b}{a} G - 2G + \frac{1}{4} \frac{b^2}{a^2} G^2\right) \qquad \text{for } b > 0 \qquad \ldots(5.9)$$

$$A = 1 - 2\sqrt{\frac{1}{2a+3}} \qquad \text{for } b = 0 \qquad \ldots(5.10)$$

Equation (5.8) is plotted as a family of solid curves passing through the origin in Fig. 5.4. The region above the curve for a given value of the roof rise factor b, represents the values of A and a for which the first plastic hinge will form at the windward knee C. Below the curve, the first hinge will form at the lee knee E.

Equations (5.9) and (5.10) are also plotted in Fig. 5.4 as a family of dashed curves. These curves divide the values of A and a for which the first plastic hinge will form at a point F in the windward rafter, from the values for which the first hinge will form at the lee knee, E. It will be noted that the first hinge can form in the rafter only for small values of b, the largest being about 0.387, when the column height is no greater than the frame span.

Fig. 5.3 showing type of mechanism and Fig. 5.4 showing the location of the first plastic hinge are sufficiently complicated in that no attempt will be made to combine them in a general way to show both the type of mechanism and location of first and last plastic hinges. However, by including the curves for only one roof height-to-frame span ratio, b, a series of simple charts may be prepared. Figs. 5.5, 5.6 and 5.7 are charts showing the limits of mechanisms for b values of 0, 0.2, and 0.5 respectively. On these charts, a shaded area above the line representing Eq. (5.3) denotes the frame sizes and loading for which a panel mechanism will occur, while the clear area, indicates the general composite mechan-

ism. An additional line in the shaded area representing Eq. (5.8), separates the regions in which the first plastic hinge will form at the windward knee C or in the lee knee E. A final line in the unshaded area separates the region in which the first hinge forms at E from the region in which the first plastic hinge forms in the rafter at F. This curve represents Eq. (5.9) or (5.10) as applicable.

It may be seen from Fig. 5.5 that a panel or sidesway mechanism will not occur in a flat-roofed frame with the proportions and loading considered in this study. From equation (5.3) it will be seen that the panel mechanism could occur when A exceeds 1.0.

Fig. (5.7) indicates that for steep-roofed frames the first hinge will not occur in the rafter as was pointed out in an earlier paragraph.

5.3 DERIVATION OF EQUATIONS FOR HINGE ANGLES

Derivation of equations for hinge angles of single span portal frames is accomplished through the use of the same slope-deflection equation as was used for the three span beam:

$$\theta_{NF} = \theta'_{NF} + R_{NF} + \frac{\ell}{3EI}\left(M_{NF} - \frac{1}{2} M_{FN}\right) \qquad \ldots(5.11)$$

For cases with sloping roofs, the θ' term is expressed in a manner which takes into account the slant of the roof. For symmetrical gabled roofs where the dimensions are measured as shown in Fig. 5.1, the expression is:

$$\theta' = \frac{w\ell_H^3}{24EI}\sqrt{1+4b^2} \qquad \ldots(5.12)$$

where ℓ_H = the horizontal projection of the length of a segment.

The nomenclature and sign conventions to be used are those given in Chapter 3.

The ultimate load moment diagram for the frame is shown in Fig. 5.8a with the effect of each type of force kept separated.

Case I. Composite Mechanism--First Hinge at Lee Knee E

The first solution will be that for the general composite type of mechanism with the first plastic hinge at the lee column top (E). The boundary conditions for this solution are the continuity at joints C and D. At joint E, the slope will be discontinuous. Substituting the moment values from Fig. 5.8a, in Eq. (5.11), will form two slope equations for each member. Since there is no transverse load on the columns, the θ' terms for those members do not exist. Pertinent lengths for use in the slope-deflection equations are given in Fig. 5.8b.

The end slope equations for each member are as follows:

Member AC

$$\theta_A = R_{AC} + \frac{aL}{3EI}\left[0 - \frac{1}{2}\left(-\frac{AwL^2}{2} + M_p\right)\right]$$

$$\theta_C = R_{AC} + \frac{aL}{3EI}\left[\left(-\frac{AwL^2}{2} + M_p\right) - 0\right]$$

Member CD

$$\theta_C = \frac{wL^3}{192EI}\sqrt{1+4b^2} + R_{CD} + \frac{L\sqrt{1+4b^2}}{6EI}\left\{\frac{AwL^2}{2} - M_p - \frac{1}{2}\left[M_p\left(1+\frac{b}{a}\right) - \frac{wL^2}{8} - \frac{AwL^2}{4}\right]\right\}$$

$$\theta_D = \frac{-wL^3}{192EI}\sqrt{1+4b^2} + R_{CD} + L\sqrt{\frac{1+4b^2}{6EI}}\left\{M_p\left(1+\frac{b}{a}\right) - \frac{wL^2}{8} - \frac{wL^2}{4} - \frac{1}{2}\left[\frac{AwL^2}{2} - M_p\right]\right\}$$

Member DE

$$\theta_D = \frac{wL^3}{192EI}\sqrt{1+4b^2} + R_{DE} + \frac{L\sqrt{1+4b^2}}{6EI}\left\{-M_p\left(1+\frac{b}{a}\right) + \frac{wL^2}{8} + \frac{AwL^2}{4} - \frac{1}{2}\left[M_p\right]\right\}$$

$$\theta_{ED} = \frac{wL^3}{192EI}\sqrt{1+4b^2} + R_{DE} + \frac{L\sqrt{1+4b^2}}{6EI}\left\{M_p - \frac{1}{2}\left[M_p\left(1+\frac{b}{a}\right) + \frac{wL^2}{8} + \frac{AwL^2}{4}\right]\right\}$$

Member EB

$$\theta_{EB} = R_{BE} + \frac{aL}{3EI}\left[0 - \frac{1}{2}\left(-M_p\right)\right] \qquad \ldots(5.13)$$

These eight equations have six unknown θ's and four unknown R's. The two additional equations necessary for the solution of the problem may be obtained by considering the relative vertical and horizontal displacements of the pinned bases. These are the equations generally used to take sidesway into account in slope-deflection solutions of structures. The relative vertical displacement of the bases is zero and is obtained by multiplying the chord rotation R of each member by the horizontal component of its length and summing these for the structure.

$$R_{CD}\frac{L}{2} + R_{DE}\frac{L}{2} = 0 \qquad \ldots(5.14)$$

The relative horizontal displacement of the bases is obtained by summing the products of the chord rotations R and the vertical components of the length of each member. Since positive rotations of members DE and EB cause negative displacements of the base B, the signs of these terms change.

$$R_{AL}\,aL + R_{CD}bL - R_{DE}\,bL - R_{BE}\,aL = 0 \qquad \ldots(5.15)$$

Solution of the equations (5.13) (5.14) and (5.15) for θ_{ED} and θ_{EB} gives the following:

$$\theta_{ED} = \frac{L\sqrt{1+4b^2}}{6EI}\left[Mp\left(3+\frac{3}{2}\frac{b}{a}\right) - \frac{1}{4}wL^2 - \frac{1}{2}AwL^2\right] \qquad \ldots(5.16)$$

$$\theta_{EB} = \frac{L\sqrt{1+4b^2}}{6EI}\left[M_p\left(-3-\frac{9}{2}\frac{b}{a} - \frac{2b^2}{a^2}\right) + wL^2\left(\frac{1}{4} + \frac{5}{16}\frac{b}{a}\right) + AwL^2\left(1 + \frac{3}{4}\frac{b}{a}\right)\right]$$

$$-\frac{2}{3}\frac{M_{pL}a}{EI}+\frac{1}{6}\frac{AwL^2a}{EI} \qquad \ldots(5.17)$$

The hinge angle at E is equal to the difference in θ_{EB} and θ_{ED}.

$$H_E=\frac{L\sqrt{1+4b^2}}{EI}\left[M_p\left(-1-\frac{b}{a}+\frac{1}{3}\frac{b^2}{a^2}\right)+wL^2\left(\frac{1}{12}+\frac{5}{96}\frac{b}{a}\right)+AwL^2\left(\frac{1}{4}+\frac{1b}{8a}\right)\right]$$

$$-\frac{2}{3}\frac{M_{pL}}{EI}a+\frac{1}{6}\frac{AwL^2}{EI}a \qquad \ldots(5.18)$$

In non-dimensional form, this equation is:

$$\frac{H_E}{\phi_{pL}}=\sqrt{1+4b^2}\left\{\frac{wL^2}{M_p}\left[\frac{1}{12}+\frac{5}{96}\frac{b}{a}+A\left(\frac{1}{4}+\frac{1b}{8a}\right)\right]-\left[1+\frac{b}{a}+\frac{1}{3}\frac{b^2}{a^2}\right]\right\}$$

$$-\frac{2}{3}a+\frac{1}{6}a\frac{wL^2}{M_p}A \qquad \ldots(5.19)$$

For a flat roofed frame, the equation reduces to:

$$\frac{H_E}{\phi_{pL}}=\frac{wL^2}{M_p}\left[\frac{1}{12}+A\left(\frac{1}{4}+\frac{1}{6}a\right)\right]-1-\frac{2}{3}a \qquad \ldots(5.20)$$

Values of M_p/wL^2 may be obtained from reference 10 thus making it possible to plot curves of hinge angles as shown in Figs. 5.11 to 5.13. Equations (5.19) and (5.20) give the hinge angles for all cases in which the values of a, b, and A fall within the domain indicating formation of a general composite mechanism with first hinge at E in Figs. 5.3, 5.4, 5.5, 5.6, and 5.7.

Case II. Composite Mechanism--First Hinge in Windward Rafter at F

As was shown in Section 5.2, for certain proportions of the frame and for certain loadings the first plastic hinge will form in the rafter. In this case, the discontinuity occurs at point F in the rafter, and elastic continuity is maintained up to ultimate load at the lee knee, E. The ultimate load moment diagram is again as shown in Fig. 5.8a.

In setting up the slope-deflection equations for this case, it is necessary to write two equations for each of the segments CF and FD of member CD. Besides the slope-deflection equations, two additional equations are again derived from considering the horizontal and vertical components of the movement of base B equal to zero. For the vertical displacement, this equation is:

$$R_{CF}\,\alpha\,L + R_{FD}\left(\frac{1}{2} - \alpha\right)L + R_{DE}\,\frac{L}{2} = 0 \qquad \ldots(5.21)$$

For the horizontal displacement the equation is:

$$R_{AC}\,aL + R_{CF}2b\,\alpha L + R_{FD}\,(bL - 2b\alpha L) - R_{DE}bL - R_{BE}aL = 0 \qquad \ldots(5.22)$$

Solution in the same manner as for the previous case results in the following equation for the hinge angle, H_F:

$$\frac{H_F}{\phi_{pL}} = \frac{1}{(1+2\frac{b}{a}\alpha)}\left\{\frac{1}{6}\,a\,\frac{wL^2}{M_p}\,A - \frac{2}{3}\,a + \sqrt{1+4b^2}\left\{\frac{wL^2}{M_p}\left[\frac{1}{12} + \frac{5}{96}\,\frac{b}{a} + A\left(\frac{1}{4} + \frac{1}{8}\,\frac{b}{a}\right)\right] - \left[1 + \frac{b}{a} + \frac{1}{3}\,\frac{b^2}{a^2}\right]\right\}\right\} \qquad \ldots(5.23)$$

Note that the second factor of the product in Eq. (5.23) is equal in magnitude to Eq. (5.19). When Eq. (5.19) and (5.23) are both zero, H_E equals H_F, and both plastic hinges form simultaneously, with zero hinge angle required.

For flat roofed frames,

$$\frac{H_F}{\phi_p L} = \frac{wL^2}{M_p}\left[\frac{1}{12} + A\left(\frac{1}{4} + \frac{1}{6}a\right)\right] - 1 - \frac{2}{3}\,a \qquad \ldots(5.24)$$

In Eq. (5.23), α is the parameter giving the horizontal distance αL from joint C to the plastic hinge F in the rafter. Values of α may be obtained from Reference 10 or the equation,

$$\alpha = \frac{1}{\frac{b}{a}} \left[\sqrt{1 - \frac{b}{a}\left[A\ (1 + \frac{b}{a}) - 1\right]} \quad -1 \right] \qquad \ldots(5.25)$$

Equations (5.23) and (5.24) give the hinge angles only for those cases in which a, b, and A fall in the domain indicated in the appropriate Figs. 5.3 to 5.7.

Case Ia. Panel Mechanism--First Hinge at Lee Knee E

For cases where the loading and dimensions are such as to make the value of α equal to zero, the rafter hinge occurs at the windward knee and a panel mechanism results. In the usual panel mechanism, the first hinge occurs at the lee knee, E, and it is there that the hinge angle is required.

The ultimate load moment diagram for the panel mechanism is as given in Fig. 5.9. The usual slope-deflection equations are written with the only discontinuity at joint E. Equations for the chord rotations, R, identical to Eq. (5.14) and (5.15) are used for the additional relationships needed to obtain a solution. The resulting expression for the hinge angle is:

$$\frac{H_E}{\phi_{pL}} = \sqrt{1+4b^2} \left[\frac{wL^2}{M_p} \left(\frac{1}{12} + \frac{5}{96} \frac{b}{a} \right) - \left(\frac{1}{2} \frac{b}{a} + \frac{1}{3} \frac{b^2}{a^2} \right) \right] \qquad \ldots(5.26)$$

For flat roofed frames, Eq. (5.26) reduces to:

$$\frac{H_E}{\phi_{pL}} = \frac{1}{12} \frac{wL^2}{M_p} \qquad \ldots(5.27)$$

Substituting Eq. (5.1) for wL^2/M_p in Eq. (5.26) and (5.27) results in the following expressions for gabled frames:

$$\frac{H_E}{\phi_{pL}} = \sqrt{1+4b^2}\left[\frac{1}{A}\left(\frac{1}{3}+\frac{5}{24}\frac{b}{a}\right)-\left(\frac{1}{2}\frac{b}{a}+\frac{1}{3}\frac{b^2}{a^2}\right)\right] \quad \ldots(5.28)$$

and for flat roofed frames:

$$\frac{H_E}{\phi_{pL}} = \frac{1}{3A} \quad \ldots(5.29)$$

Equations (5.26) to (5.28) give the hinge angle at the lee knee, E, for a panel mechanism when a, b, and A fall within the proper domain of Figs. 5.3 to 5.7.

Case IIa. Panel Mechanism--First Hinge at Windward Knee C

Certain gabled frames as shown in the domain Figs. 4, 6, and 7 may form a panel mechanism with the first plastic hinge at the windward knee, C. The slope-deflection and chord rotation equations will prove in this case to be the same as for the panel mechanism with the first hinge at E. However, in this case, the discontinuity will occur at C rather than at E. Solution of the resulting equations for the hinge angle at joint C, results in the following equation for gabled frames:

$$\frac{H_C}{\phi_{pL}} = \sqrt{1+4b^2}\left[\frac{1}{A}\left(\frac{1}{3}+\frac{5}{24}\frac{b}{a}\right)-\left(\frac{1}{2}\frac{b}{a}+\frac{1}{3}\frac{b^2}{a^2}\right)\right] \quad \ldots(5.30)$$

For flat roofed frames, it is impossible for the first plastic hinge to occur at joint C as shown by Eq. (5.8).

Though Eq. (5.30) is identical to Eq. (5.28), it must be borne in mind that they usually apply to different values of a, b and A, and thus the values of H_C and H_E will coincide only when Eq. (5.8) is satisfied.

An alternate procedure or a check on the derivation of hinge angles for the panel mechanism is to use the equations for the general (composite) mechanism and set α equal to zero. Substituting the expression (5.1) for M_p/wL^2 results in further simplification of the equations.

5.4 DESCRIPTION OF GRAPHS OF HINGE ANGLE EQUATIONS

Hinge angles for structures having three different values of roof rise factor b are plotted in Figs. 5.10, 5.11, 5.12, and 5.13. Each of these graphs utilizes results of the appropriate equations from (5.19) to 5.30).

Fig. 5.10 gives the hinge angles for frames having flat roofs. Non-dimensional values of the hinge angle, H, are plotted against values of the column height factor, a, for several values of the side load factor, A. The "curves" are actually straight lines, and most of them come from Eq. (5.20). The lines for A values from 0 to 0.5 are drawn solid. Those for A values from 0.6 to 1.0 are dashed lines to help eliminate confusion from the fact that they lie in the same region of the graph. Very large side loads are required to form a sidesway mechanism, so the only line representing Eq. (5.29) is that for A equal to 1.0. This is actually the boundary between the sidesway and the general mechanism and therefore represents Eq. (5.20) as well as Eq. (5.29). The lines for A equal to 0 and A equal to 0.1 show an additional point of interest. As the value of a increases, eventually the line crosses the zero hinge angle coordinate. At that point both the hinge at the knee E, and the hinge F in the beam form simultaneously. For greater column heights, the hinge angle H_E would

tend to be negative from Eq. (5.20). Actually, in this region, the first plastic hinge forms in the windward side of the beam at F, and the hinge angle is given by Eq. (5.24). Therefore, all values of the hinge angle above the origin of coordinates represent values of H_E, the angle at the lee knee. All values below the origin of coordinates represent values of H_F, the angle in the beam.

In Fig. 5.11 and 5.12 are shown values of hinge angles for gabled portal frames. Fig. 5.11 has values for a roof rise factor b of 0.2 representing gently sloping roofs and Fig. 5.12 has values for b equal to 0.5 representing steeper roofs. The hinge angle equations for sloping roofs result in curved lines. In both Fig. 5.11 and 5.12, values above the origin of coordinates represent H_E, the hinge at the lee knee. The region giving hinge angles, H_E, is divided into two zones by a dashed curve. The zone above the dashed curve represents hinge angles for the general mechanism as given in Eq. (5.19) while the region below the dashed curve represents hinge angles for the sidesway mechanism as given by Eq. (5.28). An exception to this is the values of the hinge angle for the portions of the A = 0 and A = 0.1 lines which extend below the dashed curve. These also represent the general mechanism. The reason for this will be discussed later.

The ordinates below the abscissa in Fig. 5.11 and 5.12 represent values of both hinge angle H_C at the windward knee (Eq. 5.30) and hinge angle H_F in the windward rafter (Eq. 5.23) depending on which occurs for a given loading and geometry. H_C occurs only for very large side loads

and relatively short columns, and H_F occurs only for low side loads and long columns. The first hinge can occur at F only for the gently sloping roof (Fig. 5.11) as indicated in Fig. 5.4.

As an aid to visualization of the total hinge angle function, the hinge angles for b equal 0.2 from Fig. 5.11 are plotted three-dimensionally in Fig. 5.13. The surface formed by combining equations (5.19), (5.23, (5.28), and (5.30) is a warped surface forming a "roof" over the portions of the A-a plane bounded by A = 0, A = 1.0, a = 0.143, and a = 1.0. The surface is bounded at a = 0.143 because tabulated values of M_p/wL^2 were not available for values of b/a greater than 1.4. This will, however, allow most practical structures to be included in the limits of the curves. A dotted line divides the surface into areas representing the general (composite) and sidesway mechanism. All values of the surface above the A-a plane represent H_E, the hinge angle at the lee knee. Near two diagonally opposite corners (A = 0, a = 1.0 and A = 1.0, a = 0.143), the surface drops below the A-a plane. Near the corner A = 1.0, a = 1.0, the surface represents values of H_F, the hinge angle in the windward rafter. In the vicinity of the corner A = 1.0, a = 0.143, the surface represents values of H_C, the hinge angle in the windward knee. If the A-a plane is considered as "sea level", hinge angles H_E are represented by the "mountain", and hinge angles H_F and H_C are represented by the surfaces below "sea level."

5.5 DERIVATION OF EQUATIONS FOR DEFLECTIONS

From the same solution which results in the equations for hinge angles, the horizontal deflections of the knees may be derived.

Case I. General Mechanism - First Hinge at Lee Knee E

The next to last of equations (5.13) gives

$$\theta_{EB} = R_{BE} - \frac{M_p La}{3EI} \qquad \ldots(5.31)$$

Eq. (5.17) gives

$$\theta_{EB} = \frac{L}{6EI}\sqrt{1+4b^2}\left[M_p\left(-3-\frac{9}{a}\frac{b}{a}-2\frac{b^2}{a^2}\right)+wL^2\left(\frac{1}{4}+\frac{5}{16}\frac{b}{a}\right)+AwL^2\left(1+\frac{3}{4}\frac{b}{a}\right)\right]$$

$$-\frac{2}{3}\frac{M_pLa}{EI}+\frac{1}{6}\frac{AwL^2}{EI} \qquad \ldots(5.32)$$

Combining these two equations gives a value for R_{BE}

$$R_{BE} = \frac{L}{EI}\sqrt{1+4b^2}\left[M_p\left(-\frac{1}{2}\frac{3}{4}\frac{b}{a}-\frac{1}{3}\frac{b^2}{a^2}\right)+wL^2\left(\frac{1}{24}+\frac{5}{96}\frac{b}{a}\right)+AwL^2\left(\frac{1}{6}+\frac{1}{8}\frac{b}{a}\right)\right]$$

$$-\frac{1}{3}\frac{M_pLa}{EI}+\frac{1}{6}\frac{AwL^2}{EI}$$

Since the horizontal deflection, δ_E, of the lee knee equals $R_{BE}\,aL$,

$$\delta_E = \frac{aL^2}{EI}\sqrt{1+4b^2}\left\{wL^2\left[\frac{1}{24}+\frac{5}{96}\frac{b}{a}+A\left(\frac{1}{6}+\frac{1}{8}\frac{b}{a}\right)\right]-M_p\left[\frac{1}{2}+\frac{3}{4}\frac{b}{a}+\frac{1}{3}\frac{b^2}{a^2}\right]\right\}$$

$$-\frac{1}{3}\frac{M_pL^2a^2}{EI}+\frac{1}{6}\frac{AwL^3}{EI}a^2 \qquad \ldots(5.34)$$

Non-dimensionally this is

$$\frac{\delta_E}{\phi_pL^2} = a\sqrt{1+4b^2}\left\{\frac{wL^2}{M_p}\left[\frac{1}{24}+\frac{5}{96}\frac{b}{a}+A\left(\frac{1}{6}+\frac{1}{8}\frac{b}{a}\right)\right]-\left[\frac{1}{2}+\frac{3}{4}\frac{b}{a}+\frac{1}{3}\frac{b^2}{a^2}\right]\right\}$$

$$-\frac{1}{3}a^2+\frac{1}{6}a^2\frac{wL^2}{M_p}A \qquad \ldots(5.35)$$

In the same manner, the results of the solution may be used to obtain the value of δ_C, the horizontal deflection of the windward knee.

$$\frac{\delta_C}{\phi_{pL^2}} = a\sqrt{1+4b^2}\left[\frac{wL^2}{M_p}\left(\frac{1}{24}+\frac{1A}{6}\right)-\left(\frac{1}{2}+\frac{1}{4}\frac{b}{a}\right)\right] \quad \ldots(5.36)$$

$$-\frac{1}{3}a^2+\frac{1a^2}{6}\frac{wL^2}{M_p}A \quad \ldots(5.36)$$

The vertical deflection of the ridge, δ_D, equals $-R_{DE}\,L/2$. Combining Eq. (5.16) with the third from last of Eq. (5.13) gives:

$$R_{DE} = \frac{L}{6}\sqrt{\frac{1+4b^2}{EI}}\left[M_p\left(\frac{3}{2}+\frac{b}{a}\right)+wL^2\left(-\frac{5}{32}-\frac{3}{8}A\right)\right]$$

The resulting δ_D is then:

$$\frac{\delta_D}{\phi_{pL^2}} = \sqrt{1+4b^2}\left[\frac{wL^2}{M_p}\left(\frac{5}{384}+\frac{1}{32}A\right)-\left(\frac{1}{8}+\frac{1}{12}\frac{b}{a}\right)\right] \quad \ldots(5.37)$$

Similar methods give equations for deflections for all the cases. These are summarized in the appendix in Eq. (5.38) to (5.53).

5.6 DESCRIPTION OF GRAPHS OF DEFLECTION EQUATIONS

Results of the equations for deflections are plotted in Figs. 5.14 through 5.18. Figs. 5.14 and 5.15 are the deflections of flat-roofed frames, while Figs. 5.16, 5.17 and 5.18 are the deflections of gabled frames having a roof-rise factor b of 0.2.

The horizontal deflections at ultimate load of the knees in flat-roofed portal frames are plotted in Fig. 5.14 which shows the curves from Eq. (5.38) and (5.40). For several values of the side load factor A, the deflection is plotted against the column height factor a. If a three-dimensional plot of these deflections were made as was done for hinge angles in Fig. 5.13, the several curves would represent sloping lines formed on the side of a hill sliced at equally spaced A

intervals. Viewed from the front, the curves for A values above 0.7 would be invisible because they would be below the crest on the far side of the hill. These are therefore shown by dashed lines. A dotted line near the lower right hand corner divides the region in which the first hinge forms at the knee from that in which the first hinge forms in the beam. Where the first hinge forms in the beam, Eq. (5.40) gives the deflection.

The maximum horizontal deflection at ultimate load for any frame is seen to be 0.69 $\emptyset_{pL}2$ for an A value of 0.7, a very extreme side load, and for a column height factor a of 1.0.

Fig. 5.15 shows the vertical deflection at the center of the beam of flat-roofed frames, as given by Eq. (5.42) and (5.44). The major portion of the surface represented would be a cylinder with a horizontal generator. For values of A greater than 0.2, the curves would be out of sight on the far side of the cylinder. These are shown by dashed lines. The region above the dotted line represents the zone where Eq. (5.44) gives the deflection, that is where the first hinge forms in the beam.

The curves show that the vertical deflection of the beam is most severe for cases of very long columns with no side load, a case when the first plastic hinge forms in the middle of the beam. In this case, the maximum deflection may approach 0.17 $\emptyset_{pL}2$, whereas for shorter columns or higher side loads, a maximum less than 0.09 $\emptyset_{pL}2$ is obtained.

As an example of the horizontal knee deflection of gabled frames, Figs. 5.16 and 5.17 show the deflections δ_E and δ_C of the lee and windward knees respectively for frames having a roof rise factor b of 0.2. It is obvious that the δ function is quite complex, but it can be pictured more easily if the curves are visualized as the outlines of vertical slices cut into a "hill" at even intervals representing the side load factor A. Both δ_E and δ_C curves are similar in appearance with the curves well-spaced up to A values of 0.5, and then being crowded together behind the crest of the hill for the higher values of A. For certain very small side loads, δ_C appears as a negative deflection. This is the case when the spreading of the columns due to the vertical deflection of the gables is greater than the horizontal deflection due to side loads. Dotted lines separate the regions where two mechanisms form simultaneously. The first dotted line, which is between the A = 0 and A = 0.1 curves in the long column range, separates the regions for which the first hinge forms in the lee column and in the windward rafter. The second dotted line, which follows almost the same slant as the A = 0.7 line and covers the entire range of column heights, separates the region of the panel mechanism from that of the general composite mechanism. The third dotted line touches the minimum points of the A = 0.5 to A = 1.0 curves where column heights are less than 0.306L. This line marks the beginning of the cases where the panel mechanism forms with the first hinge in the windward knee, C. Maximum values of the horizontal deflections of b = 0.2 gable frames are about $0.76\ \phi_p L^2$.

The vertical deflections of the ridges of gabled frames having a roof rise factor b of 0.2 are given in Fig. 5.18. The greatest deflections occur for low side loads with A = 0 and A = 0.1. A large peak occurs where the first hinge forms in the rafter as was the case for the flat roofed frames. The curves for the "behind-the-hill" values of A are not dashed in this figure, because they are spaced well enough to prevent confusion. Dotted lines again separate the regions for the cases of different mechanisms and first plastic hinges. One dotted line between the A = 0 and A = 0.1 curves indicates when the first plastic hinge forms in the rafter for the general mechanism. The long dotted line in the vicinity of the A = 0.7 and A = 0.8 curves separates the sidesway and general mechanisms. A short dotted line just below the abscissa denotes that the first plastic hinge forms in the windward knee for a sidesway mechanism. The maximum vertical deflection is between $0.10\ \phi_{pL}2$ and $0.14\ \phi_{pL}2$. For values of A above 0.5 and columns between 0.1 L and 0.3 L, the vertical deflection is negative. This means that the extremely high side loads, combined with the relatively stiff columns, cause the ridge to bulge upward as the windward knee moves closer to the lee knee. It will be shown in later discussion that loading cases of this type should be rare and consideration of this effect is primarily of academic interest.

5.7 ILLUSTRATIVE EXAMPLES

The equations derived here make it possible to determine the hinge angles required to form a mechanism as well as the deflections of joints of a large variety of portal frames. The equations will

serve for all symmetrical frames with pinned bases as long as the loads may be approximated by uniformly distributed vertical loads. The effect of horizontal loads is replaced by a concentrated horizontal load at the eaves of such magnitude as to cause the same moment about the base. Use of the results of this study will be illustrated by some examples which will be compared, where possible, with experimental results.

5.7.1 Flat Roofed Frame

Given: Span length, L = 120 ft.

Height , aL = 30 ft.

Bent Spacing = 25 ft.

Vertical Working Loads:
Dead plus Live plus show 60 psf

Horizontal Working Load:
Wind 20 psf

Load Factors:
Dead plus live load 1.88
Dead plus live plus wind load 1.41
σ_y = 33 ksi
E = 30,000 ksi

Find: Rolled structural shape for this frame.

Hinge angle required to form a mechanism.

Deflections at maximum load.

a. Design

From the given data, the parameters for geometry of the frame are found to be:

a = 0.25

b = 0

Considering the 25 ft. bent spacing and a 60 psf working load, the vertical design load for the dead load plus the live load becomes;

$$w = 60 \text{ psf} \times 25 \text{ ft.} \times 1.88 = 2820 \text{ lb/ft.}$$

When a wind load is added, a load factor of 1.41 applies and the working load is:

$$w = 60 \text{ psf} \times 25 \text{ ft.} \times 1.41 = 2115 \text{ lb/ft.}$$

The wind load will be represented by a concentrated load P which will have the same moment about the base as a uniform pressure of 20 psf distributed over the whole frame height.

$$P = 20 \text{ psf} \times 25 \text{ ft} \times 30 \text{ ft} \times \frac{15 \text{ ft}}{30 \text{ ft}} \times 1.41 = 10{,}580 \text{ lb.}$$

The side load parameter A is determined from the expression for P given in Fig 5.1.

$$A = \frac{2Pa}{wL} = \frac{2 \times 10{,}580 \text{ lb.} \times 0.25}{2115 \text{ lb/ft,} \times 120 \text{ ft.}} = 0.0208$$

Fig 5.5 shows that this structure will form a general composite mechanism under either loading, and M_p will be given by Eq (5.2), or the appropriate curve from Ref 10.

Without wind load, when A = 0,

$$M_p = 0.0625\ wL^2$$

With wind load, when A = 0.0208,

$$M_p = 0.0650\ wL^2$$

Without wind, the section modulus required is:

$$Z = \frac{M_p}{\sigma_y} = \frac{0.0625 \times 2.82 \text{ k/ft.} \times 120 \text{ ft} \times 12 \times 120 \text{ in.}}{33 \text{ ksi}}$$

$$= 924 \text{ in}^3$$

With wind, the section modulus required is:

$$Z = \frac{M_p}{\sigma_y} = \frac{0.0650 \times 2.115 \text{ k/ft.} \times 120 \text{ ft} \times 12 \times 120 \text{ in.}}{33 \text{ ksi}}$$

$$= 721 \text{ in}^3$$

The case without wind controls, and a 36 WF 230 shape having $Z = 942.7 \text{ in}^3$ is selected from the section economy tables.

b. Hinge Angle and Deflections

The hinge angle and deflections may be obtained from Figs. 5.10, 5.14, 5.15 once a and A are known.

From Fig 5.10,

$$H_E = 0.167 \, \phi_p L$$

From Fig 5.14,

$$\delta_E = 0.022 \, \phi_p L^2$$

From Fig 5.15,

$$\delta_D = 0.0832 \, \phi_p L^2$$

By substituting for ϕ_p and L, these functions may be evaluated.

$$\phi_p L = \frac{M_p L}{EI} = \frac{33 \text{ ksi} \times 942.7 \text{ in.}^3 \times 1440 \text{ in.}}{30 \times 10^3 \text{ ksi} \times 14{,}988 \text{ in.}^4}$$

$$\phi_p L^2 = 143.4 \text{ in.}$$

$$H_E = 0.167 \, \phi_p L = 0.0166 \text{ rad.}$$

$$\delta_E = 0.022 \, \phi_p L^2 = 3.16 \text{ in.}$$

$$\delta_D = 0.0832 \, \phi_p L^2 = 11.94 \text{ in.}$$

c. Comparison With Experimental Results

A 36 WF 230 connection of the type which might be used in such a frame was tested as part of a research program on corner connections.[5] A total rotation of 0.0293 radians over a length of 38 inches spanning the corner was measured at a point in the test where the moment was still above the theoretical plastic moment. This is greater than the hinge angle of 0.0166 radians required at the corner of the theoretical frame.

Fig. 5.19 compares the moment diagram of the tested connection with that of the theoretical frame, thus giving an indication of the validity of this comparison.

5.7.2 Gabled Frame

Given: Span length, 40 ft.

Column height 10 ft.

Roof rise 8 ft.

Vertical working loads:

Dead plus live, plus snow 60 psf.

Horizontal working load:

Wind, 20 psf

Load factors:

Dead plus live load, 1.88
Dead plus live plus wind load 1.41
σ_y, 33 ksi
E, 30,000 ksi

Find: Rolled structural shape for the frame.

Hinge angle required to form a mechanism.

Deflections at maximum load.

a. Design

The frame parameters are as follows:

$$a = 0.25$$

$$b = 0.20$$

$$b/a = 0.8$$

The vertical design load for dead load plus live load for the 17 ft. bent spacing and 60 psf working load is:

$$w = 60 \text{ psf} \times 17 \text{ ft.} \times 1.88 = 1918 \text{ lb./ft.}$$

Using the load factor for dead plus live plus wind load, the design load becomes:

$$w = 60 \text{ psf} \times 17 \text{ ft.} \times 1.41 = 1438 \text{ lb./ft.}$$

The horizontal wind load will be:

$$P = \frac{20 \text{ psf} \times 18 \text{ ft.} \times 17 \text{ ft} \times 9 \text{ ft} \times 1.41}{10 \text{ ft}} = 7770 \text{ lb.}$$

Then

$$A = \frac{2Pa}{wL} = \frac{2 \times 7770 \text{ lb.} \times 0.25}{1438 \text{ lb./ft} \times 40 \text{ ft.}} = 0.0675$$

Fig 5.6 shows that the frame will form a composite mechanism under either loading. M_p as given by Eq (5.2) or the appropriate curve from Ref 10 will be:

$$M_p = 0.0456 \, wL^2$$

when A = 0 and

$$M_p = 0.0532 \, wL^2$$

when A = 0.0675

The section modulus required without wind is

$$Z = \frac{M_p}{\sigma_y} = \frac{0.0456 \times 1.918 \text{ k/ft} \times 40 \text{ ft} \times 12 \times 40 \text{ in}}{33 \text{ ksi}}$$

$$= 50.8 \text{ in}^3$$

The section modulus required with wind is:

$$Z = \frac{0.0532 \times 1.438 \text{ k/ft} \times 40 \text{ ft} \times 12 \times 40 \text{ in}}{33 \text{ ksi}}$$

$$= 45.6 \text{ in}^3$$

The case without wind again controls.

Section economy tables will give a 14 WF 34 with $Z = 54.5 \text{ in}^3$. However, in the event delivery on 14 WF 34 could not be obtained, or for some reason it was desired to use a shallower member, a 12 WF 36 with $Z = 51.4 \text{ in}^3$ would suffice. The 12 WF 36 member will be selected for this example.

b. Hinge Angle and Deflections

The hinge angles and deflections for this frame are given in Fig 5.11, 5.16, 5.17, and 5.18. Entering the charts with b = 0.2, a = 0.25, and A = 0, the following values are obtained:

From Fig 5.11,

$$H_E = 0.62 \, \phi_p L$$

From Fig 5.16,

$$\delta_E = 0.117 \, \phi_p L^2$$

From Fig 5.17,

$$\delta_C = 0.036 \, \phi_p L^2$$

From Fig 5.18,

$$\delta_D = 0.1005 \, \phi_p L^2$$

By substituting the known values for ϕp and L, these functions may be evaluated as follows:

$$\phi_{pL} = \frac{M_p L}{EI} = \frac{33 \text{ ksi} \times 51.4 \text{ in.}^3 \times 480 \text{ in.}}{30 \times 10^3 \text{ ksi} \times 280.8 \text{ in}^4}$$

$$= 0.0966 \text{ rad.}$$

$$\phi_{pL}^2 = 46.4 \text{ in.}$$

$$H_E = 0.62\ \phi_{pL} = 0.060 \text{ rad.}$$

$$\delta_E = 0.117\ \phi_{pL}^2 = 5.43 \text{ in.}$$

$$\delta_C = 0.036\ \phi_{pL}^2 = 1.67 \text{ in.}$$

$$\delta_D = 0.1005\ \phi_{pL}^2 = 4.66 \text{ in.} \qquad \ldots (5.55)$$

c. Comparison with Experimental Results

Test results are available for a 40 ft. span gabled frame with 12 WF 36 members.[4] This frame was loaded with four vertical concentrated loads and had fixed bases and a slightly different roof slope, but was similar enough to allow the hinge angles to be compared. The moment diagrams for the two frames are plotted in Fig 5.20 showing this similarity. The lee knee of the test frame rotated through a measured angle of 0.077 radians at the end of the test with the frame still at maximum load as compared with the 0.060 radian requirement for the theoretical frame. Of course a small part of this measured rotation was due to bending of the members in the length spanned by the rotation indicator and should not be included in the comparison of hinge angles. This amount was calculated as approximately 0.005 radians. This result indicates that the theoretical frame would probably be satisfactory just as the test frame was.

The vertical deflection of the test frame just as it reached maximum load was 5.3 inches as compared with 4.57 inches required for

the theoretical frame. However, the test frame was able to sustain the maximum load through a total deflection of 9.9 inches.

Due to the fixity of the bases and the smaller roof slope of the test frame, it is not surprising that the total horizontal deflections of the knees were less than those theoretically required for the pinned-base frame. The experimental deflections were 3.9 in. for the lee knee and 1.6 in. for the windward knee as compared with 5.43 in. and 1.67 in. respectively, for the theoretical pinned-base frame.

5.8 PROBABLE EXTREME VALUES OF LOADING AND GEOMETRY

Since one of the primary objectives of this study is to determine extreme values of the hinge angles, some attention will be given to the extreme ranges of the factors controlling hinge angles. In the proceeding sections it has been shown that a frame may be designed and the magnitude of the required angle determined if the following factors are known:

(1) Span length, L.

(2) Bent spacing, s

(3) Column height, aL

(4) Roof rise, bL

(5) Vertical load intensity, w.

(6) Horizontal concentrated load, $P = AwL/2a$

The first four factors are geometric factors which are generally controlled by architectural considerations. The last two factors are the load factors which are determined by the design allowances made to take care of dead load, live load, and wind load. The probable range of each of these variables in typical rigid frame designs will be established in the following paragraphs.

a. Geometric Design

Spans of typical rigid frame construction are determined primarily by the amount of space to be covered with a roof, and range from about 30 ft. with 16 ft. bent spacing to over 200 ft. with bent spacing varying from 1/5 to 1/8 of the span length.[7,13]

Column heights must be great enough to give sufficient headroom for the purpose of the building and therefore may be as large as the span length for short span-frames. For longer span frames, it is considered good practice to have the minimum column height at least 1/6 of the span. Therefore the column height factor, a, may range from 0.167 to 1.0.

Roof rise is influenced by drainage considerations and by special problems related to the type of roof covering used. Flat roofs are frequently used, and other roof pitches are in the order of 1/6, 1/5, 1.4, 1/3 and 1/2 the span length.[14] Thus, the roof rise factor, b, may range from 0 to 0.5. The ratio of roof rise to column height, b/a will rarely exceed 1.0 except for special architectural problems like churches, in which case b may greatly exceed 0.5.

b. Loading Factors

Vertical design loads consist of the dead weight of the roof and structure averaging about 20 psf, and live and snow loads totalling up to about 40 psf.[11,21] A total of 60 psf will be used here as an average and combined with allowances for horizontal loads ranging from zero to a maximum extreme.

Horizontal design loads are generally wind loads which may be present or absent arbitrarily and so must be considered either way. Usual wind loads are about 20 psf on the vertical projection of the structure as given in the AISC specifications.[21] However, in areas subject to severe windstorms, greater wind loads are specified. The National Building Code recommends increasingly larger wind pressures as the height of the structure increases. For buildings from 100 to 499 ft. high, a pressure of 70 psf is recommended.[22]

The maximum and minimum of the several factors are tabulated in Table I as a preliminary to the calculation of the side load factor, A.

TABLE I

Extreme Values of Geometry and Loading

	Column Height Factor a	Roof Rise Factor b	b/a	Bent Spacing s	Horizontal Wind Pressure p	Vertical Unit Load
Minimum	0.167	0	0	L/8	20 psf	60 psf
Maximum	1.0	0.5	1.0	L/2	70 psf	60 psf

c. Values of Side Load Factor A

The concentrated load, P, at the eaves is that force which will give the same overturning moment about the base as a uniformly distributed wind load on the vertical projection of the frame. Expressed in terms of the previously tabulated variables, the concentrated load for a flat roofed frame would be

$$P = 1/2 \text{ pas LF} \qquad \ldots(5.56)$$

and for a gabled frame would be

$$P = 1/2 \text{ pas } (1 + b/a)^2 \text{ LF.} \qquad \ldots(5.57)$$

where F is the load factor 1.41 applied to increase the working load to the design full load of the structure considering wind.

The side load factor, A, is defined as the quantity 2Pa/wL. Substituting in this the expressions for P, and noting that the linear distributed load wF is equal to the product qsF of the uniformly distributed roof load q in psf, the bent spacing s, and the load factor F, the following expressions are obtained for A:

$$A = 1/2 \text{ pas LF} \times 2a/q \text{ sLF} = a^2 \, p/q \qquad \ldots(5.58)$$

for flat roofed frames, and

$$A = a^2 \frac{p}{q} (1 + b/a)^2 \qquad \ldots(5.59)$$

for gabled frames.

For both cases, the value of A without wind is zero. This value will control many designs.

In most areas the design wind load specified is 20 psf. Therefore the p and q values to be used in Eq (5.58) and (5.59) would be 20 psf and 60 psf respectively. The maximum possible values of A would result when a and b/a are a maximum. This would occur when a is 1.0 and b is 0.5 giving

$$A = (1.0)^2 \frac{20}{60} \times 1.0 = 0.333 \quad \ldots (5.60)$$

for flat roofed frames and

$$A = (1.0)^2 \times \frac{20}{60} \times (1.5)^2 = 0.750 \quad \ldots (5.61)$$

for gabled frames. These constitute the maximum probable values of A for the standard 20 psf wind loading. However, the values of a and b used to obtaine these values are not the most typical. For long span frames, "a" would ordinarily be closer to 1/5 and even for short spans would be nearer to 1/2. For either of these values, b/a could be as great as 1.0. Values of A calculated for the 20 psf wind loading are tabulated in Table II for a value of 0.2, 0.5 and 1.0.

In areas subject to severe storms, the 70 psf wind would govern, and values of 70 psf and 60 psf would be used for p and q respectively. The results of these calculations are included in Table II.

TABLE II

Maximum Values of Side Load Factor A

Wind Load	Column Height Factor a	Roof Rise Factor b	Maximum Side Load Factor A
Flat Roofed Frames			
20 psf	0.2	0	0.01333
	0.5	0	0.0833
	1.0	0	0.333
70 psf	0.2	0	0.0467
	0.5	0	0.292
	1.0	0	1.166
Gabled Frames			
20 psf	0.2	0.2	0.0533
	0.5	0.5	0.333
	1.0	0.2	0.480
	1.0	0.5	0.750
70 psf	0.2	0.2	0.1867
	0.5	0.5	1.167
	1.0	0.2	1.680
	1.0	0.5	2.62

It has been shown by these calculations that for the typical 20 psf wind load, the side load factors may range from 0 to 0.333 for flat roofed frames and from 0 to 0.750 for gabled frames. Thus the possibilities of actual loads cover the whole range of A values for which hinge angles have been calculated and charted. For the extreme case of a 70 psf wind load, "A"-values less than 1.0 will include all structures except those with the largest column heights. For the cases with long columns, it is probable that the hinge angles will be smaller than the values plotted for A = 1 and at least an upper bound for the hinge angles is included in the curves. (Fig 5.11 & 5.12)

5.9 PROBABLE EXTREME VALUES OF HINGE ANGLES

The maximum probable values of hinge angles can either depend on the maximum angle shown on Fig 5.10, 5.11, or 5.12, or on the maximum angle possible within the limits of the probable side load factors, A, given in Table II. For example, in flat roofed frames with 20 psf wind loading, the maximum hinge angle at the lee knee with long columns would be about 0.32 $\emptyset_p L$ with A = 0.333. At the same time the maximum for short columns would be about 0.22 $\emptyset_p L$ with A limited to 0.01333 even though, for a = 0.2, greater values of the hinge angle are indicated for values of A up to 0.5. Another limit for flat-roofed frames would be a hinge angle, H_F, in the beam of 0.33 $\emptyset_p L$ for no side load and a column height equal to the span.

If a 70 psf wind is specified on a flat-roofed frame, the same maximum value of $H_F = 0.33\ \emptyset_p L$ would apply (with no load and a = 1.0).

The hinge angle, H_E, at the lee knee could increase to 0.42 $\emptyset_p L$.

Applying the same type of reasoning to gabled frames shows that the intensity of the wind pressure has little effect on the maximum values of the hinge angles H_E and H_F. H_E has its maximum value for very short columns and relatively light side loads; thus, the greater side loads actually mean a decrease in required hinge angle. The hinge angle H_F in the rafter has its maximum value with no side load and with the longest columns and flattest roofs. One additional factor is introduced in gabled frames -- this is the possibility of a hinge angle H_C at the windward knee. The maximum angle occurs with a high wind load on a frame with short columns and a steep roof.

The maximum probable hinge angles for these several extremes of size and loading are shown in Table III along with a list of the factors causing the extreme values of each. It is seen there that the maximum hinge angle at a lee knee would be about 1.03 $\emptyset_p L$ for a steep gabled frame. (b = 0.5, a = 0.5, A = 0.1). The maximum hinge angle for a windward knee would also occur in a steep gabled frame, (b = 0.5, a = 0.5, A = 1.17) with a value of about 0.49 $\emptyset_p L$. The maximum hinge angle in the rafter would occur with a flat roofed frame and would be 0.33 $\emptyset_p L$. (b = 0. a = 1.0, A = 0).

TABLE III

Maximum Probable Hinge Angles for Single Span Frames

	Hinge Angle at Lee Knee H_E	Hinge Angle At Windward Knee H_C	Hinge Angle In Windward Rafter H_F
Factors Causing Maximum Hinge Angle	Small side Load Short Columns Steep Roofs	High Side Load Short Columns Steep Roofs	No Side Load Tall Columns Low Roofs
<u>Wind Load</u>			
Flat Roofed Frames			
b = 0			
Up to 20 psf	0.32 $\emptyset_p L$	——	0.33 $\emptyset_p L$
Up to 20 psf	0.42 $\emptyset_p L$	——	0.33 $\emptyset_p L$
Gabled Frames			
b = 0.2			
Up to 20 psf	0.80 $\emptyset_p L$	——	0.15 $\emptyset_p L$
Up to 70 psf	0.86 $\emptyset_p L$	——	0.15 $\emptyset_p L$
b = 0.5			
Up to 20 psf	1.03 $\emptyset_p L$	——	——
Up to 70 psf	1.03 $\emptyset_p L$	0.44 $\emptyset_p L$	——

5.10 SUMMARY

The following summarizes the contributions of this chapter and gives the results of the calculations made for single-span gabled portal frames with pinned bases and including the special case of flat-roofed frames.

(1) Equations were developed determining the domains of two types of mechanisms (Eq. (5.3), Fig. 5.3)

(2) Equations were developed determining the domains in which any of three possible plastic hinges could be the first to form (Eq. (5.8), (5.9), and (5.10), Fig. 5.4).

(3) Combining the graphs for type of mechanism and location of the first plastic hinge gives graphs indicating four combinations of mechanism and first plastic hinge. (Fig. 5.6).

(4) Expressions were developed for the hinge angles, H, for the four cases of failure mode (Fig. 5.10 through 5.13).

(5) Equations and charts were developed for the horizontal deflections of the columns and for the vertical deflections of the roofs (Fig. 5.14 through 5.18).

(6) A flat-roofed frame and a gabled frame were designed and the hinge angle requirements were calculated. These were compared with the actual hinge angles measured on test specimens using the same rolled structural sections. Though the experimental loadings differed slightly from the theoretical loadings, they were considered similar enough for a rough comparison (Fig. 5.19 and 5.20). The comparisons showed the theoretical and experimental hinge angles to be of the same order of magnitude.

(7) The maximum possible hinge angles were determined for a complete range of frame proportions and for wind loadings ranging from zero to 70 psf, including the usually specified wind load of 20 psf.

These calculations showed the maximum hinge angle at a lee knee to be about 1.03 $\emptyset_p L$ for gabled frames with small side loads, short columns and steep roofs. The maximum hinge angle at a windward knee would be about 0.44 $\emptyset_p L$ for gabled frames with large side loads, short columns, and steep roofs. The maximum hinge angle in a beam or rafter would be about 0.33 $\emptyset_p L$ for flat-roofed frames with tall columns and no side load.

6. MULTI - SPAN FRAMES WITH FLAT ROOFS

A method of plastic design of multi-span rigid frames by separation into subassemblages has been presented by Ketter.[10] With certain modifications in the concepts of subassemblages, the determination of rotations and deflections for multi-span rigid frames may also be accomplished by the use of graphical charts for subassemblages. The solution of this problem will be presented in the following discussions. In order to keep the number of complicating factors to a minimum, only flat-roofed frames will be considered in this chapter. Gabled frames will be treated in Chapter 7.

To solve the problem of rotations and deflections of subassemblages for multi-span frames, the necessary alterations to the concept of subassemblages will first be made. In Ketter's method, the effects of adjacent spans on the span being considered are grouped together in the moment terms $AwL^2/2$ and $DwL^2/2$ applied to each side of the subassemblage (Fig 6.1a). A and D are dimensionless parameters relating the side loads and moments to the vertical loads. Unfortunately, these side load terms do not define the moment diagrams in the columns sufficiently to allow calculation of deflections and rotations.

If the moment terms in Fig 6.1(a) are replaced by a pair of thrusts, AwL/2a and DwL/2a, as shown in Fig 6.1(b), the moment diagram in the columns may be determined. However, replacing the external moments $AwL^2/2$ and $DwL^2/2$ does not change the loading statically. Therefore, the design method may still be used without alteration. In a multi-span frame, it would be expected that there would be external moments at the knees caused by adjacent spans as well as external thrusts at the knees. To take these external moments into account, the moments M_{Q_L} and M_{Q_R} and negative thrusts M_{Q_L}/aL and M_{Q_R}/aL will be added as in Fig 6.1(c). The three loading cases given in Fig 6.1 are all identical with respect to the plastic design of the subassemblage by means of charts because the charts actually select only the member for the roof beam. For the calculation of rotations and deflections, the loading of Fig 6.1(c) will be used. For the determination of the first plastic hinge, the loading of Fig 6.1(b) will be used.

6.1 POSSIBLE MECHANISMS AND DOMAINS

As in the case of the single span frame, each subassemblage

might form one of two possible mechanisms. Equating the plastic hinge moments for these two mechanisms gives an equation separating the domains for which each will occur.

For a general composite mechanism, the plastic hinge moment is:[10]

$$\frac{M_p}{wL^2} = \frac{1}{16}(A-D+1)^2 \qquad \ldots(6.1)$$

For a panel mechanism, the plastic hinge moment is:[10]

$$\frac{M_p}{wL^2} = \frac{1}{4}(A-D) \qquad \ldots(6.2)$$

Equating these, the boundary between the two mechanisms is:

$$A - D = 1 \qquad \ldots(6.3)$$

6.2 LOCATION OF FIRST AND LAST PLASTIC HINGES

The locations of the first and last plastic hinges within a subassemblage are determined by the location of the maximum elastic moment. Expressions for the elastic moments in the subassemblages are as follows:

$$M_E = -wL^2\left[\frac{1}{8a+12} + \frac{1}{4}(A - D)\right]$$

$$M_F = wL^2\left[\frac{1}{8} + \frac{1}{8}(A-D)^2 - \frac{1}{8a+12}\right]$$

$$M_C = wL^2\left[\frac{1}{4}(A-D) - \frac{1}{8a+12}\right] \qquad \ldots(6.4)$$

It is only possible for the maximum moment to occur at the lee knee E

and in the beam at F. Equating the expressions for M_E and M_F gives an expression as follows for the desired boundary.

$$A\text{-}D = 1 - 2\sqrt{\frac{1}{2a+3}} \qquad \ldots(6.5)$$

6.3 SELF-SUPPORTING AND NON-SELF-SUPPORTING SUBASSEMBLAGES

A typical design of a three span frame might result in a mechanism similar to that shown in Fig. 6.3. To determine the required rotation capacity of this structure, calculations of rotations and deflections must be made considering continuity at the last plastic hinge to form. This brings out two important points:

(1) The last plastic hinge must be located.

(2) Only one of the three subassemblages possesses the continuity at maximum load which makes a structure determinate and stable. The other two subassemblages are truly mechanisms and must depend on the self-supporting span for support.

These two contitions in multi-span frames may be handled by deriving a set of equations for non-self-supporting subassemblages as well as for the self-supporting subassemblages. The location of the last plastic hinge may be determined by assuming each span in turn to be the self-supporting span and calculating deflections. It has been shown that the greatest deflection will occur when the true last plastic hinge has been assumed.

The unusual condition in the non-self-supporting spans is that,

having two plastic hinges free to rotate, they are overdeterminate, and deflections and rotations may not be calculated without further information. This further information is supplied by the known deflection of the self-supporting span at the point to which the adjacent span must remain attached. For instance, suppose it is determined that the left span in Fig. 6.3 is to be the self-supporting span. Then the deflection δ_E of the lee knee can be calculated. This deflection is then a known deflection when considering the behavior of the span to its right. If the desired functions in the non-self-supporting span are solved in terms of the loading, geometry, and this controlled deflection, Δ_C, all results may be obtained.

6.4 HINGE ANGLES AND DEFLECTIONS FOR SELF-SUPPORTING SUBASSEMBLAGES

The moment diagram for flat-roofed multi-span frames is given in Fig. 6.4. The moments shown are applicable to both the self-supporting and non-self-supporting subassemblages. Because the interior columns in multi-span frames are, in general, different members than the rafters, the different moments of inertia are used directly rather than deriving the equations for constant section throughout. These moments of inertia are designated as I_O for the rafters, I_L for the left hand column, and I_R for the right hand column.

The derivation of the hinge angles for the self-supporting subassemblage proceeds exactly as in the case of single span frames with the simple addition of the DwL^2, M_{Q_L}, and M_{QR} terms. The resulting hinge angle equation for the general mechanism with the first hinge at

the lee knee E is now given.

Case I. -- Composite Mechanism with First Hinge at Lee Knee E

$$\frac{H_E}{\emptyset pL} = \frac{wL^2}{M_p}\left[\frac{1}{12} + \frac{1}{4}(A - D)\right] - 1$$
$$+ \frac{1}{6}a\frac{wL^2}{M_p}(A-D)\frac{I_o}{I_L} - \frac{1}{3}a\frac{I_o}{I_L} - \frac{1}{3}a\frac{I_o}{I_R}$$
$$- \frac{1}{3}a\frac{I_o}{I_L}\frac{M_{Q_L}}{M_p} - \frac{1}{3}a\frac{M_{Q_R}}{M_p}\frac{I_o}{I_R} \qquad \ldots(6.6)$$

If, temporarily, the I of the columns is made equal to that of the rafters, and M_{Q_L} and M_{Q_R} are set equal to zero, the equation reduces to a function of A, D, and a.

$$\frac{H_E}{\emptyset pL} = \frac{wL^2}{M_p}\left[\frac{1}{12} + (A-D)\left(\frac{1}{4} + \frac{1}{6}a\right)\right] - 1 - \frac{2}{3}a \qquad \ldots(6.7)$$

This equation is seen to be identical to Eq. (5.20) for single span frames except that the expression (A-D) replaces A. It thus becomes convenient to set up the equations for multi-span frames as a graphic portion consisting of the solution of a single-span frame with side loads from both sides, and a set of corrections for the differences in moments of inertia of the columns and beam and for the moments at the eaves due to adjoining subassemblages.

Graphic

$$\frac{H_E}{\emptyset pL} = \frac{wL^2}{M_p}\left[\frac{1}{12} + (A-D)\left(\frac{1}{4} + \frac{1}{6}a\right)\right] - 1 - \frac{2}{3}a \qquad \ldots(6.7)$$

Corrections

$$\frac{H_E}{\phi_p L} = -\frac{1}{3}a\frac{I_o}{I_L}\frac{M_{Q_L}}{M_p} - \frac{1}{3}a\frac{I_o}{I_R}\frac{M_{Q_R}}{M_p}$$
$$-\frac{1}{3}\left(\frac{I_o}{I_L}+\frac{I_o}{I_R}-2\right)+\frac{1}{6}a\left(\frac{I_o}{I_L}-1\right)\frac{wL^2}{M_p}\quad (A\text{-}D) \qquad ...(6.8)$$

The sum of eq. (6.7) and (6.8) is eq. (6.6) fulfilling the requirement that the graphic solution plus the corrections equal the total result.

Similarly, hinge angles may be derived for two other cases:

Case II. COMPOSITE MECHANISM -- FIRST HINGE IN BEAM AT F

$$\frac{H_F}{\phi pL} = \frac{wL^2}{M_p}\left[\frac{1}{12}+\quad (A\text{-}D)\left(\frac{1}{4}+\frac{1}{6}a\right)\right] -1 - \frac{2}{3}a$$
$$-\frac{1}{3}\frac{I_o}{I_L}\frac{M_{Q_L}}{M_p} - \frac{1}{3}a\frac{I_o}{I_R}\frac{M_{Q_R}}{M_p}$$
$$-\frac{1}{3}a\left(\frac{I_o}{I_L}+\frac{I_o}{I_R}-2\right)+\frac{1}{6}a\left(\frac{I_o}{I_L}-1\right)\frac{wL^2}{M_p}\quad (A\text{-}D) \qquad ...(6.9)$$

Case Ia. Panel Mechanism -- First Hinge at Lee Knee E

$$\frac{H_E}{\phi pL} = \frac{1}{3(A\text{-}D)}$$
$$-\frac{1}{3}a\frac{I_o}{I_L}\frac{M_{Q_L}}{M_p} - \frac{1}{3}a\frac{I_o}{I_R}\frac{M_{Q_R}}{M_p}$$
$$+\frac{1}{3}a\left(\frac{I_o}{I_L}-\frac{I_o}{I_R}\right) \qquad ...(6.10)$$

The graphic portions of Eq. (6.7), (6 .9) and (6.10) are plotted as a family

of curves in Fig. 6.5. This figure is identical to Fig. 5.10.

As a result of the derivations of hinge angles it becomes possible to compute the horizontal deflections of the knees, δ_E, and the vertical deflections of the midpoint of the beams δ_D. These are summarized in the appendix in Eq. (6.11) to (6.17). Curves of the graphic portions of the δ_E equations are plotted in Fig. 6.6.

6.5 HINGE ANGLES AND DEFLECTIONS FOR NON-SELF-SUPPORTING SUBASSEMBLAGES

The only different step in the procedure for deriving hinge angles for non-self-supporting subassemblages is using the horizontal deflection Δ_C produced by the adjacent span as a boundary condition. Also there are two hinge angles instead of one. The use of the deflection boundary condition is actually accomplished by using the chord rotation F_{AC} as the known quantity in the slope-deflection equations and substituting its value Δ_C/aL into the resulting solution.

The following equations result from the slope-deflection calculations:

Case I and II: Composite Mechanism -- Hinges at Lee Knee E and in Beam at F.

$$\frac{H_E}{\emptyset pL} = \frac{1}{(1-\alpha)}\left\{ \frac{wL^2}{M_p}\left[\frac{1}{24} - \frac{1}{12}\alpha + (A\text{-}D)\left(\frac{1}{12} - \frac{1}{4}\alpha - \frac{1}{3}a\,\alpha\right)\right] - \left[\frac{1}{2} - \alpha - \frac{1}{3}a\alpha\right]\right\} - \frac{1}{3}a$$
$$+ \frac{\Delta C}{a\,\emptyset pL^2}\left(\frac{1}{1-\alpha}\right) + \frac{1}{3}a\left(\frac{\alpha}{1-\alpha}\right)\frac{I_o}{I_L}\frac{M_{QL}}{M_p} - \frac{1}{3}a\frac{I_o}{I_R}\frac{M_{QR}}{M_p}$$
$$+ \left(\frac{\alpha}{1-\alpha}\right)\frac{1}{3}a\left(\frac{I_o}{I_L} - 1\right) - \left(\frac{\alpha}{1-\alpha}\right)\frac{1}{3}a\frac{wL^2}{M_p}(A\text{-}D)\left(\frac{I_o}{I_L} - 1\right)$$
$$- \frac{1}{3}a\left(\frac{I_o}{I_R} - 1\right) \qquad \ldots(6.18)$$

$$\frac{H_F}{\emptyset pL} = \left(\frac{1}{1-\alpha}\right)\left\{\frac{wL^2}{M_p}\left[\frac{1}{24} + (A-D)\left(\frac{1}{6} + \frac{1}{6}a\right)\right] - \left[\frac{1}{2} + \frac{1}{3}a\right]\right.$$

$$- \left(\frac{1}{1-\alpha}\right)\frac{\Delta_C}{a\emptyset pL^2} - \frac{1}{3}a\,\frac{I_o}{I_L}\,\frac{M_{QL}}{M_p}\,\frac{1}{(1-\alpha)}$$

$$\left. - \frac{1}{3}a\left(\frac{I_o}{I_L} - 1\right)\frac{1}{(1-\alpha)} + \frac{1}{6}a\,\frac{wL^2}{M_p}(A-D)\left(\frac{I_o}{I_L} - 1\right)\frac{1}{(1-\alpha)}\right. \qquad \ldots(6.19)$$

Case Ia: Panel Mechanism -- Hinges at Lee Knee E and Windward Knee C

$$\frac{H_E}{\emptyset pL} = \frac{1}{6}\left(\frac{1}{A-D}\right) - \frac{1}{6} - \frac{1}{3}a$$

$$+ \frac{\Delta_C}{a\emptyset pL^2} - \frac{1}{3}a\,\frac{I_o}{I_R}\,\frac{M_{QR}}{M_p}$$

$$- \frac{1}{3}a\left(\frac{I_o}{I_L} - 1\right) \qquad \ldots(6.20)$$

$$\frac{H_C}{\emptyset pL} = \frac{1}{6}\left(\frac{1}{A-D}\right) + \frac{1}{6} + \frac{1}{3}a$$

$$- \frac{\Delta_C}{a\emptyset pL^2} - \frac{1}{3}a\,\frac{I_o}{I_L}\,\frac{M_{QL}}{M_p}$$

$$+ \frac{1}{3}a\left(\frac{I_o}{I_L} - 1\right) \qquad \ldots(6.21$$

Eq. (6.18) is plotted as a family of curves in Fig. 6.7, and Eq. (6.19) is plotted in Fig. 6.8. Eq. (6.20) and (6.21) appear in their respective charts only as the A-D = 1 curve since no greater values of A-D are plotted.

Since the horizontal deflection δ_E of the lee knee equals the given deflection Δ_C of the Windward Knee for flat roof frames, no further

derivation of horizontal deflections is required. (Eq (6.21). Equations (6.22) and (6.23) for the vertical deflections of the center of the beam are given in the appendix, but are not plotted.

Rather than describing the steps in the procedure for using the equations and graphs derived immediately, and the procedure will be demonstrated with an example in the following section. The steps in the procedure will then be summarized in section 6.7.

6.6 SAMPLE SOLUTION OF A FLAT ROOFED MULTI-SPAN FRAME

The use of the results of this chapter will be illustrated by means of the two-span frame shown in Fig 6.9. The "known" information which can be obtained from the figure is as follows:

Left Span	Right Span
$b/a = 0$	$b/a = 0$
$a_1 = 0.333$	$a_2 = 0.200$
$A_1 = 0.0555$	$D_2 = 0$
$L_1 = 3L_o$	$L_2 = 5L_o$

The required information for a design is as follows:

Left Span	Right Span
$D_1 = ?$	$A_2 = ?$
$M_{p1} = ?$	$M_{p2} = ?$

The design full load for the frame is desired as w = 2k/ft and the column height L_o is 20 ft. Using a yield stress σ_y = 33ksi and following the necessary procedures of Ref 10, the following results are

obtained:

Left Span	Right Span	Center Column
$D_1 = 0.030$	$A_2 = 0.0108$	
$\frac{M_{p1}}{wL_1^2} = 0.0658$	$\frac{M_{p2}}{wL_2^2} = 0.0641$	
$A\text{-}D = 0.0256$	$A\text{-}D = 0.0108$	
$\alpha = 0.487$	$\alpha = 0.495$	
$\frac{M_Q}{M_{p1}} = -0.085$	$\frac{M_Q}{M_{p2}} = -0.916$	

21 WF 73	33 WF 130	27 WF 94
$Z_1 = 172.1$	$Z_2 = 466.0$	$Z_3 = 277.7$
$I_1 = 1600.3$	$I_2 = 6699.0$	$I_3 = 3266.7$
$M_{p1} = M_p$	$M_{p2} = 2.70\ M_p$	$M_{p3} = 1.61\ M_p$

The moment diagram at maximum load is shown in Fig 6.10.

The next step is to decide which span is the self-supporting span. This is done by calculating the horizontal deflection assuming each span in turn to be the self-supporting span. For the left span, using A-D = 0.0256 and a = 0.333, a $\delta_E / \emptyset_p L^2$ value of 0.035 is taken from Fig 6.6. The corrections to this graphic value are given by Eq. (6.11). Since there is no external moment to the left, and since the left column is the same section as the beam, all corrections equal zero. Then,

$$\delta_E = 0.035 \frac{M_{p1} L_1^2}{E I_1}$$

$$\delta_E = 0.035 \frac{M_p(3L_o)^2}{EI_1}$$

$$\delta_E = 0.316 \frac{M_p L_o^2}{EI_1} \quad \text{(Left Span)} \qquad \ldots(6.22)$$

For the right hand span, the graphic δ_E-value is $0.023\ \phi_p L^2$. Since there is an external moment to the left of this span, and the left column of the span differs from the beam, all corrections apply to this span. The additional factors necessary are:

$$\frac{M_{Q_L}}{M_p} = \frac{-1.00}{2.70}$$

$$\frac{I_o}{I_L} = \frac{6699.0\ in^4}{3266.7\ in^4} = 2.05$$

The correction terms of Eq (6.11) become:

$$\frac{\delta'_E}{\phi_p L^2} = -\frac{1}{3}a^2 \frac{I_o}{I_L}\frac{M_{Q_L}}{M_p} - \frac{1}{3}a^2\left(\frac{I_o}{I_L} - 1\right) + \frac{1}{6}a^2 \frac{wL^2}{M_p}(A-D)\left(\frac{I_o}{I_L} - 1\right)$$

$$= -\frac{1}{3}(0.2)^2 \frac{(2.05)}{(-2.70)} - \frac{1}{3}(0.2)^2 (1.05) + \frac{1}{6}(0.2)^2 \frac{(0.0108)}{0.0641}(1.05)$$

$$\frac{\delta'_E}{\phi_p L^2} = -0.00269 \qquad \ldots(6.23)$$

Adding this correction to the graphic value of δ_E gives the total value of δ_E.

$$\delta_E = \delta_E \text{ (graphic)} + \delta'_E$$

$$= (0.023 - 0.003)\frac{M_{p2}L_2^2}{EI_2}$$

$$\delta_E = 0.020 \frac{M_{p2}L_2^2}{EI_2} \qquad \ldots(6.24)$$

To compare this deflection with that of the left span, they must be put into the same dimensions.

$$\delta_E = \frac{0.020\ (2.70\ M_p)\ (5L_o)^2}{E\ (4.18\ I_1)}$$

$$\delta_E = 0.323\ \frac{M_p L_o^2}{EI_1} \qquad \text{(Right Span)} \qquad \ldots(6.25)$$

Since the horizontal deflection of the frame would be greater with the last plastic hinge in the right span, that span must be the self-supporting span. Therefore, hinge angles for the left span must be calculated using the charts and corrections for non-self-supporting subassemblages, and those for the right span using the functions for self-supporting subassemblages.

The first hinge angle to be calculated will be that for the right span. The graphic value of H_E from Fig. 6.5 is 0.216 $\emptyset pL$. Additional data needed for the corrections is provided below:

$$\frac{M_{Q_L}}{M_p} = \frac{-1.00}{2.70} \qquad \frac{M_{Q_R}}{M_p} = 0$$

$$\frac{I_o}{I_L} = 2.05 \qquad \frac{I_o}{I_R} = 1$$

The corrections to be made are included in Eq. (6.6).

$$\frac{H_E'}{\emptyset pL} = -\frac{1}{3}a\ \frac{I_o}{I_L}\ \frac{M_{Q_L}}{M_p} - \frac{1}{3}a\ \frac{I_o}{I_R}\ \frac{M_{Q_R}}{M_p}$$

$$-\frac{1}{3}a\ \left(\frac{I_o}{I_L} + \frac{I_o}{I_R} - 2\right) + \frac{1}{6}a\ \left(\frac{I_o}{I_L} - 1\right)\ \frac{wL^2}{M_p} \qquad \text{(A-D)}$$

$$\frac{H_E'}{\emptyset pL} = -\frac{1}{3}(0.2)\frac{(2.05)}{(-2.70)} - 0$$

$$-\frac{1}{3}(0.2)\ (1.05) + \frac{1}{6}(0.2)\ (1.05)\ \frac{(0.0108)}{0.0641}$$

$$\frac{H_E'}{\emptyset pL} = -0.0134 \qquad \ldots(6.26)$$

Therefore,

$$\frac{H_E}{\emptyset pL} = 0.216 - 0.013 = 0.203 \qquad \ldots(6.27)$$

Substituting quantities for $\emptyset_p$ and L,

$$H_E = 0.203\ \frac{(2.48\ M_p)(5L_o)}{E\ (4.18\ I_1)}$$

$$H_E = 0.602\ \frac{M_p L_o}{EI_1} \qquad \text{(Right Span)} \qquad \ldots(6.28)$$

For the left hand span, two hinge angles, H_E and H_F are to be calculated. These calculations will use the following additional data:

$$\frac{M_Q}{M_p} = 0 \qquad \frac{M_{Q_R}}{M_p} = \frac{-2.48}{1.00}$$

$$\frac{I_o}{I_L} = 1.00 \qquad \frac{I_o}{I_R} = 0.490$$

$$\frac{\alpha}{1-\alpha} = \frac{0.487}{0.513} = 0.950$$

The graphic value of the H_E from Fig. 6.7 is -0.051 ØpL. The corrections from Eq. (6.18) are:

$$\frac{H_E'}{\emptyset_p L} = \frac{\Delta_C}{a\emptyset pL^2}\left(\frac{1}{1-\alpha}\right) + \frac{1}{3}a\ \frac{I_o}{I_L}\ \frac{MQ_L}{M_p}\left(\frac{\alpha}{1-\alpha}\right) - \frac{1}{3}a\ \frac{I_o}{I_R}\ \frac{M_{Q_R}}{M_p}$$

$$+ \left(\frac{I_o}{I_L} - 1\right) \frac{1}{3}a \left(\frac{\alpha}{1-\alpha}\right) \left[1 - \frac{wL^2}{M_p} (A-D) \right]$$

$$- \frac{1}{3}a \left(\frac{I_o}{I_R} - 1\right) \qquad \ldots(6.29)$$

Substituting for ΔC the value obtained in Eq. (6.25) and for the other quantities their known values,

$$\frac{H_E'}{\phi_p L} = \frac{0.323 \frac{M_p L_o^2}{EI_1}}{0.333 M_p (3L_o)^2 (0.513)} + 0 - \frac{1}{3} (0.333) (0.490) (-2.48)$$

$$+ 0 - \frac{1}{3} (0.333) (-0.510)$$

$$\frac{H_E'}{\phi_p L} = 0.402 \qquad \ldots(6.30)$$

Then,

$$H_E = -0.051 \frac{M_p L_1}{EI_1} + 0.402 \frac{M_p L_1}{EI_1} = 0.351 \frac{M_p L_1}{EI_1}$$

$$H_E = 0.351 \frac{M_p (3L_o)}{EI_1} = 1.053 \frac{M_p L_o}{EI_1} \qquad \text{(Left Span)} \qquad \ldots(6.31)$$

The graphic value of H_F from Fig. 6.6 is $0.191 \phi_p L$. The corrections from Eq. (6.19) are:

$$\frac{H_F'}{\phi_p L} = - \frac{\Delta C}{a \phi_p L^2} \left(\frac{1}{1-\alpha}\right) - \frac{1}{3}a \frac{I_o}{I_L} \frac{MQ_L}{M_p} \left(\frac{1}{1-\alpha}\right)$$

$$- \left(\frac{I_o}{I_L} - 1\right) \frac{1}{3}a \left(1 - \frac{1}{2} \frac{wL^2}{M_p} [A-D]\right) \qquad \ldots(6.32)$$

Substituting,

$$\frac{H_F'}{\phi_p L} = - \frac{0.323 \frac{M_p L_o^2}{EI_1}}{0.333 \frac{M_p}{EI_1} (3l_o)^2 (0.513)} - 0 - 0$$

$$\frac{H_F'}{\phi_p L} = - 0.210 \qquad \ldots(6.33)$$

Then the hinge angle at Section F is given by

$$H_F = 0.191 \frac{M_p L_1}{EI_1} - 0.210 \frac{M_p L_1}{EI_1} = - 0.019 \frac{M_p L_1}{EI_1}$$

$$H_F = - 0.057 \frac{M_p L_o}{EI_1} \qquad \text{(Left Span)} \qquad \ldots(6.34)$$

Summarizing, the hinge angles for the structure are as follows:

	Left Span	Right Span
Knee	$H_E = 1.053 \frac{M_p L_o}{EI_1}$	$H_E = 0.602 \frac{M_p L}{EI_1}$
Beam	$H_F = - 0.057 \frac{M_p L_o}{EI_1}$	$H_F = 0$

$\ldots(6.35)$

The magnitude of the hinge angles at the knees would indicate that they were the first to form. This is expected because elastic solutions of two-span frames generally show the greatest moment at the center support and a large moment at the lee knee. The meaning of the negative sign of the hinge angle in the left beam is that the hinge has tension on the bottom of the beam as is expected from the physical picture of the structure. The hinge angle in the right beam is zero by its definition as the last plastic hinge to form.

6.7 SUMMARY

In this chapter, a method of determining the required hinge angles of flat-roofed multi-span frames by separation of the structure into subassemblages is described. This method is consistant with the method of designing similar frames presented by Ketter.[10] The following

summarizes this chapter:

(1) Due to the requirement that only one plastic hinge can have continuity just prior to the formation of mechanism, only one of the subassemblages of a multi-span frame may be self-supporting. All remaining subassemblages must depend upon this subassemblage for part of their support. Therefore, it is necessary to derive a set of equations for non-self-supporting subassemblages as well as for the self-supporting subassemblage.

(2) Equations for the domains for mechanisms, hinge angles, and deflections were derived for the self-supporting subassemblages in the same way as was done for single-span flat-roofed frames. In fact, the resulting equations were the same with three exceptions: (i) The term A-D in the multi-span equations replaced the term A in the single-span equations, (ii) Correction terms were included for the moments of the knees due to the effect of adjacent spans; and (iii) Correction terms were included for differences between the moments of inertia of columns and beams. Graphs of the graphic portions of these equations are given in Fig 6.5 and 6.6. To these values must be added the appropriate corrections.

(3) Additional equations were derived for non-self-supporting subassemblages. The derivations assumed discontinuity at both plastic hinges rather than one. The boundary condition substituted to make the problem solvable was that the horizontal deflection of the knees must be the same as the "known" deflection of the self-supporting span.

Thus a term Δ_C, which is determined by the self-supporting subassemblage, appears in each equation for non-self-supporting subassemblages. Graphs of the graphic portions of these equations are given in Fig 6.7 and 6.8. Correction terms must be added to these values.

(4) The method of solving rotation capacity problems for multi-span frames was established as follows: First, assume each span in turn to be the self-supporting span and calculate the corresponding horizontal deflection; the correct assumption will be indicated by the largest deflection so computed. Second, having determined the self supporting span, calculate the hinge angle for that span causing the "self-supporting" equations, and calculate the hinge angles for all other spans using the angles for all other spans using the "non-self-supporting" equations.

(5) An example of a non-symmetrical two span frame was solved to indicate the use of the charts and equations.

7. MULTI-SPAN GABLED FRAMES

The principles to be used in the solution of gabled multi-span frames are the same as for flat-roofed frames. However, added complications arise in the form of additional possible mechanisms resulting from the gabled roof. These possible mechanisms could result when the side loads on both sides of a span are quite high, causing the rafters to bulge upward with a plastic hinge forming at the ridge. This mechanism will be designated a "reverse" mechanism in the sense that some of the loads move in a direction opposite to that in which they are applied. It can occur either with hinges at the ridge D and in the windward rafter at F or with hinges at D and at the windward knee C. The second form is actually a special case of the first with an α value equal to zero.

It is considered doubtful that the value of the side load factor D could become large enough in most practical cases to cause a reverse mechanism. However, a case can be shown where it would form, so the equations will be presented for completeness.

7.1 TYPE OF MECHANISMS

The equations for the plastic hinge moments for the composite and panel mechanisms are available from Ref 10.

Composite Mechanism (Fig 7.1a)

$$\frac{M_p}{wL^2} = \frac{1}{4}\left[\frac{(1-\alpha)\ (A+\alpha\ -D)\ -\ D\left(\frac{2b}{a}\right)\alpha}{1+\frac{b}{a}\alpha}\right]$$

$$\alpha = \frac{1}{b/a}\left[\sqrt{1 - \frac{b}{a}\left[A\left(1+\frac{b}{a}\right) - D\left(1-\frac{b}{a}\right) - 1\right]} \quad -1\right] \text{ for } \frac{b}{a} > 0 \qquad \ldots(7.1)$$

Panel Mechanism (Fig 7.1b)

$$\frac{M_p}{wL^2} = \frac{A-D}{4} \qquad \ldots(7.2)$$

The panel mechanism is a special case of the composite mechanism with $\alpha = 0$.

Equations for the two forms of the "reverse" mechanism may be derived in the same manner that was used for the others. The resulting expressions are:

Reverse Composite Mechanism (Fig 7.1c)

$$\frac{M_p}{wL^2} = \frac{1}{4}\left\{\frac{(1-2\alpha)\left[A\left(\frac{1+2b}{a}\right) - D - \frac{1}{2} + \alpha\left(\frac{1+b}{a}\right)\right]}{2 + \frac{b}{a} + 2\frac{b}{a}\alpha}\right\}$$

$$\alpha = \frac{1}{b/a}\left[\sqrt{1 + 2\frac{b}{a} + \frac{1}{2}\frac{b^2}{a^2} - \frac{b}{a}\left[A\left(1+2\frac{b}{a}\right) - D\right]} \quad -1\right] - \frac{1}{2} \qquad \ldots(7.3)$$

Reverse Gable Mechanism (Fig 7.1d)

$$\frac{M_p}{wL^2} = \frac{1}{4}\left[\frac{A\left(1 + 2b/a\right) - D - 1/2}{(2 + b/a)}\right] \qquad \ldots(7.4)$$

The limits of the mechanisms are determined by equating the M_p/wL^2 expressions for each pair of mechanisms.

Relationship Separating Composite Mechanism from Negative Composite Mechanism

$$\frac{\frac{3}{4}\left(2+\frac{b}{a}\right)}{\frac{b}{a}} - A + D = \frac{\left(1+\frac{b}{a}\right)}{b^2/a^2}\sqrt{1 + 2b/a + \frac{1}{2}\frac{b^2}{a^2} - \frac{b}{a}\left[A\left(1+2\frac{b}{a}\right) - D\right]} - \frac{1}{b^2/a^2}\sqrt{1 - \frac{b}{a}\left[A\left(1+\frac{b}{a}\right) - D\left(1-\frac{b}{a}\right) - 1\right]} \qquad \ldots(7.5)$$

Relationship Separating Composite Mechanism from Panel Mechanism

$$A = \frac{1 + D\ (1 - b/a)}{1 + b/a} \qquad \ldots(7.6)$$

Relationship Separating Panel Mechanism from Reverse Gable Mechanism

$$D = \frac{A\ (1 - b/a) + 1/2}{1 + b/a} \qquad \ldots(7.7)$$

Relationship Separating Reverse Composite Mechanism from Reverse Gable Mechanism

$$A = \frac{(1 + 1/4\ b/a) + D}{1 + 2\ b/a} \qquad \ldots(7.8)$$

Eq. (7.5) to (7.8) when plotted in the A vs D plane as in Fig 7.2 form the boundaries of four regions, one for each mechanism. The general region for each mechanism is as follows:

Southwest -- Composite Mechanism
Southeast -- Panel Mechanism
Northeast -- Reverse Gable Mechanism
Northwest -- Reverse Composite Mechanism

The equations for plastic hinge moment and for limits of mechanisms include the roof rise factor b and the column height factor a in each case only in the ratio b/a. However, it will be shown later, that for the location of first plastic hinges, the separate values of a and b must be used.

Plotting Eqs (7.5) to (7.8) for several b/a values would show that the intersection moves toward the northeast as b/a decreases. Thus for b/a = 1.0 (equal column height and roof rise), there are significant areas for each mechanism within the limits of A and D no greater than 1.0 (Fig 7.3). However, for smaller values, i.e. b/a = 0.2 (column

height much greater than roof rise), only the composite mechanism would occur for most values of A and D less than 1.0. This puts more emphasis on the composite mechanism for the purposes of analysis and design problems.

7.2 LOCATION OF FIRST AND LAST PLASTIC HINGES

In locating the first and last plastic hinges, the maximum elastic moments are needed. Because of the addition of the reverse mechanism, the moment at the ridge D must be considered in addition to those sections considered in the earlier solutions. The equations for the elastic moments are:

$$M_C = \frac{wL^2}{8}\left[(A-D)\,F - G + AJ\right] \qquad \ldots(7.9)$$

$$M_D = \frac{wL^2}{8}\left[2\,(A+D) - (A+D)\,F + 1 - G - \frac{b}{a}G - (A+D)\,F\,\frac{b}{a}\right] \qquad \ldots(7.10)$$

$$M_E = \frac{wL^2}{8}\left[-(A-D)\,F - G + DJ\right] \qquad \ldots(7.12)$$

$$M_F = \frac{wL^2}{8}\left[1 + 2\,(A+D) + (A-D)^2 + \frac{b}{a}F\,(A^2 - D^2 - A-D) - F\,(A+D) + \frac{b}{a}G\,(A-D) - \frac{b}{a}G - G + \frac{1}{4}\frac{b^2}{a^2}\left\{G+(A-D)\,F\right\}^2\right] \qquad \ldots(7.13)$$

where the values of A and D are as defined previously and

$$N = \frac{8a}{\sqrt{1+4b^2}} + 12 + 12\,\frac{b}{a} + 4\,\frac{b^2}{a^2} \qquad G = \frac{8 + 5\,b/a}{N}$$

$$F = \frac{\sqrt{\frac{16a}{1 + 4b^2}} + 24 + 12\frac{b}{a}}{N} \qquad J = \frac{24\,b/a + 16b^2/a^2}{N} \qquad \ldots(7.14)$$

These equations were derived with the aid of equations given in Ref. 7. The regions in which each plastic hinge is first to form are bounded by

curves derived by equating the elastic moments in pairs as was done previously. These equations are:

a) Boundary Between First Hinge at Lee Knee E and In Windward Rafter at F

$$M_E = - M_F$$

$$0 = A^2 \left(1+\frac{b}{a} + \frac{1}{4} \frac{b^2}{a^2} F^2\right) + A\left(2 - \frac{b}{a}F - 2F + \frac{b}{a}G + \frac{1}{2} \frac{b^2}{a^2}FG + D\left[\frac{1}{2} \frac{b^2}{a^2} F^2 - 2\right]\right)$$
$$+ D \left(2 - \frac{b}{a} F - \frac{b}{a} G + \frac{1}{2} \frac{b^2}{a^2} FG + J\right) + D^2 \left(1 - \frac{b}{a} F + \frac{1}{4} \frac{b^2}{a^2} F^2\right)$$
$$+ \left(1 - \frac{b}{a} G - 2G + \frac{1}{4} \frac{b^2}{a^2} G^2\right) \qquad \ldots(7.15)$$

b) Boundary Between First Hinge at Lee Knee E and at Windward Knee C

$$M_E = -M_C$$

$$A + D = \frac{8 + 5b/a}{12b/a + 8\ b^2/a^2} \qquad \ldots(7.16)$$

c) Boundary Between First Hinge at Lee Knee E and at Ridge D

$$M_E = M_D$$

$$D = \frac{A(2 - Fb/a) + \left(1 - \frac{b}{a} G\right)}{(Fb/a + 2F + J - 2)} \qquad \ldots(7.17)$$

d) Boundary Between First Hinge at Ridge D and at Windward Knee C

$$M_D = -M_C$$

$$D = \frac{A\left(2 - F\frac{b}{a} + J\right) + \left(1 - 2G - \frac{b}{a} G\right)}{(AF + Fb/a - 2)} \qquad \ldots(7.18)$$

e) Boundary Between First Hinge at Ridge D and in Windward Rafter at F

$$M_F = -M_D$$

$$0 = A^2 \left(1 + \frac{b}{a}F + \frac{1}{4}\frac{b^2}{a^2}F^2\right) + A\left(4 - 2F - 2\frac{b}{a}F + \frac{b}{a}G + \frac{1}{2}\frac{b^2}{a^2}FG\right.$$
$$\left. + D\left[\frac{1}{2}\frac{b^2}{a^2}F^2 - 2\right]\right) + \left(2 - 2G - 2\frac{b}{a}G + \frac{1}{4}\frac{b^2}{a^2}G^2\right)$$
$$+ D\left(4 - 2F - 2\frac{b}{a}F - \frac{b}{a}G + \frac{1}{2}\frac{b^2}{a^2}FG\right)$$
$$+ D^2\left(1 - \frac{b}{a}F + \frac{1}{4}\frac{b^2}{a^2}F^2\right) \quad \ldots (7.19)$$

As an example, equations (7.15) to (7.19) are plotted for the case of b = 0.2a = 0.2 in Fig 7.4. The segments applicable to each equation are indicated. Limiting the curves to one a and b value is necessary because of the radical form $a/\sqrt{1 + 4b^2}$ in the expressions for F, G and J. The first hinge is at the lee knee E for values in domain D1. It is in the windward rafter at F or at the windward knee G in domain D2. In domain D3, the first plastic hinge forms at the ridge D.

In Fig 7.5 are shown the domains for three cases of column height, all with the constant roof rise factor b of 0.2. These show that the point of intersection of a given set of curves moves upward and to the right with increasing column height. Of special interest is the curve for b = 0.2, a = 1.0. Here the

curve (Eq 7.15) separating the first hinge at E and first hinge at F does not intersect the A = D line, but continues downward until it touches the abscissa. This is another example of the effect seen in single span frames where the first hinge may form in the windward rafter of very tall frames with gently sloping roofs under little or no side load.

Comparable sets of curves for frames with steeper roofs are similar in shape to those in Fig 7.5, but the intersection point of each comparable set of curves occurs at a lower value of D. For example, considering two cases with the column height factor a = 1.0, the point of intersection of the curves for roof rise factor b = 0.5 is below D = 0.6, whereas the intersection point given in Fig 7.5 for b = 0.2 is near D = 1.5.

Charts of the type given in Fig 7.2 and 7.4 make it possible to determine the mechanism in one instance and the location of the first plastic hinge in the other. For the solution of a hinge angle problem however, it is necessary to know both at once for a given frame and loading. By combining these two figures, Fig 7.6

is obtained for frames with b = 0.2 and a = 0.2, giving the domains both for mechanism and first plastic hinge on one graph. Thus, the several cases for which hinge angles must be derived are defined. These domains are labelled as follows:

I. Composite Mechanism -- First Hinge at E

Ia. Panel Mechanism (α= 0) -- First Hinge at E

II. Composite Mechanism -- First Hinge at F

IIa. Panel Mechanism (α= 0) -- First Hinge at C

III. Reverse Composite Mechanism -- First Hinge at F

IIIa. Reverse Gable Mechanism (α= 0) -- First Hinge at C

IV. Reverse Composite Mechanism -- First Hinge at D

IVa. Reverse Gable Mechanism (α=0) -- First Hinge at D

All equations for multi-span gabled frames will be classified by this system so that selection of the proper equations for a given example may be made by reference to the domain chart, Fig 7.6.

7.3 HINGE ANGLES AND DEFLECTION OF SELF-SUPPORTING SUBASSEMBLAGES

The derivation of equations for hinge angles and deflections is accomplished in exactly the same manner as was done for single-span frames and flat-roofed multi-span frames. The slope-deflection equations are used with the addition of terms considering the effect of thrusts and bending moments applied to the column tops by the adjoining sub-assemblages. The necessary additional equations are obtained as before

by considering the relative horizontal and vertical displacements of the bases as given in Eq (5.21) and (5.22). The boundary conditions relating to continuity of slope are used as applicable to the particular mechanism being considered.

Bending moment diagrams for the two general types of mechanisms are given in Fig 7.7 and 7.8. Fig 7.7 is applicable to the composite and panel mechanisms, Cases I and II, while Fig 7.8 is applicable to the reverse mechanisms, Cases III and IV. Using those bending moment diagrams to set up the slope-deflection equations, hinge angles and deflections were derived for each case. For Case I (the composite mechanism with the first hinge at the lee knee) the hinge angle is:

$$\frac{H_E}{\phi_p L} = \sqrt{1+4b^2}\left\{\frac{wL^2}{M_p}\left[\frac{1}{12}+\frac{5}{96}\frac{b}{a}+A\left(\frac{1}{4}+\frac{1}{8}\frac{b}{a}\right)-D\left(\frac{1}{4}+\frac{3}{8}\frac{b}{a}+\frac{1}{6}\frac{b^2}{a^2}\right)\right]-\left[1+\frac{b}{a}+\frac{1}{3}\frac{b^2}{a^2}\right]\right\} - \frac{2a}{3} + \frac{1}{6}a\frac{wL^2}{M_p}(A-D)$$
$$-\frac{1}{3}a\frac{I_o}{I_L}\frac{M_{Q_L}}{M_p} - \frac{1}{3}\frac{I_o}{I_R}\frac{M_{Q_R}}{M_p}$$
$$-\frac{1}{3}a\left(\frac{I_o}{I_L}+\frac{I_o}{I_R}-2\right)+\frac{1}{6}a\left(\frac{I_o}{I_L}-1\right)\frac{wL^2}{M_p}(A-D) \qquad \ldots(7.20)$$

In this form, the equation has already been separated into its graphic and correction parts.

The hinge angle equations for the remaining cases are as follows:

Case Ia: Panel Mechanism -- First Hinge at Lee Knee E

$$\frac{H_E}{\phi_{pL}} = \sqrt{1+4b^2}\left\{\frac{1}{A-D}\left[\frac{1}{3}+\frac{5}{24}\frac{b}{a}-D\left(\frac{b}{a}+\frac{2}{3}\frac{b^2}{a^2}\right)\right]-\left[\frac{1}{2}\frac{b}{a}+\frac{1}{3}\frac{b^2}{a^2}\right]\right\}$$
$$-\frac{1}{3}a\,\frac{I_o}{I_L}\,\frac{M_{Q_L}}{M_p}-\frac{1}{3}a\,\frac{I_o}{I_R}\,\frac{M_{Q_R}}{M_p}$$
$$+\frac{1}{3}a\left(\frac{I_o}{I_L}-\frac{I_o}{I_R}\right) \qquad \ldots(7.21)$$

Case II: Composite Mechanism -- First Hinge in Windward Rafter at F

$$\frac{H_F}{\phi_{pL}} = \frac{1}{(1+2\frac{b}{a})}\left[\sqrt{1+4b^2}\left\{\frac{wL^2}{M_p}\left[\frac{1}{12}+\frac{5}{96}\frac{b}{a}+A\left(\frac{1}{4}+\frac{1}{8}\frac{b}{a}\right)-D\left(\frac{1}{4}+\frac{3}{8}\frac{b}{a}+\frac{1}{6}\frac{b^2}{a^2}\right)\right]\right.\right.$$
$$\left.\left.-\left[1+\frac{b}{a}+\frac{1}{3}\frac{b^2}{a^2}\right]\right\}-\frac{2}{3}+\frac{1}{6}a\,\frac{wL^2}{M_p}(A-D)\right]$$
$$-\frac{1}{3}a\,\frac{I_o}{I_L}\,\frac{M_{Q_L}}{M_p}\,\frac{1}{(1+2\frac{b}{a}\alpha)}-\frac{1}{3}a\,\frac{I_o}{I_R}\,\frac{M_{Q_R}}{M_p}\,\frac{1}{(1+2\frac{b}{a}\alpha)}$$
$$-\frac{1}{3}a\left(\frac{I_o}{I_L}+\frac{I_o}{I_R}-2\right)\frac{1}{(1+2\frac{b}{a}\alpha)}+\frac{1}{6}a\left(\frac{I_o}{I_L}-1\right)\frac{wL^2}{M_p}(A-D)\,\frac{1}{(1+2\frac{b}{a}\alpha)}$$
$$\ldots(7.22)$$

Case IIa: Panel Mechanism -- First Hinge at Windward Knee C

$$\frac{H_C}{\phi_{pL}} = \sqrt{1+4b^2}\left\{\frac{1}{A-D}\left[\frac{1}{3}+\frac{5}{24}\frac{b}{a}-D\left(\frac{b}{a}+\frac{2}{3}\frac{b^2}{a^2}\right)\right]-\left[\frac{1}{2}\frac{b}{a}+\frac{1}{3}\frac{b^2}{a^2}\right]\right\}$$
$$-\frac{1}{3}a\,\frac{I_o}{I_L}\,\frac{M_{Q_L}}{M_p}-\frac{1}{3}a\,\frac{I_o}{I_R}\,\frac{M_{Q_R}}{M_p}$$
$$+\frac{1}{3}a\left(\frac{I_o}{I_L}-\frac{I_o}{I_R}\right) \qquad \ldots(7.23)$$

Case III. Reverse Mechanism -- First Hinge in Windward Rafter at F

$$\frac{H_F}{\phi_{pL}} = \frac{1}{(1+b/a)}\,\frac{1}{(1+2\frac{b}{a}\alpha)}\left[\sqrt{1+4b^2}\left\{\frac{-wL^2}{M_p}\left[\frac{1}{24}-\frac{1}{96}\frac{b}{a}-\frac{1}{96}\frac{b^2}{a^2}\right.\right.\right.$$
$$\left.\left.\left.-(A+D)\left(\frac{1}{8}\frac{b}{a}+\frac{1}{24}\frac{b^2}{a^2}\right)\right]\right.$$

$$- \left[1+ \frac{b}{a} + \frac{1}{3} \frac{b^2}{a^2}\right]\Bigg\} - \frac{2}{3}a + \frac{wL^2}{M_p} \left\{ \frac{1}{6}b\ (A+D) - \frac{1}{12}a \right\}\Bigg]$$

$$- \frac{1}{3}\ a\ \frac{I_o}{I_L}\ \frac{M_{Q_L}}{M_p}\ \frac{1}{(1+2\frac{b}{a}\ \alpha)} - \frac{1}{3}a\ \frac{I_o}{I_R}\ \frac{M_{Q_R}}{M_p}\ \frac{1}{(1+2\frac{b}{a}\ \alpha)}$$

$$+ \frac{1}{(1+b/a)}\ \frac{1}{(1+2\frac{b}{a}\alpha)}\Bigg\{ - \frac{1}{3}a\ (\frac{I_o}{I_L} + \frac{I_o}{I_R} - 2) + \frac{wL^2}{M_p}\Bigg[\frac{1}{12}a\ (\frac{I_o}{IL} - \frac{I_o}{I_R})(A-D)$$

$$- \frac{1}{24}a\ (\frac{I_o}{I_L} + \frac{I_o}{I_R} - 2) + \frac{1}{6}b\ A\ (\frac{I_o}{I_L} - 1) + \frac{1}{6}b\ D\ (\frac{I_o}{I_R} - 1)\Bigg]\Bigg\} \qquad \ldots(7.24)$$

Case IIIa Reverse Mechanism ($\alpha = 0$) -- First Hinge at Windward Knee C

$$\frac{H_C}{\emptyset_p L} = \frac{1}{(1+\frac{b}{a})}\Bigg[\sqrt{1+4b^2}\Bigg\{ - \frac{wL^2}{M_p}\Bigg[\frac{1}{24} - \frac{1}{96}\frac{b}{a} - \frac{1}{96}\frac{b^2}{a^2} - (A+D)\left(\frac{1}{8}\frac{b}{a} + \frac{1}{24}\frac{b^2}{a^2}\right)\Bigg]$$

$$- \left[1 + \frac{b}{a} + \frac{1}{3}\frac{b^2}{a^2}\right]\Bigg\} - \frac{2}{3}\alpha + \frac{wL^2}{M_p}\left\{\frac{1}{6}b\ (A+D) - \frac{1}{12}a\right\}\Bigg]$$

$$- \frac{1}{3}a\ \frac{I_o}{I_L}\ \frac{M_{Q_L}}{M_p} - \frac{1}{3}a\ \frac{I_o}{I_R}\ \frac{M_{Q_R}}{M_p}$$

$$+ \frac{1}{(1+\frac{b}{a})}\Bigg\{ - \frac{1}{3}a\ (\frac{I_o}{I_L} + \frac{I_o}{I_R} - 2) + \frac{wL^2}{M_p}\Bigg[\frac{1}{12}a\ (\frac{I_o}{I_L} - \frac{I_o}{I_R})\ (A-D) - \frac{1}{24}a\left(\frac{I_o}{I_L} + \frac{I_o}{I_R} - 2\right)$$

$$+ \frac{1}{6}\ bA\ (\frac{I_o}{I_L} - 1) + \frac{1}{6}bD\ (\frac{I_o}{I_R} - 1)\Bigg]\Bigg\} \qquad \ldots(7.25)$$

Case IV & IVa. Reverse Mechanism -- First Hinge at Ridge D

$$\frac{H_D}{\emptyset_p L} = \frac{1}{(1+\frac{b}{a})^2}\Bigg[\sqrt{1+4b^2}\Bigg\{\frac{wL^2}{M_p}\Bigg[\left(\frac{1}{96}\frac{b}{a} + \frac{1}{96}\frac{b^2}{a^2} - \frac{1}{24}\right) + (A+D)\ \left(\frac{1}{8}\frac{b}{a} + \frac{1}{24}\frac{b^2}{a^2}\right)\Bigg]$$

$$- \left[1 + \frac{b}{a} + \frac{1}{3}\frac{b^2}{a^2}\right]\Bigg\} - \frac{2a}{3} + \frac{wL^2}{M_p}\left\{\frac{1}{6}b\ (A+D) - \frac{1}{12}a\right\}\Bigg]$$

$$- \frac{1}{3}a\ \frac{I_o}{I_L}\ \frac{M_{Q_L}}{M_p}\ \frac{1}{(1+\frac{b}{a})} - \frac{1}{3}a\ \frac{I_o}{I_R}\ \frac{M_{Q_R}}{M_p}\ \frac{1}{(1+\frac{b}{a})}$$

$$+\frac{1}{(1+\frac{b}{a})^2}\left\{-\frac{1}{3}a\left(\frac{I_o}{I_L}+\frac{I_o}{I_R}-2\right)+\frac{WL^2}{M_p}\left[\frac{1}{12}a\left(\frac{I_o}{I_L}-\frac{I_o}{I_R}\right)(A-D)\right.\right.$$

$$\left.\left.-\frac{1}{24}a\left(\frac{I_o}{I_L}+\frac{I_o}{I_R}-2\right)+\frac{1}{6}bA\left(\frac{I_o}{I_L}-1\right)+\frac{1}{6}bD\left(\frac{I_o}{I_R}-1\right)\right]\right\} \quad \ldots(7.26)$$

Equations for the horizontal deflections of the lee and windward knees are listed in the Appendix in Eq (7.27) through (7.40). Expressions for the vertical deflection of the ridge are listed in Eq (7.41) through (7.47).

Curves of the hinge angles for the specific case of b = 0.2, a = 0.2 are plotted in Fig 7.9. In this figure, values of H_E are plotted above the abscissa with solid lines, and values of H_F are plotted below the abscissa with solid lines. Values of H_D are plotted as dashed lines above the abscissa, and H_C are plotted as dashed lines below the abscissa. To these values must be added the necessary corrections for variation in moment of inertia and for external knee moments.

Similarly, curves of the horizontal deflections δ_E of the lee knee and δ_C of the windward knee are plotted in Fig 7.10 and 7.11 respectively. These figures apply only to the case of b = 0.2, a = 0.2. Curves of the vertical deflection of the ridge are not included since they are unnecessary for the rotation capacity studies.

7.4 HINGE ANGLES AND DEFLECTIONS OF NON-SELF-SUPPORTING SUBASSEMBLAGES

The equations for hinge angles and deflections of non-self-supporting subassemblages with gabled roofs are derived in the same manner as were those for flat-roofed subassemblages in section 6.5. That is, freedom to rotate is assumed at each of two plastic hinges. Since this condition implies a mechanism for which deflection and rotation are not bounded, an additional condition must be imposed. This is handled by constraining the deflection, Δ_C of the windward knee to be equal to the deflection of the same knee as obtained from the solution of a self-supporting case for the adjacent span.

The actual equations are derived by using the moments of Fig. 7.7 or 7.8 to set up the slope-deflection equations. These equations are then solved for the required hinge angles and deflections. The resulting equations for hinge angles follow. In each case, all terms preceding the Δ_C term form the graphic part of the function and the remainder form the corrections for change of cross section and external moments applied to the knees.

Cases I & II: Composite Mechanism

$$\frac{H_E}{\emptyset_{pL}} = \frac{1}{(1-\alpha)}\left[\sqrt{1+4b^2}\left\{\frac{wL^2}{M_p}\left[\frac{1}{24}+\frac{5}{96}\frac{b}{a}-\frac{1}{12}\alpha-\frac{13}{96}\frac{b}{a}\alpha\right.\right.\right.$$
$$+A\left(\frac{1}{12}+\frac{1}{8}\frac{b}{a}-\frac{1}{4}\alpha-\frac{11}{24}\frac{b}{a}\alpha\right)$$
$$\left.\left.\left.-D\left(\frac{1}{12}+\frac{1}{4}\frac{b}{a}+\frac{1}{6}\frac{b^2}{a^2}-\frac{1}{4}\alpha-\frac{17}{24}\frac{b}{a}\alpha-\frac{5}{12}\frac{b^2}{a^2}\alpha\right)\right]\right.$$

$$- \left[\frac{1}{2} + \frac{3}{4}\frac{b}{a} + \frac{1}{3}\frac{b^2}{a^2} - \alpha - 2\frac{b}{a}\alpha - \frac{5}{6}\frac{b^2}{a^2}\alpha \right] \Bigg\}$$

$$+ \frac{1}{3}a\alpha \left(1+2\frac{b}{a}\right)\left\{1 - \frac{wL^2}{M_p}(A-D)\right\} \Bigg] - \frac{1}{3}a$$

$$+ \frac{\Delta C}{a\phi pL^2} \frac{(1+2\frac{b}{a}\alpha)}{(1-\alpha)} + \frac{1}{3}a\alpha\frac{I_o}{I_L}\frac{MQ_L}{M_p}\frac{(1+2\frac{b}{a})}{(1-\alpha)} - \frac{1}{3}a\frac{I_o}{I_R}\frac{M_{QR}}{M_p}$$

$$+ \frac{1}{3}a\alpha\left(\frac{I_o}{I_L} - 1\right)\left(\frac{1+2\frac{b}{a}}{1-\alpha}\right)\left\{1 - \frac{wL^2}{M_p}(A-D)\right\} - \frac{1}{3}a\left(\frac{I_o}{I_R} - 1\right) \qquad \ldots(7.48)$$

$$\frac{H_F}{\phi_p L} = \frac{1}{(1-\alpha)}\left\{\sqrt{1+4b^2}\left\{\frac{wL^2}{M_p}\left[\frac{1}{24} + \frac{1}{6}(A-D) - \frac{1}{8}\frac{b}{a}D\right] - \left[\frac{1}{2}+\frac{1}{4}\frac{b}{a}\right]\right\}\right.$$

$$\left. - \frac{1}{3}a + \frac{1}{6}a\frac{wL^2}{M_p}(A-D)\right\}$$

$$- \frac{1}{(1-\alpha)}\frac{\Delta C}{a\phi pL^2} - \frac{1}{3}a\frac{I_o}{I_L}\frac{M_{QL}}{M_p}\frac{1}{(1-\alpha)}$$

$$- \frac{1}{3}a\left(\frac{I_o}{I_L} - 1\right)\frac{1}{(1-\alpha)}\left\{1 - \frac{1}{2}\frac{wL^2}{M_p}(A-D)\right\} \qquad \ldots(7.49)$$

Cases Ia & IIa: Panel Mechanism.

$$\frac{H_E}{\phi_{pL}} = \sqrt{1+4b^2}\left\{\frac{1}{A-D}\left[\frac{1}{6} + \frac{5}{24}\frac{b}{a} - D\left(\frac{1}{2}\frac{b}{a} + \frac{2}{3}\frac{b^2}{a^2}\right)\right] - \left[\frac{1}{6}+\frac{1}{4}\frac{b}{a}+\frac{1}{3}\frac{b^2}{a^2}\right]\right.$$

$$\left. = \frac{1}{3}a\right.$$

$$+ \frac{\Delta C}{a\phi pL^2} - \frac{1}{3}a\frac{I_o}{I_R}\frac{M_{QR}}{M_p}$$

$$- \frac{1}{3}a\left(\frac{I_o}{I_R} - 1\right) \qquad \ldots(7.50)$$

$$\frac{H_C}{\phi_{pL}} = \sqrt{1+4b^2}\left\{\frac{1}{A-D}\left[\frac{1}{6} - \frac{1}{2}\frac{b}{a}D\right] + \left[\frac{1}{6} - \frac{1}{4}\frac{b}{a}\right]\right\} + \frac{1}{3}a$$

$$- \frac{\Delta C}{a\phi pL^2} - \frac{1}{3} a \frac{I_o}{I_L} \frac{M_{QL}}{M_p}$$

$$+ \frac{1}{3} a \left(\frac{I_o}{I_L} - 1 \right) \qquad \ldots(7.51)$$

Cases III & IV: Reverse Composite Mechanism

$$\frac{H_D}{\phi_{pL}} = \frac{1}{(1+\frac{b}{a})(1+2\frac{b}{a})(1-2\alpha)} \left\{ \sqrt{1+4b^2} \left\{ - \left[1+\frac{3}{2}\frac{b}{a}+\frac{2}{3}\frac{b^2}{a^2} - 2\alpha - 4\frac{b}{a}\alpha - \frac{5}{3}\frac{b^2}{a^2}\alpha \right] \right.\right.$$

$$- \frac{wL^2}{M_p} \left[\frac{1}{24} - \frac{1}{48}\frac{b^2}{a^2} - \frac{1}{12}\alpha - \frac{1}{16}\frac{b}{a}\alpha + \frac{1}{16}\frac{b^2}{a^2}\alpha + A\left(\frac{1}{12} - \frac{1}{24}\frac{b}{a} - \frac{1}{12}\frac{b^2}{a^2} - \frac{5}{12}\frac{b}{a}\alpha + \frac{1}{2}\frac{b^2}{a^2}\alpha \right) \right.$$

$$\left.\left. - D\left(\frac{1}{12} + \frac{5}{24}\frac{b}{a} + \frac{1}{12}\frac{b^2}{a^2} - \frac{1}{12}\frac{b}{a}\alpha - \frac{1}{6}\frac{b^2}{a^2}\alpha \right) \right] \right\}$$

$$- \frac{2}{3} a(1-\alpha) \left\{ 1 + \frac{wL^2}{M_p} \left[\frac{1}{8} + \frac{1}{4}(A-D) - \frac{1}{2}\frac{b}{a} D \right] \right\}$$

$$+ \frac{1}{(1+\frac{b}{a})(1-2\alpha)} \frac{2}{3} a \left\{ 1 + \frac{wL^2}{M_p} \left[\frac{1}{8} - \frac{1}{4}(A-D) - \frac{1}{2}\frac{b}{a} A \right] \right\}$$

$$+ \frac{2\Delta C}{a\phi pL^2} \frac{(1+2\frac{b}{a}\alpha)}{(1+2\frac{b}{a})(1-2\alpha)}$$

$$+ \frac{2}{3} a \frac{I_o}{I_L} \frac{M_{QL}}{M_p} \frac{\alpha}{(1-2\alpha)} - \frac{2}{3} a \frac{I_o}{I_R} \frac{M_{QR}}{M_p} \frac{(1-\alpha)}{(1+2\frac{b}{a})(1-2\alpha)}$$

$$+ \left(\frac{I_o}{I_L} - 1 \right) \frac{1}{(1+\frac{b}{a})(1-2\alpha)} \frac{2}{3} a \left\{ 1 + \frac{wL^2}{M_p} \left[\frac{1}{8} - \frac{1}{4}(A-D) - \frac{1}{2}\frac{b}{a} A \right] \right\}$$

$$- \left(\frac{I_o}{I_R} - 1 \right) \frac{(1-\alpha)}{(1+\frac{b}{a})(1+2\frac{b}{a})(1-2\alpha)} \frac{2}{3} a \left\{ 1 + \frac{wL^2}{M_p} \left[\frac{1}{8} + \frac{1}{4}(A-D) - \frac{1}{2}\frac{b}{a} D \right] \right\}$$

$$\ldots(7.52)$$

$$\frac{H_F}{\phi_{pL}} = \frac{1}{(1+\frac{b}{a})(1+2\frac{b}{a})(1-2\alpha)} \left\{ \sqrt{1+4b^2} \left\{ \frac{wL^2}{M_p} \left[\frac{1}{32}\frac{b}{a} + \frac{1}{96}\frac{b^2}{a^2} + A\left(\frac{1}{12} + \frac{1}{6}\frac{b}{a} + \frac{1}{6}\frac{b^2}{a^2} \right) \right. \right. \right.$$

$$-D\left(\frac{1}{12}+\frac{1}{6}\frac{b}{a}\right)\Bigg] - \left[\frac{1}{2}\frac{b}{a}+\frac{1}{6}\frac{b^2}{a^2}\right]\Bigg\}$$

$$+\frac{1}{3}a\left\{1+\frac{wL^2}{M_p}\left[\frac{1}{8}+\frac{1}{4}(A-D)-\frac{1}{2}\frac{b}{a}D\right]\right\}\Bigg]$$

$$-\frac{1}{3}a\frac{1}{(1+\frac{b}{a})(1-2\alpha)}\left\{1+\frac{wL^2}{M_p}\left[\frac{1}{8}-\frac{1}{4}(A-D)-\frac{1}{2}\frac{b}{a}A\right]\right\}$$

$$-\frac{2\Delta_C}{a\phi pL^2}\frac{(1+\frac{b}{a})}{(1+2\frac{b}{a})(1-2\alpha)}-\frac{1}{3}a\frac{I_o}{I_L}\frac{M_{QL}}{M_p}\frac{1}{(1-2\alpha)}+\frac{1}{3}a\frac{I_o}{I_R}\frac{M_{QR}}{M_p}\frac{1}{(1+2\frac{b}{a})(1-2\alpha)}$$

$$-\frac{1}{3}a\left(\frac{I_o}{I_L}-1\right)\frac{1}{(1+\frac{b}{a})(1-2\alpha)}\left\{1+\frac{wL^2}{M_p}\left[\frac{1}{8}-\frac{1}{4}(A-D)-\frac{1}{2}\frac{b}{a}A\right]\right\}$$

$$+\frac{1}{3}a\left(\frac{I_o}{I_R}-1\right)\frac{1}{(1+\frac{b}{a})(1+2\frac{b}{a})(1-2\alpha)}\left\{1+\frac{wL^2}{M_p}\left[\frac{1}{8}+\frac{1}{4}(A-D)-\frac{1}{2}\frac{b}{a}D\right]\right\} \quad \ldots(7.53)$$

Cases IIIa & IVa: Reverse Gable Mechanism

$$\frac{H_D}{\phi_{pL}}=\frac{1}{(1+\frac{b}{a})(1+2\frac{b}{a})}\Bigg\{\sqrt{1+4b^2}\left\{-\left[1+\frac{3}{2}\frac{b}{a}+\frac{2}{3}\frac{b^2}{a^2}\right]-\frac{wL^2}{M_p}\left[\frac{1}{24}-\frac{1}{48}\frac{b^2}{a^2}\right.\right.$$

$$+A\left(\frac{1}{12}-\frac{1}{24}\frac{b}{a}-\frac{1}{12}\frac{b^2}{a^2}\right)-D\left(\frac{1}{12}+\frac{5}{24}\frac{b}{a}+\frac{1}{12}\frac{b^2}{a^2}\right)$$

$$-\frac{2}{3}a\left\{1+\frac{wL^2}{M_p}\left[\frac{1}{8}+\frac{1}{4}(A-D)-\frac{1}{2}\frac{b}{a}D\right]\right\}\Bigg]$$

$$+\frac{1}{(1+\frac{b}{a})}\frac{2}{3}a\left\{1+\frac{wL^2}{M_p}\left[\frac{1}{8}-\frac{1}{4}(A-D)-\frac{1}{2}\frac{b}{a}A\right]\right\}$$

$$+\frac{2\Delta_C}{a\phi pL^2}\frac{1}{(1+2\frac{b}{a})}-\frac{2}{3}a\frac{I_o}{I_R}\frac{M_{QR}}{M_p}\frac{1}{(1+2\frac{b}{a})}$$

$$+\frac{2}{3}\,a\left(\frac{I_o}{I_L}-1\right)\frac{1}{(1+\frac{b}{a})}\left\{1+\frac{wL^2}{M_p}\left[\frac{1}{8}-\frac{1}{4}\,(A-D)-\frac{1}{2}\,\frac{b}{a}\,A\right]\right\}$$

$$-\frac{2}{3}\,a\left(\frac{I_o}{I_R}-1\right)\frac{1}{(1+\frac{b}{a})(1+2\frac{b}{a})}\left\{1+\frac{wL^2}{M_p}\left[\frac{1}{8}+\frac{1}{4}\,(A-D)-\frac{1}{2}\,\frac{b}{a}\,D\right]\right\} \quad \ldots(7.54)$$

$$\frac{H_C}{\phi_{pL}}=\frac{1}{(1+\frac{b}{a})(1+2\frac{b}{a})}\left\{\sqrt{1+4b^2}\left\{\frac{wL^2}{M_p}\left[-\frac{1}{32}\,\frac{b}{a}+\frac{1}{96}\,\frac{b^2}{a^2}+A\left(\frac{1}{12}+\frac{1}{6}\,\frac{b}{a}+\frac{1}{6}\,\frac{b^2}{a^2}\right)\right.\right.\right.$$

$$\left.\left.\left.-D\left(\frac{1}{12}+\frac{1}{6}\,\frac{b}{a}\right)\right]-\left[\frac{1}{2}\,\frac{b}{a}+\frac{1}{6}\,\frac{b^2}{a^2}\right]\right\}$$

$$+\frac{1}{3}\,a\left\{1+\frac{wL^2}{M_p}\left[\frac{1}{8}+\frac{1}{4}\,(A-D)-\frac{1}{2}\,\frac{b}{a}\,D\right]\right\}$$

$$-\frac{1}{3}\,a\,\frac{1}{(1+\frac{b}{a})}\left\{1+\frac{wL^2}{M_p}\left[\frac{1}{8}-\frac{1}{4}\,(A-D)-\frac{1}{2}\,\frac{b}{a}\,A\right]\right\}$$

$$-\frac{2\triangle C}{a\phi pL^2}\,\frac{(1+\frac{b}{a})}{(1+2\frac{b}{a})}-\frac{1}{3}\,a\,\frac{I_o}{I_L}\,\frac{M_{QL}}{M_p}+\frac{1}{3}\,a\,\frac{I_o}{I_R}\,\frac{M_{QR}}{M_p}\,\frac{1}{(1+2\frac{b}{a})}$$

$$-\frac{1}{3}\,a\left(\frac{I_o}{I_L}-1\right)\frac{1}{(1+\frac{b}{a})}\left\{1+\frac{wL^2}{M_p}\left[\frac{1}{8}-\frac{1}{4}\,(A-D)-\frac{1}{2}\,\frac{b}{a}\,A\right]\right\}$$

$$+\frac{1}{3}\,a\left(\frac{I_o}{I_R}-1\right)\frac{1}{(1+\frac{b}{a})(1+2\frac{b}{a})}\left\{1+\frac{wL^2}{M_p}\left[\frac{1}{8}+\frac{1}{4}\,(A-D)-\frac{1}{2}\,\frac{b}{a}\,D\right]\right\} \quad \ldots(7.55)$$

Comparable equations for the horizontal deflection of the lee knee and the vertical deflection of the ridge for these cases are given in Eq. (7.56) to Eq. (7.61) in Appendix E.

The graphic portions of these hinge angle equations are plotted in Figs. 7.12 through 7.15. The graphic portions of the equations for deflection of the lee knee are plotted in Figs. 7.16 and 7.17.

Summarizing the results on multi-span gabled frames, equations are available for the following types of functions:

(1) Equations determining the loading combinations for which each type of mechanism may form and for which each plastic hinge of a self-supporting subassemblage may be first to form are represented graphically in Fig. 7.6 (b=0.2, a=0.2)

(2) Hinge angles and deflections for self-supporting subassemblages are given in equations represented by Fig. 7.9 to 7.11. (b=0.2, a=0.2)

(3) Hinge angles and deflections for non-self-supporting subassemblages are given in equations represented by Fig. 7.12 to 7.17. (b=0.2, a=0.2)

For application to an actual problem, the mechanism must first be determined by the usual methods of plastic analysis. Then it must be determined which subassemblage is self-supporting. Knowing this, data from the appropriate curves or equations may be used to calculate the hinge angles and deflections of the self-supporting subassemblage and all non-

self-supporting subassemblages.

In order to determine which assemblage is self-supporting, it is assumed that each subassemblage, in turn, is self-supporting and the corresponding deflection of the total structure is calculated. The greatest deflection will occur when the true self-supporting structure is assumed.

The method of using the equations and charts developed here will be illustrated by an example in the following section.

7.5 SAMPLE SOLUTION OF A MULTI-SPAN GABLED FRAME

(a) Design.

To illustrate the use of the results of the development for multi-span gabled frames, a sample frame will be designed and the required hinge rotation calculated. The example to be discussed will be the symmetrical two-span frame shown in Fig. 7.18. The information to be used in the design part of the problem is as follows:

Left Span	Right Span
$a_1=b_1= 0.2$	$a_1=b_1= 0.2$
$b/a = 1.0$	$b/a = 1.0$
$L_1 = L$	$L_2 = L$
$A_1 = 0.1$	$A_2 = ?$
$D_1 = ?$	$D_2 = 0$
$w = 2k/ft$	$w = 2k/ft$
$L = 50$ ft	$L = 50$ ft

σ_y = 33 ksi σ_y = 33 ksi

Because of the symmetry of the frame and the fact that the wind might blow from either direction, the same M_p value will be assumed for each span.

Without further discussion, it will be stated that the results of a design following the methods of reference 10 are as follows:

Left Span	Right Span	Center Column
D_1 = 0.032	A_2 = 0.032	
$\frac{M_p}{wL^2}$ = 0.0463	$\frac{M_p}{wL^2}$ = 0.0463	
α = 0.342	α = 0.381	
16 WF 50	16 WF 50	14 WF 30*
Z = 92.7 in^3	Z = 92.7 in^3	Z = 47.1
I = 655.4 in^4	I = 655.4 in^4	I = 289.6 in^4

Because the section modulus of 92.7 in^3 actually supplied is greater than the value of 84.2 which would be required to support a design full load of 2 kips per foot, this structure would actually require 2.20 kips per foot to form a mechanism. The hinge angles to be determined will be based on the assumption that the frame will be loaded to

*Columns were checked for resistance to buckling at maximum load by methods of Ref. 6.

its true ultimate load. Therefore, the moment diagram to be considered will be that in Fig. 7.19.

(b) Calculation of Deflection and Determination of Self-Supporting Subassemblage

Next, it must be determined which is the self-supporting subassemblage. By entering Fig. 7.10 with the appropriate values of A and D, the following values of $\delta_E/\phi_{pL}{}^2$ are obtained.**

Left Span	Right Span
$\frac{\delta_E}{\phi_{pL}{}^2} = 0.141$	$\frac{\delta_E}{\phi_{pL}{}^2} = 0.129$

To these "graphic" values of the deflection must be added the correction terms of Eq. (7.27):

$$\text{Correction} = \frac{1}{3} a^2 \frac{I_o'}{I_L} \frac{M_{QL}}{M_p} - \frac{1}{3} a^2 \left(\frac{I_o}{I_L} - 1 \right)$$

$$+ \frac{1}{6} a^2 \left(\frac{I_o}{I_L} - 1 \right) \frac{wL^2}{M_p} \text{ (A-D)}$$

For the left span, there is no external moment applied to the left knee, and the column and rafter have equal moments of inertia, so the corrections equal zero. Therefore, the deflection of the lee knee (E) of the left span is:

$$\delta_E = 0.141 \, \phi_{pL}{}^2 \qquad \ldots(7.62)$$

** Though the joints of the multi-span frame are labelled A through K, the subscripts for δ & H to be used here will be those of the primary subassemblage in order to indicate which graph or equation is used.

For the right span, the corrections will apply because there is an external moment $-M_p$ at the left knee, and the left column differs from the rafter. Substituting into the correction terms of Eq. (7.27) the following results are obtained:

$$-\frac{1}{3}(0.2)^2\frac{(655.4\ in^4)}{(289.6\ in^4)}(-1.00)-\frac{1}{3}(0.2)^2\left(\frac{655.4}{289.6}-1\right)$$

$$+\frac{1}{6}(0.2)^2\left(\frac{655.4}{289.6}-1\right)\frac{(0.032)}{0.0463}$$

$$=0.0192$$

This correction added to the "graphic" value gives for a final value of the deflection of the lee knee (J) of the right span:

$$\delta_E = 0.148\ \phi_{pL}^2 \qquad \ldots(7.63)$$

Considering the structure as a whole, equation (7.63) gives the deflection of the lee knee (J) if the <u>right</u> hand span is the self-supporting subassemblage. Equation (7.62) gives the deflection of the center column top (E) if the <u>left</u> span is the self-supporting subassemblage. To determine which is the true self-supporting span, it is next necessary to determine the deflection of the lee knee (J) assuming the <u>right</u> span to be non-self-supporting and compare this with Eq. (7.63). This is done by using the deflection of $0.141\ \phi_{pL}^2$ of the center column as the Δ_C term in Eq. (7.56) and applying this equation to the right span. A "graphic" value of $\delta_E/\phi_{pL}^2 = 0.018$ is obtained from Fig. 7.16 and to it are added the following correction terms from Eq. (7.56):

$$\frac{\Delta_C}{\phi_{pL}^2}\frac{(1+2\frac{b}{a}\alpha-\alpha)}{(1-\alpha)} + \frac{2}{3}\,a\,b\,\frac{I_o}{I_L}\,\frac{M_{QL}}{M_p}\left(\frac{\alpha}{1-\alpha}\right)$$

$$+\frac{2}{3}\,a\,b\left(\frac{I_o}{I_L}-1\right)\left(\frac{\alpha}{1-\alpha}\right)-\frac{1}{3}\,a\,b\left(\frac{I_o}{I_L}-1\right)\frac{wL^2}{M_p}\,(A-D)\left(\frac{\alpha}{1-\alpha}\right)$$

$$=\frac{0.141(1.391)}{0.609}+\frac{2}{3}\,(0.2)^2\,\frac{(655.4)\quad(-1.00)\quad 0.391}{(289.6)\qquad\qquad 0.609}$$

$$+\frac{2}{3}\,(0.2)^2\left(\frac{655.4}{289.6}-1\right)\frac{0.391}{0.609}$$

$$-\frac{1}{3}\,(0.2)^2\left(\frac{655.4}{289.6}-1\right)\frac{(0.032)\quad 0.391}{(0.0463)\quad 0.609}$$

$$=0.300$$

This correction added to the "graphic" value of 0.018 gives the following result for the deflection of the lee knee (J):

$$\delta_E = 0.318\ \phi_{pL}^2 \qquad \ldots(7.64)$$

The deflection of knee (J) is $0.318\ \phi_{pL}^2$ when the left span is assumed to be self-supporting as against only $0.148\ \phi_{pL}^2$ when the right span is assumed to be self-supporting. The conclusion is that the left span is the self-supporting span.

(c) Calculation of Hinge Angle for Self-supporting Subassemblage

It is then possible to complete the calculations of hinge angles for both spans. The hinge angle at the center top is obtained from the H_E/ϕ_{pL} value of Fig. 7.9 and from

the corrections of Eq. (7.20).

$$\frac{H_E}{\phi_{pL}} \text{ (Graphic)} = 0.786$$

The corrections are:

$$-\frac{1}{3}\, a\, \frac{I_o}{I_L}\, \frac{M_{QL}}{M_p} - \frac{1}{3}\, a\, \frac{I_o}{I_R}\, \frac{M_{QR}}{M_p}$$

$$-\frac{1}{3}\, a \left(\frac{I_o}{I_L} + \frac{I_o}{I_R} - 2 \right) + \frac{1}{6}\, a \left(\frac{I_o}{I_L} - 1 \right) \frac{wL^2}{M_p} \text{ (A-D)}$$

Substitution of numerical values into the corrections gives:

$$0 - \frac{1}{3}\,(0.2)\, \frac{(655.4)}{(289.6)}\, (-0.654)$$

$$-\frac{1}{3}\,(0.2) \left(1.0 + \frac{655.4}{289.6} - 2 \right) + 0$$

$$= +0.0145$$

The final sum of the graphic and correction terms is the hinge angle at the center column top (E).

$$H_E = 0.800\, \phi_{pL} \qquad \ldots(7.65)$$

(d) Calculation of Hinge Angles for Non-self-supporting Subassemblage.

The non-self-supporting right-hand subassemblage will have hinge angles at the lee knee (J) and in the windward rafter

(G). The magnitudes of these hinge angles will be obtained from the H_E and H_F values of the basic non-self-supporting subassemblage. Each of these will require the use of a ΔC value equal to the 0.141 ϕ_{pL} value for the deflection of the center knee given by Eq. (7.62).

From Fig. 7.12 is obtained a value of 0.058 $\phi_p L$ for H_E, and substitution of the appropriate data in the correction terms of Eq. (7.48) results in a total correction of 1.371 ϕ_{pL}.

$$\frac{H_E}{\phi_{pL}} = \frac{H_E}{\phi_{pL}}\ (\text{Graphic}) + \frac{\Delta C}{a\phi_{pL}^2}\ \frac{(1+2\frac{b}{a}\alpha)}{(1-\alpha)}$$

$$+ \frac{1}{3}\ a\alpha\ \frac{I_o}{I_L}\ \frac{M_{QL}}{M_p}\ \frac{(1+2\frac{b}{a})}{(1-\alpha)} - \frac{1}{3}\ a\ \frac{I_o}{I_R}\ \frac{M_{QR}}{M_p}$$

$$+ \frac{1}{3}\ a\alpha\left(\frac{I_o}{I_L} - 1\right)\frac{(1+2\frac{b}{a})}{(1-\alpha)}\left\{1 - \frac{wL^2}{M_p}\ (A-D)\right\}$$

$$- \frac{1}{3}\ a\left(\frac{I_o}{I_L} - 1\right)$$

$$= 0.058 + 1.612 - 0.291 - 0$$

$$+ 0.0501 - 0$$

Then,

$$H_E = 1.429\ \phi_{pL} \qquad \ldots(7.66)$$

This is the hinge angle at the lee knee (J). It is noted that the predominant factor in this summation is the Δ_C term. This was also true in the case of the horizontal deflection of knee (J), (Eq. 7.64), and for every other function so far calculated in examples of non-self-supporting subassemblages.

Similarly, the hinge angle in the windward rafter (G) of the right span may be obtained by combining a "graphic" value of H_F equal to $0.390\ \phi_p L$ as taken from Fig. 7.13 with $0.390\ \phi_{pL}$ as taken from Fig. 7.13 with the sum of correction terms totalling $-1.001\ \phi_{pL}$ as calculated from Eq. (7.49). The hinge angle in the windward rafter at (G) is:

$$H_F = -0.611\ \phi_p L \qquad \ldots(7.67)$$

The negative sign for H_F is a remnant of the slope-deflection equations used in deriving the formulas and may be construed as indicating that the plastic hinge has tension on the inside of the frame.

(e) Discussion.

All hinge angles and deflections have been determined, and putting them in summary form will make it possible to compare the results.

HINGE ANGLES			
	Left Span	Right Span	
	Center Column Top (E)	Windward Rafter (G)	Lee Knee (J)
Equation	$0.800\ \phi_{pL}$	$0.611\ \phi_{pL}$	$1.429\ \phi_{pL}$
Radians	0.0747	0.0571	0.1333
Degrees	4.28^{o}	3.28^{o}	7.64^{o}

HORIZONTAL DEFLECTIONS OF COLUMNS

	Left Column (B)	Center Column (E)	Right Column (J)
Equation	$0.0636\ \phi_{pL}{}^2$	$0.141\ \phi_{pL}{}^2$	$0.318\ \phi_{pL}{}^2$
Inches	3.54	7.90	17.8

The quantities substituted for ϕ_{pL} in order to obtain dimensional values of the hinge angles and deflections are as follows:

$$\phi_{pL} = \frac{M_{pL}}{EI} = \frac{\sigma_{yZL}}{EI}$$

$$= \frac{33\ \text{ksi} \times 92.7\ \text{in}^3 \times 600\ \text{in}}{30 \times 10^3\ \text{ksi} \times 655.4\ \text{in}^4}$$

$$= 0.0934 \text{ radians}$$

Also, $\phi_{pL}{}^2 = 56.1$ inches.

The relative magnitude of the hinge angles tabulated is consistent with the order of formation of plastic hinges calculated for two frames previously tested.[3,4] That is, the greatest hinge angle and the first plastic hinge generally form at the leeward knee. The next hinge in a multi-span frame would probably form at the lee knee of the span next to the leeward span. Following would be a hinge in the windward rafter of a lee span, and finally the last hinge would form in the windward rafter of the windward span. In this example, the last hinge would form at joint C, with a hinge angle required of zero at reaching ultimate load.

By comparing Eq. (7.66) with Eq. (7.55) it is seen that the order of magnitude of hinge angles for the multi-span frame is greater than that for the single span frame. This increased rotation capacity requirement may be regarded as the "penalty" paid to gain the benefits of redistribution of moment realized as a result of continuity.

From a practical standpoint, deflections at maximum load of 8 and 18 inches might seem excessive at first sight. However, it must be remembered that these are ultimate load deflections and not working load deflections. The calculation of deflections at working load may prove to be quite tedious. Fortunately, the theoretical load-deflection curve is available for a two-span gabled frame which has been tested.[3] Though this frame had fixed bases, the curve will serve to illustrate qualitatively the point in question. Fig. 7.20 shows a non-dimensional load-deflection curve of the two span frame tested. The deflection at maximum load, or at formation of the last plastic hinge is shown as about $0.19PL^3/EI$. A possible range of plastic design working loads ranging from 50 to 71% of

the maximum load is also shown. (This is an extreme range allowing for increase in loads due to wind load in one direction, and a very conservative factor for static loads in the other direction.) The deflections for the working range are from 0.02 to $0.03PL^3/EI$, or one-ninth to one-sixth of the maximum load deflections. It is expected that even with pinned bases, the deflections at working loads would follow a pattern similar to this.

7.6 SUMMARY

This chapter extends the work on the rotation capacity requirements for multi-span portal frames to cover the case of gabled roofs. Introduced here is an additional type of mechanism possible only when a subassemblage having a gabled roof is loaded heavily from both sides to such an extent that negative work is done by the vertical loads. This type of mechanism is designated a "reverse" mechanism.

The results of the chapter are summarized as follows:

(1) Domains for four possible mechanisms were determined by equating plastic hinge moments, and domains for four possible locations of the first plastic hinge in a subassemblage were determined by equating expressions for elastic moments. Combining these sets of domains resulted in eight cases of possible mechanisms and locations of first plastic hinge. (Fig. 7.6).

(2) Equations for the hinge angles and deflections for all eight cases were derived for self-supporting subassemblages, and the portions of these equations which could be shown in graphical form were plotted

for a family of subassemblages. (Eq. 7.20 through 7.47) (Fig. 7.9 to 7.11).

(3) For a non-self-supporting subassemblage, a determination as to which is the first and the last plastic hinge is not pertinent information, so only consideration of the four possible mechanisms is necessary. Equations for the hinge angles and deflections for all four cases were derived, and "graphic" portions of these equations were also plotted for a family of subassemblages. (Eq. 7.48 to 7.61) (Fig. 7.12 to 7.17).

(4) All equations for hinge angles and deflections contained terms which corrected for differences in moment of inertia of columns and rafters, and for the effects of adjacent spans on moments at the knees. In using graphs for the solution of hinge angle problems, these corrections must be calculated and added to the graphic values when applicable.

(5) Equations for functions of a non-self-supporting subassemblage also included a term Δ_C, the deflection of the windward knee. This was the controlling boundary condition for a non-self-supporting subassemblage, and is actually determined in a given structure by the deflection of the self-supporting span.

(6) The method of solving multi-span gabled frames proved to be the same as that established for multi-span flat-roofed frames. The steps are as follows: First, assume each span in turn to be the self-supporting span and calculate the corresponding horizontal deflection; the correct assumption will be indicated by the largest deflection so computed. Second, having determined the self-supporting span, calculate the hinge

angles for that span using the "self-supporting" graphs and correction equations, and calculate the hinge angles for all other spans using the "non-self-supporting" graphs and appropriate correction equations.

(7) An example of a symmetrical two span gabled frame was solved to indicate the use of the charts and the equations. The example showed that the order of magnitude of hinge angles calculated was larger than that calculated for single span frames. This is not unexpected in view of the fact that more extensive redistribution of moment is likely in these more highly redundant structures.

(8) A complete theoretical load-deflection curve for a two-span gabled frame calculated in connection with a test program was compared with the deflections of the frame used in the example. This showed that though calculated deflections at maximum load may be large, the deflections at working loads will probably remain ~~the~~ in the elastic range, and thus will probably be small fractions of the maximum load deflections. This leads to the conclusion that there should be no reason why deflections of structures designed by plastic methods could not be either calculated or neglected with the same reservations as are now made in elastic analysis.

8. SUMMARY AND CONCLUSIONS

This dissertation discusses the problem of required rotation as it affects the application of plastic analysis to structural design. Rotation capacity has been defined as the ability of a plastic hinge to rotate at or near the maximum moment. In order that redistribution of moment may occur and allow a structure to reach its computed full plastic load, the first plastic hinges forming in an indeterminate structure are required to rotate through some hinge angle. Methods are presented for calculating the amount of hinge rotation required at plastic hinges in a given structure. These required hinge angles may then be compared with the actual rotation capacity of structural elements as determined from tests or from theoretical analyses.

The study made here is directed toward the determination of the rotation capacity requirements for multi-span gabled portal frames with pinned bases. In solving the problem, advantage is taken of the fact that plastic analysis and design of multi-span frames may be accomplished by separation of the structure into single-span elements called subassemblages. Hinge angles and deflections at ultimate load are determined in general terms for subassemblages, and methods for determining the interaction of the several subassemblages which make up a structure are presented. As a special case, the behavior of a single subassemblage represents the behavior of a single span gabled portal frame.

Certain of the principles and results of this required rotation study apply to all the problems in required rotation covered. These are as follows:

(1) For any subassemblage or multi-span beam two or more possible mechanisms may form depending on the loading and geometry of the structure. By plastic analysis, equations relating the applied load to the required plastic hinge moment for each mechanism may be derived, and from them, expressions for M_p/wL^2 may be obtained in general terms relating the geometry and loading. Combining in pairs the equations for M_p/wL^2 of different mechanisms results in expressions defining the combinations of loading and geometry for which both of a pair of mechanisms will form simultaneously. Graphs of these expressions may be plotted to separate the domains of structural geometry and loading in which each possible mechanism will form. (For example, see Fig. 4.2 or 7.2).

(2) For any structure or subassemblage, one of two or more plastic hinges may be the first to form depending on the loading and geometry of the structure. By elastic analysis methods, expressions for the elastic moment at each hinge location may be derived in general terms. The largest elastic moment will occur at the location of the first plastic hinge. Equating the expressions for elastic moments in pairs results in equations for the loading and geometry for which each of a pair of first plastic hinges will form simultaneously. Graphs of these expressions may be plotted to separate the domains of structural geometry and loading in which each possible plastic hinge will be first to form. (For example, see Fig. 4.3 or 7.4).

(3) Combining the graphs for possible mechanisms and first plastic hinges results in an additional graph for the domains defining the rotation capacity problem. In each of these domains, the structure or subassemblage will form a definite mechanism with the first plastic hinge at a given point. Location of the structure or subassemblage in its proper domain gives the key to the use of the proper boundary conditions in deriving rotation equations, or indicates the proper hinge angle equations to use if they are already derived. (See Fig. 4.4 or 7.6)

(4) Hinge angles and deflections at maximum load are calculated for any structure or subassemblage by using slope deflection equations and applying boundary conditions which recognize the lack of continuity at all plastic hinges except the last to form. By using the slope-deflection equations, the assumption is implicit that all members are perfectly elastic except at plastic hinges which are implied to be of zero length. These assumptions neglect a part of the deflections and rotations resulting from the true yielding process of steel, but the error is usually small.

(5) For applications to numerical problems, deflections and hinge angles may be determined directly from the equations derived, or graphs covering selected ranges of variables may be prepared and used.

Certain additional principles and results of this study apply only to the more complicated problems of multi-span portal frames. These are summarized in the following paragraphs.

(6) At maximum load, but just before the entire structure begins to deflect as a mechanism, continuity exists at the point where the last plastic hinge is about to form. All other plastic hinges will display a discontinuity of slope across the hinges and will have reached the stage where they could rotate without addition of moment. Since the last plastic hinge forms at only one point for the general multi-span rigid frame, only one subassemblage may contain this continuity. The remaining subassemblages will contain two plastic hinges and would not be able to stand by themselves if set apart as single subassemblages. The subassemblages with two plastic hinges are called non-self-supporting plastic hinges. The one subassemblage which contains the continuity at the location of the eventual last plastic hinge is called a self-supporting subassemblage. (Special cases exist which violate the letter of these statements, but do not alter the method of solution of the problem. First of these cases is the symmetrical case in which two equivalent plastic hinges form simultaneously, either of which would be sufficient to fulfill the conditions causing a mechanism. A second special case is that case in which by mere chance two or more of the last hinges will form simultaneously. This second case results in a required hinge angle of zero at all plastic hinges forming simultaneously with the last hinge.)

(7) Equations for hinge angles and deflections of self-supporting subassemblages are derived by the same methods as used for single span frames. However, the resulting equations contain terms which correct for differences in moment of inertia of the rolled sections in the

columns and rafter, and for the effects of adjoining spans on the moments at the knees.

(8) In deriving equations for hinge angles and deflections of non-self-supporting subassemblages, it is found that with two plastic hinges having freedom to rotate without additional moment, there are insufficient independent boundary conditions to solve the problem. The required additional boundary condition is obtained by setting the deflection of the windward knee of a non-self-supporting subassemblage equal to the deflection determined by the adjoining self-supporting subassemblage.

(9) It is necessary to determine which is the last plastic hinge in order to calculate the correct hinge angles for a multi-span frame. If this were done by making a step-by-step analysis of the frame up to maximum load, the process would be too complicated. Also, only the deflections and rotations at ultimate load are actually required. A trial-and-error method of determining the last plastic hinge is therefore used. Each span in turn is assumed to be the self-supporting span, and the corresponding horizontal deflection is calculated. The correct assumption is indicated by the largest deflection of the total structure so computed. Knowing which are self-supporting and non-self-supporting subassemblages makes it possible to use the proper graphs or equations for each span in a given problem.

Specific examples using typical structures were designed and the hinge angles and deflections were calculated to illustrate the use of the methods presented. These examples were:

(a) Three-span continuous beam (Chap. 4, page 25).

(b) Flat-roofed single span frame (Chap. 5, page 50).

(c) Single-span gabled frame (Chap. 5, page 53).

(d) Flat-roofed multi-span frame (Chap. 6, page 77).

(e) Multi-span gabled frame (Chap. 7, page 104).

Detailed summaries of the results for each type of structure are presented at the end of the appropriate chapters.

As a result of the derivations and numerical calculations made in this dissertation, the following conclusions were reached:

(10) The hinge rotations required in typical structures studies were of the same order of magnitude as rotations which have been measured in tests of rigid frames and corner connections.

(11) The hinge angles required for multi-span frames are of larger magnitude than those required for single-span frames. This must be expected in view of the more extensive redistribution of moment likely in these more highly redundant structures.

(12) The question of whether or not to calculate deflections and rotations arises in structural design. In present elastic methods of design, engineers find that with a certain amount of experience and use of judgement, the calculation of deflections may be omitted without danger of having excessive deflections of the erected structure for many average cases. This saves the spending of many unnecessary hours making complicated calculations of deflections.

Admittedly, the calculation of deflections at ultimate load is just as complicated as the calculation of deflections in the elastic range when both calculations start with the moment diagram. (However the moment diagram is easier to obtain in the plastic range.) It is, therefore, desirable to omit the calculation of deflections in structures designed by plastic analysis. All theoretical and experimental evidence disclosed to date suggests that for plastic design of many average structures, the calculation of deflections may safely be omitted without any more danger of excessive deflections than is experienced for comparable structures designed elastically. The types of structures for which deflection calculations may be omitted will be approximately the same for both elastic and plastic analysis.

If knowledge of the deflection at working load is necessary for a given case, it will be necessary to make an elastic analysis once the members have been selected by plastic design.

N O M E N C L A T U R E

Symbols:

A	non-dimensional parameter relating the horizontal force acting on a structure (or the "overturning" moment of one part of a structure on the adjacent part) to the vertical loading. It is assumed that "A" results in positive work being done as the structure fails.
D	non-dimensional parameter relating the horizontal resisting force or "over turning" moment acting on a structure to its vertical loading. It is assumed that "D" results in negative work being done as the structure fails.
E	Young's modulus of elasticity
F	load factor of safety
F	dimensionless parameter in elastic moment equation
G	dimensionless parameter in elastic moment equation
H	hinge angle
I	moment of inertia of cross section
I_o	moment of inertia of frame rafter
I_L	moment of inertia of left column
I_R	moment of inertia of right column
J	dimensionless parameter in elastic moment equations
L	span length
M	moment
M_{FN}	moment at far end of member
M_{NF}	moment at near end of member
M_p	plastic hinge moment
M_{Q_L}	external moment at left knee
M_{Q_R}	external moment at right knee
N	dimensionless parameter in elastic moment equations
P	concentrated horizontal load

R	rotation of a chord between ends of a member
Z	fully plastic section modulus
a	ratio of column height to frame span
b	pitch, ratio of frame rise to span
ℓ	length of a member or portion of a member (variable)
p	horizontal wind pressure per unit area
q	uniformly distributed vertical roof load per unit area
s	bent spacing
w	uniformly distributed load per unit length of span
x	distance along member
y	deflection of neutral axis of a member from the original straight line
α	ratio of side span unit load to main span unit load in beam calculations
α	non-dimensional parameter defining the distance to the location of the plastic hinge in the rafter of a structure
β	ratio of side span length to main span length in beam calculations
δ	deflection
ϵ	strain
ζ	ratio of distance to plastic hinge in side span of a beam to side span length
θ	slope or rotation of a member from undeformed shape
ρ	radius of curvature of member
σ	stress
σ_y	yield stress of steel
ϕ	curvature of member
ϕ_p	curvature parameter M_p / EI

Δ virtual displacement

Subscripts in Slope-Deflection Equations:

Single letter -- joint
Double letter -- member
First letter -- near end
Second letter -- far end

Important Functions for Frames or Subassemblages:

δ_C horizontal deflection of windward knee

δ_D vertical deflection of ridge or center of flat roof

δ_E horizontal deflection of lee knee

Δ_C horizontal deflection of windward knee of non-self-supporting subassemblage.

H_C hinge angle in windward knee

H_D hinge angle at ridge

H_E hinge angle in lee knee

H_F hinge angle in windward rafter

Definitions:

Plastic Hinge A yielded section of a beam which acts as if it were hinged, except that it has a constant restraining moment.

Hinge Angle The required rotation of a given plastic hinge in a structure that is necessary to assure that the structure reaches the ultimate load.

Rotation Capacity The ability of a structural member to rotate at near-maximum moment.

Mechanism A system of members (and/or segments of members) that can deform at constant load. It is used in the special sense that all hinges are plastic hinges (except pin ends).

Plastification of cross section	The development of full plastic yield of the cross section.
Redistribution of Moment	A process in which plastic hinges form successively in a redundant structure until the ultimate load of the structure is reached. In the process, a new distribution of moments is achieved in which portions of the structure which are less highly-stressed in the elastic state subsequently reach the plastic hinge value. Redistribution is accomplished by rotation through the hinge angle of earlier-formed plastic hinges.
Subassemblage	A single-span element into which a multi-span frame may be separated for the purpose of simplification of design.
Non-self supporting subassemblage	A subassemblage in which all plastic hinges are formed before the total structure has reached maximum load. It would not be able to stand without the support of an adjacent subassemblage.
Self-supporting subassemblage	The one subassemblage in a multi-span structure which has continuity at its last plastic hinge until the maximum load of the total structure is reached. If it were set apart as a free body with its complete system of forces it would be able to stand.

10. REFERENCES

1. Beedle, L. S.
Thurlimann, B.
Ketter, R. L.
PLASTIC DESIGN IN STRUCTURAL STEEL 1955 Summer Course Lecture Notes, Lehigh University--AISC 1955.

2. Driscoll, G. C.
ROTATION CAPACITY OF A THREE-SPAN CONTINUOUS BEAM, Fritz Laboratory Report 268.2, Lehigh University, 1956.

3. Driscoll, G. C.
TEST OF TWO-SPAN GABLED PORTAL FRAME, Proceedings, 1956 AISC National Engineering Conference.

4. Driscoll, G. C.
Beedle, L. S.
THE PLASTIC BEHAVIOR OF STRUCTURAL MEMBERS AND FRAMES, Progress Report No. 21, Welded Continuous Frames and Their Components, The Welding Journal, Research Suppl., June 1957, page 275-s.

5. Fisher, J. W.
Driscoll, G. C.
Schutz, F. W.
BEHAVIOR OF WELDED CORNER CONNECTIONS, Progress Report 23, Welded Continuous Frames and Their Components, Fritz Laboratory Report 205C.21 (To be published in The Welding Journal).

6. Galambos, T. V.
Ketter, R. L.
FURTHER STUDIES OF COLUMNS UNDER COMBINED BENDING AND THRUST, Interim Report No. 36, Welded Continuous Frames and Their Components, Fritz Laboratory Report No. 205A.19, 1957.

7. Griffiths, J. D.
SINGLE SPAN RIGID FRAMES IN STEEL, AISC, 1948.

8. Haaijer, G.
PLATE BUCKLING IN THE STRAIN HARDENING RANGE, ASCE Proceedings Paper 1212, April 1957.

9. Haaijer, G.
Thurlimann, B.
ON INELASTIC LOCAL BUCKLING IN STEEL, Presented at ASCE 1956 Annual Convention, Pittsburgh, Pa., October 1956.

10. Ketter, R. L.
PLASTIC DESIGN OF MULTI-SPAN RIGID FRAMES, Ph.D Dissertation, Lehigh University, 1956.

11. Knudsen, K.E.
Schutz, F.W.
Beedle, L.S.
PROPOSAL FOR THE CONTINUATION OF PORTAL FRAME TESTS, Fritz Laboratory Report 205D.4 (Unpublished).

12. Knudsen, K.E.
Yang, C.H.
Johnston, B.G.
Beedle, L.S.
PLASTIC STRENGTH AND DEFLECTION OF CONTINUOUS BEAMS, The Welding Journal, May 1953, page 240-s.

13. Korn, M.P.
A SHORT COURSE IN WELDED RIGID FRAME DESIGN, The Welding Journal, 36(3), p 236-239, March 1957.

14. Shedd, T.C.
STRUCTURAL DESIGN IN STEEL, John Wiley & Sons, Inc., 1934.

15. Symonds, P.S.
A REVIEW OF METHODS FOR THE PLASTIC ANALYSIS OF RIGID FRAMES OF DUCTILE METAL, Tech. Rep. A 11-86/86, Brown University to Office of Naval Research, May 1950, pp 44-49.

16. Symonds, P.S.
Neal, B.G.
RECENT PROGRESS IN THE PLASTIC METHODS OF STRUCTURAL ANALYSIS, Journal of the Franklin Institute, 252 (5 & 6), 1951.

17. Sutherland, H.
Bowman, H.L.
STRUCTURAL THEORY, Fourth Edition, John Wiley and Sons, New York, 1950, p. 242.

18. Toprac, A.A.
Beedle, L.S.
Johnston, B.G.
CONNECTIONS FOR WELDED CONTINUOUS PORTAL FRAMES, Part I--"Test Results and Requirements for Connections", The Welding Journal 30(7) Research Supplement 357-s, 1951. Part II--"Theoretical Analysis of Straight Knees" Ivid., 30(8), Research Suppl. 397-s, 1951. Part III--"Discussion of Test Results and Conclusions", Ibid., 31(11), Research Suppl. 543-s, 1952.

19. White, M.W.
THE LATERAL-TORSIONAL BUCKLING OF YIELDED STRUCTURAL STEEL MEMBERS, Ph.D Dissertation, Lehigh University, 1956.

20. Yang, C.H. RESIDUAL STRESS AND THE YIELD STRENGTH OF STEEL BEAMS, Progress Report No. 5, Welded Continuous Frames and Their Components, The Welding Journal 31(4), Research Suppl. 205-s to 229-s (1952).

21. STEEL CONSTRUCTION, American Institute of Steel Construction Handbook

22. NATIONAL BUILDING CODE, National Board of Fire Underwriters, 1955, p 111, 272.

A P P E N D I X A

EQUATIONS FOR THREE-SPAN BEAM

PLASTIC HINGE MOMENTS

Main Span Mechanism

$$M_p = \frac{wL^2}{16} \qquad \ldots(4.1)$$

Side Span Mechanism

$$M_p = \frac{\alpha\beta^2 wL^2}{11.66} \qquad \ldots(4.2)$$

LIMITS

Between Main Span and Side Span Mechanisms

$$\alpha\beta^2 = 0.728 \qquad \ldots(4.4)$$

Between First Hinge at B and E

$$\frac{\beta + 1.5}{\alpha\beta^3 + 1} = 2 \qquad \ldots(4.8)$$

Between First Hinge at B and F

$$\frac{(3\alpha\beta^3 + 6\alpha\beta^2 - 1)^2}{\alpha\beta^2(2\beta + 3)(\alpha\beta^3+1)} = 8 \qquad \ldots(4.9)$$

HINGE ANGLES

Main Span Mechanism -- First Hinge at Support B

$$\frac{H_B}{\phi_{pL}} = \frac{2}{3}\alpha\beta^3 - \frac{1}{3}\beta + \frac{1}{6} \qquad \ldots(4.24)$$

Main Span Mechanism -- First Hinge in Span at E

$$\frac{H_E}{\phi_{pL}} = \frac{2}{3}\beta - \frac{1}{3} - \frac{4}{3}\alpha\beta^3 \qquad \ldots(4.18)$$

Side Span Mechanism -- First Hinge at Support B

$$\frac{H_B}{\phi_{pL}} = 0.1524\beta - \frac{1}{2} + \frac{0.486}{\alpha\beta^2} \qquad \ldots(4.29)$$

Side Span Mechanism -- First Hinge in Span at F

$$\frac{H_F}{\phi_{pL}} = 0.368\beta - 1.207 + \frac{1.173}{\alpha\beta^2} \qquad \ldots(4.31)$$

A P P E N D I X B

EQUATIONS FOR SINGLE SPAN FRAMES WITH FLAT ROOFS

PLASTIC HINGE MOMENTS

Composite Mechanism

$$\frac{M_p}{wL^2} = \frac{1}{16}(A+1)^2$$

$$\alpha = \frac{1 - A}{2} \qquad \ldots(5.2)$$

Panel Mechanism

$$\frac{M_p}{wL^2} = \frac{A}{4} \qquad \ldots(5.1)$$

LIMITS

Between Panel and Composite Mechanism

$$A = 1 \qquad \ldots(5.3)$$

Between First Plastic Hinge at Lee Knee E and in Beam at F

$$A = 1 - 2\sqrt{\frac{1}{2a + 3}} \qquad \ldots(5.10)$$

HINGE ANGLES

Case I. Composite Mechanism -- First Hinge at Lee Knee E

$$\frac{H_E}{\phi_{pL}} = \frac{wL^2}{M_p}\left[\frac{1}{12} + A\left(\frac{1}{4} + \frac{1}{6}a\right)\right] - 1 - \frac{2}{3}a \qquad \ldots(5.20)$$

Case Ia. Panel Mechanism -- First Hinge at Lee Knee E

$$\frac{H_E}{\phi_{pL}} = \frac{1}{3A} \qquad \ldots(5.29)$$

Case II. Composite Mechanism -- First Hinge in Beam at F

$$\frac{H_F}{\phi_{pL}} = \frac{wL^2}{M_p}\left[\frac{1}{12} + A\left(\frac{1}{4} + \frac{1}{6}a\right)\right] - 1 - \frac{2}{3}a \qquad \ldots(5.24)$$

DEFLECTIONS -- LEE KNEE

Case I.

$$\frac{\delta_E}{\phi_{pL^2}} = a\frac{wL^2}{M_p}\left[\frac{1}{24} + A\left(\frac{1}{6} + \frac{1}{6}a\right)\right] - a\left[\frac{1}{2} + \frac{1}{3}a\right] \qquad \ldots(5.38)$$

Case Ia.

$$\frac{\delta_E}{\phi_{pL^2}} = \frac{1}{6}a\left(1 + \frac{1}{A}\right) + \frac{1}{3}a^2 \qquad \ldots(5.39)$$

Case II.

$$\frac{\delta_E}{\phi_{pL^2}} = a\left[\frac{1}{2} + \frac{1}{3}a - \alpha - \frac{2}{3}a\alpha\right] - a\frac{wL^2}{M_p}\left[\frac{1}{24} - \frac{1}{12}\alpha + A\left(\frac{1}{12} - \frac{1}{4}\alpha - \frac{1}{6}a\alpha\right)\right] \qquad \ldots(5.40)$$

DEFLECTIONS -- WINDWARD KNEE

All cases

$$\delta_C = \delta_E \qquad \ldots(5.41)$$

DEFLECTIONS -- CENTER OF BEAM

Case I.

$$\frac{\delta_D}{\phi_{pL^2}} = \frac{wL^2}{M_p}\left(\frac{5}{384} + \frac{1}{32}A\right) - \frac{1}{8} \qquad \ldots(5.42)$$

Case Ia.

$$\frac{\delta_D}{\phi_{pL^2}} = \frac{5}{96A} \qquad \ldots(5.43)$$

Case II.

$$\frac{\delta_D}{\phi_{pL}{}^2} = \frac{wL^2}{M_p}\left[\frac{5}{384} - \frac{1}{24}\alpha + A\left(\frac{1}{32} - \frac{1}{8}\alpha - \frac{1}{12}a\dot{\alpha}\right)\right] - \left[\frac{1}{8} - \frac{1}{2}\alpha - \frac{1}{3}a\dot{\alpha}\right] \quad \ldots(5.44)$$

APPENDIX C

EQUATIONS FOR SINGLE-SPAN GABLED FRAMES

PLASTIC HINGE MOMENTS

Composite Mechanism

$$\frac{M_p}{wL^2} = \frac{1}{4}\left[\frac{(1-\alpha)(A+\alpha)}{1+\frac{b}{a}\alpha}\right]$$

$$\alpha = \frac{1}{\frac{b}{a}}\left[\sqrt{1-\frac{b}{a}\left[A\left(1+\frac{b}{a}\right)-1\right]}-1\right] \quad \text{...for } \frac{b}{a}>0$$

...(5.2)

Panel Mechanism

$$\frac{M_p}{wL^2} = \frac{A}{4}$$

...(5.1)

LIMITS

Between Composite Mechanism and Panel Mechanism

$$A = \frac{1}{1+\frac{b}{a}}$$

...(5.3)

Between First Hinge at Lee Knee E and Windward Knee C

$$A = \frac{8 + 5\frac{b}{a}}{12\frac{b}{a} + 8\frac{b^2}{a^2}}$$

...(5.8)

Between First Hinge at Lee Knee E and in Windward Rafter at F

$$0 = A^2\left(1+\frac{b}{a}F+\frac{1}{4}\frac{b^2}{a^2}F^2\right) + A\left(2-\frac{b}{a}F-2F+\frac{b}{a}G+\frac{1}{2}\frac{b^2}{a^2}FG\right)$$

$$+\left(1-\frac{b}{a}G-2G+\frac{1}{4}\frac{b^2}{a^2}G^2\right)$$

...(5.9)

where:

$$N = \left[\frac{8a}{\sqrt{1+4b^2}} + 12 + 12\frac{b}{a} + 4\frac{b^2}{a^2} \right]$$

$$F = \left[\frac{\frac{16a}{\sqrt{1+4\ b^2}} + 24 + 12\ \frac{b}{a}}{N} \right]$$

$$G = \left[\frac{8 + 5\frac{b}{a}}{N} \right].$$

...(5.7)

HINGE ANGLES

Case I. Composite Mechanism --First Hinge at Lee Knee E

$$\frac{H_E}{\phi_{pL}} = \sqrt{1+4b^2} \left\{ \frac{wL^2}{M_p} \left[\frac{1}{12} + \frac{5}{96}\frac{b}{a} + A\left(\frac{1}{4} + \frac{1}{8}\frac{b}{a}\right) \right] - \left[1 + \frac{b}{a} + \frac{1}{3}\frac{b^2}{a^2} \right] \right\}$$

$$- \frac{2}{3}a + \frac{1}{6}a\frac{wL^2}{M_p}A$$

...(5.19)

Case Ia. Panel Mechanism -- First Hinge at Lee Knee E

$$\frac{H_E}{\phi_{pL}} = \sqrt{1+4b^2} \left\{ \frac{1}{A}\left(\frac{1}{3} + \frac{5}{24}\frac{b}{a}\right) - \left(\frac{1}{2}\frac{b}{a} + \frac{1}{3}\frac{b^2}{a^2}\right) \right\}$$

...(5.28)

Case II. Composite Mechanism -- First Hinge in Windward Rafter at F

$$\frac{H_F}{\phi_{pL}} = \frac{1}{(1+2\frac{b}{a}\alpha)} \left[\sqrt{1+4b^2} \left\{ \frac{wL^2}{M_p} \left[\frac{1}{12} + \frac{5}{96}\frac{b}{a} + A\left(\frac{1}{4} + \frac{1}{8}\frac{b}{a}\right) \right] - \left[1+\frac{b}{a} + \frac{1}{3}\frac{b^2}{a^2} \right] \right\} \right.$$

$$\left. - \frac{2}{3}a + \frac{1}{6}a\frac{wL^2}{M_p}A \right]$$

...(5.23)

Case IIa. Panel Mechanism -- First Hinge at Windward Knee C

$$\frac{H_C}{\phi_{pL}} = \sqrt{1+4b^2} \left\{ \frac{1}{A}\left(\frac{1}{3} + \frac{5}{24}\frac{b}{a}\right) - \left(\frac{1}{2}\frac{b}{a} + \frac{1}{3}\frac{b^2}{a^2}\right) \right\}$$

...(5.30)

DEFLECTIONS -- LEE KNEE

Case I.

$$\frac{\delta_E}{\phi_{pL^2}} = a\sqrt{1+4b^2}\left\{\frac{wL^2}{M_p}\left[\frac{1}{24}+\frac{5}{96}\frac{b}{a}+A\left(\frac{1}{6}+\frac{1}{8}\frac{b}{a}\right)\right]-\left[\frac{1}{2}+\frac{3}{4}\frac{b}{a}+\frac{1}{3}\frac{b^2}{a^2}\right]\right\}$$

$$-\frac{1}{3}a^2+\frac{1}{6}a^2\frac{wL^2}{M_p} \qquad \ldots(5.35)$$

Case Ia.

$$\frac{\delta_E}{\phi_{pL^2}} = a\sqrt{1+4b^2}\left\{\frac{1}{A}\left(\frac{1}{6}+\frac{5}{24}\frac{b}{a}\right)+\left(\frac{1}{6}-\frac{1}{4}\frac{b}{a}-\frac{1}{3}\frac{b^2}{a^2}\right)\right\}+\frac{1}{3}a^2 \qquad \ldots(5.45)$$

Case II.

$$\frac{\delta_E}{\phi_{pL^2}} = \frac{1}{(1+2\frac{b}{a}\alpha)}\left[a\sqrt{1+4b^2}\left\{\left[\frac{1}{2}+\frac{1}{4}\frac{b}{a}-\alpha+\frac{1}{6}\frac{b^2}{a^2}\alpha\right]-\frac{wL^2}{M_p}\left[\frac{1}{24}-\frac{1}{12}\alpha+\frac{1}{32}\frac{b}{a}\alpha\right.\right.\right.$$

$$\left.\left.\left.+A\left(\frac{1}{12}+\frac{1}{24}\frac{b}{a}\alpha-\frac{1}{4}\alpha\right)\right]\right\}-\frac{2}{3}a^2\alpha+\frac{1}{6}a^2\alpha\frac{wL^2}{M_p}A\right]+\frac{1}{3}a^2 \qquad \ldots(5.36)$$

Case IIa.

$$\frac{\delta_E}{\phi_{pL^2}} = a\sqrt{1+4b^2}\left\{\frac{1}{6}+\frac{1}{4}\frac{b}{a}-\frac{1}{6A}\right\}+\frac{1}{3}a^2 \qquad \ldots(5.46)$$

DEFLECTIONS -- WINDWARD KNEE

Case I.

$$\frac{\delta_C}{\phi_{pL^2}} = a\sqrt{1+4b^2}\left\{\frac{wL^2}{M_p}\left[\frac{1}{24}+\frac{1}{6}A\right]-\left[\frac{1}{2}+\frac{1}{4}\frac{b}{a}\right]\right\}-\frac{1}{3}a^2+\frac{1}{6}a^2\frac{wL^2}{M_p}A$$

$$\ldots(5.47)$$

Case Ia.

$$\frac{\delta_C}{\emptyset_{pL^2}} = a\sqrt{1+4b^2}\left\{\frac{1}{6A}+\frac{1}{6}-\frac{1}{4}\frac{b}{a}\right\}+\frac{1}{3}a^2 \qquad \ldots(5.48)$$

Case II.

$$\frac{\delta_C}{\emptyset_{pL^2}} = \frac{1}{(1+2\frac{b}{a}\alpha)}\left[a\sqrt{1+4b^2}\left\{\left[\frac{1}{2}+\frac{3}{4}\frac{b}{a}+\frac{1}{3}\frac{b^2}{a^2}-\alpha-2\frac{b}{a}\alpha-\frac{5}{6}\frac{b^2}{a^2}\alpha\right]\right.\right.$$
$$\left.\left.-\frac{wL^2}{M_p}\left[\frac{1}{24}+\frac{5}{96}\frac{b}{a}-\frac{1}{12}\alpha-\frac{13}{96}\frac{b}{a}\alpha+A\left(\frac{1}{12}+\frac{1}{8}\frac{b}{a}-\frac{1}{4}\alpha-\frac{11}{24}\frac{b}{a}\alpha\right)\right]\right\}\right.$$
$$\left.+(1-\alpha)\left\{\frac{2}{3}a^2-\frac{1}{6}a^2\frac{wL^2}{M_p}A\right\}\right]-\frac{1}{3}a^2+\frac{1}{6}a^2\frac{wL^2}{M_p}A \qquad \ldots(5.49)$$

Case IIa.

$$\frac{\delta_C}{\emptyset_{pL^2}} = a\sqrt{1+4b^2}\left\{\left[\frac{1}{6}+\frac{1}{4}\frac{b}{a}+\frac{1}{3}\frac{b^2}{a^2}\right]-\frac{1}{A}\left[\frac{1}{6}+\frac{5}{24}\frac{b}{a}\right]\right\}+\frac{1}{3}a^2 \qquad \ldots(5.50)$$

DEFLECTIONS -- RIDGE

Case I.

$$\frac{\delta_D}{\emptyset_{pL^2}} = \sqrt{1+4b^2}\left\{\frac{wL^2}{M_p}\left[\frac{5}{384}+\frac{1}{32}A\right]-\left[\frac{1}{8}+\frac{1}{12}\frac{b}{a}\right]\right\} \qquad \ldots(5.37)$$

Case Ia.

$$\frac{\delta_D}{\emptyset_{pL^2}} = \sqrt{1+4b^2}\left\{\frac{5}{96A}-\frac{1}{12}\frac{b}{a}\right\} \qquad \ldots(5.51)$$

Case II.

$$\frac{\delta_D}{\emptyset_{pL^2}} = \frac{1}{(1+2\frac{b}{a}\alpha)}\left[\sqrt{1+4b^2}\left\{\frac{wL^2}{M_p}\left[\frac{5}{384}-\frac{1}{24}\alpha+A\left(\frac{1}{32}-\frac{1}{8}\alpha\right)\right]\right.\right.$$
$$\left.\left.-\left[\frac{1}{8}+\frac{1}{12}\frac{b}{a}-\frac{1}{2}\alpha-\frac{1}{4}\frac{b}{a}\alpha\right]\right\}+\frac{1}{3}a\alpha-\frac{1}{12}a\alpha\frac{wL^2}{M_p}A\right] \qquad \ldots(5.52)$$

Case IIa.

$$\frac{\delta_D}{\phi_{pL^2}} = \sqrt{1+4b^2}\left\{\frac{5}{96A} - \frac{1}{12}\frac{b}{a}\right\} \qquad \ldots(5.53)$$

A P P E N D I X D

EQUATIONS FOR MULTI-SPAN FRAMES WITH FLAT ROOFS

PLASTIC HINGE MOMENTS

Composite Mechanism

$$\frac{M_p}{wL^2} = \frac{1}{16}(A-D+1)^2$$

$$\alpha = \frac{1-A+D}{2} \qquad \ldots(6.1)$$

Panel Mechanism

$$\frac{M_p}{wL^2} = \frac{1}{4}(A-D) \qquad \ldots(6.2)$$

LIMITS

Between Composite and Panel Mechanisms

$$A-D=1 \qquad \ldots(6.3)$$

Between First Plastic Hinge at Lee Knee E and in Beam at F.

$$A-D=1-2\sqrt{\frac{1}{2a+3}} \qquad \ldots(6.5)$$

HINGE ANGLES -- SELF-SUPPORTING SUBASSEMBLAGE

Case I. Composite Mechanism -- First Hinge at Lee Knee E

$$\frac{H_E}{\phi_{pL}} = \frac{wL^2}{M_p}\left[\frac{1}{12} + (A-D)\left(\frac{1}{4} + \frac{1}{6}a\right)\right] - 1 - \frac{2}{3}a \qquad \text{(Graphic)}$$

$$- \frac{1}{3}a\frac{I_o}{I_L}\frac{M_{QL}}{M_p} - \frac{1}{3}a\frac{I_o}{I_R}\frac{M_{QR}}{M_p} \qquad \text{(Corrections)}$$

$$- \frac{1}{3}a\left(\frac{I_o}{I_L} + \frac{I_o}{I_R} - 2\right) + \frac{1}{6}a\left(\frac{I_o}{I_L} - 1\right)\frac{wL^2}{M_p}(A-D) \qquad \ldots(6.6)$$

Case Ia. Panel Mechanism -- ~~Flat~~ First Hinge at Lee Knee E

$$\frac{H_E}{\phi_{pL}} = \frac{1}{3(A-D)}$$

$$- \frac{1}{3} a \frac{I_o}{I_L} \frac{M_{QL}}{M_p} - \frac{1}{3} a \frac{I_o}{I_R} \frac{M_{QR}}{M_p}$$

$$+ \frac{1}{3} a \left(\frac{I_o}{I_L} - \frac{I_o}{I_R} \right) \qquad \ldots(6.10)$$

Case II. Composite Mechanism -- First Hinge in Beam at F

$$\frac{H_F}{\phi_{pL}} = \frac{wL^2}{M_p} \left[\frac{1}{12} + (A-D) \left(\frac{1}{4} + \frac{1}{6} a \right) \right] - 1 - \frac{2}{3} a$$

$$- \frac{1}{3} a \frac{I_o}{I_L} \frac{M_{QL}}{M_p} - \frac{1}{3} a \frac{I_o}{I_R} \frac{M_{QR}}{M_p}$$

$$- \frac{1}{3} a \left(\frac{I_o}{I_L} + \frac{I_o}{I_R} - 2 \right) + \frac{1}{6} a \left(\frac{I_o}{I_L} - 1 \right) \frac{wL^2}{M_p} \quad (A-D) \qquad \ldots(6.9)$$

DEFLECTIONS -- LEE KNEE -- SELF-SUPPORTING SUBASSEMBLAGE

Case I.

$$\frac{\delta_E}{\phi_{pL}{}^2} = a \frac{wL^2}{M_p} \left[\frac{1}{24} + (A-D) \left(\frac{1}{6} + \frac{1}{6} a \right) \right] - a \left[\frac{1}{2} + \frac{1}{3} a \right]$$

$$- \frac{1}{3} a^2 \frac{I_o}{I_L} \frac{M_{QL}}{M_p}$$

$$- \frac{1}{3} a^2 \left(\frac{I_o}{I_L} - 1 \right) + \frac{1}{6} a^2 \left(\frac{I_o}{I_L} - 1 \right) \frac{wL^2}{M_p} \quad (A-D) \qquad \ldots(6.11)$$

Case Ia.

$$\frac{\delta_E}{\phi_{pL}{}^2} = \frac{1}{A-D} \left(\frac{1}{6} a \right) + \frac{1}{6} a + \frac{1}{3} a^2$$

$$- \frac{1}{3} a^2 \frac{I_o}{I_L} \frac{M_{QL}}{M_p}$$

$$+ \frac{1}{3} a^2 \left(\frac{I_o}{I_L} - 1 \right) \qquad \ldots(6.12)$$

Case II.

$$\frac{\delta_E}{\phi_{pL}{}^2} = a \left[\frac{1}{2} + \frac{1}{3} a - \alpha - \frac{2}{3} a\alpha \right] - a \frac{wL^2}{M_p} \left[\frac{1}{24} - \frac{1}{12} \alpha + (A-D) \left(\frac{1}{12} - \frac{1}{4} \alpha - \frac{1}{6} a\alpha \right) \right]$$

$$- \frac{1}{3} a^2 \alpha \frac{I_o}{I_L} \frac{M_{QL}}{M_p} + \frac{1}{3} a^2 \frac{I_o}{I_R} \frac{M_{QR}}{M_p} (1-\alpha)$$

$$- \alpha \left\{ \frac{1}{3} a^2 \left(\frac{I_o}{I_L} + \frac{I_o}{I_R} - 2 \right) - \frac{1}{6} a^2 \left(\frac{I_o}{I_L} - 1 \right) \frac{wL^2}{M_p} \text{ (A-D)} \right\}$$

$$+ \frac{1}{3} a^2 \left(\frac{I_o}{I_R} - 1 \right) \qquad \ldots(6.13)$$

DEFLECTIONS -- WINDWARD KNEE

All cases.

$$\delta_C = \delta_E \qquad \ldots(6.14)$$

DEFLECTIONS -- CENTER OF BEAM
SELF-SUPPORTING SUBASSEMBLAGE

Case I.

$$\frac{\delta_D}{\phi_{pL}{}^2} = \frac{wL^2}{M_p} \left[\frac{5}{384} + \frac{1}{32} \text{ (A-D)} \right] - \frac{1}{8} \qquad \ldots(6.15)$$

No corr.

Case Ia.

$$\frac{\delta_D}{\phi_{pL}{}^2} = \frac{1}{\text{(A-D)}} \frac{5}{96} \qquad \ldots(6.16)$$

No corr.

Case II.

$$\frac{\delta_D}{\phi_{pL}{}^2} = \frac{wL^2}{M_p} \left[\frac{5}{384} - \frac{1}{24} \alpha + \text{(A-D)} \left(\frac{1}{32} - \frac{1}{8}\alpha - \frac{1}{12} a\alpha \right) \right] - \left[\frac{1}{8} - \frac{1}{2}\alpha - \frac{1}{3} a\alpha \right]$$

$$+ \frac{1}{6} a\alpha \frac{I_o}{I_L} \frac{M_{QL}}{M_p} + \frac{1}{6} a\alpha \frac{I_o}{I_R} \frac{M_{QR}}{M_p}$$

$$+ \frac{1}{6} a\alpha \left\{ \left(\frac{I_o}{I_L} + \frac{I_o}{I_R} - 2 \right) - \frac{1}{2} \left(\frac{I_o}{I_L} - 1 \right) \frac{wL^2}{M_p} \text{ (A-D)} \right\} \qquad \ldots(6.17)$$

HINGE ANGLES -- NON-SELF-SUPPORTING SUBASSEMBLAGE

Cases I & II.

$$\frac{H_E}{\phi_{pL}} = \frac{1}{(1-\alpha)} \left\{ \frac{wL^2}{M_p} \left[\frac{1}{24} - \frac{1}{12}\alpha + \text{(A-D)} \left(\frac{1}{12} - \frac{1}{4}\alpha - \frac{1}{3} a\alpha \right) \right] - \left[\frac{1}{2} - \alpha - \frac{1}{3} a\alpha \right] \right\} - \frac{1}{3} a$$

$$+\frac{\Delta C}{a\phi_{pL}{}^2}\frac{1}{(1-\alpha)}+\frac{1}{3}a\frac{I_o}{I_L}\frac{M_{QL}}{M_p}\frac{\alpha}{(1-\alpha)}-\frac{1}{3}a\frac{I_o}{I_R}\frac{M_{QR}}{M_p}$$
$$+\frac{\alpha}{(1-\alpha)}\left\{\frac{1}{3}a\left(\frac{I_o}{I_L}-1\right)-\frac{1}{3}a\left(\frac{I_o}{I_L}-1\right)\frac{wL^2}{M_p}(A-D)\right\}$$
$$-\frac{1}{3}a\left(\frac{I_o}{I_R}-1\right) \qquad \ldots(6.18)$$

Cases I & II

$$\frac{H_F}{\phi_{pL}}=\frac{1}{(1-\alpha)}\left\{\frac{wL^2}{M_p}\left[\frac{1}{24}+(A-D)\left(\frac{1}{6}+\frac{1}{6}a\right)\right]-\left[\frac{1}{2}+\frac{1}{3}a\right]\right\}$$

$$-\frac{\Delta C}{a\phi_{pL}{}^2}\frac{1}{(1-\alpha)}-\frac{1}{3}a\frac{I_o}{I_L}\frac{M_{QL}}{M_p}\frac{1}{(1-\alpha)}$$
$$-\left(\frac{I_o}{I_L}-1\right)\left(\frac{1}{1-\alpha}\right)\frac{1}{3}a\left\{1-\frac{1}{2}\frac{wL^2}{M_p}(A-D)\right\} \qquad \ldots(6.19)$$

Case Ia

$$\frac{H_E}{\phi_{pL}}=\frac{1}{6(A-D)}-\frac{1}{6}-\frac{1}{3}a$$

$$+\frac{\Delta C}{a\phi_{pL}{}^2}-\frac{1}{3}a\frac{I_o}{I_R}\frac{M_{QR}}{M_p}$$
$$-\frac{1}{3}a\left(\frac{I_o}{I_R}-1\right) \qquad \ldots(6.20)$$

Case Ia.

$$\frac{H_C}{\phi_{pL}}=\frac{1}{6(A-D)}+\frac{1}{6}+\frac{1}{3}a$$

$$-\frac{\Delta C}{a\phi_{pL}{}^2}-\frac{1}{3}a\frac{I_o}{I_L}\frac{M_{QL}}{M_p}$$
$$+\frac{1}{3}a\left(\frac{I_o}{I_L}-1\right) \qquad \ldots(6.21)$$

DEFLECTIONS -- LEE KNEE --
NON-SELF-SUPPORTING SUBASSEMBLAGE

All cases

$$\delta_E = \Delta_C \qquad \ldots(6.21)$$

DEFLECTIONS -- CENTER OF BEAM
NON-SELF-SUPPORTING SUBASSEMBLAGE

Cases I & II

$$\frac{\delta_D}{\phi_{pL}{}^2} = \frac{1}{(1-\alpha)}\left[\left\{\frac{wL^2}{M_p}\left[\frac{5}{384} + (A-D)\left(\frac{1}{32} - \frac{11}{96}\alpha\right)\right] - \left[\frac{1}{8} - \frac{3}{8}\alpha\right]\right\} + \frac{1}{6}a\alpha\left\{1 - \frac{1}{2}\frac{wL^2}{M_p}(A-D)\right\}\right]$$

$$- \frac{\Delta_C}{a\phi_{pL}{}^2}\frac{\alpha}{(1-\alpha)} + \frac{1}{6}a\frac{I_o}{I_L}\frac{M_{QL}}{M_p}\frac{\alpha}{1-\alpha}$$

$$+ \frac{1}{6}a\left(\frac{I_o}{I_L} - 1\right)\frac{\alpha}{(1-\alpha)}\left\{1 - \frac{1}{2}\frac{wL^2}{M_p}(A-D)\right\} \qquad \ldots(6.22)$$

Cases Ia & IIa

$$\frac{\delta_D}{\phi_{pL}{}^2} = \frac{5}{96(A-D)}$$

No corr. $\qquad \ldots(6.23)$

APPENDIX E

EQUATIONS FOR MULTI-SPAN GABLED FRAMES

PLASTIC HINGE MOMENTS

Composite Mechanism

$$\frac{M_p}{wL^2} = \frac{1}{4}\left[\frac{(1-\alpha)(A+\alpha-D)-D\left(\frac{2b}{a}\right)\alpha}{1+\frac{b}{a}\alpha}\right]$$

$$\alpha = \frac{1}{\frac{b}{a}}\left[\sqrt{1-\frac{b}{a}\left[A\left(1+\frac{b}{a}\right)-D\left(1-\frac{b}{a}\right)-1\right]}-1\right]$$

... for $\frac{b}{a} > 0$

...(7.1)

Panel Mechanism

$$\frac{M_p}{wL^2} = \left[\frac{A-D}{4}\right]$$

...(7.2)

Reverse Composite Mechanism

$$\frac{M_p}{wL^2} = \frac{1}{4}\left[\frac{(1-2\alpha)\left\{A\left(1+\frac{2b}{a}\right)-D-\frac{1}{2}+\alpha\left(1+\frac{b}{a}\right)\right\}}{2+\frac{b}{a}+\frac{2b}{a}\alpha}\right]$$

$$\alpha = \frac{1}{\frac{b}{a}}\left[\sqrt{1+\frac{2b}{a}+\frac{b^2}{2a^2}-\frac{b}{a}\left[A\left(1+\frac{2b}{a}\right)-D\right]}-1\right]-\frac{1}{2}$$

...(7.3)

Reverse Gable Mechanism ($\alpha = 0$)

$$\frac{M_p}{wL^2} = \frac{1}{4}\left[\frac{A\left(1+\frac{2b}{a}\right)-D-\frac{1}{2}}{2+\frac{b}{a}}\right]$$

...(7.4)

LIMITS

Between Composite Mechanism and Reverse Composite Mechanism

$$\frac{\frac{3}{4}(2+\frac{b}{a})}{\frac{b}{a}} - A + D = \frac{(1+\frac{b}{a})}{\frac{b^2}{a^2}} \sqrt{1+\frac{2b}{a}+\frac{b^2}{2a^2}-\frac{b}{a}\left[A(1+\frac{2b}{a})-D\right]} - \frac{1}{\frac{b^2}{a^2}} \sqrt{1-\frac{b}{a}\left[A(1+\frac{b}{a})-D(1-\frac{b}{a})-1\right]}$$

...(7.5)

Between Composite Mechanism and Panel Mechanism

$$A = \frac{1+D(1-\frac{b}{a})}{1+\frac{b}{a}}$$

...(7.6)

Between Panel Mechanism and Reverse Gable Mechanism

$$D = \frac{A(1-\frac{b}{a})+\frac{1}{2}}{1+\frac{b}{a}}$$

...(7.7)

Between Reverse Composite Mechanism and Reverse Gable Mechanism

$$A = \frac{(1+\frac{b}{2a})+D}{1+\frac{2b}{a}}$$

...(7.8)

Parameters for First Hinge Limits

$$N = \frac{8a}{\sqrt{1+4b^2}} + 12 + 12\frac{b}{a} + 4\frac{b^2}{a^2}$$

$$F = \left[\frac{\frac{16a}{\sqrt{1+4b^2}} + 24 + 12\frac{b}{a}}{N}\right]$$

$$G = \frac{8+5\frac{b}{a}}{N}$$

$$J = \frac{24\frac{b}{a}+16\frac{b^2}{a^2}}{N}$$

...(7.14)

Between First Hinge at Lee Knee E and in Windward Rafter at F

$$M_E = -M_F$$

$$0 = A^2\left(1+\frac{b}{a}+\frac{1}{4}\frac{b^2}{a^2}F^2\right)+A\left(2-\frac{b}{a}F-2F+\frac{b}{a}G+\frac{1}{2}\frac{b^2}{a^2}FG\right.$$
$$\left.+D\left[\frac{1}{2}\frac{b^2}{a^2}F^2-2\right]\right)+D\left(2-\frac{b}{a}F-\frac{b}{a}G+\frac{1}{2}\frac{b^2}{a^2}FG+J\right)$$
$$+D^2\left(1-\frac{b}{a}F+\frac{1}{4}\frac{b^2}{a^2}F^2\right)+\left(1-\frac{b}{a}G-2G+\frac{1}{4}\frac{b^2}{a^2}G^2\right)$$

...(7.15)

Between First Hinge at Lee Knee E and at Windward Knee C

$$M_E = -M_C$$

$$A+D = \frac{8+5\frac{b}{a}}{12\frac{b}{a}+8\frac{b^2}{a^2}}$$

...(7.16)

Between First Hinge at Lee Knee E and at Ridge D

$$M_E = M_D$$

$$D = \frac{A\left(2-F\frac{b}{a}\right)+\left(1-\frac{b}{a}G\right)}{\left(F\frac{b}{a}+2F+J-2\right)}$$

...(7.17)

Between First Hinge at Ridge D and at Windward Knee C

$$M_D = -M_C$$

$$D = \frac{A\left(2-F\frac{b}{a}+J\right)+\left(1-2G-\frac{b}{a}G\right)}{\left(2F+F\frac{b}{a}-2\right)}$$

...(7.18)

Between First Hinge at Ridge D and in Windward Rafter at F

$$M_F = -M_D$$

$$0 = A^2\left(1+\frac{b}{a}F+\frac{1}{4}\frac{b^2}{a^2}F^2\right)+A\left(4-2F-2\frac{b}{a}F+\frac{b}{a}G+\frac{1}{2}\frac{b^2}{a^2}FG\right.$$
$$\left.+D\left[\frac{1}{2}\frac{b^2}{a^2}F^2-2\right]+D\left(4-2F-2\frac{b}{a}F-\frac{b}{a}G+\frac{1}{2}\frac{b^2}{a^2}FG\right)\right.$$
$$+D^2\left(1-\frac{b}{a}F+\frac{1}{4}\frac{b^2}{a^2}F^2\right)+\left(2-2G-2\frac{b}{a}G+\frac{1}{4}\frac{b^2}{a^2}G^2\right)$$

...(7.19)

HINGE ANGLES -- SELF-SUPPORTING SUBASSEMBLAGE

Case I. Composite Mechanism -- First Hinge at Lee Knee E

$$\frac{H_E}{\phi_p L} = \sqrt{1+4b^2}\left\{\frac{WL^2}{M_p}\left[\frac{1}{12}+\frac{5}{96}\frac{b}{a}+A\left(\frac{1}{4}+\frac{1}{8}\frac{b}{a}\right)-D\left(\frac{1}{4}+\frac{3}{8}\frac{b}{a}+\frac{1}{6}\frac{b^2}{a^2}\right)\right]\right.$$

$$\left.-\left[1+\frac{b}{a}+\frac{1}{3}\frac{b^2}{a^2}\right]\right\}-\frac{2}{3}a+\frac{1}{6}a\frac{WL^2}{M_p}(A-D)$$

(Graphic) / (Corrections)

$$-\frac{1}{3}a\frac{I_o}{I_L}\frac{M_{QL}}{M_p}-\frac{1}{3}a\frac{I_o}{I_R}\frac{M_{QR}}{M_p}$$

$$-\frac{1}{3}a\left(\frac{I_o}{I_L}+\frac{I_o}{I_R}-2\right)+\frac{1}{6}a\left(\frac{I_o}{I_L}-1\right)\frac{WL^2}{M_p}(A-D)$$

...(7.20)

Case Ia. Panel Mechanism -- First Hinge at Lee Knee E

$$\frac{H_E}{\phi_p L} = \sqrt{1+4b^2}\left\{\frac{1}{A-D}\left[\frac{1}{3}+\frac{5}{24}\frac{b}{a}-D\left(\frac{b}{a}+\frac{2}{3}\frac{b^2}{a^2}\right)\right]-\left[\frac{1}{2}\frac{b}{a}+\frac{1}{3}\frac{b^2}{a^2}\right]\right\}$$

$$-\frac{1}{3}a\frac{I_o}{I_L}\frac{M_{QL}}{M_p}-\frac{1}{3}a\frac{I_o}{I_R}\frac{M_{QR}}{M_p}+\frac{1}{3}a\left(\frac{I_o}{I_L}-\frac{I_o}{I_R}\right)$$

...(7.21)

Case II. Composite Mechanism -- First Hinge in Windward Rafter at F

$$\frac{H_F}{\phi_p L} = \frac{1}{\left(1+2\frac{b}{a}\alpha\right)}\left[\sqrt{1+4b^2}\left\{\frac{WL^2}{M_p}\left[\frac{1}{12}+\frac{5}{96}\frac{b}{a}+A\left(\frac{1}{4}+\frac{1}{8}\frac{b}{a}\right)\right.\right.\right.$$

$$\left.\left.\left.-D\left(\frac{1}{4}+\frac{3}{8}\frac{b}{a}+\frac{1}{6}\frac{b^2}{a^2}\right)\right]-\left[1+\frac{b}{a}+\frac{1}{3}\frac{b^2}{a^2}\right]\right\}-\frac{2}{3}a+\frac{1}{6}a\frac{WL^2}{M_p}(A-D)\right]$$

$$-\frac{1}{3}a\frac{I_o}{I_L}\frac{M_{QL}}{M_p}\frac{1}{\left(1+2\frac{b}{a}\alpha\right)}-\frac{1}{3}a\frac{I_o}{I_R}\frac{M_{QR}}{M_p}\frac{1}{\left(1+2\frac{b}{a}\alpha\right)}$$

$$-\frac{1}{3}a\left(\frac{I_o}{I_L}+\frac{I_o}{I_R}-2\right)\frac{1}{\left(1+2\frac{b}{a}\alpha\right)}+\frac{1}{6}a\left(\frac{I_o}{I_L}-1\right)\frac{WL^2}{M_p}\frac{(A-D)}{\left(1+2\frac{b}{a}\alpha\right)}$$

...(7.22)

Case IIa. Panel Mechanism -- First Hinge at Windward Knee C

$$\frac{H_c}{\phi_p L} = \sqrt{1+4b^2}\left\{\frac{1}{A-D}\left[\frac{1}{3}+\frac{5}{24}\frac{b}{a}-D\left(\frac{b}{a}+\frac{2}{3}\frac{b^2}{a^2}\right)\right]-\left[\frac{1}{2}\frac{b}{a}+\frac{1}{3}\frac{b^2}{a^2}\right]\right\}$$

$$-\frac{1}{3}a\frac{I_o}{I_L}\frac{M_{QL}}{M_P}-\frac{1}{3}a\frac{I_o}{I_R}\frac{M_{QR}}{M_P}$$

$$+\frac{1}{3}a\left(\frac{I_o}{I_L}-\frac{I_o}{I_R}\right) \qquad \ldots(7.23)$$

Case III. Reverse Composite Mechanism -- First Hinge in Windward Rafter at F

$$\frac{H_F}{\phi_p L} = \left(\frac{1}{1+\frac{b}{a}}\right)\left(\frac{1}{1+2\frac{b}{a}\alpha}\right)\left[\sqrt{1+4b^2}\left\{-\frac{WL^2}{M_P}\left[\frac{1}{24}-\frac{1}{96}\frac{b}{a}-\frac{1}{96}\frac{b^2}{a^2}\right.\right.\right.$$

$$\left.\left.\left.-(A+D)\left(\frac{1}{8}\frac{b}{a}+\frac{1}{24}\frac{b^2}{a^2}\right)\right]-\left[1+\frac{b}{a}+\frac{1}{3}\frac{b^2}{a^2}\right]\right\}-\frac{2}{3}a+\frac{WL^2}{M_P}\left\{\frac{1}{6}b(A+D)-\frac{1}{12}\right.\right.$$

$$-\frac{1}{3}a\frac{I_o}{I_L}\frac{M_{QL}}{M_P}\frac{1}{(1+2\frac{b}{a}\alpha)}-\frac{1}{3}a\frac{I_o}{I_R}\frac{M_{QR}}{M_P}\frac{1}{(1+2\frac{b}{a}\alpha)}$$

$$+\left(\frac{1}{1+\frac{b}{a}}\right)\left(\frac{1}{1+2\frac{b}{a}\alpha}\right)\left\{-\frac{1}{3}a\left(\frac{I_o}{I_L}+\frac{I_o}{I_R}-2\right)+\frac{WL^2}{M_P}\left[\frac{1}{12}a\left(\frac{I_o}{I_L}-\frac{I_o}{I_R}\right)(A-D)\right.\right.$$

$$\left.\left.-\frac{1}{24}a\left(\frac{I_o}{I_L}+\frac{I_o}{I_R}-2\right)+\frac{1}{6}bA\left(\frac{I_o}{I_L}-1\right)+\frac{1}{6}bD\left(\frac{I_o}{I_R}-1\right)\right]\right\} \qquad \ldots(7.24)$$

Case IIIa. Reverse Gable Mechanism ($\alpha = 0$) -- First Hinge at Windward Knee C

$$\frac{H_c}{\phi_p L} = \frac{1}{1+\frac{b}{a}}\left[\sqrt{1+4b^2}\left\{-\frac{WL^2}{M_P}\left[\frac{1}{24}-\frac{1}{96}\frac{b}{a}-\frac{1}{96}\frac{b^2}{a^2}-(A+D)\left(\frac{1}{8}\frac{b}{a}+\frac{1}{24}\frac{b^2}{a^2}\right)\right]\right.\right.$$

$$\left.\left.-\left[1+\frac{b}{a}+\frac{1}{3}\frac{b^2}{a^2}\right]\right\}-\frac{2}{3}a+\frac{WL^2}{M_P}\left\{\frac{1}{6}b(A+D)-\frac{1}{12}a\right\}\right]$$

$$-\frac{1}{3}a\frac{I_o}{I_L}\frac{M_{QL}}{M_P}-\frac{1}{3}a\frac{I_o}{I_R}\frac{M_{QR}}{M_P}$$

$$+\frac{1}{1+\frac{b}{a}}\left\{-\frac{1}{3}a\left(\frac{I_o}{I_L}+\frac{I_o}{I_R}-2\right)+\frac{WL^2}{M_P}\left[\frac{1}{12}a\left(\frac{I_o}{I_L}-\frac{I_o}{I_R}\right)(A-D)\right.\right.$$

$$\left.\left.-\frac{1}{24}a\left(\frac{I_o}{I_L}+\frac{I_o}{I_R}-2\right)+\frac{1}{6}bA\left(\frac{I_o}{I_L}-1\right)-\frac{1}{6}bD\left(\frac{I_o}{I_R}-1\right)\right]\right\} \qquad \ldots(7.25)$$

Cases IV & IVa. Reverse Composite Mechanism and Reverse Gable Mechanism -- First Hinge at Ridge D

$$\frac{H_o}{\phi_p L} = \frac{1}{(1+\frac{b}{a})^2}\left[\sqrt{1+4b^2}\left\{\frac{WL^2}{M_p}\left[\frac{1}{96}\frac{b}{a}+\frac{1}{96}\frac{b^2}{a^2}-\frac{1}{24}+(A+D)\left(\frac{1}{8}\frac{b}{a}+\frac{1}{24}\frac{b^2}{a^2}\right)\right]\right.\right.$$
$$\left.\left.-\left[1+\frac{b}{a}+\frac{1}{3}\frac{b^2}{a^2}\right]\right\}-\frac{2}{3}a+\frac{WL^2}{M_p}\left\{\frac{1}{6}b(A+D)-\frac{1}{12}a\right\}\right]$$

$$-\frac{1}{3}a\frac{I_o}{I_L}\frac{M_{QL}}{M_p}\frac{1}{(1+\frac{b}{a})}-\frac{1}{3}a\frac{I_o}{I_R}\frac{M_{QR}}{M_p}\frac{1}{(1+\frac{b}{a})}$$
$$+\frac{1}{(1+\frac{b}{a})^2}\left\{-\frac{1}{3}a\left(\frac{I_o}{I_L}+\frac{I_o}{I_R}-2\right)+\frac{WL^2}{M_p}\left[\frac{1}{12}a\left(\frac{I_o}{I_L}-\frac{I_o}{I_R}\right)(A-D)\right.\right.$$
$$\left.\left.-\frac{1}{24}a\left(\frac{I_o}{I_L}+\frac{I_o}{I_R}-2\right)+\frac{1}{6}bA\left(\frac{I_o}{I_L}-1\right)+\frac{1}{6}bD\left(\frac{I_o}{I_R}-1\right)\right]\right\}$$

...(7.26)

DEFLECTIONS -- LEE KNEE
SELF-SUPPORTING SUBASSEMBLAGE

Case I.

$$\frac{\delta_E}{\phi_p L^2} = a\sqrt{1+4b^2}\left\{\frac{WL^2}{M_p}\left[\frac{1}{24}+\frac{5}{96}\frac{b}{a}+A\left(\frac{1}{6}+\frac{1}{8}\frac{b}{a}\right)-D\left(\frac{1}{6}+\frac{1}{4}\frac{b}{a}+\frac{1}{6}\frac{b^2}{a^2}\right)\right]\right.$$
$$\left.-\left[\frac{1}{2}+\frac{3}{4}\frac{b}{a}+\frac{1}{3}\frac{b^2}{a^2}\right]\right\}-\frac{1}{3}a^2+\frac{1}{6}a^2\frac{WL^2}{M_p}(A-D)$$

$$-\frac{1}{3}a^2\frac{I_o}{I_L}\frac{M_{QL}}{M_p}$$
$$-\frac{1}{3}a^2\left(\frac{I_o}{I_L}-1\right)+\frac{1}{6}a^2\left(\frac{I_o}{I_L}-1\right)\frac{WL^2}{M_p}(A-D)$$

...(7.27)

Case Ia.

$$\frac{\delta_E}{\phi_p L^2} = a\sqrt{1+4b^2}\left\{\frac{1}{A-D}\left[\frac{1}{6}+\frac{5}{24}\frac{b}{a}-D\left(\frac{1}{2}\frac{b}{a}+\frac{2}{3}\frac{b^2}{a^2}\right)\right]\right.$$

$$\left.+\left[\frac{1}{6}-\frac{1}{4}\frac{b}{a}-\frac{1}{3}\frac{b^2}{a^2}\right]+\frac{1}{3}a^2\right.$$

$$-\frac{1}{3}a^2\frac{I_o}{I_L}\frac{M_{QL}}{M_p}$$

$$+\frac{1}{3}a^2\left(\frac{I_o}{I_L}-1\right) \qquad \ldots(7.28)$$

Case II.

$$\frac{\delta_E}{\phi_p L^2} = \frac{1}{(1+2\frac{b}{a}\alpha)}\left[a\sqrt{1+4b^2}\left\{\left[\frac{1}{2}+\frac{1}{4}\frac{b}{a}-\alpha+\frac{1}{6}\frac{b^2}{a^2}\alpha\right]-\frac{WL^2}{M_p}\left[\frac{1}{24}-\frac{1}{12}\alpha\right.\right.\right.$$

$$\left.+\frac{1}{32}\frac{b}{a}\alpha+A\left(\frac{1}{12}+\frac{1}{24}\frac{b}{a}\alpha-\frac{1}{4}\alpha\right)-D\left(\frac{1}{12}+\frac{1}{8}\frac{b}{a}-\frac{1}{4}\alpha-\frac{5}{24}\frac{b}{a}\alpha\right.\right.$$

$$\left.\left.+\frac{1}{12}\frac{b^2}{a^2}\alpha\right)\right]\Big\}-\frac{2}{3}a^2\alpha+\frac{1}{6}a^2\alpha\frac{WL^2}{M_p}(A-D)\Big]+\frac{1}{3}a^2$$

$$-\frac{1}{3}a^2\frac{I_o}{I_L}\frac{M_{QL}}{M_p}\left[\frac{\alpha}{1+2\frac{b}{a}\alpha}\right]+\frac{1}{3}a^2\frac{I_o}{I_R}\frac{M_{QR}}{M_p}\left[\frac{1+2\frac{b}{a}\alpha-\alpha}{1+2\frac{b}{a}\alpha}\right]$$

$$-\frac{\alpha}{(1+2\frac{b}{a}\alpha)}\left\{\frac{1}{3}a^2\left(\frac{I_o}{I_L}+\frac{I_o}{I_R}-2\right)-\frac{1}{6}a^2\left(\frac{I_o}{I_L}-1\right)\frac{WL^2}{M_p}(A-D)\right\}$$

$$-\frac{1}{3}a^2\left(\frac{I_o}{I_R}-1\right) \qquad \ldots(7.29)$$

Case IIa.

$$\frac{\delta_E}{\phi_p L^2} = a\sqrt{1+4b^2}\left\{\left[\frac{1}{6}+\frac{1}{4}\frac{b}{a}\right]-\frac{1}{A-D}\left[\frac{1}{6}-\frac{1}{2}\frac{b}{a}D\right]\right\}+\frac{1}{3}a^2$$

$$+\frac{1}{3}a^2\frac{I_o}{I_R}\frac{M_{QR}}{M_p}$$

$$+\frac{1}{3}a^2\left(\frac{I_o}{I_R}-1\right) \qquad \ldots(7.30)$$

Case III.

$$\frac{\delta_E}{\phi_p L^2} = \frac{1}{(1+\frac{b}{a})(1+2\frac{b}{a}\alpha)}\left[\alpha\sqrt{1+4b^2}\left\{\left[\frac{1}{2}+\frac{1}{4}\frac{b}{a}-\alpha+\frac{1}{6}\frac{b^2}{a^2}\alpha\right]\right.\right.$$

$$+\frac{WL^2}{M_p}\left[\frac{1}{48}-\frac{1}{96}\frac{b}{a}-\frac{1}{24}\alpha+\frac{5}{96}\frac{b}{a}\alpha-\frac{1}{96}\frac{b^2}{a^2}\alpha+A\left(\frac{1}{24}-\frac{1}{48}\frac{b}{a}+\frac{5}{24}\frac{b}{a}\alpha\right)\right.$$

$$\left.\left.-D\left(\frac{1}{24}+\frac{5}{48}\frac{b}{a}-\frac{1}{24}\frac{b}{a}\alpha+\frac{1}{6}\frac{b^2}{a^2}\alpha\right)\right]\right\}$$

$$+a^2\left\{\left[\frac{1}{3}-\frac{2}{3}\alpha+\frac{2}{3}\frac{b}{a}\alpha\right]+\frac{WL^2}{M_p}\left[\frac{1}{24}-\frac{1}{12}\alpha+\frac{1}{12}\frac{b}{a}\alpha\right.\right.$$

$$\left.\left.+A\left(\frac{1}{12}+\frac{1}{3}\frac{b}{a}\right)-D\left(\frac{1}{12}+\frac{1}{6}\frac{b}{a}+\frac{1}{3}\frac{b^2}{a^2}\alpha\right)\right]\right\}\Bigg]$$

$$-\frac{1}{3}a^2\frac{I_o}{I_L}\frac{M_{QL}}{M_p}\left[\frac{\alpha}{1+2\frac{b}{a}\alpha}\right]-\frac{1}{3}a^2\frac{I_o}{I_R}\frac{M_{QR}}{M_p}\left[\frac{1+2\frac{b}{a}\alpha-\alpha}{1+2\frac{b}{a}\alpha}\right]$$

$$-a^2\alpha\left(\frac{I_o}{I_L}-1\right)\left(\frac{1}{1+\frac{b}{a}}\right)\left(\frac{1}{1+2\frac{b}{a}\alpha}\right)\left\{\frac{1}{3}+\frac{WL^2}{M_p}\left[\frac{1}{24}-\frac{1}{12}(A-D)-\frac{1}{6}\frac{b}{a}A\right]\right\}$$

$$+a^2\left(\frac{I_o}{I_R}-1\right)\left(\frac{1}{1+\frac{b}{a}}\right)\left(\frac{1}{1+2\frac{b}{a}\alpha}\right)\left[\left\{\frac{1}{3}+\frac{WL^2}{M_p}\left[\frac{1}{24}+\frac{1}{12}(A-D)-\frac{1}{6}\frac{b}{a}D\right]\right\}\right.$$

$$\left.-\alpha\left\{\left[\frac{1}{3}-\frac{2}{3}\frac{b}{a}\right]+\frac{WL^2}{M_p}\left[\frac{1}{24}-\frac{1}{12}\frac{b}{a}+A\left(\frac{1}{12}-\frac{1}{6}\frac{b}{a}\right)-D\left(\frac{1}{12}-\frac{1}{3}\frac{b^2}{a^2}\right)\right]\right\}\right] \quad \ldots(7.31)$$

Case IIIa.

$$\frac{\delta_E}{\phi_p L^2} = \frac{1}{(1+\frac{b}{a})}\left[\alpha\sqrt{1+4b^2}\left\{\left[\frac{1}{2}+\frac{1}{4}\frac{b}{a}\right]+\frac{WL^2}{M_p}\left[\frac{1}{48}-\frac{1}{96}\frac{b}{a}+A\left(\frac{1}{24}-\frac{1}{48}\frac{b}{a}\right)\right.\right.\right.$$

$$\left.\left.\left.-D\left(\frac{1}{24}+\frac{5}{48}\frac{b}{a}\right)\right]\right\}+\frac{1}{3}a^2+a^2\frac{WL^2}{M_p}\left\{\frac{1}{24}+\frac{1}{12}(A-D)-\frac{1}{6}\frac{b}{a}D\right\}\right]$$

$$+\frac{1}{3}a^2\frac{I_o}{I_R}\frac{M_{QR}}{M_p}$$

$$+a^2\left(\frac{I_o}{I_R}-1\right)\left(\frac{1}{1+\frac{b}{a}}\right)\left\{\frac{1}{3}+\frac{WL^2}{M_p}\left[\frac{1}{24}+\frac{1}{12}(A-D)-\frac{1}{6}\frac{b}{a}D\right]\right\} \quad \ldots(7.32)$$

Case IV & IVa.

$$\frac{\delta_E}{\phi_p L^2} = \frac{1}{(1+\frac{b}{a})^2}\left[a\sqrt{1+4b^2}\left\{\left[\frac{1}{4}\frac{b}{a}+\frac{1}{12}\frac{b^2}{a^2}\right]+\frac{WL^2}{M_p}\left[\frac{1}{64}\frac{b}{a}-\frac{1}{192}\frac{b^2}{a^2}\right.\right.\right.$$

$$\left.\left.+A\left(\frac{1}{24}+\frac{1}{12}\frac{b}{a}\right)-D\left(\frac{1}{24}+\frac{1}{12}\frac{b}{a}+\frac{1}{12}\frac{b^2}{a^2}\right)\right]\right\}+\frac{1}{3}ab$$

$$\left.+\frac{1}{6}a^2\frac{WL^2}{M_p}\left\{\frac{1}{4}\frac{b}{a}+A\left(\frac{1}{2}+\frac{b}{a}\right)-D\left(\frac{1}{2}+\frac{b}{a}+\frac{b^2}{a^2}\right)\right\}\right]$$

$$-\frac{1}{6}a^2\frac{I_o}{I_L}\frac{M_{QL}}{M_p}\left[\frac{1}{1+\frac{b}{a}}\right]+\frac{1}{6}a^2\frac{I_o}{I_R}\frac{M_{QR}}{M_p}\left[\frac{1+2\frac{b}{a}}{1+\frac{b}{a}}\right]$$

$$+\frac{1}{6}a^2\left(\frac{1}{1+\frac{b}{a}}\right)^2\left(\frac{I_o}{I_L}-1\right)\left\{-1+\frac{WL^2}{M_p}\left[-\frac{1}{8}+\frac{1}{4}(A-D)+\frac{1}{2}\frac{b}{a}A\right]\right\}$$

$$+\frac{1}{6}a^2\left(\frac{1}{1+\frac{b}{a}}\right)^2\left(\frac{I_o}{I_R}-1\right)\left\{\left[1+2\frac{b}{a}\right]+\frac{WL^2}{M_p}\left[\frac{1}{8}+\frac{1}{4}\frac{b}{a}+A\left(\frac{1}{4}+\frac{1}{2}\frac{b}{a}\right)\right.\right.$$

$$\left.\left.-D\left(\frac{1}{4}+\frac{b}{a}+\frac{b^2}{a^2}\right)\right]\right\}$$

...(7.33)

DEFLECTIONS -- WINDWARD KNEE --
SELF-SUPPORTING SUBASSEMBLAGE

Case I.

$$\frac{\delta_c}{\phi_p L^2} = a\sqrt{1+4b^2}\left\{\frac{WL^2}{M_p}\left[\frac{1}{24}+\frac{1}{6}(A-D)-\frac{1}{8}\frac{b}{a}D\right]-\left[\frac{1}{2}+\frac{1}{4}\frac{b}{a}\right]\right\}$$

$$-\frac{1}{3}a^2+\frac{1}{6}a^2\frac{WL^2}{M_p}(A-D)$$

$$-\frac{1}{3}a^2\frac{I_o}{I_L}\frac{M_{QL}}{M_p}$$

$$-\frac{1}{3}a^2\left(\frac{I_o}{I_L}-1\right)+\frac{1}{6}a^2\left(\frac{I_o}{I_L}-1\right)\frac{WL^2}{M_p}(A-D)$$

...(7.34)

Case Ia.

$$\frac{\delta_c}{\phi_p L^2} = a\sqrt{1+4b^2}\left\{\frac{1}{A-D}\left[\frac{1}{6}-\frac{1}{2}\frac{b}{a}D\right]+\left[\frac{1}{6}-\frac{1}{4}\frac{b}{a}\right]\right\}+\frac{1}{3}a^2$$

$$-\frac{1}{3}a^2\frac{I_o}{I_L}\frac{M_{QL}}{M_p}$$

$$+\frac{1}{3}a^2\left(\frac{I_o}{I_L}-1\right)$$

...(7.35)

Case II.

$$\frac{\delta_c}{\phi_p L^2} = \frac{1}{\left(1+2\frac{b}{a}\alpha\right)}\left[a\sqrt{1+4b^2}\left\{\left[\frac{1}{2}+\frac{3}{4}\frac{b}{a}+\frac{1}{3}\frac{b^2}{a^2}\alpha-2\frac{b}{a}\alpha-\frac{5}{6}\frac{b^2}{a^2}\alpha\right]\right.\right.$$

$$-\frac{WL^2}{M_p}\left[\frac{1}{24}+\frac{5}{96}\frac{b}{a}-\frac{1}{12}\alpha-\frac{13}{96}\frac{b}{a}\alpha+A\left(\frac{1}{12}+\frac{1}{8}\frac{b}{a}-\frac{1}{4}\alpha-\frac{11}{24}\frac{b}{a}\alpha\right)\right.$$

$$\left.\left.-D\left(\frac{1}{12}+\frac{1}{4}\frac{b}{a}+\frac{1}{6}\frac{b^2}{a^2}-\frac{1}{4}\alpha-\frac{17}{24}\frac{b}{a}\alpha-\frac{5}{12}\frac{b^2}{a^2}\alpha\right)\right]\right\}$$

$$\left.+(1-\alpha)\left\{\frac{2}{3}a^2-\frac{1}{6}a^2\frac{WL^2}{M_p}(A-D)\right\}\right]-\frac{1}{3}a^2+\frac{1}{6}a^2\frac{WL^2}{M_p}(A-D)$$

$$-\frac{1}{3}a^2\alpha\frac{I_o}{I_L}\frac{M_{QL}}{M_p}\left[\frac{1+2\frac{b}{a}}{1+2\frac{b}{a}\alpha}\right]+\frac{1}{3}a^2\frac{I_o}{I_R}\frac{M_{QR}}{M_p}\left[\frac{1-\alpha}{1+2\frac{b}{a}\alpha}\right]$$

$$+\frac{1-\alpha}{1+2\frac{b}{a}\alpha}\left\{\frac{1}{3}a^2\left(\frac{I_o}{I_L}+\frac{I_o}{I_R}-2\right)-\frac{1}{6}a^2\left(\frac{I_o}{I_L}-1\right)\frac{WL^2}{M_p}(A-D)\right\}$$

$$-\frac{1}{3}a^2\left(\frac{I_o}{I_L}-1\right)+\frac{1}{6}a^2\left(\frac{I_o}{I_L}-1\right)\frac{WL^2}{M_p}(A-D)$$

...(7.36)

Case IIa.

$$\frac{\delta_c}{\phi_p L^2} = a\sqrt{1+4b^2}\left\{\left[\frac{1}{6}+\frac{1}{4}\frac{b}{a}+\frac{1}{3}\frac{b^2}{a^2}\right]-\frac{1}{A-D}\left[\frac{1}{6}+\frac{5}{24}\frac{b}{a}-D\left(\frac{1}{2}\frac{b}{a}+\frac{2}{3}\frac{b^2}{a^2}\right)\right]\right\}+\frac{1}{3}a^2$$

$$+\frac{1}{3}a^2\frac{I_o}{I_R}\frac{M_{QR}}{M_p}$$

$$+\frac{1}{3}a^2\left(\frac{I_o}{I_R}-1\right) \qquad \ldots(7.37)$$

Case III.

$$\frac{\delta_c}{\phi_p L^2} = \frac{1}{(1+\frac{b}{a})}\frac{1}{(1+2\frac{b}{a}\alpha)}\left\{a\sqrt{1+4b^2}\left\{\frac{1}{2}+\frac{3}{4}\frac{b}{a}+\frac{1}{3}\frac{b^2}{a^2}-\alpha-2\frac{b}{a}\alpha-\frac{5}{6}\frac{b^2}{a^2}\alpha\right\}\right.$$

$$+\frac{WL^2}{M_p}\left[\frac{1}{48}-\frac{1}{96}\frac{b^2}{a^2}-\frac{1}{24}\alpha-\frac{1}{32}\frac{b}{a}\alpha+\frac{1}{32}\frac{b^2}{a^2}\alpha\right.$$

$$+A\left(\frac{1}{24}-\frac{1}{48}\frac{b}{a}-\frac{1}{24}\frac{b^2}{a^2}+\frac{5}{24}\frac{b}{a}\alpha+\frac{1}{4}\frac{b^2}{a^2}\alpha\right)$$

$$\left.\left.-D\left(\frac{1}{24}+\frac{5}{48}\frac{b}{a}+\frac{1}{24}\frac{b^2}{a^2}-\frac{1}{24}\frac{b}{a}\alpha-\frac{1}{12}\frac{b^2}{a^2}\alpha\right)\right]\right\}$$

$$-a^2\alpha\left(1+2\frac{b}{a}\right)\left\{\frac{1}{3}+\frac{WL^2}{M_p}\left[\frac{1}{24}-\frac{1}{12}(A-D)-\frac{1}{6}\frac{b}{a}A\right]\right\}$$

$$\left.+a^2(1-\alpha)\left\{\frac{1}{3}+\frac{WL^2}{M_p}\left[\frac{1}{24}+\frac{1}{12}(A-D)-\frac{1}{6}\frac{b}{a}D\right]\right\}\right]$$

$$\frac{1}{3}a^2\alpha\frac{I_o}{I_L}\frac{M_{QL}}{M_p}\frac{(1+2\frac{b}{a})}{(1+2\frac{b}{a}\alpha)}+\frac{1}{3}a^2\frac{I_o}{I_R}\frac{M_{QR}}{M_p}\frac{(1-\alpha)}{(1+2\frac{b}{a}\alpha)}$$

$$-a^2\alpha\left(\frac{I_o}{I_L}-1\right)\frac{1+2\frac{b}{a}}{(1+\frac{b}{a})(1+2\frac{b}{a}\alpha)}\left\{\frac{1}{3}+\frac{WL^2}{M_p}\left[\frac{1}{24}-\frac{1}{12}(A-D)-\frac{1}{6}\frac{b}{a}A\right]\right\}$$

$$+a^2\left(\frac{I_o}{I_R}-1\right)\frac{(1-\alpha)}{(1+\frac{b}{a})(1+2\frac{b}{a}\alpha)}\left\{\frac{1}{3}+\frac{WL^2}{M_p}\left[\frac{1}{24}+\frac{1}{12}(A-D)-\frac{1}{6}\frac{b}{a}D\right]\right\}$$

$$\ldots(7.38)$$

Case IIIa.

$$\frac{\delta_c}{\phi_p L^2} = \frac{1}{1+\frac{b}{a}}\left[a\sqrt{1+4b^2}\left\{\left[\frac{1}{2}+\frac{3}{4}\frac{b}{a}+\frac{1}{3}\frac{b^2}{a^2}\right]+\frac{WL^2}{M_p}\left[\frac{1}{48}-\frac{1}{96}\frac{b^2}{a^2}\right.\right.\right.$$
$$\left.+A\left(\frac{1}{24}-\frac{1}{48}\frac{b}{a}-\frac{1}{24}\frac{b^2}{a^2}\right)-D\left(\frac{1}{24}+\frac{5}{48}\frac{b}{a}+\frac{1}{24}\frac{b^2}{a^2}\right)\right]\Bigg\}$$
$$\left.+a^2\left\{\frac{1}{3}+\frac{WL^2}{M_p}\left[\frac{1}{24}+\frac{1}{12}(A-D)-\frac{1}{6}\frac{b}{a}D\right]\right\}\right]$$

$$+\frac{1}{3}a^2\frac{I_o}{I_R}\frac{M_{QR}}{M_p}$$
$$+\left(\frac{I_o}{I_R}-1\right)\left(\frac{1}{1+\frac{b}{a}}\right)a^2\left\{\frac{1}{3}+\frac{WL^2}{M_p}\left[\frac{1}{24}+\frac{1}{12}(A-D)-\frac{1}{6}\frac{b}{a}D\right]\right\}$$

...(7.39)

Case IV & IVa.

$$\frac{\delta_c}{\phi_p L^2} = \frac{1}{\left(1+\frac{b}{a}\right)^2}\left[a\sqrt{1+4b^2}\left\{\frac{WL^2}{M_p}\left[\frac{1}{192}\frac{b^2}{a^2}-\frac{1}{64}\frac{b}{a}+A\left(\frac{1}{24}+\frac{1}{12}\frac{b}{a}+\frac{1}{12}\frac{b^2}{a^2}\right)\right.\right.\right.$$
$$\left.-D\left(\frac{1}{24}+\frac{1}{12}\frac{b}{a}\right)\right]-\left[\frac{1}{4}\frac{b}{a}+\frac{1}{12}\frac{b^2}{a^2}\right]\Bigg\}-\frac{1}{3}ab$$
$$\left.+\frac{1}{6}a^2\frac{WL^2}{M_p}\left[-\frac{1}{4}\frac{b}{a}+(A-D)\left(\frac{1}{2}+\frac{b}{a}\right)+\frac{b^2}{a^2}A\right]\right]$$

$$-\frac{1}{6}a^2\frac{I_o}{I_L}\frac{M_{QL}}{M_p}\frac{\left(1+2\frac{b}{a}\right)}{\left(1+\frac{b}{a}\right)}+\frac{1}{6}a^2\frac{I_o}{I_R}\frac{M_{QR}}{M_p}\left(\frac{1}{1+\frac{b}{a}}\right)$$
$$-\left(\frac{I_o}{I_L}-1\right)\frac{1}{\left(1+\frac{b}{a}\right)^2}\frac{1}{6}a^2\left\{\left[1+2\frac{b}{a}\right]+\frac{WL^2}{M_p}\left[\frac{1}{8}+\frac{1}{4}\frac{b}{a}-A\left(\frac{1}{4}+\frac{b}{a}+\frac{b^2}{a^2}\right)\right.\right.$$
$$\left.+D\left(\frac{1}{4}+\frac{1}{2}\frac{b}{a}\right)\right\}+\left(\frac{I_o}{I_R}-1\right)\frac{1}{\left(1+\frac{b}{a}\right)^2}\frac{1}{6}a^2\left\{1+\frac{WL^2}{M_p}\left[\frac{1}{8}\right.\right.$$
$$\left.\left.+\frac{1}{4}(A-D)-\frac{1}{2}\frac{b}{a}D\right]\right\}$$

...(7.40)

DEFLECTIONS -- RIDGE --
SELF-SUPPORTING SUBASSEMBLAGE

Case I.

$$\frac{\delta_D}{\phi_p L^2} = \sqrt{1+4b^2}\left\{\frac{WL^2}{M_p}\left[\frac{5}{384}+\frac{1}{32}(A-D)-\frac{1}{24}\frac{b}{a}D\right]-\left[\frac{1}{8}+\frac{1}{12}\frac{b}{a}\right]\right\}$$

No corr. ...(7.41)

Case Ia.

$$\frac{\delta_D}{\phi_p L^2} = \sqrt{1+4b^2}\left\{\frac{1}{A-D}\left[\frac{5}{96}-\frac{1}{6}\frac{b}{a}D\right]-\frac{1}{12}\frac{b}{a}\right\}$$

No corr. ...(7.42)

Case IIa.

$$\frac{\delta_D}{\phi_p L^2} = \sqrt{1+4b^2}\left\{\frac{1}{A-D}\left[\frac{5}{96}-\frac{1}{6}\frac{b}{a}D\right]-\frac{1}{12}\frac{b}{a}\right\}$$

No corr. ...(7.44)

Case II.

$$\frac{\delta_D}{\phi_p L^2} = \frac{1}{1+2\frac{b}{a}\alpha}\left[\sqrt{1+4b^2}\left\{\frac{WL^2}{M_p}\left[\frac{5}{384}-\frac{1}{24}\times+A\left(\frac{1}{32}-\frac{1}{8}\alpha\right)\right.\right.\right.$$

$$\left.-D\left(\frac{1}{32}+\frac{1}{24}\frac{b}{a}-\frac{1}{8}\alpha-\frac{1}{8}\frac{b}{a}\alpha\right)\right]-\left[\frac{1}{8}+\frac{1}{12}\frac{b}{a}-\frac{1}{12}\alpha-\frac{1}{4}\frac{b}{a}\alpha\right]\Bigg\}$$

$$\left.+\frac{1}{3}a\alpha-\frac{1}{12}a\alpha\frac{WL^2}{M_p}(A-D)\right]$$

$$+\frac{1}{6}a\frac{\alpha}{1+2\frac{b}{a}\alpha}\left\{\frac{I_o}{I_L}\frac{M_{QL}}{M_p}+\frac{I_o}{I_R}\frac{M_{QR}}{M_p}\right\}$$

$$+\frac{1}{6}a\frac{\alpha}{1+2\frac{b}{a}\alpha}\left\{\left(\frac{I_o}{I_L}+\frac{I_o}{I_R}-2\right)-\frac{1}{2}\left(\frac{I_o}{I_L}-1\right)\frac{WL^2}{M_p}(A-D)\right\}$$

...(7.43)

Case III.

$$\frac{\delta_D}{\phi_p L^2} = -\frac{1}{(1+\frac{b}{a})}\frac{1}{(1+2\frac{b}{a}\alpha)}\left[\sqrt{1+4b^2}\left\{\left[\frac{1}{8}+\frac{1}{12}\frac{b}{a}-\frac{1}{2}\alpha-\frac{1}{4}\frac{b}{a}\alpha\right]\right.\right.$$
$$+\frac{WL^2}{M_p}\left[\frac{1}{384}-\frac{1}{384}\frac{b}{a}-\frac{1}{48}\alpha+\frac{1}{96}\frac{b}{a}\alpha-(A-D)\left(\frac{1}{96}\frac{b}{a}-\frac{1}{16}\frac{b}{a}\right)\right]\Big\}$$
$$\left.-a\alpha\left\{\frac{1}{3}+\frac{WL^2}{M_p}\left[\frac{1}{24}-(A+D)\frac{1}{12}\frac{b}{a}\right]\right\}\right]$$

$$+\frac{1}{6}a\frac{\alpha}{(1+2\frac{b}{a}\alpha)}\left\{\frac{I_o}{I_L}\frac{M_{QL}}{M_p}+\frac{I_o}{I_R}\frac{M_{QR}}{M_p}\right\}$$
$$+a\alpha\left(\frac{I_o}{I_L}-1\right)\frac{1}{(1+\frac{b}{a})}\frac{1}{(1+2\frac{b}{a}\alpha)}\left\{\frac{1}{6}+\frac{WL^2}{M_p}\left[\frac{1}{48}-\frac{1}{24}(A-D)\right.\right.$$
$$\left.\left.-\frac{1}{12}\frac{b}{a}A\right]\right\}$$
$$+a\alpha\left(\frac{I_o}{I_R}-1\right)\frac{1}{(1+\frac{b}{a})}\frac{1}{(1+2\frac{b}{a}\alpha)}\left\{\frac{1}{6}+\frac{WL^2}{M_p}\left[\frac{1}{48}+\frac{1}{24}(A-D)\right.\right.$$
$$\left.\left.-\frac{1}{12}\frac{b}{a}D\right]\right\} \qquad \ldots(7.45)$$

Case IIIa.

$$\frac{\delta_D}{\phi_p L^2} = -\frac{1}{(1+\frac{b}{a})}\left[\sqrt{1+4b^2}\left\{\left[\frac{1}{8}+\frac{1}{12}\frac{b}{a}\right]+\frac{WL^2}{M_p}\left[\frac{1}{384}-\frac{1}{384}\frac{b}{a}\right.\right.\right.$$
$$\left.\left.\left.-\frac{1}{96}\frac{b}{a}(A+D)\right]\right\}\right]$$

No corr. ...(7.46)

Cases IV & IVa.

$$\frac{\delta_D}{\phi_p L^2} = \frac{1}{(1+\frac{b}{a})^2}\left[\sqrt{1+4b^2}\left\{\left[\frac{1}{8}+\frac{1}{24}\frac{b}{a}\right]+\frac{WL^2}{M_p}\left[\frac{3}{64}-\frac{1}{64}\frac{b}{a}\right.\right.\right.$$
$$\left.\left.\left.-\frac{1}{8}\frac{b}{a}(A+D)\right]\right\}-\frac{1}{6}a\left\{1+\frac{WL^2}{M_p}\left[\frac{1}{8}-\frac{1}{4}\frac{b}{a}(A+D)\right]\right\}\right]$$

(Graphic)

Cases IV & IVa. .(Correction)

$$+\frac{1}{12}a\frac{1}{(1+\frac{b}{a})}\left\{\frac{I_o}{I_L}\frac{MQ_L}{M_P}+\frac{I_o}{I_R}\frac{MQ_R}{M_P}\right\}$$

$$+\frac{1}{12}a\frac{1}{(1+\frac{b}{a})^2}\left\{\left(\frac{I_o}{I_L}+\frac{I_o}{I_R}-2\right)+\frac{WL^2}{M_P}\left[\frac{1}{8}\left(\frac{I_o}{I_L}+\frac{I_o}{I_R}-2\right)\right.\right.$$

$$\left.\left.+\frac{1}{4}(A-D)\left(\frac{I_o}{I_R}-\frac{I_o}{I_L}\right)-\frac{1}{2}\frac{b}{a}A\left(\frac{I_o}{I_L}-1\right)-\frac{1}{2}\frac{b}{a}D\left(\frac{I_o}{I_R}-1\right)\right]\right\}$$

...(7.47)

HINGE ANGLES -- NON-SELF-SUPPORTING SUBASSEMBLAGE

Cases I & II

$$\frac{H_E}{\phi_P L}=\frac{1}{(1-\alpha)}\left[\sqrt{1+4b^2}\left\{\frac{WL^2}{M_P}\left[\frac{1}{24}+\frac{5}{96}\frac{b}{a}-\frac{1}{12}\alpha-\frac{13}{96}\frac{b}{a}\alpha\right.\right.\right.$$

$$+A\left(\frac{1}{12}+\frac{1}{8}\frac{b}{a}-\frac{1}{4}\alpha-\frac{11}{24}\frac{b}{a}\alpha\right)-D\left(\frac{1}{12}+\frac{1}{4}\frac{b}{a}+\frac{1}{6}\frac{b^2}{a^2}-\frac{1}{4}\alpha\right.$$

$$\left.\left.\left.-\frac{17}{24}\frac{b}{a}\alpha-\frac{5}{12}\frac{b^2}{a^2}\alpha\right)\right]-\left[\frac{1}{2}+\frac{3}{4}\frac{b}{a}+\frac{1}{3}\frac{b^2}{a^2}-\alpha-2\frac{b}{a}\alpha-\frac{5}{6}\frac{b^2}{a^2}\alpha\right]\right\}$$

$$\left.+\frac{1}{3}a\alpha\left(1+2\frac{b}{a}\right)\left\{1-\frac{WL^2}{M_P}(A-D)\right\}\right]-\frac{1}{3}a$$

$$+\frac{\Delta c}{a\phi_P L^2}\frac{(1+2\frac{b}{a}\alpha)}{(1-\alpha)}+\frac{1}{3}a\alpha\frac{I_o}{I_L}\frac{MQ_L}{M_P}\frac{(1+2\frac{b}{a})}{(1-\alpha)}-\frac{1}{3}a\frac{I_o}{I_R}\frac{MQ_R}{M_P}$$

$$+\frac{1}{3}a\alpha\left(\frac{I_o}{I_L}-1\right)\left(\frac{1+2\frac{b}{a}}{1-\alpha}\right)\left\{1-\frac{WL^2}{M_P}(A-D)\right\}-\frac{1}{3}a\left(\frac{I_o}{I_R}-1\right)$$

...(7.48)

Cases I & II.

$$\frac{H_F}{\phi_p L} = \frac{1}{(1-\alpha)}\left[\sqrt{1+4b^2}\left\{\frac{WL^2}{M_p}\left[\frac{1}{24}+\frac{1}{6}(A-D)-\frac{1}{8}\frac{b}{a}D\right]\right.\right.$$
$$\left.\left.-\left[\frac{1}{2}+\frac{1}{4}\frac{b}{a}\right]\right\}-\frac{1}{3}a+\frac{1}{6}a\frac{WL^2}{M_p}(A-D)\right]$$

$$-\frac{1}{(1-\alpha)}\frac{\Delta c}{a\phi_p L^2}-\frac{1}{3}a\frac{I_o}{I_L}\frac{M_{QL}}{M_p}\frac{1}{(1-\alpha)}$$
$$-\frac{1}{3}a\left(\frac{I_o}{I_L}-1\right)\frac{1}{(1-\alpha)}\left\{1-\frac{1}{2}\frac{WL^2}{M_p}(A-D)\right\}$$

...(7.49)

Cases Ia & IIa.

$$\frac{H_E}{\phi_p L} = \sqrt{1+4b^2}\left\{\frac{1}{A-D}\left[\frac{1}{6}+\frac{5}{24}\frac{b}{a}-D\left(\frac{1}{2}\frac{b}{a}+\frac{2}{3}\frac{b^2}{a^2}\right)\right]\right.$$
$$\left.-\left[\frac{1}{6}+\frac{1}{4}\frac{b}{a}+\frac{1}{3}\frac{b^2}{a^2}\right]\right\}-\frac{1}{3}a$$

$$+\frac{\Delta c}{a\phi_p L^2}-\frac{1}{3}a\frac{I_o}{I_R}\frac{M_{QR}}{M_p}$$
$$-\frac{1}{3}a\left(\frac{I_o}{I_R}-1\right)$$

...(7.50)

Cases Ia & IIa.

$$\frac{H_c}{\phi_p L} = \sqrt{1+4b^2}\left\{\frac{1}{A-D}\left[\frac{1}{6}-\frac{1}{2}\frac{b}{a}D\right]+\left[\frac{1}{6}-\frac{1}{4}\frac{b}{a}\right]\right\}+\frac{1}{3}a$$

$$-\frac{\Delta c}{a\phi_p L^2}-\frac{1}{3}a\frac{I_o}{I_L}\frac{M_{QL}}{M_p}$$
$$+\frac{1}{3}a\left(\frac{I_o}{I_L}-1\right)$$

...(7.51)

Cases III & IV.

$$\frac{H_D}{\phi_p L} = \frac{1}{\left(1+\frac{b}{a}\right)\left(1+2\frac{b}{a}\right)(1-2\alpha)}\left[\sqrt{1+4b^2}\left\{-\left[1+\frac{3}{2}\frac{b}{a}+\frac{2}{3}\frac{b^2}{a^2}2\alpha\right.\right.\right.$$

$$-4\frac{b}{a}\alpha-\frac{5}{3}\frac{b^2}{a^2}\alpha\Big]-\frac{WL^2}{M_p}\left[\frac{1}{24}-\frac{1}{48}\frac{b^2}{a^2}-\frac{1}{12}\alpha-\frac{1}{16}\frac{b}{a}\alpha+\frac{1}{16}\frac{b^2}{a^2}\alpha\right.$$

$$+A\left(\frac{1}{12}-\frac{1}{24}\frac{b}{a}-\frac{1}{12}\frac{b^2}{a^2}\frac{5}{12}\frac{b}{a}\alpha+\frac{1}{2}\frac{b^2}{a^2}\alpha\right)-D\left(\frac{1}{12}+\frac{5}{24}\frac{b}{a}+\frac{1}{12}\frac{b^2}{a^2}\right.$$

$$\left.\left.\left.-\frac{1}{12}\frac{b}{a}\alpha-\frac{1}{6}\frac{b^2}{a^2}\alpha\right)\right]\right\}-\frac{2}{3}a(1-\alpha)\left\{1+\frac{WL^2}{M_p}\left[\frac{1}{8}+\frac{1}{4}(A-D)\right.\right.$$

$$\left.\left.-\frac{1}{2}\frac{b}{a}D\right]\right\}\Bigg]+\frac{1}{\left(1+\frac{b}{a}\right)(1-2\alpha)}\frac{2}{3}a\left\{1+\frac{WL^2}{M_p}\left[\frac{1}{8}-\frac{1}{4}(A-D)-\frac{1}{2}\frac{b}{a}A\right]\right\}$$

$$+\frac{2}{3}a\frac{I_o}{I_L}\frac{M_{QL}}{M_p}\frac{\alpha}{(1-2\alpha)}-\frac{2}{3}a\frac{I_o}{I_R}\frac{M_{QR}}{M_p}\frac{(1-\alpha)}{\left(1+2\frac{b}{a}\right)(1-2\alpha)}$$

$$+\frac{2\Delta_c}{a\phi_p L^2}\frac{\left(1+2\frac{b}{a}\alpha\right)}{\left(1+2\frac{b}{a}\right)(1-2\alpha)}$$

$$+\left(\frac{I_o}{I_L}-1\right)\frac{1}{\left(1+\frac{b}{a}\right)(1-2\alpha)}\frac{2}{3}a\left\{1+\frac{WL^2}{M_p}\left[\frac{1}{8}-\frac{1}{4}(A-D)-\frac{1}{2}\frac{b}{a}A\right]\right\}$$

$$-\left(\frac{I_o}{I_R}-1\right)\frac{(1-\alpha)}{\left(1+\frac{b}{a}\right)\left(1+2\frac{b}{a}\right)(1-2\alpha)}\frac{2}{3}a\left\{1+\frac{WL^2}{M_p}\left[\frac{1}{8}+\frac{1}{4}(A-D)-\frac{1}{2}\frac{b}{a}D\right]\right\}$$

...(7.52)

Cases III & IV

$$\frac{H_F}{\phi_p L} = \frac{1}{(1+\frac{b}{a})(1+2\frac{b}{a})(1-2\alpha)}\left[\sqrt{1+4b^2}\left\{\frac{WL^2}{M_p}\left[-\frac{1}{32}\frac{b}{a}+\frac{1}{96}\frac{b^2}{a^2}\right.\right.\right.$$

$$\left.+A\left(\frac{1}{12}+\frac{1}{6}\frac{b}{a}+\frac{1}{6}\frac{b^2}{a^2}\right)-D\left(\frac{1}{12}+\frac{1}{6}\frac{b}{a}\right)\right]-\left[\frac{1}{2}\frac{b}{a}+\frac{1}{6}\frac{b^2}{a^2}\right]\Bigg\}$$

$$\left.+\frac{1}{3}a\left\{1+\frac{WL^2}{M_p}\left[\frac{1}{8}+\frac{1}{4}(A-D)-\frac{1}{2}\frac{b}{a}D\right]\right\}\right]$$

$$-\frac{1}{3}a\frac{1}{(1+\frac{b}{a})(1-2\alpha)}\left\{1+\frac{WL^2}{M_p}\left[\frac{1}{8}-\frac{1}{4}(A-D)-\frac{1}{2}\frac{b}{a}A\right]\right\}$$

$$-\frac{2\Delta_c}{a\phi_p L^2}\frac{(1+\frac{b}{a})}{(1+2\frac{b}{a})(1-2\alpha)}-\frac{1}{3}a\frac{I_o}{I_L}\frac{M_{QL}}{M_p}\frac{1}{(1-2\alpha)}$$

$$+\frac{1}{3}a\frac{I_o}{I_R}\frac{M_{QR}}{M_p}\frac{1}{(1+2\frac{b}{a})(1-2\alpha)}$$

$$-\frac{1}{3}a\left(\frac{I_o}{I_L}-1\right)\frac{1}{(1+\frac{b}{a})(1-2\alpha)}\left\{1+\frac{WL^2}{M_p}\left[\frac{1}{8}-\frac{1}{4}(A-D)-\frac{1}{2}\frac{b}{a}A\right]\right\}$$

$$+\frac{1}{3}a\left(\frac{I_o}{I_R}-1\right)\frac{1}{(1+\frac{b}{a})(1+2\frac{b}{a})(1-2\alpha)}\left\{1+\frac{WL^2}{M_p}\left[\frac{1}{8}+\frac{1}{4}(A-D)-\frac{1}{2}\frac{b}{a}D\right]\right\}$$

...(7.53)

Cases IIIa & IVa.

$$\frac{H_D}{\phi_p L} = \frac{1}{(1+\frac{b}{a})(1+2\frac{b}{a})}\left[\sqrt{1+4b^2}\left\{-\left[1+\frac{3}{2}\frac{b}{a}+\frac{2}{3}\frac{b^2}{a^2}\right]-\frac{WL^2}{M_p}\left[\frac{1}{24}-\frac{1}{48}\frac{b^2}{a^2}\right.\right.\right.$$

$$\left.+A\left(\frac{1}{12}-\frac{1}{24}\frac{b}{a}-\frac{1}{12}\frac{b^2}{a^2}\right)-D\left(\frac{1}{12}+\frac{5}{24}\frac{b}{a}+\frac{1}{12}\frac{b^2}{a^2}\right)\right]\Bigg\}$$

$$\left.-\frac{2}{3}a\left\{1+\frac{WL^2}{M_p}\left[\frac{1}{8}+\frac{1}{4}(A-D)-\frac{1}{2}\frac{b}{a}D\right]\right\}\right]$$

$$+\frac{1}{(1+\frac{b}{a})}\frac{2}{3}a\left\{1+\frac{WL^2}{M_p}\left[\frac{1}{8}-\frac{1}{4}(A-D)-\frac{1}{2}\frac{b}{a}A\right]\right\}$$

.(Graphic)

Cases IIIa & IVa. .(Correction)

$$+\frac{2\Delta c}{a\phi_p L^2}\frac{1}{(1+2\frac{b}{a})}-\frac{2}{3}a\frac{I_o}{I_R}\frac{M_{QR}}{M_p}\frac{1}{(1+2\frac{b}{a})}$$

$$+\frac{2}{3}a\left(\frac{I_o}{I_L}-1\right)\frac{1}{(1+\frac{b}{a})}\left\{1+\frac{WL^2}{M_p}\left[\frac{1}{8}-\frac{1}{4}(A-D)-\frac{1}{2}\frac{b}{a}A\right]\right\}$$

$$-\frac{2}{3}a\left(\frac{I_o}{I_R}-1\right)\frac{1}{(1+\frac{b}{a})(1+2\frac{b}{a})}\left\{1+\frac{WL^2}{M_p}\left[\frac{1}{8}+\frac{1}{4}(A-D)-\frac{1}{2}\frac{b}{a}D\right]\right\}$$

...(7.54)

Cases IIIa & IVa.

$$\frac{H_c}{\phi_p L}=\frac{1}{(1+\frac{b}{a})(1+2\frac{b}{a})}\left[\sqrt{1+4b^2}\left\{\frac{WL^2}{M_p}\left[-\frac{1}{32}\frac{b}{a}+\frac{1}{96}\frac{b^2}{a^2}\right.\right.\right.$$

$$\left.+A\left(\frac{1}{12}+\frac{1}{6}\frac{b}{a}+\frac{1}{6}\frac{b^2}{a^2}\right)-D\left(\frac{1}{12}+\frac{1}{6}\frac{b}{a}\right)\right]-\left[\frac{1}{2}\frac{b}{a}+\frac{1}{6}\frac{b^2}{a^2}\right]$$

$$\left.\left.+\frac{1}{3}a\left\{1+\frac{WL^2}{M_p}\left[\frac{1}{8}+\frac{1}{4}(A-D)-\frac{1}{2}\frac{b}{a}D\right]\right\}\right]$$

$$-\frac{1}{3}a\frac{1}{(1+\frac{b}{a})}\left\{1+\frac{WL^2}{M_p}\left[\frac{1}{8}-\frac{1}{4}(A-D)-\frac{1}{2}\frac{b}{a}A\right]\right\}$$

$$-\frac{2\Delta c}{a\phi_p L^2}\frac{(1+\frac{b}{a})}{(1+2\frac{b}{a})}-\frac{1}{3}a\frac{I_o}{I_L}\frac{M_{QL}}{M_p}+\frac{1}{3}a\frac{I_o}{I_R}\frac{M_{QR}}{M_p}\frac{1}{(1+2\frac{b}{a})}$$

$$-\frac{1}{3}a\left(\frac{I_o}{I_L}-1\right)\frac{1}{(1+\frac{b}{a})}\left\{1+\frac{WL^2}{M_p}\left[\frac{1}{8}-\frac{1}{4}(A-D)-\frac{1}{2}\frac{b}{a}A\right]\right\}$$

$$+\frac{1}{3}a\left(\frac{I_o}{I_R}-1\right)\frac{1}{(1+\frac{b}{a})(1+2\frac{b}{a})}\left\{1+\frac{WL^2}{M_p}\left[\frac{1}{8}+\frac{1}{4}(A-D)-\frac{1}{2}\frac{b}{a}D\right]\right\}$$

...(7.55)

DEFLECTIONS -- LEE KNEE --
NON-SELF-SUPPORTING SUBASSEMBLAGE

Cases I & II.

$$\frac{\delta_E}{\phi_p L^2} = \frac{b}{1-\alpha}\left[\sqrt{1+4b^2}\left\{\frac{WL^2}{M_p}\left[\frac{5}{96}-\frac{13}{96}\alpha+A\left(\frac{1}{8}-\frac{11}{24}\alpha\right)\right.\right.\right.$$
$$\left.\left.-D\left(\frac{1}{8}+\frac{1}{6}\frac{b}{a}-\frac{11}{24}\alpha-\frac{5}{12}\frac{b}{a}\alpha\right)\right]-\left[\frac{1}{2}+\frac{1}{3}\frac{b}{a}-\frac{3}{2}\alpha-\frac{5}{6}\frac{b}{a}\alpha\right]\right\}$$
$$\left.+\frac{2}{3}a\alpha-\frac{1}{3}a\alpha\frac{WL^2}{M_p}(A-D)\right]$$

$$+\frac{\Delta_c}{\phi_p L^2}\frac{(1+2\frac{b}{a}\alpha-\alpha)}{(1-\alpha)}+\frac{2}{3}ab\frac{I_o}{I_L}\frac{M_{QL}}{M_p}\frac{\alpha}{(1-\alpha)}$$
$$+\frac{2}{3}ab\left(\frac{I_o}{I_L}-1\right)\frac{\alpha}{(1-\alpha)}-\frac{1}{3}ab\left(\frac{I_o}{I_L}-1\right)\frac{WL^2}{M_p}(A-D)\frac{\alpha}{(1-\alpha)}$$

...(7.56)

Cases Ia & IIa.

$$\frac{\delta_E}{\phi_p L^2} = b\sqrt{1+4b^2}\left\{\frac{1}{A-D}\left[\frac{5}{24}-\frac{2}{3}\frac{b}{a}D\right]-\frac{1}{3}\frac{b}{a}\right\}$$

$$+\frac{\Delta_c}{\phi_p L^2}$$

...(7.57)

Cases III, IV, IIIa, & IVa.

$$\frac{\delta_E}{\phi_p L^2} = \frac{1}{(1+\frac{b}{a})(1+2\frac{b}{a})}\left[b\sqrt{1+4b^2}\left\{\left[\frac{1}{2}+\frac{1}{6}\frac{b}{a}\right]+\frac{WL^2}{M_p}\left[\frac{1}{32}-\frac{1}{96}\frac{b}{a}\right.\right.\right.$$
$$\left.\left.+\frac{1}{12}(A-D)-\frac{1}{6}\frac{b}{a}D\right]\right\}+\frac{2}{3}ab\left\{1+\frac{WL^2}{M_p}\left[\frac{1}{8}+\frac{1}{4}(A-D)-\frac{1}{2}\frac{b}{a}D\right]\right\}\Bigg]$$

$$+\frac{\Delta_c}{\phi_p L^2}\frac{1}{(1+2\frac{b}{a})}+\frac{2}{3}ab\frac{I_o}{I_R}\frac{M_{QR}}{M_p}\frac{1}{(1+2\frac{b}{a})}$$
$$+\frac{2}{3}ab\left(\frac{I_o}{I_R}-1\right)\left\{1+\frac{WL^2}{M_p}\left[\frac{1}{8}+\frac{1}{4}(A-D)-\frac{1}{2}\frac{b}{a}D\right]\right\}$$

...(7.58)

DEFLECTIONS -- RIDGE --
NON-SELF-SUPPORTING SUBASSEMBLAGE

Cases I & II.

$$\frac{\delta_D}{\phi_p L^2} = \frac{1}{(1-\alpha)}\left[\sqrt{1+4b^2}\left\{\frac{WL^2}{M_p}\left[\frac{5}{384}-\frac{13}{384}\alpha+A\left(\frac{1}{32}-\frac{11}{96}\alpha\right)\right.\right.\right.$$
$$\left.\left.-D\left(\frac{1}{32}+\frac{1}{24}\frac{b}{a}-\frac{11}{96}\alpha-\frac{5}{48}\frac{b}{a}\alpha\right)\right]-\left[\frac{1}{8}+\frac{1}{12}\frac{b}{a}-\frac{3}{8}\alpha-\frac{5}{24}\frac{b}{a}\alpha\right]\right\}$$
$$\left.+\frac{1}{6}a\alpha\left\{1-\frac{1}{2}\frac{WL^2}{M_p}(A-D)\right\}\right]$$

$$-\frac{\Delta c}{a\phi_p L^2}\frac{\alpha}{(1-\alpha)}+\frac{1}{6}a\frac{I_o}{I_L}\frac{M_{QL}}{M_p}\frac{\alpha}{(1-\alpha)}$$
$$+\frac{1}{6}a\left(\frac{I_o}{I_L}-1\right)\frac{\alpha}{(1-\alpha)}\left\{1-\frac{1}{2}\frac{WL^2}{M_p}(A-D)\right\}$$

...(7.59)

Cases Ia & IIa.

$$\frac{\delta_D}{\phi_p L^2} = \sqrt{1+4b^2}\left\{\frac{1}{(A-D)}\left[\frac{5}{96}-\frac{1}{6}\frac{b}{a}D\right]-\frac{1}{12}\frac{b}{a}\right\}$$

No corr.

...(7.60)

Cases III, IV, IIIa, & IVa.

$$\frac{\delta_D}{\phi_p L^2} = \frac{1}{(1+\frac{b}{a})(1+2\frac{b}{a})}\left[\sqrt{1+4b^2}\left\{\left[\frac{1}{8}+\frac{1}{24}\frac{b}{a}\right]+\frac{WL^2}{M_p}\left[\frac{1}{128}-\frac{1}{384}\frac{b}{a}\right.\right.\right.$$
$$\left.\left.+\frac{1}{48}(A-D)-\frac{1}{24}\frac{b}{a}D\right]\right\}+\frac{1}{6}a\left\{1+\frac{WL^2}{M_p}\left[\frac{1}{8}+\frac{1}{4}(A-D)-\frac{1}{2}\frac{b}{a}D\right]\right\}$$

$$-\frac{1}{2}\frac{\Delta c}{a\phi_p L^2}\frac{1}{(1+2\frac{b}{a})}+\frac{1}{6}a\frac{I_o}{I_R}\frac{M_{QR}}{M_p}\frac{1}{(1+2\frac{b}{a})}$$
$$+\frac{1}{6}\left(\frac{I_o}{I_R}-1\right)\frac{1}{(1+\frac{b}{a})(1+2\frac{b}{a})}\left\{1+\frac{WL^2}{M_p}\left[\frac{1}{8}+\frac{1}{4}(A-D)-\frac{1}{2}\frac{b}{a}D\right]\right\}$$

...(7.61)

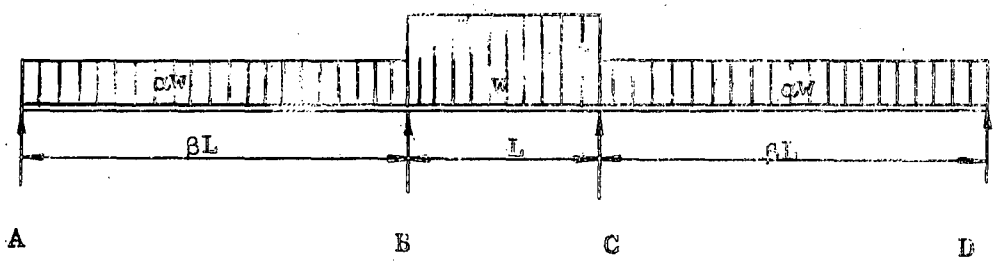

FIG. 2.1 THREE SPAN CONTINUOUS BEAM

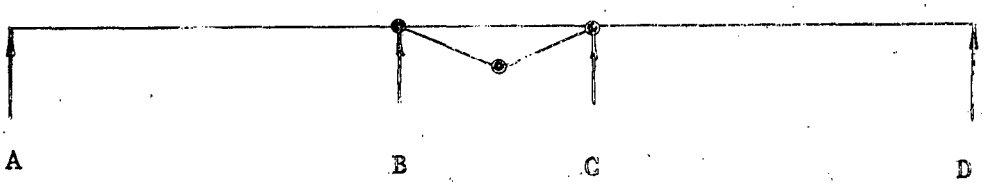

FIG. 2.2 POSSIBLE MECHANISM FOR THREE SPAN CONTINUOUS BEAM

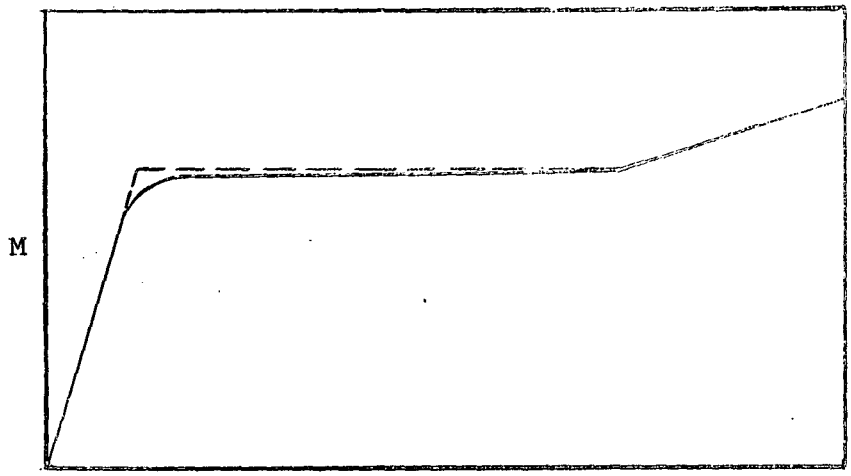

FIG. 2.3—ACTUAL M-ø CURVE FOR WF SHAPE

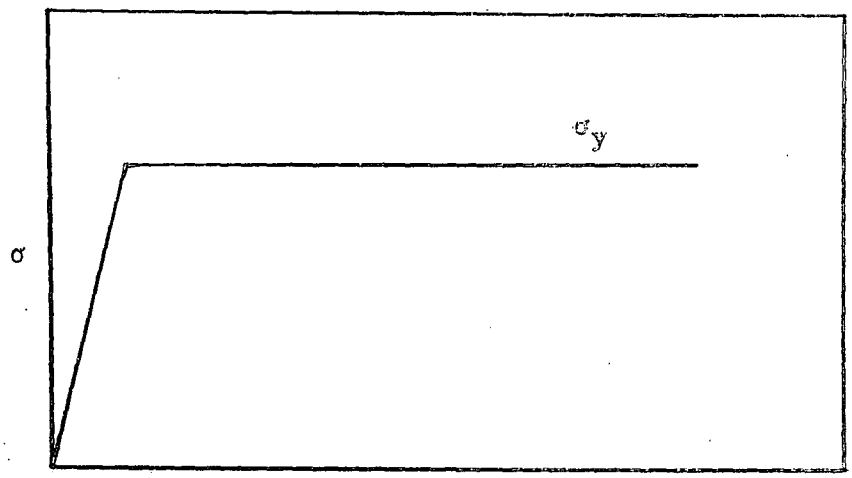

FIG. 2.4 IDEALIZED STRESS-STRAIN CURVE

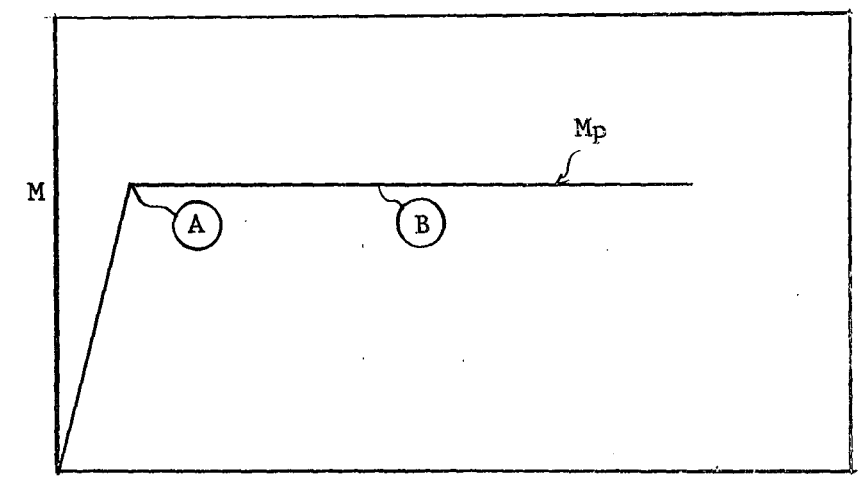

FIG. 2.5 IDEALIZED M-ø CURVE

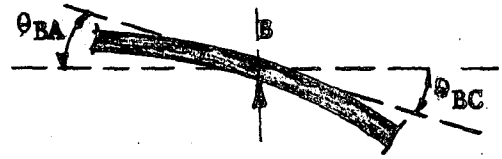

$$\theta_{BA} = \theta_{BC}$$

Elastic slope or
slope prior to formation
of plastic hinge

FIG. 2.6a

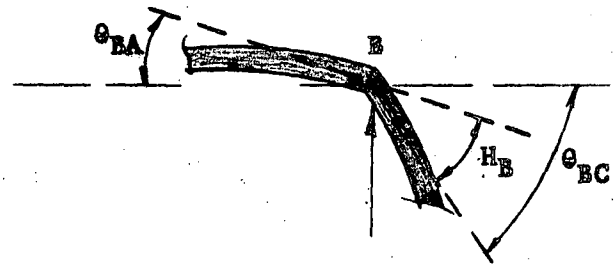

$$\theta_{BA} \neq \theta_{BC}$$

$$H_B = \theta_{BC} - \theta_{BA}$$

FIG. 2.6b

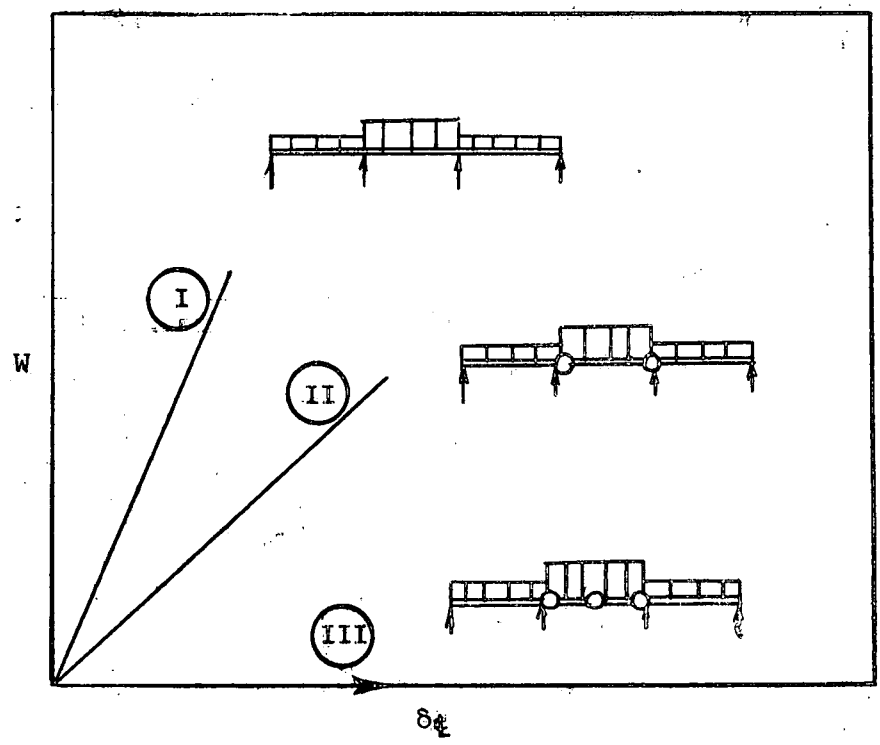

FIG. 2.7 INCREMENTAL BEHAVIOR OF BEAM FORMING A MECHANISM

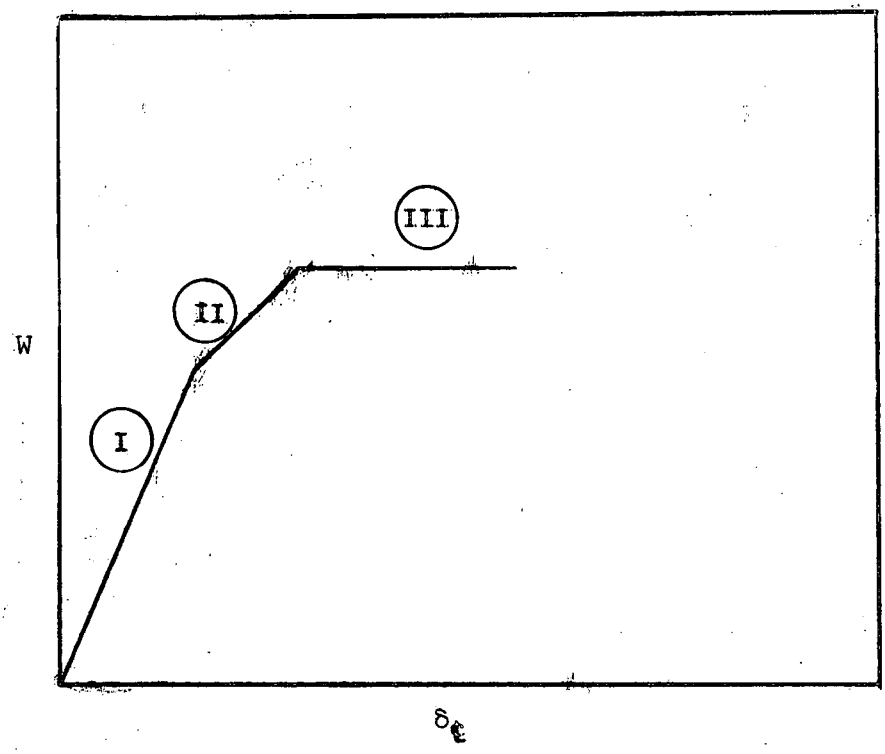

FIG. 2.8 TOTAL BEHAVIOR OF BEAM FORMING A MECHANISM

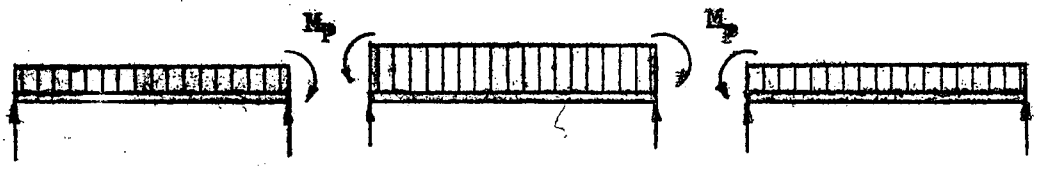

FIG. 2.9

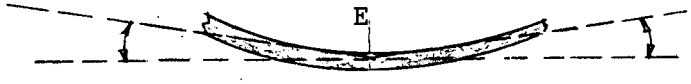

$\theta_{EB} = \theta_{EC}$

FIG. 2.10a

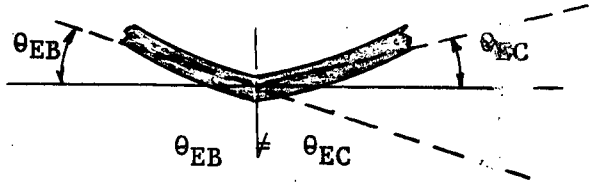

FIG. 2.10b

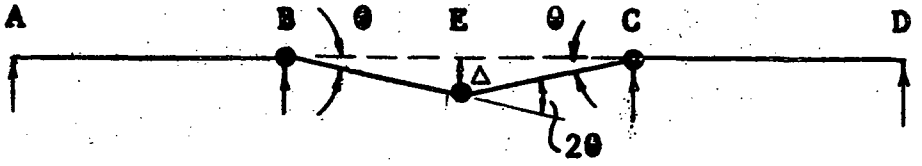

FIG. 2.11a

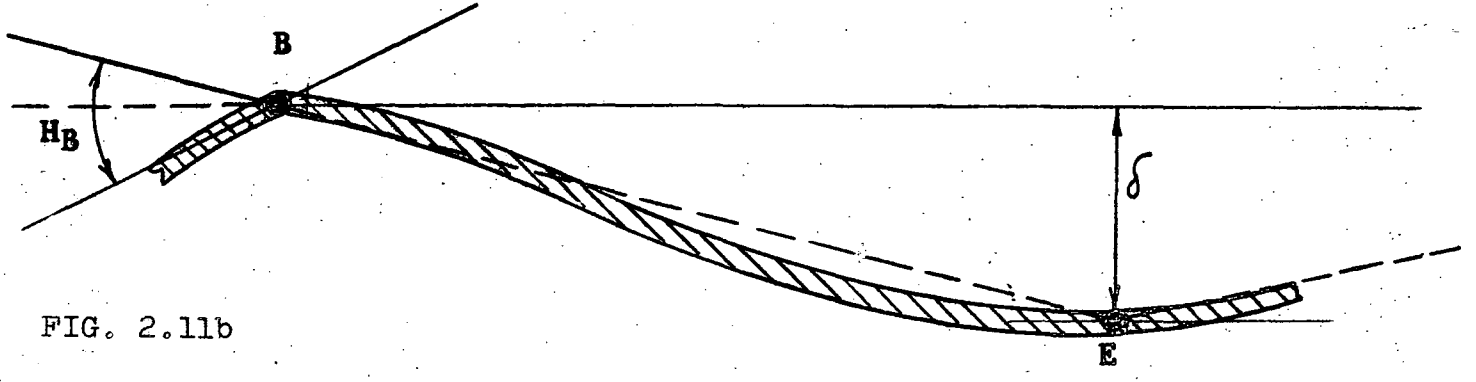

FIG. 2.11b

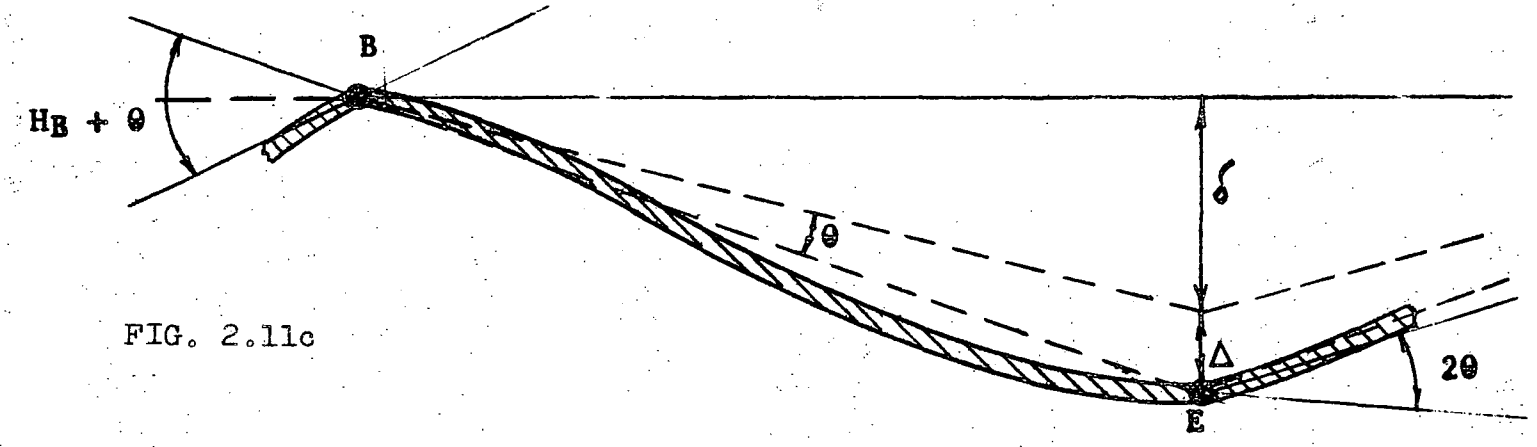

FIG. 2.11c

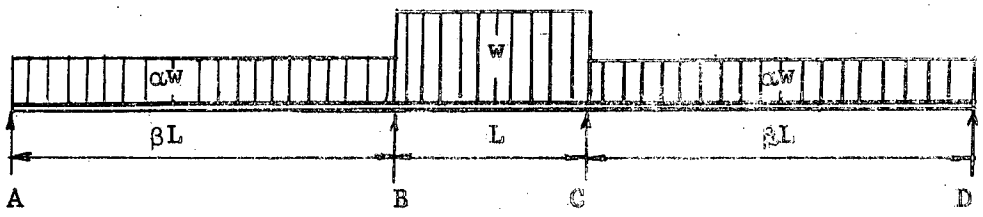

(a) Beam Dimensions and Loading

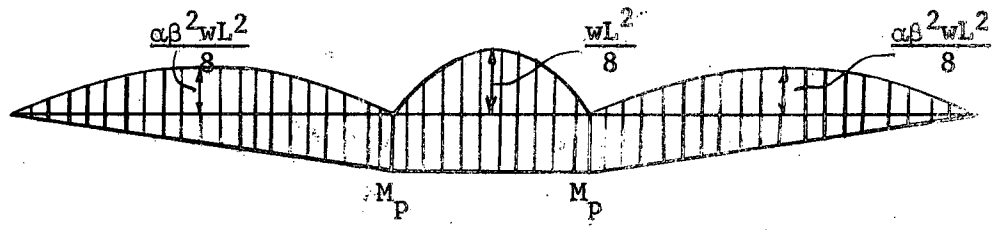

(b) Moment Diagram

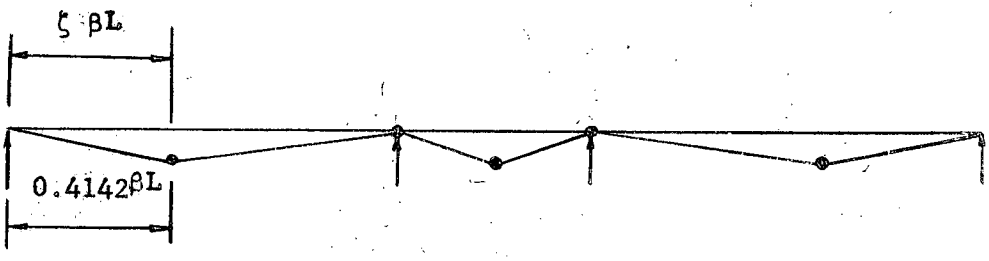

(c) Possible Mechanisms

FIG. 4.1 BEAM DIMENSIONS, LOADING, MOMENT DIAGRAM, AND POSSIBLE MECHANISMS

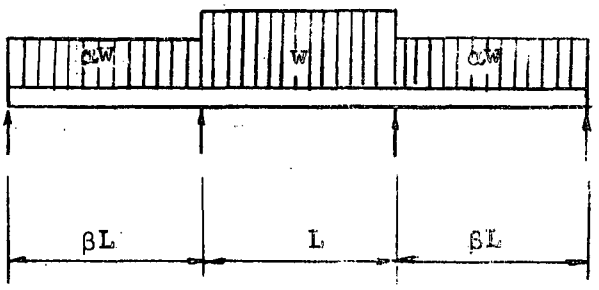

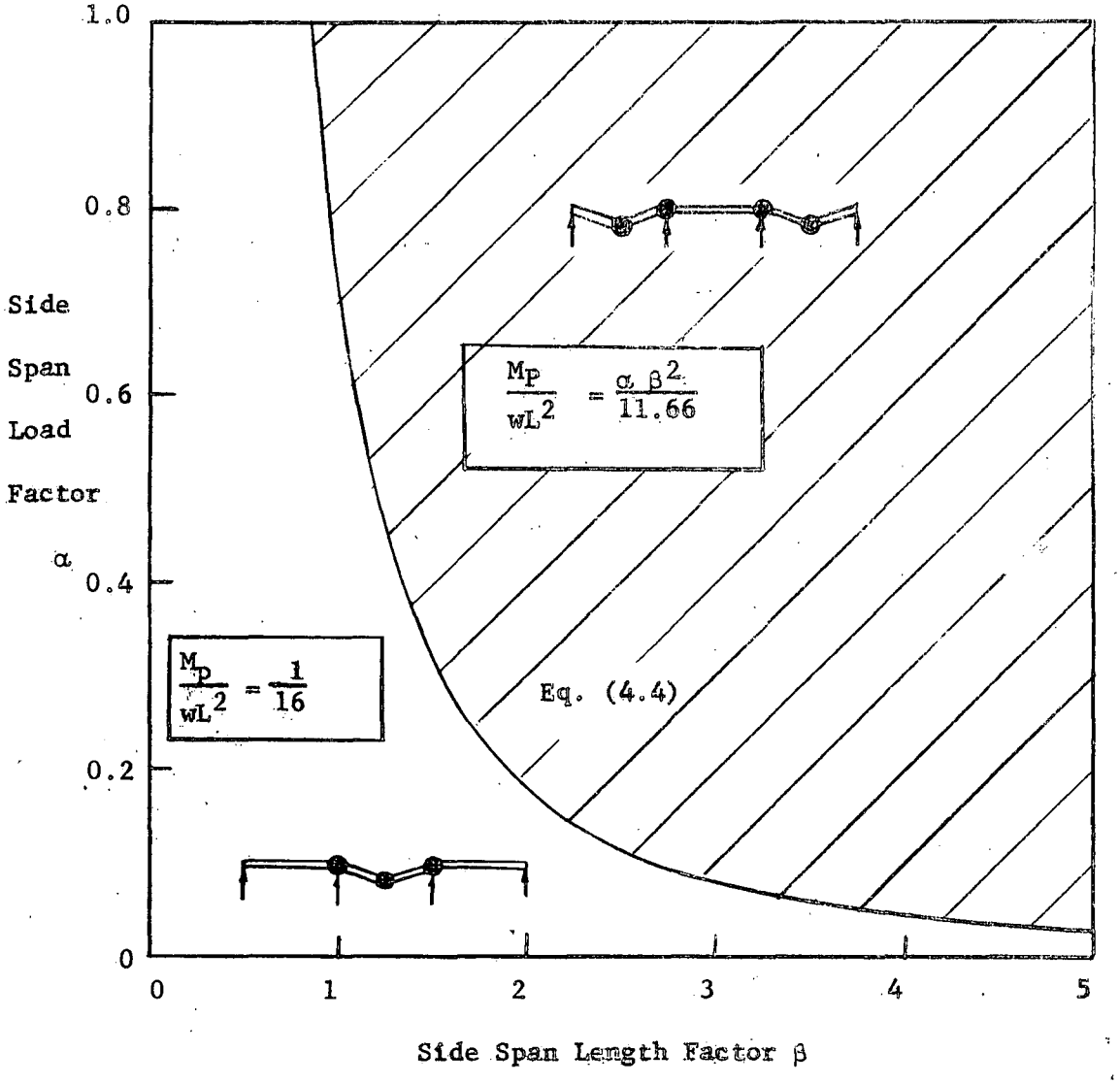

FIG. 4.2 TYPE OF MECHANISM

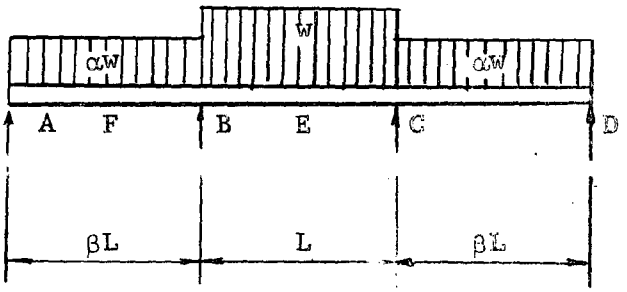

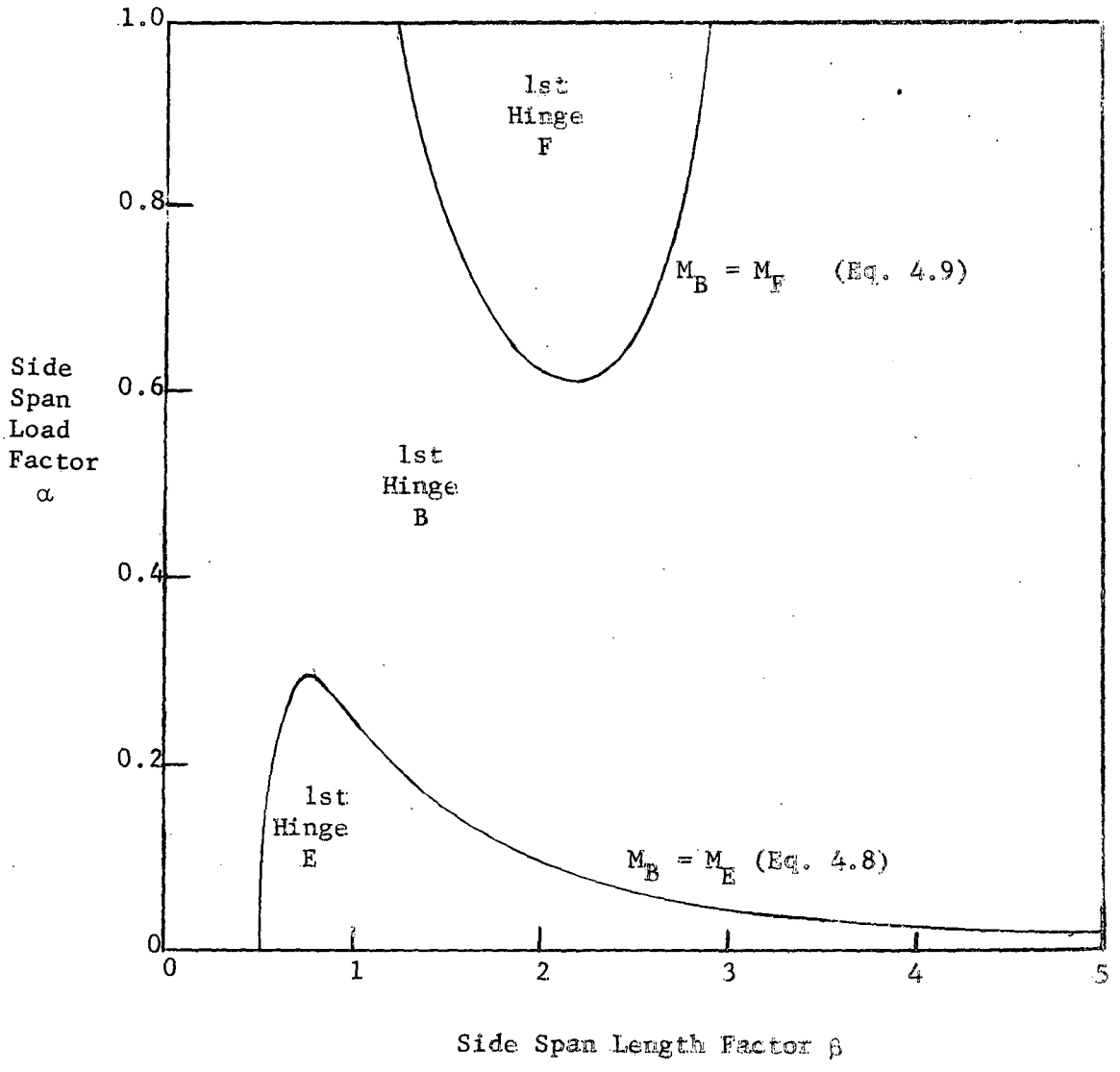

FIG. 4.3 LOCATION OF FIRST PLASTIC HINGE

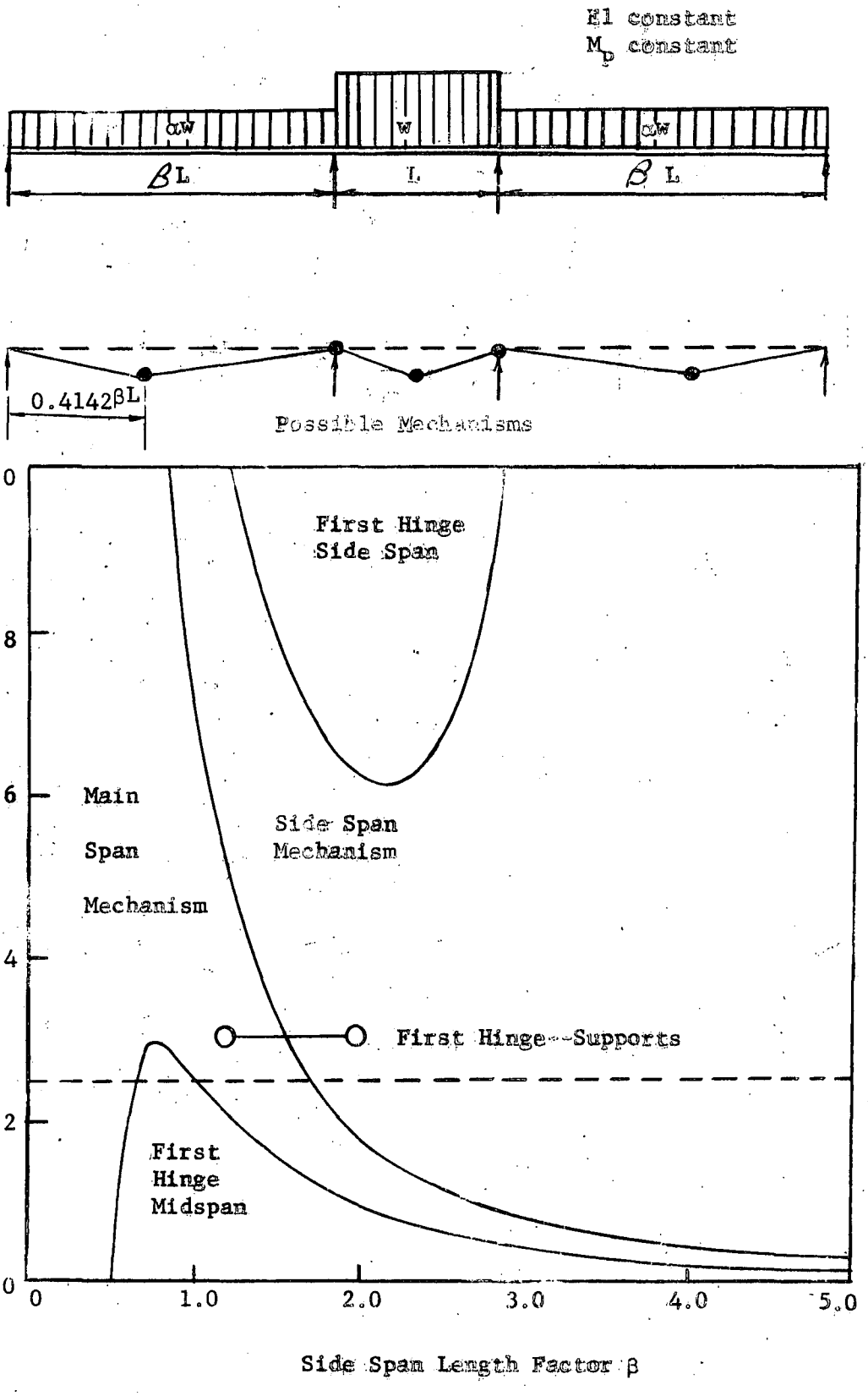

FIG. 4.4 LIMITS OF MECHANISMS

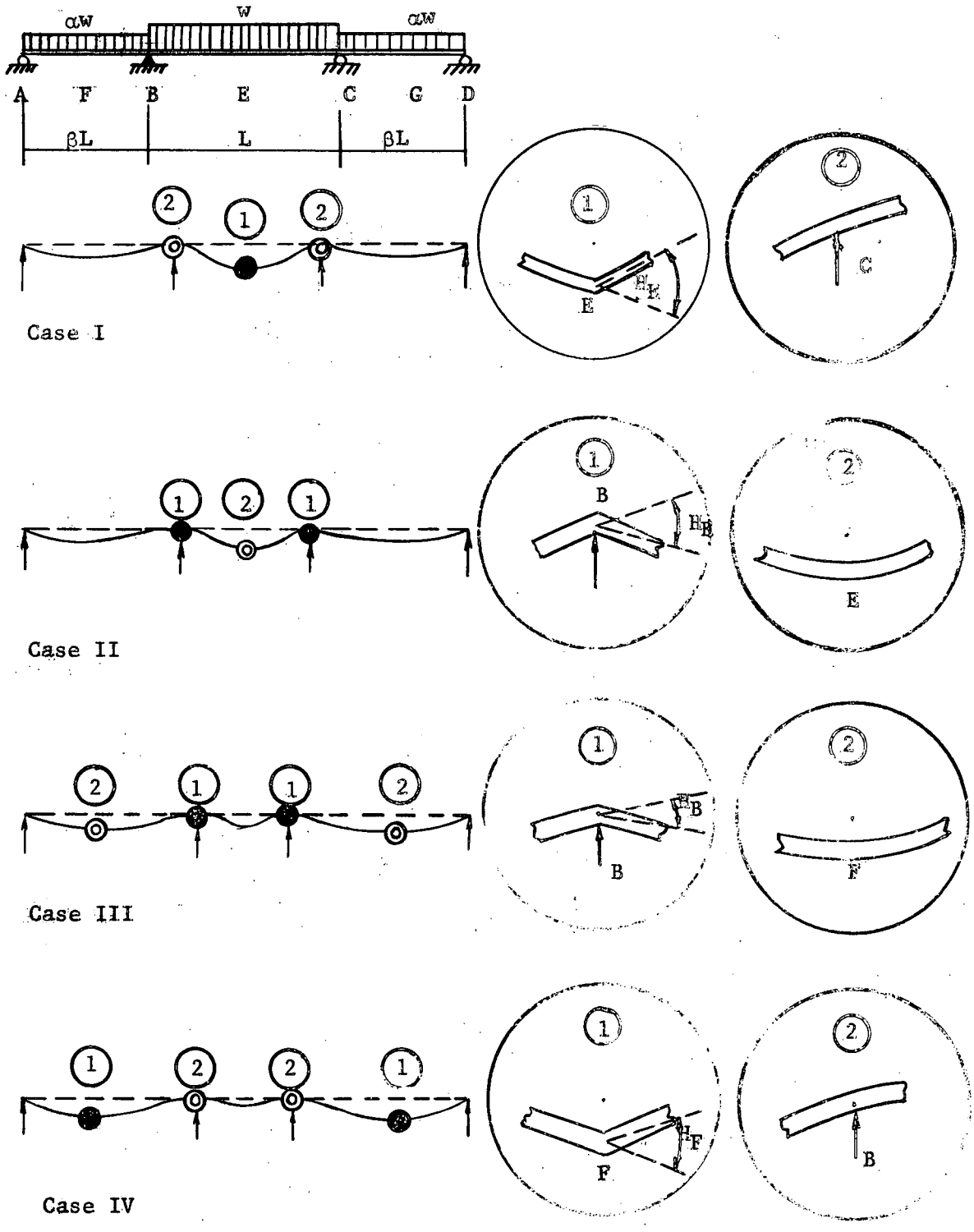

FIG. 4.5 POSSIBLE ORDER OF FORMATION OF PLASTIC HINGES

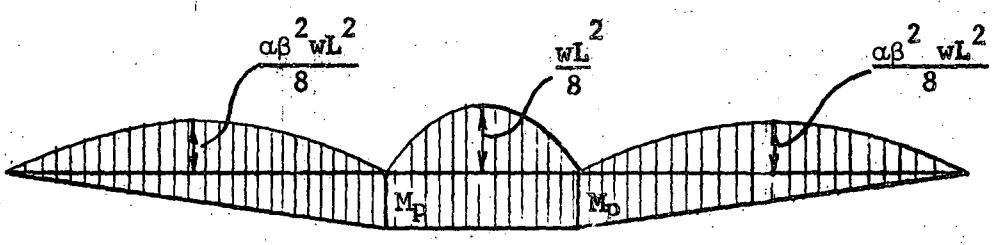

Case I First Hinge in Main Span

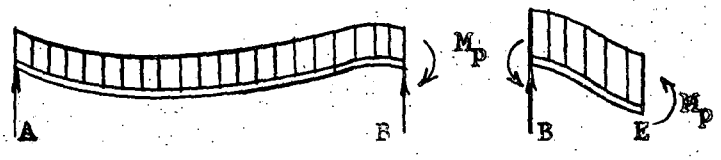

$\delta = 0$	$\delta = 0$	$\delta = ?$
$\theta = ?$	$\theta_{BA} = \theta_{BE}$	$\theta = ? = \theta_{EB}$
$M = 0$	$M = M_p$	$M = M_p$

Case II & **Case III** First Hinge at Interior Support

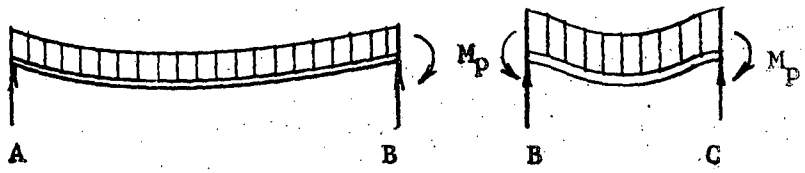

$\delta = 0$	$\delta = 0$	$\delta = 0$
$\theta = ?$	$\theta = ? = \theta_{BA}$	$\theta = ? = \theta_{BC}$
$M = 0$	$M = M_p$	$M = M_p$

Case IV First Hinge in Side Span

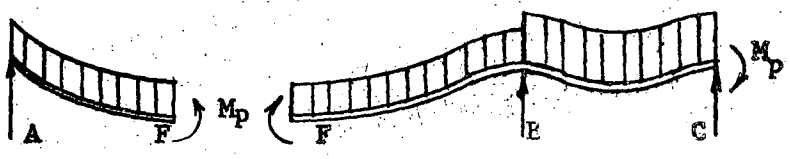

$\delta = 0$	$\delta = ?$	$\delta = ?$	$\delta = 0$
$\theta = ?$	$\theta = ? = \theta_{FA}$	$\theta = ? = \theta_{FB}$	$\theta_{BF} = \theta_{BC}$
$M = 0$	$M = M_p$	$M = M_p$	$M = M_p$

FIG. 4.6 BOUNDARY CONDITIONS FOR CALCULATING HINGE ANGLES

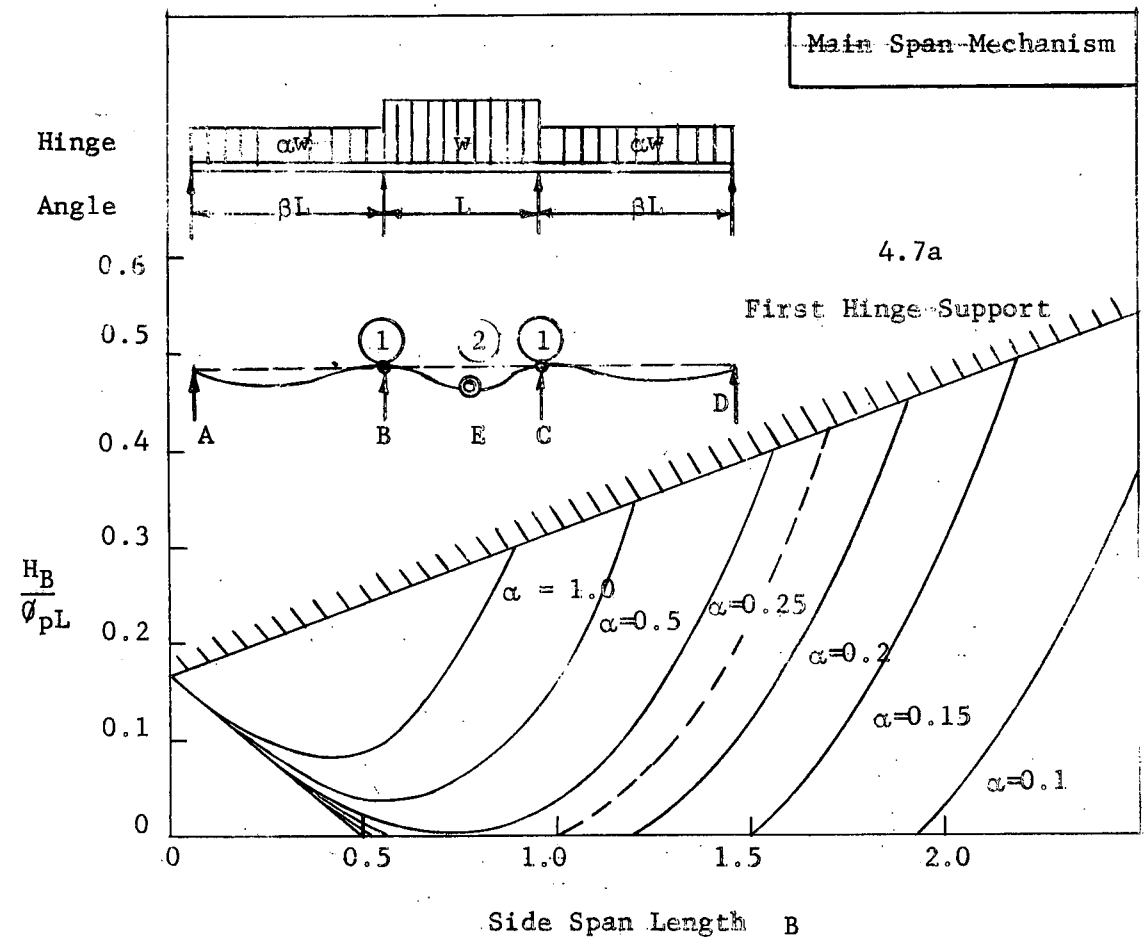

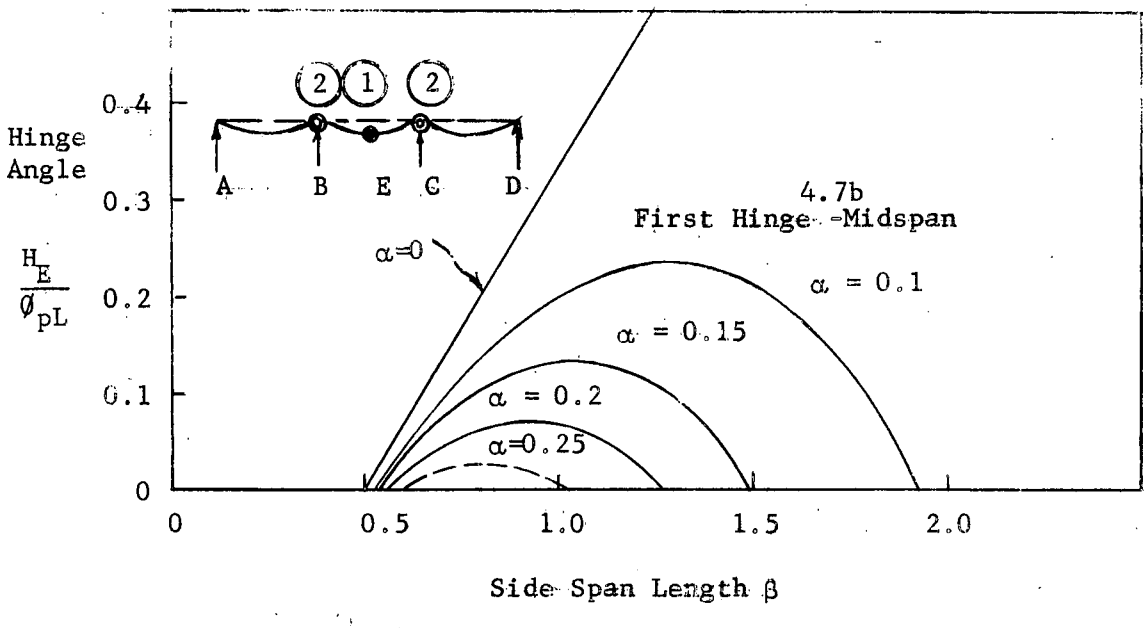

FIG. 4.7 HINGE ANGLES FOR MAINSPAN MECHANISM

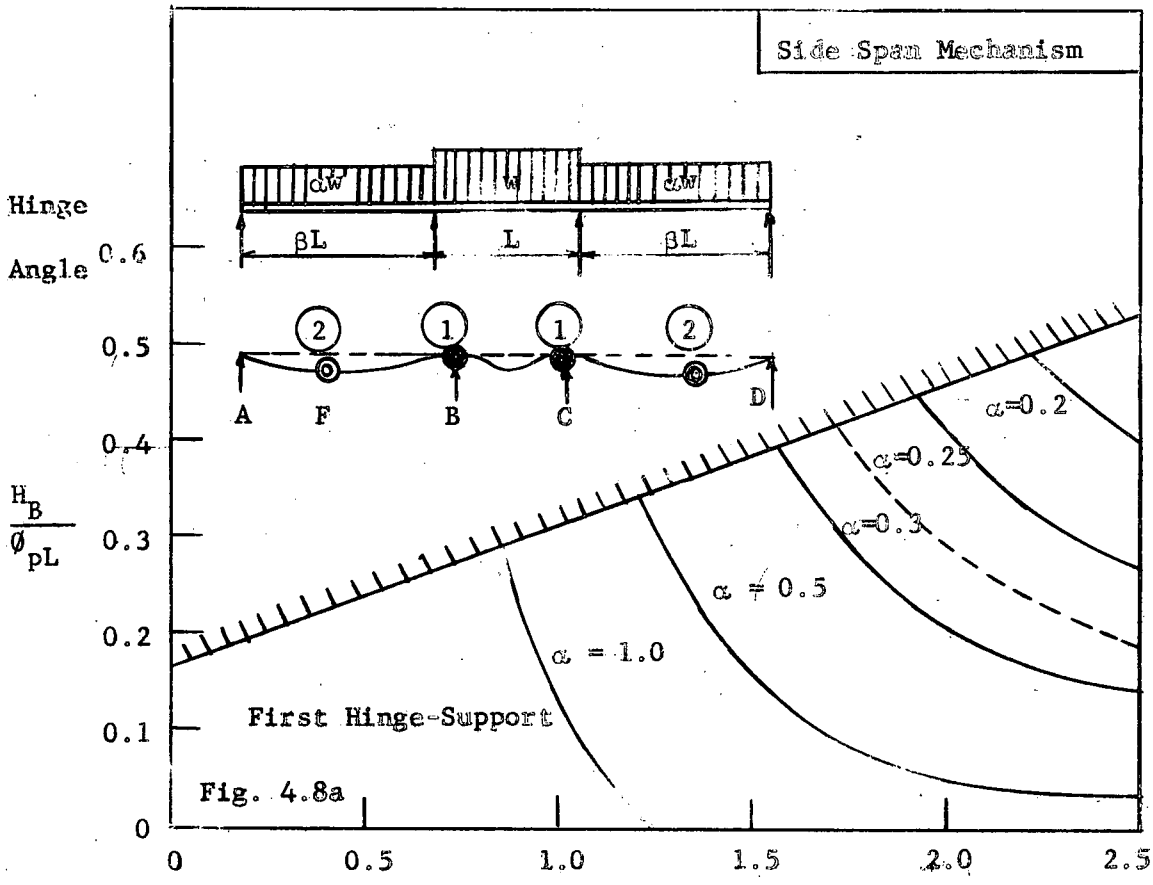

Fig. 4.8a

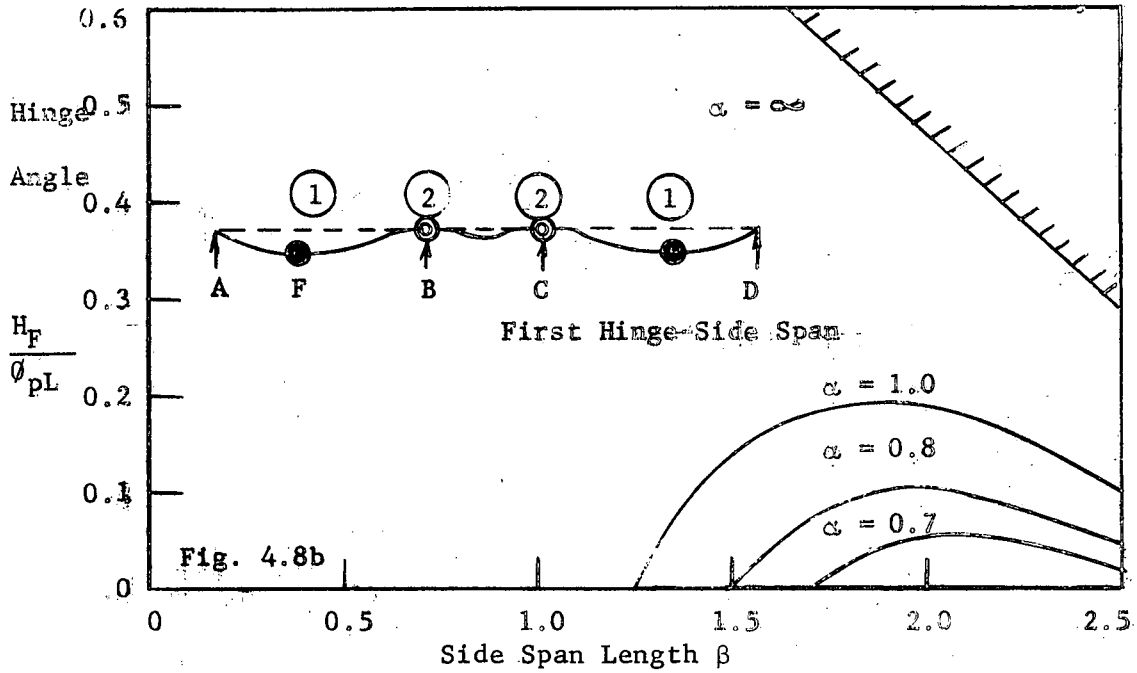

Fig. 4.8b

FIG. 4.8 HINGE ANGLES FOR SIDE SPAN MECHANISM

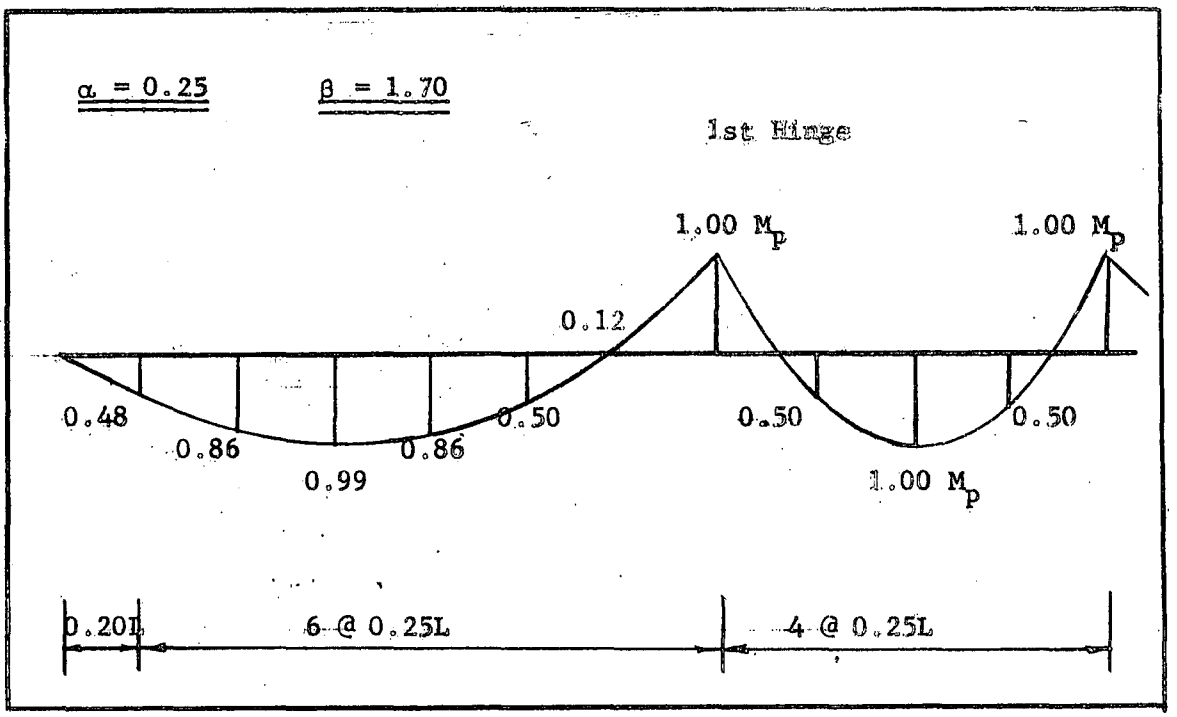

(a) Moment Diagram for Three-Span Beam (14WF30)

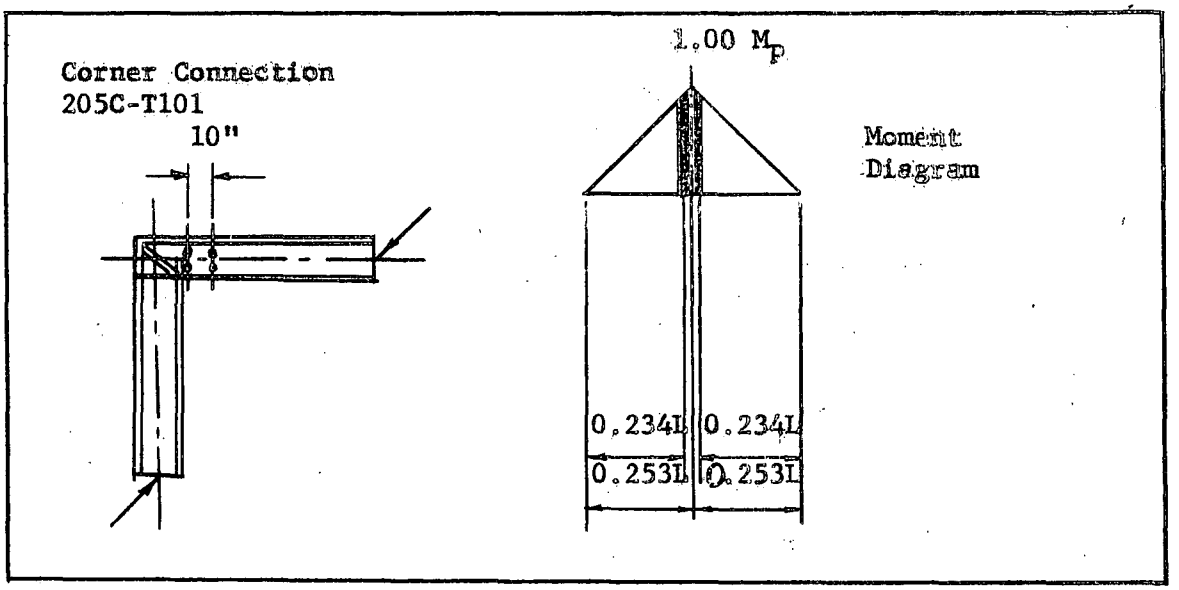

(b) Moment Diagram for Corner Connection (14WF30)

FIG. 4.9 COMPARISON OF MOMENT DIAGRAM FOR THEORETICAL EXAMPLE OF THREE-SPAN BEAM WITH MOMENT DIAGRAM FOR EXPERIMENTAL TEST OF CORNER CONNECTION

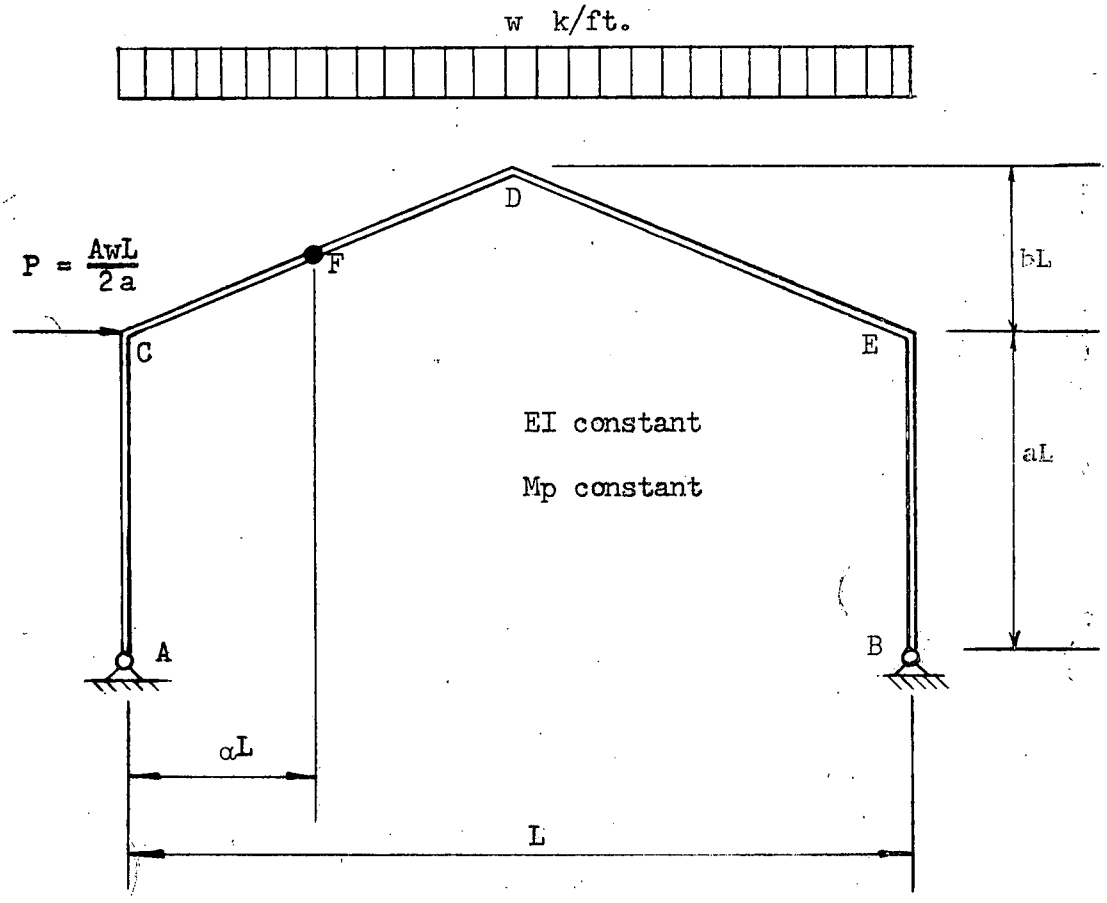

FIG. 3.1 FRAME DIMENSIONS AND LOADING

Panel Mechanism (a)

Composite Mechanism (b)

FIG. 5.2 POSSIBLE MECHANISMS FOR SINGLE-SPAN FRAME

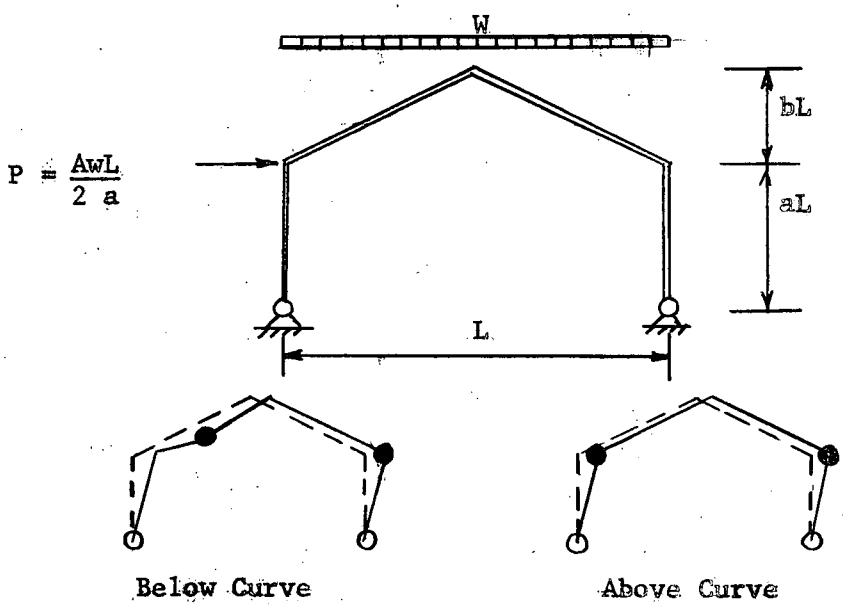

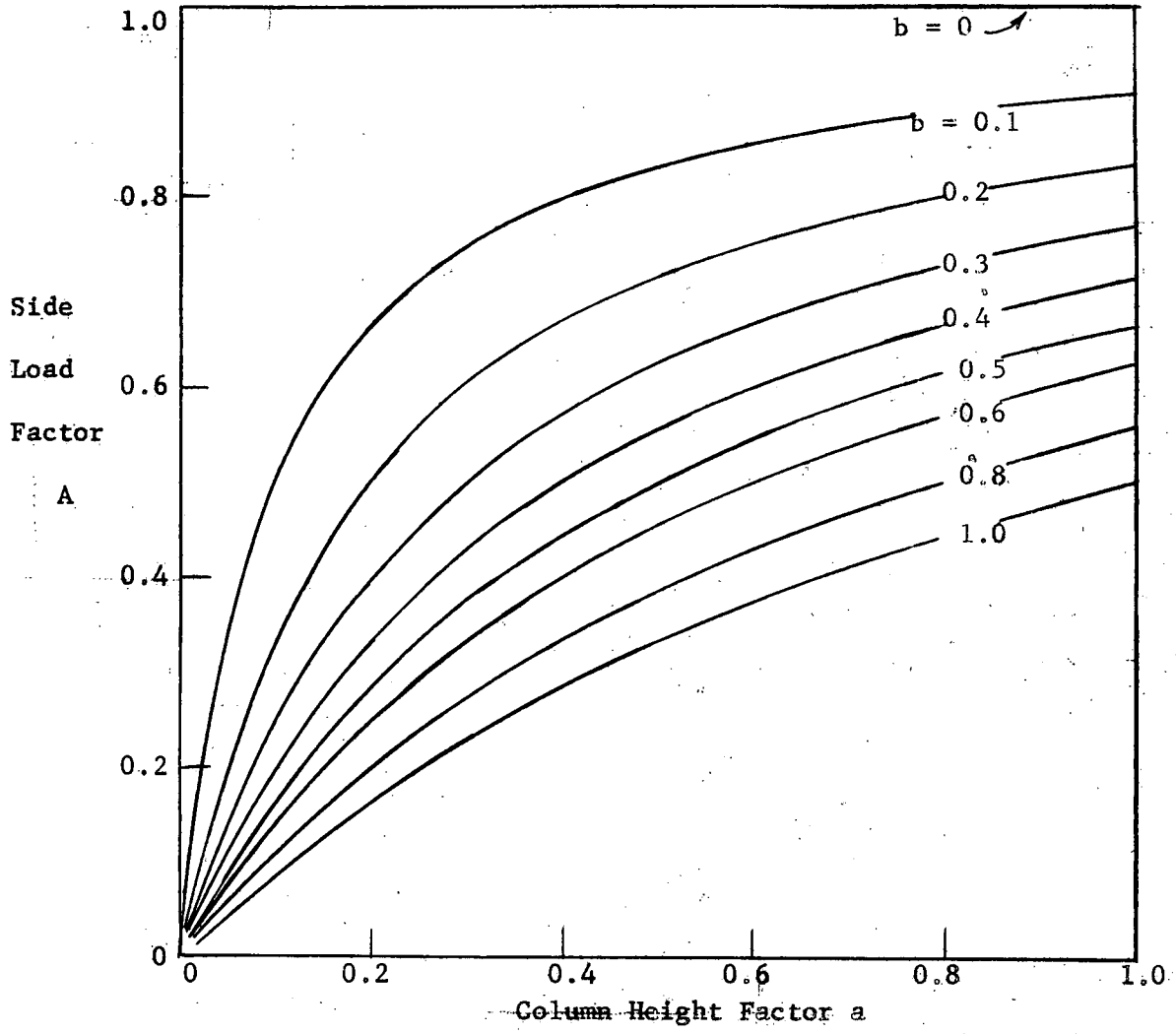

Fig. 5.3. TYPE OF MECHANISM

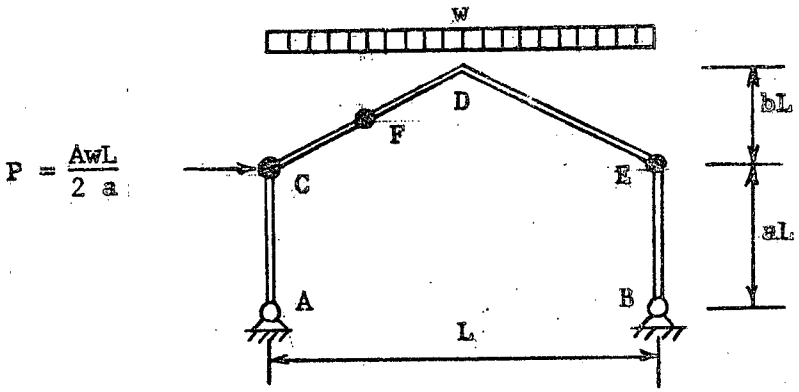

KEY:

Above Solid Line	-	First Hinge C
Below Dashed Line	-	" " F
Between Lines	-	" " E

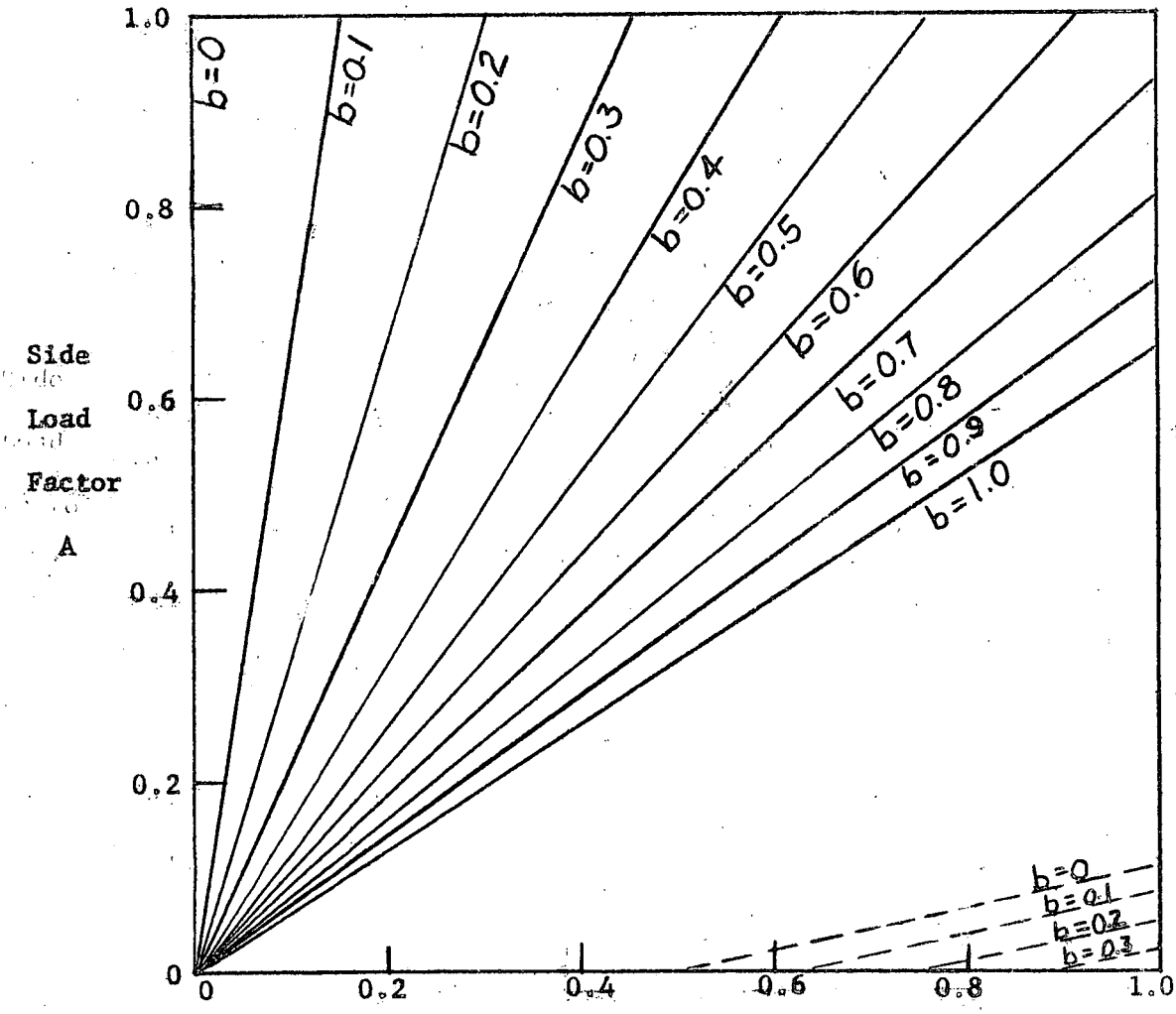

Fig. 5.4 LOCATION OF FIRST PLASTIC HINGE

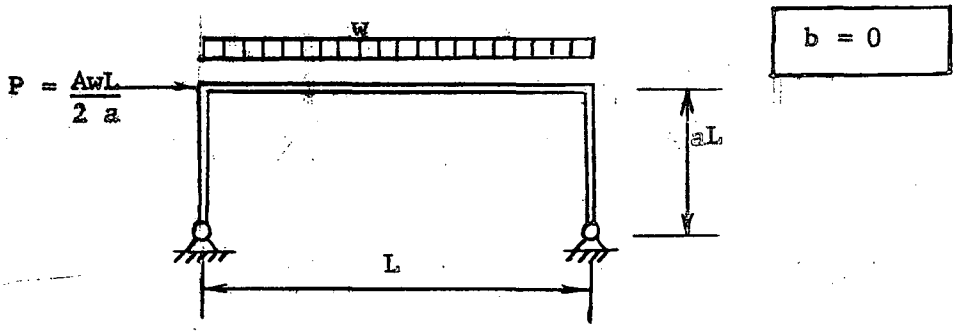

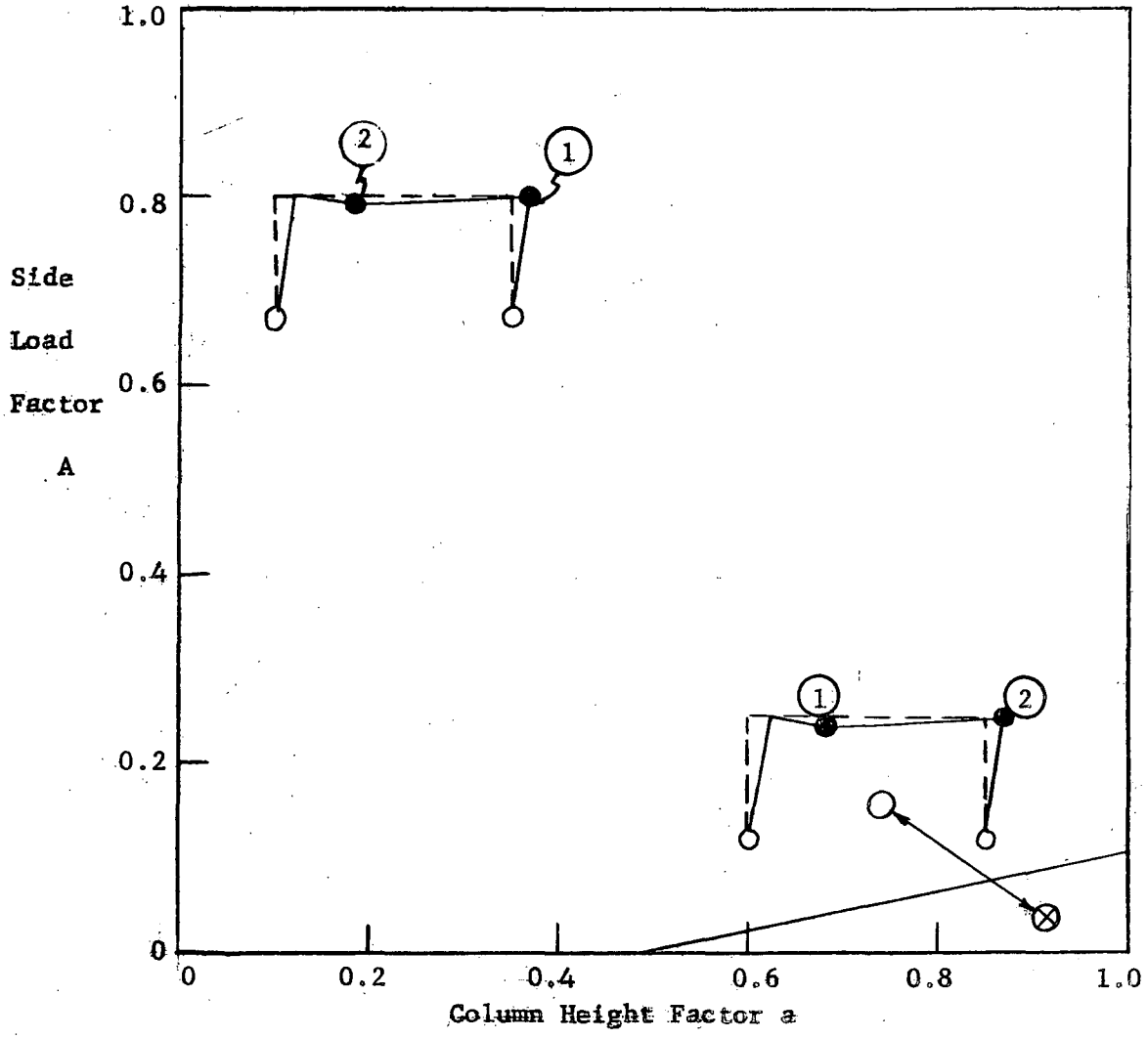

Fig. 5.5 LIMITS OF MECHANISMS (b = 0)

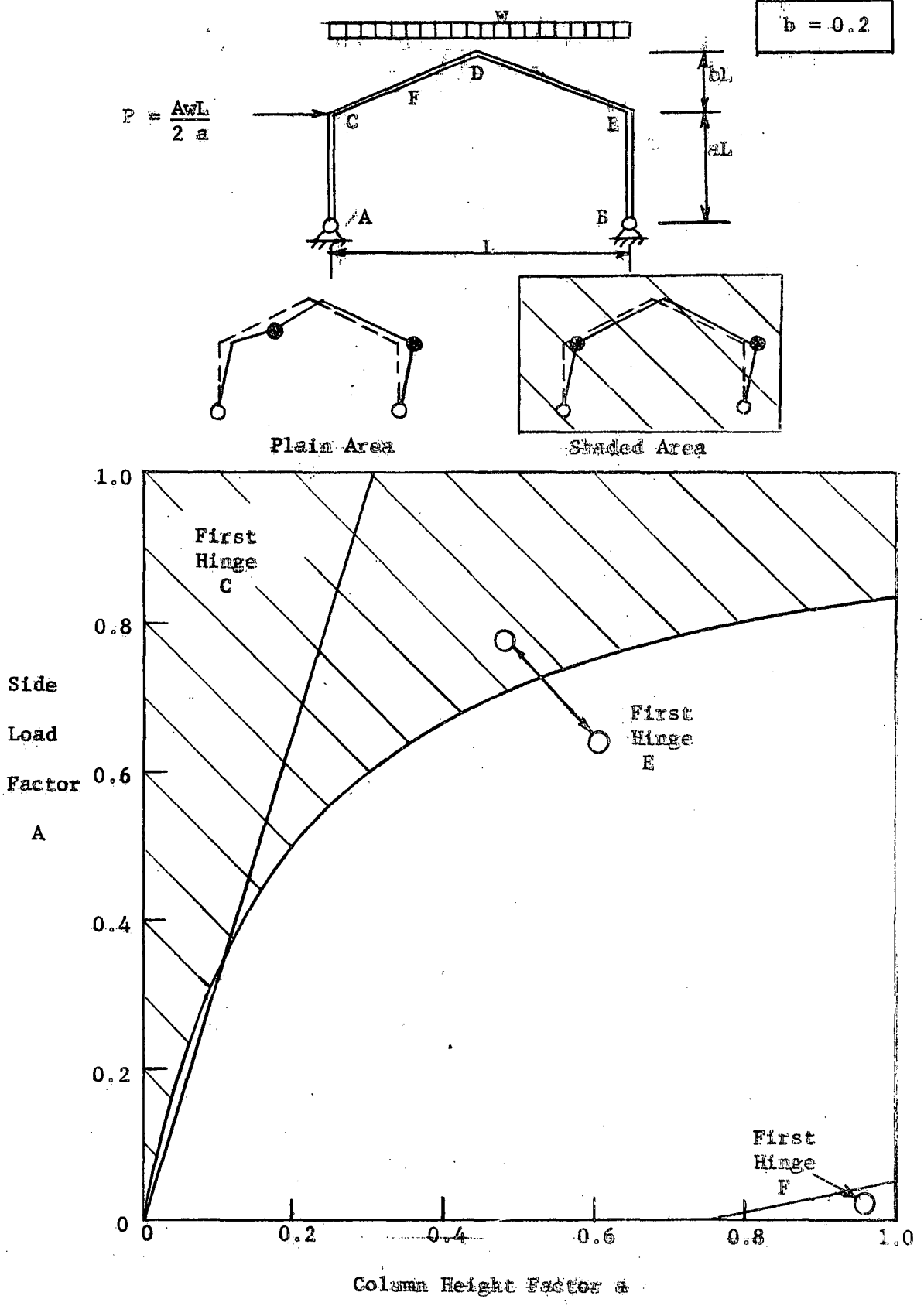

Fig. 5.6 LIMITS OF MECHANISMS (b = 0.2)

b = 0.5

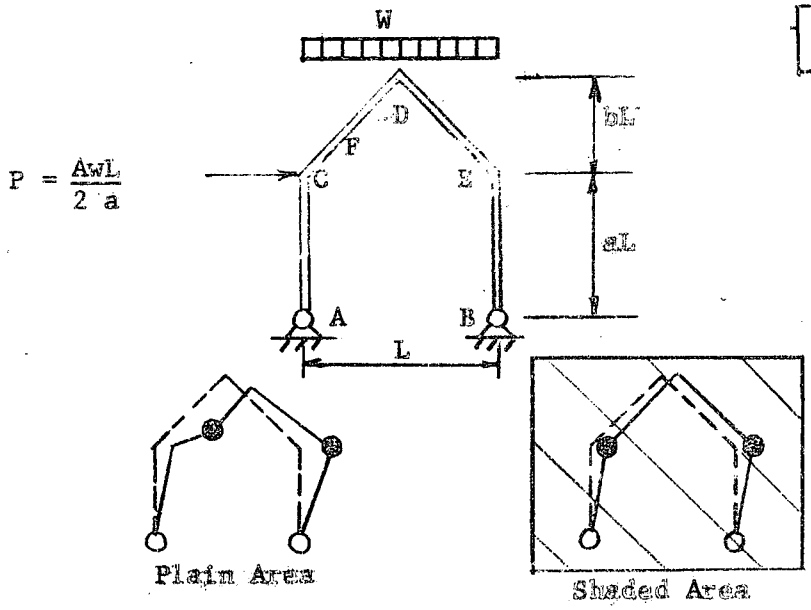

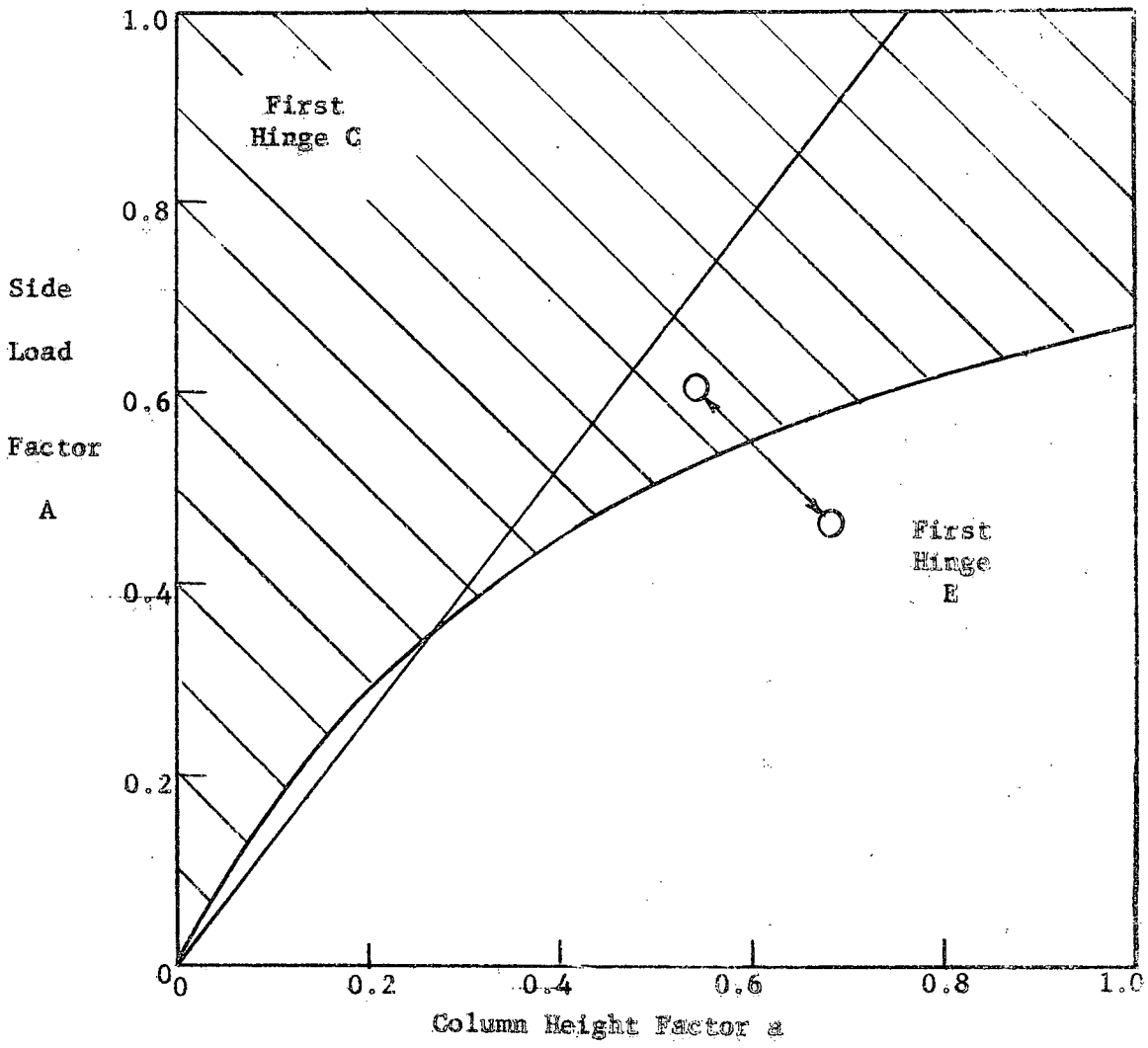

Fig. 5.7 LIMITS OF MECHANISMS (b=0.5)

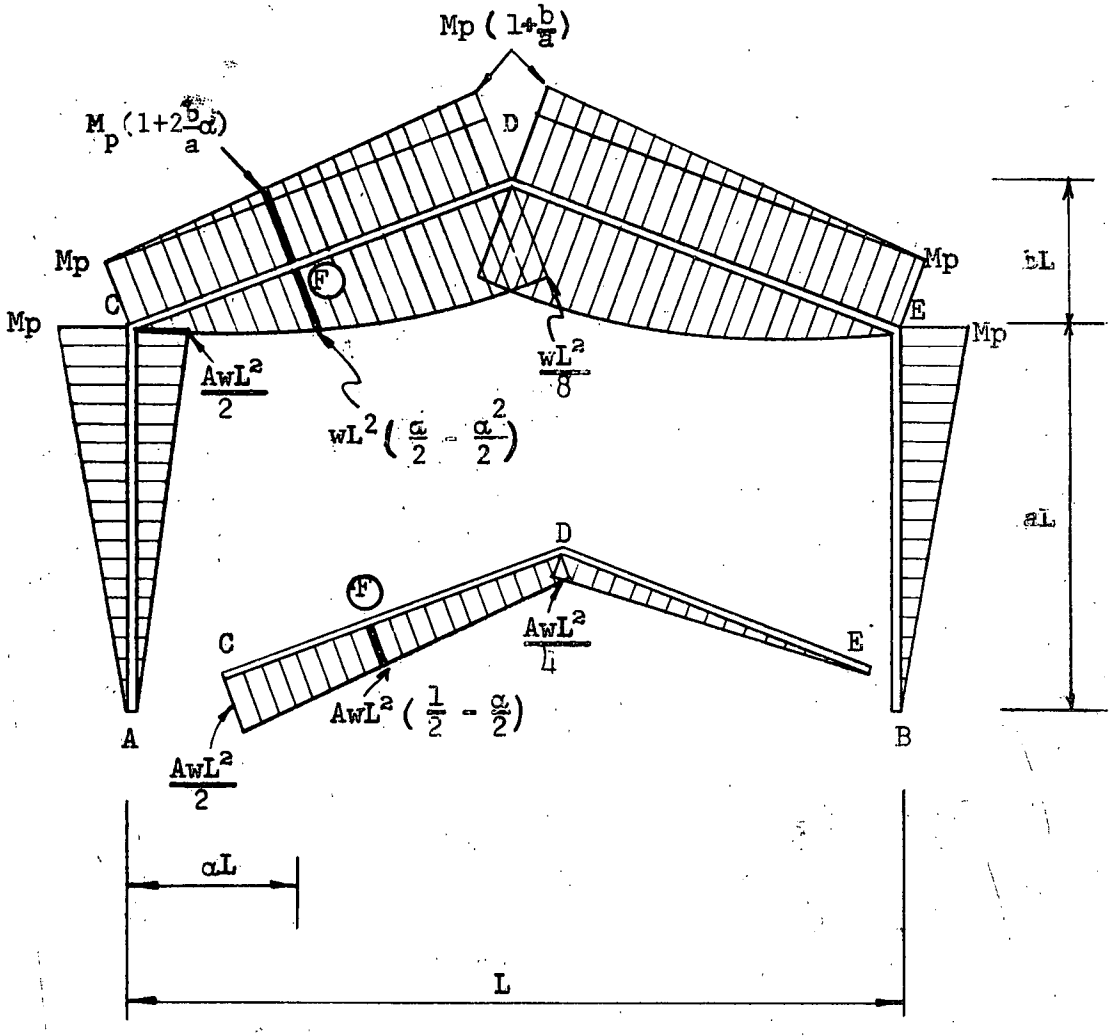

FIG.5.8a. ULTIMATE LOAD MOMENT DIAGRAM

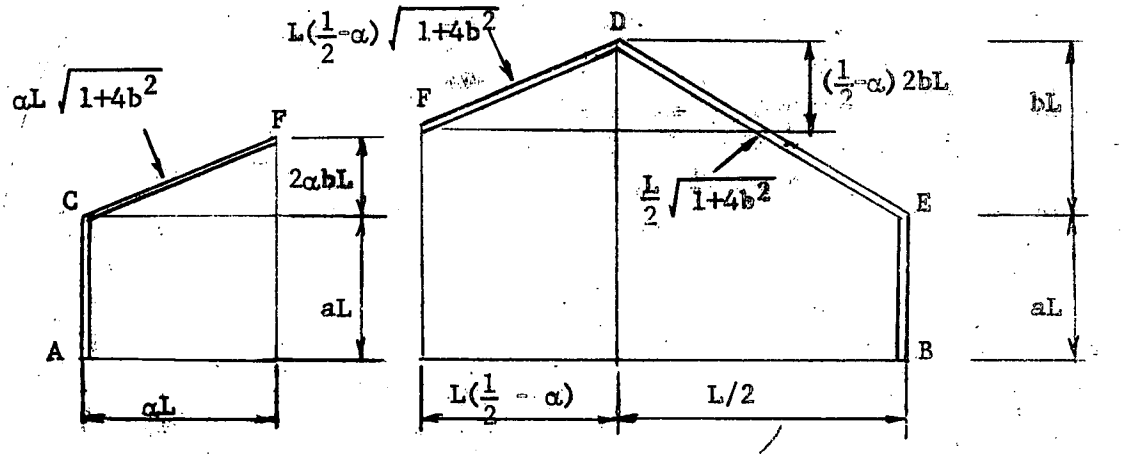

Fig. 5.8b. LENGTHS OF MEMBERS

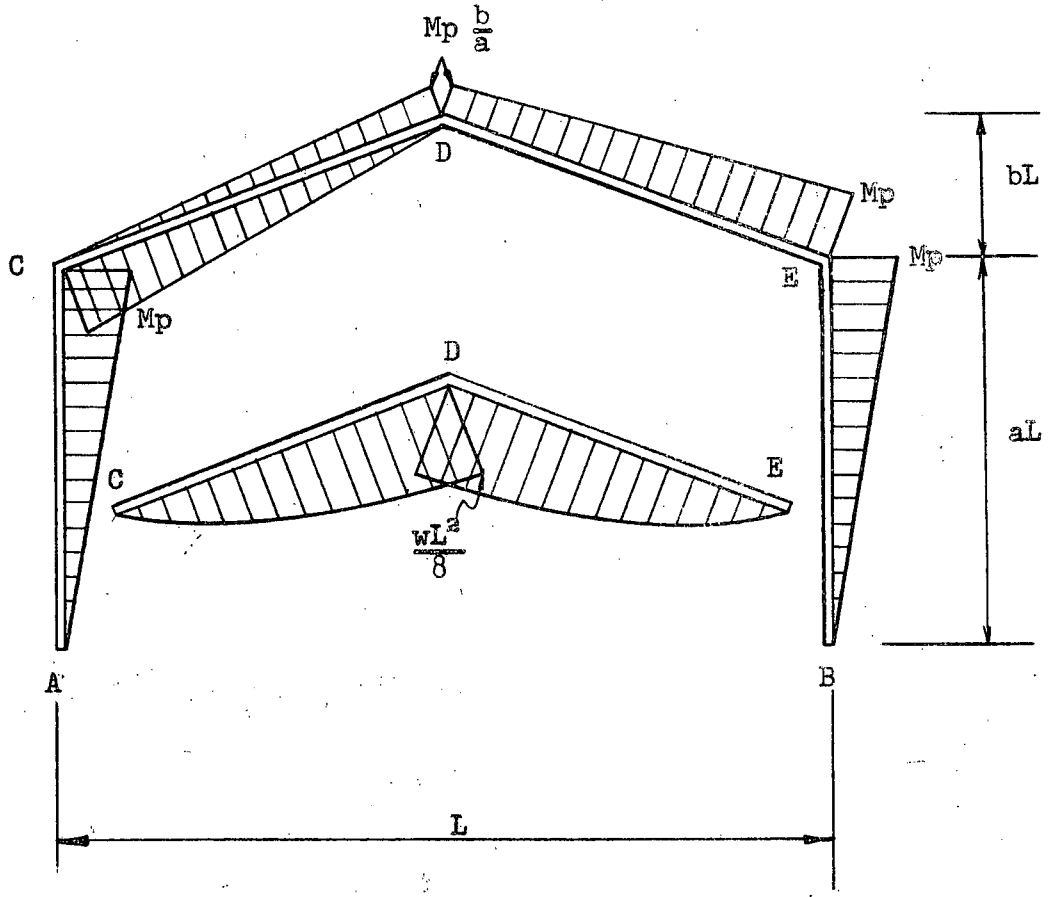

FIG. 5.9 ULTIMATE LOAD MOMENT DIAGRAM

(Panel Mechanism)

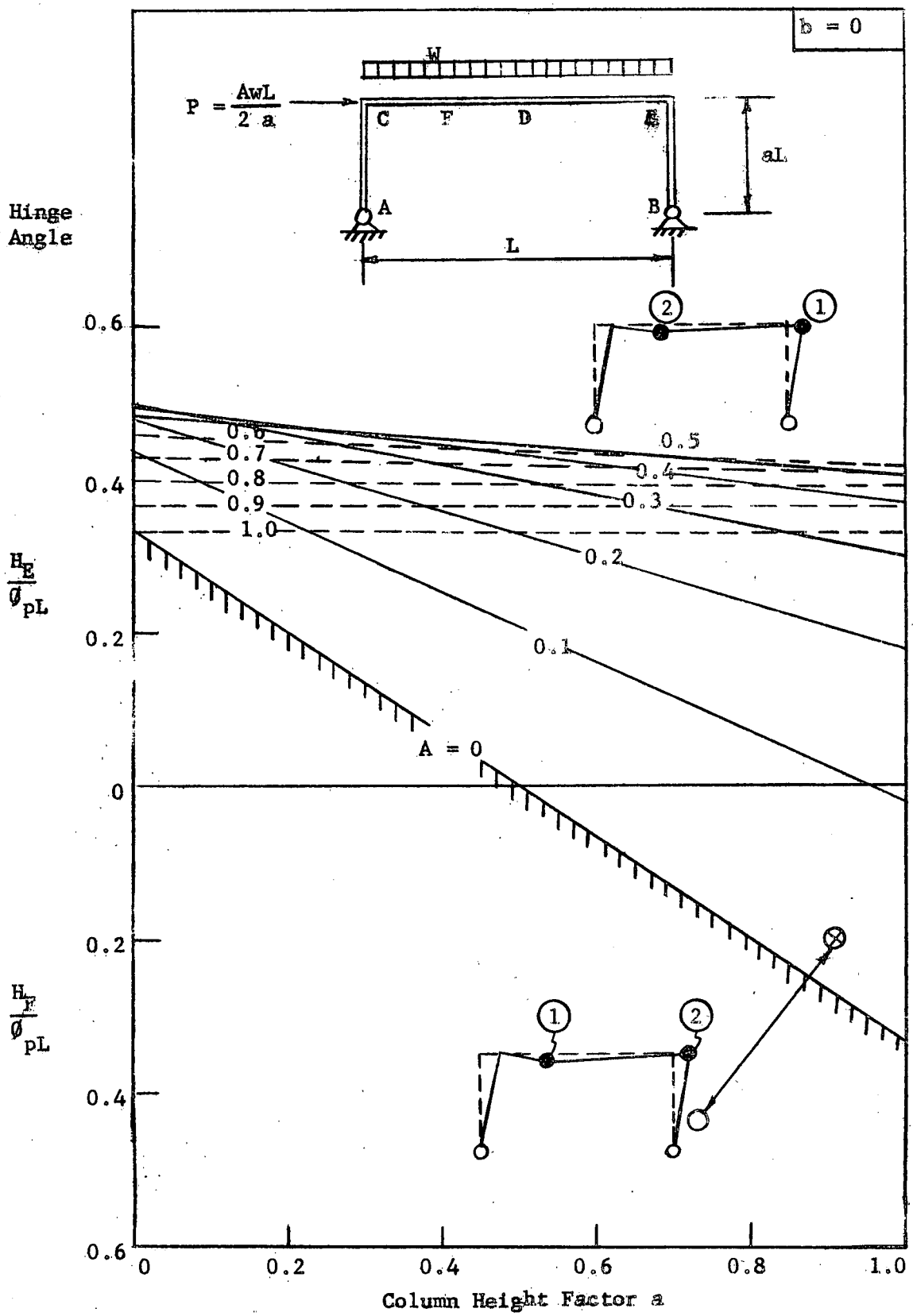

Fig. 5.10 HINGE ANGLES (b = 0)

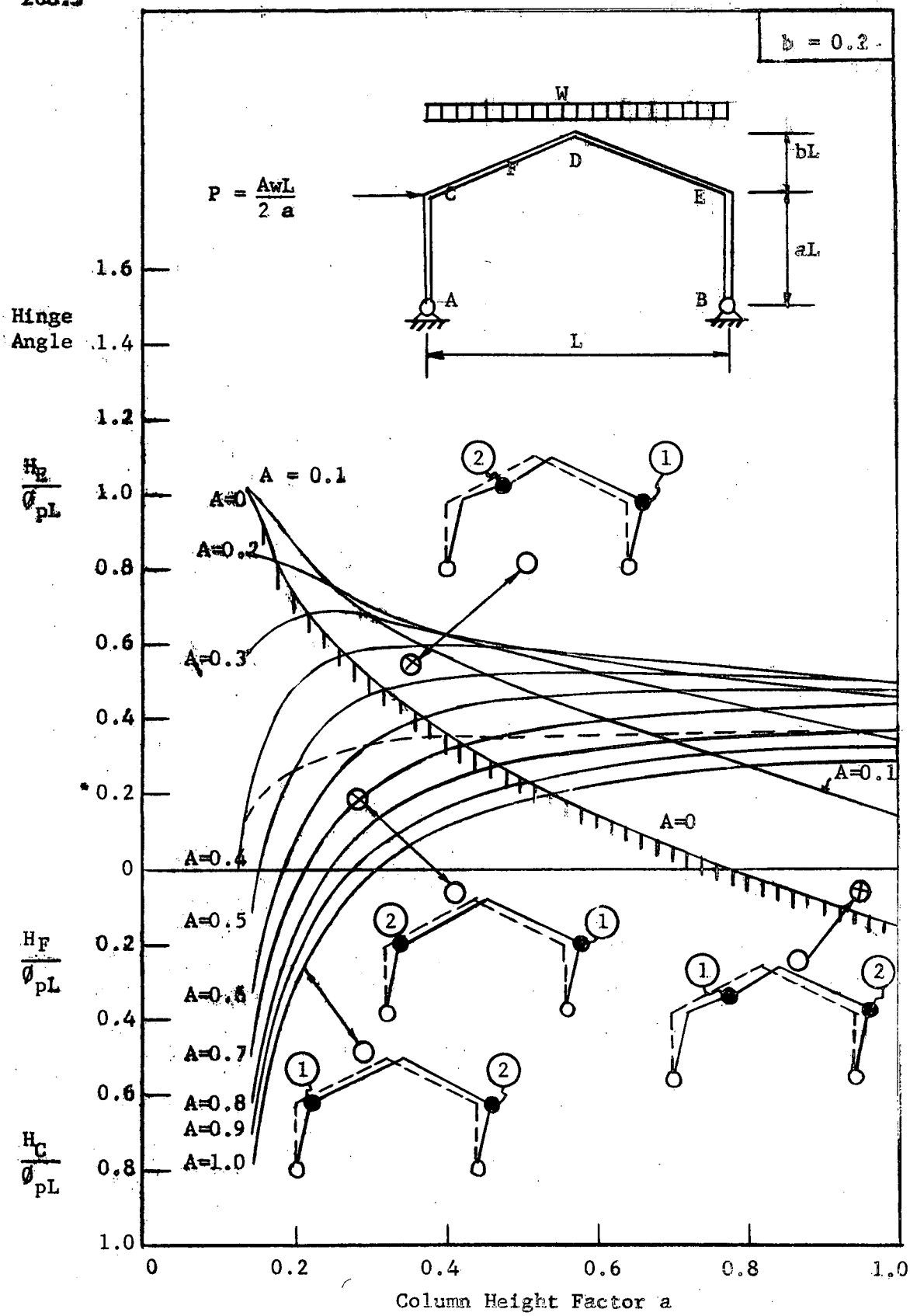

Fig. 5.11 HINGE ANGLES (b=0.2)

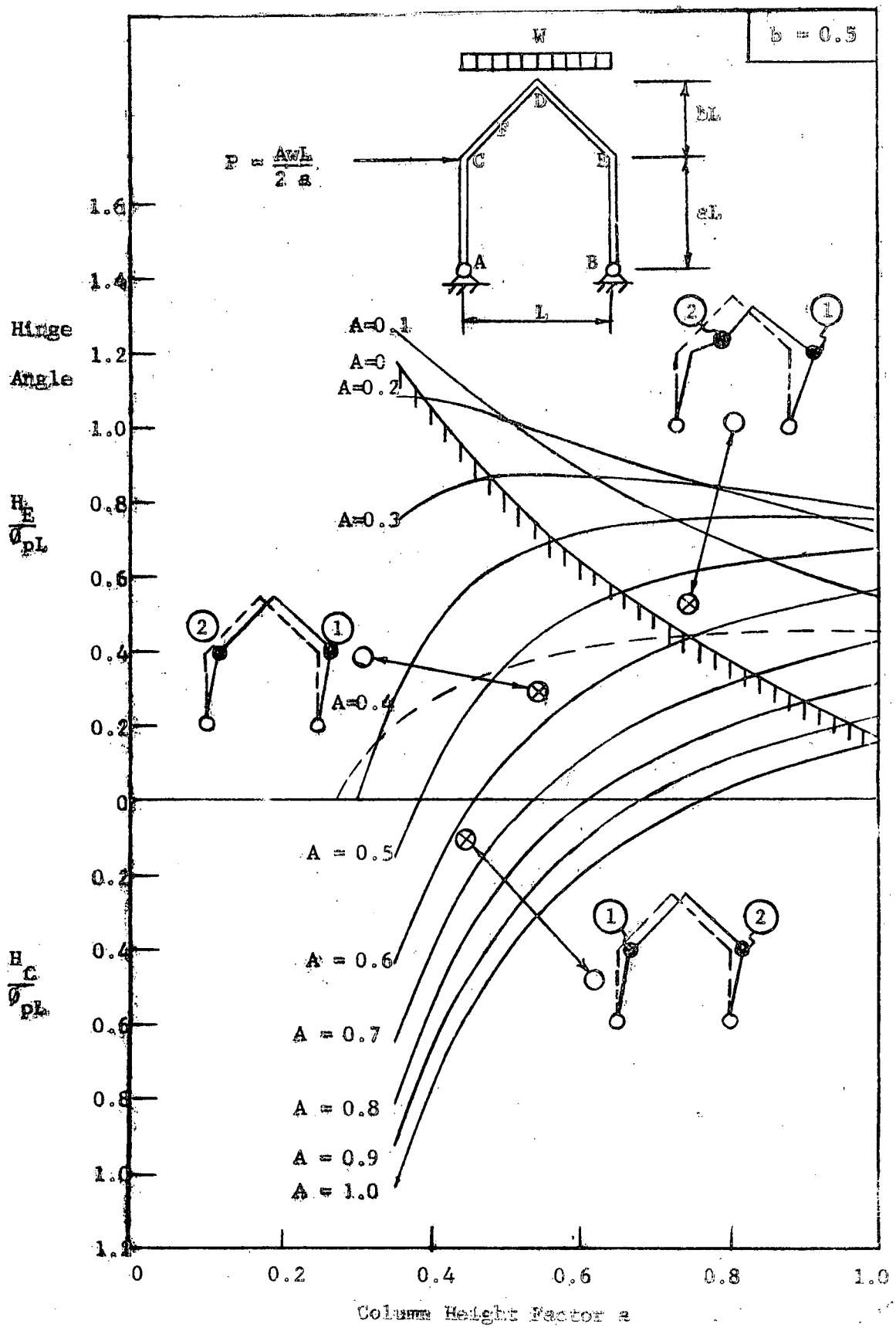

Fig. 5.12 HINGE ANGLES (b=0.5)

b=0.2

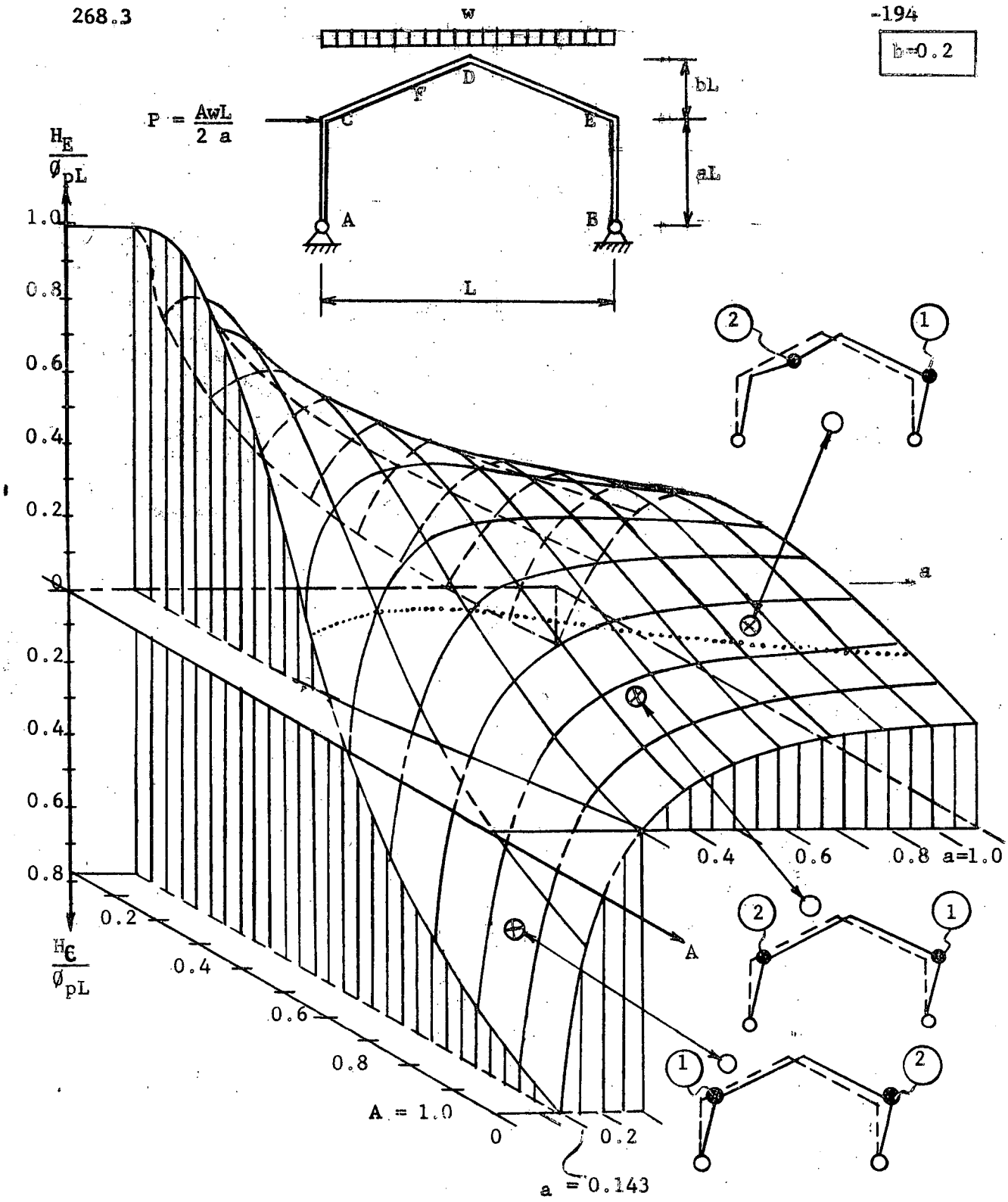

FIG. 5.13 HINGE-ANGLES (b=0.2) THREE-DIMENSIONAL PLOT

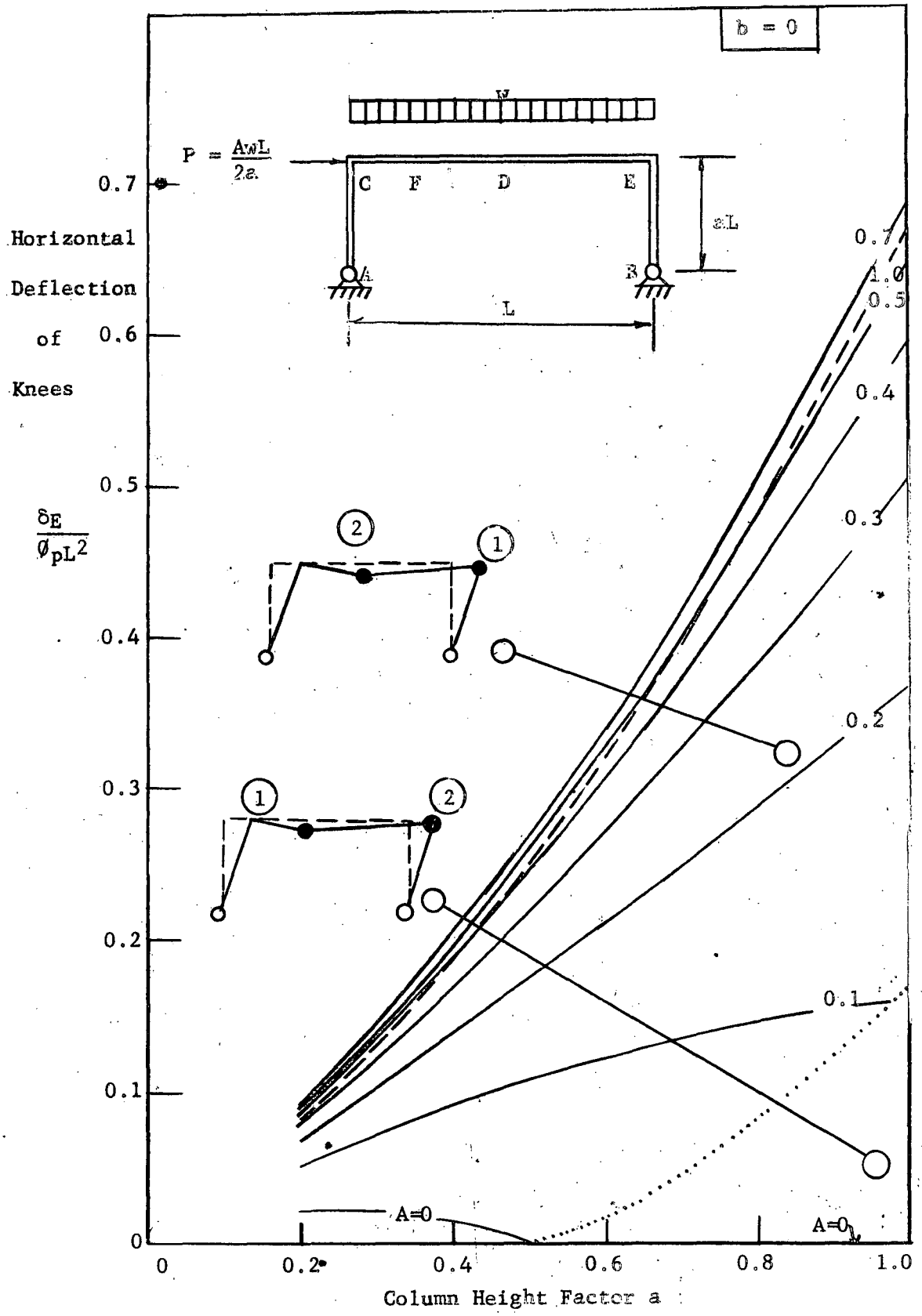

FIG. 5.14 HORIZONTAL DEFLECTION OF KNEES (b=0)

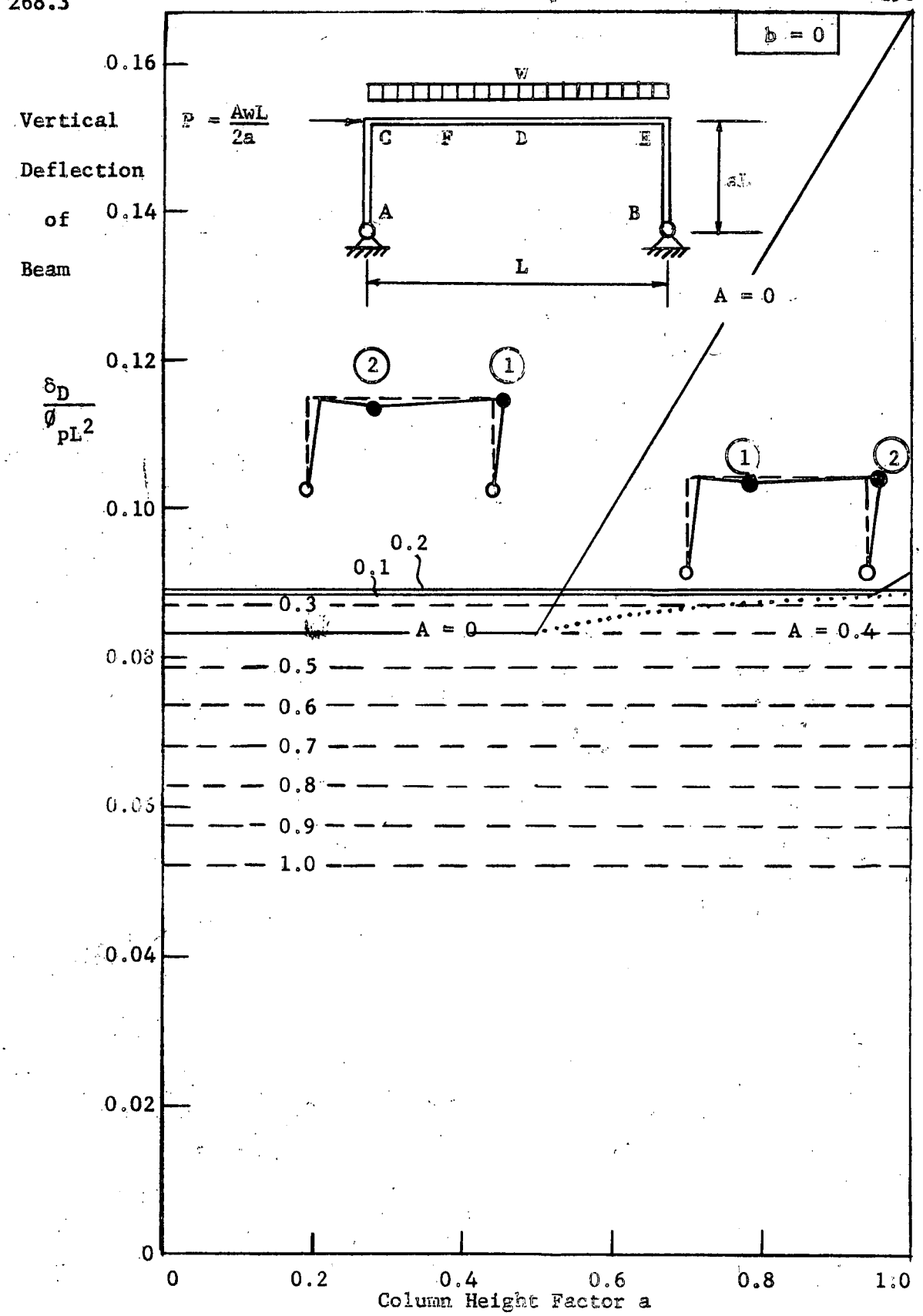

FIG. 5.15 VERTICAL DEFLECTION OF BEAM (b=0)

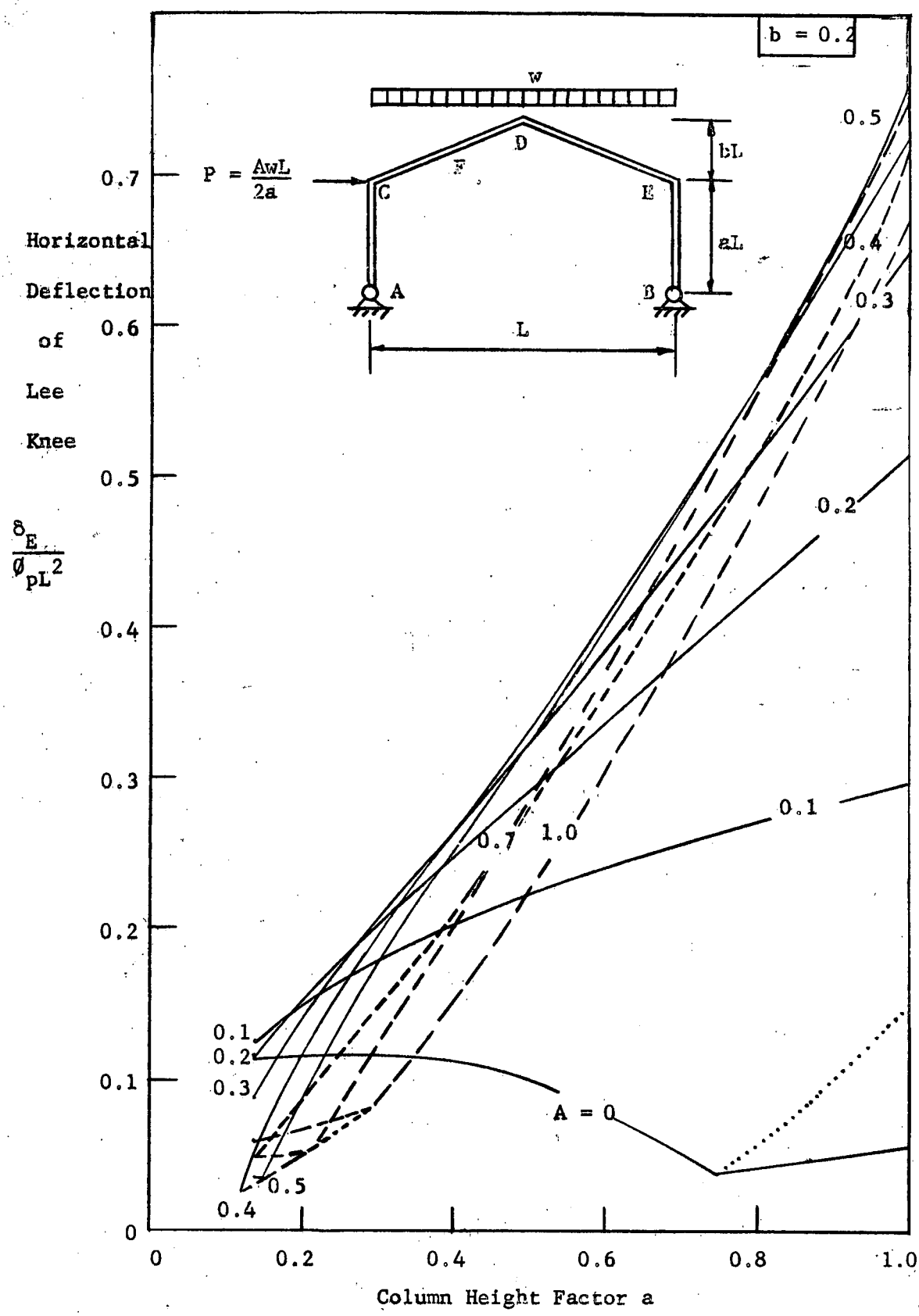

FIG. 5.16 HORIZONTAL DEFLECTION OF LEE KNEE (b=0.2)

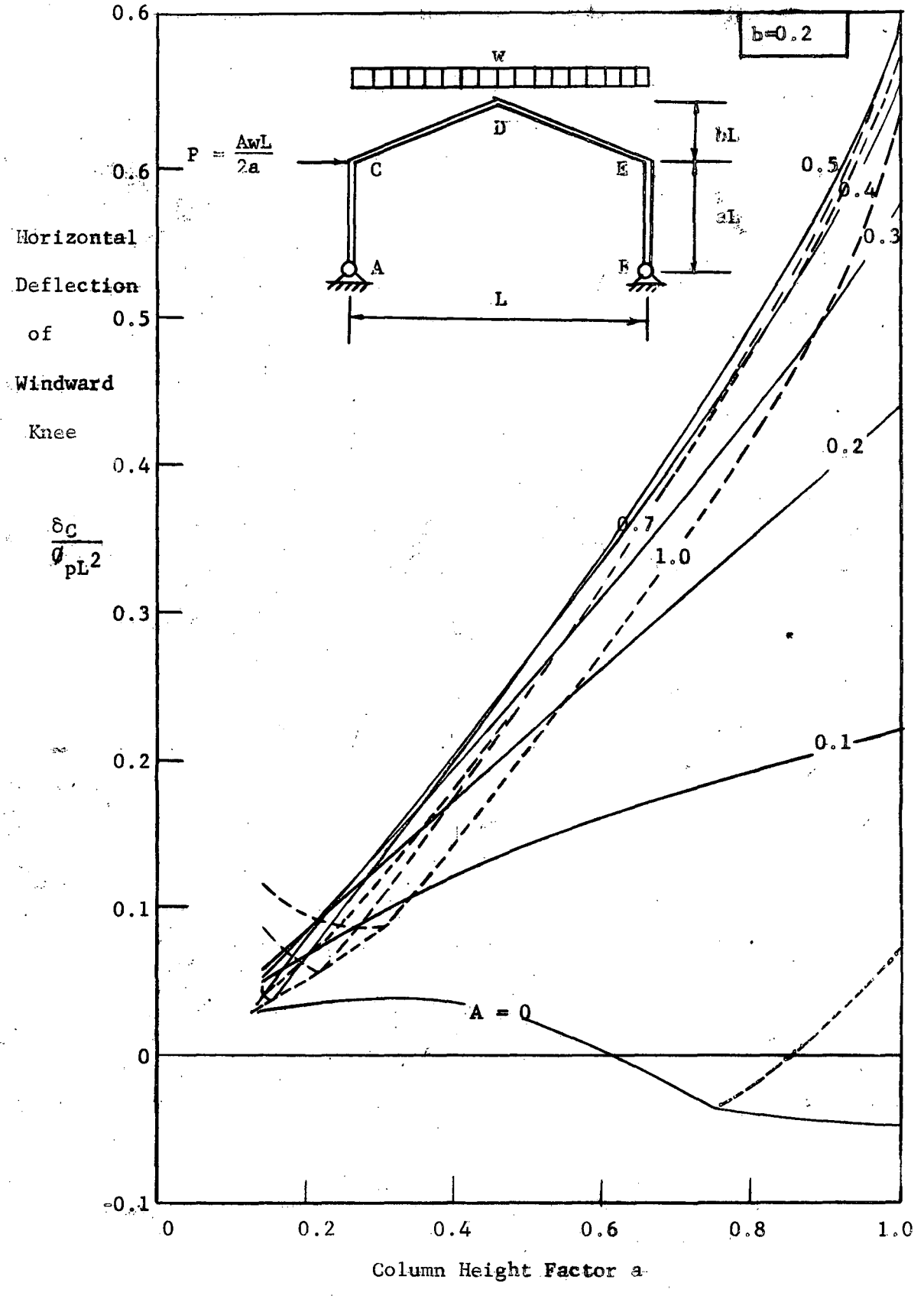

FIG. 5.17 HORIZONTAL DEFLECTION OF WINDWARD KNEE (b=0.2)

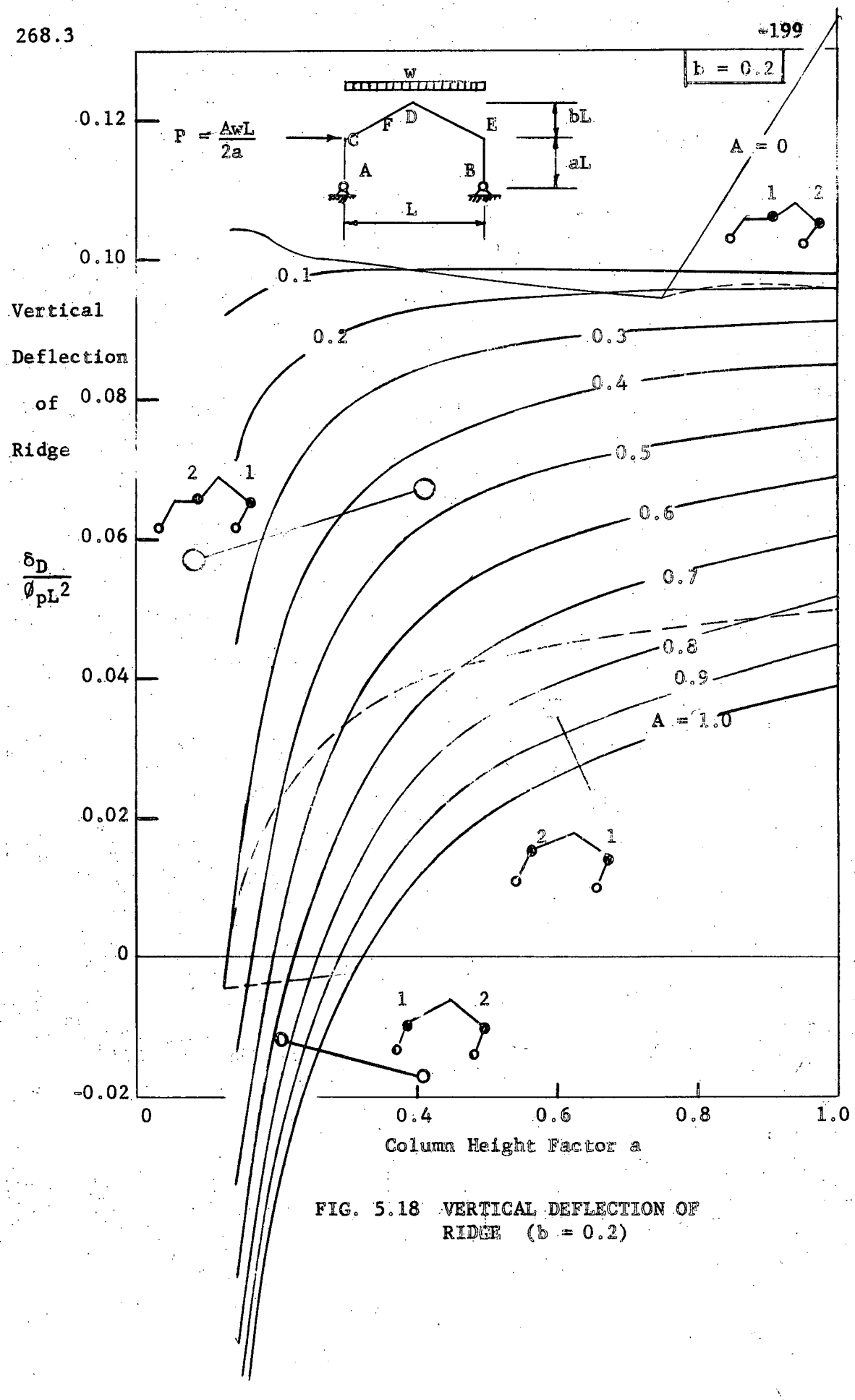

FIG. 5.18 VERTICAL DEFLECTION OF RIDGE (b = 0.2)

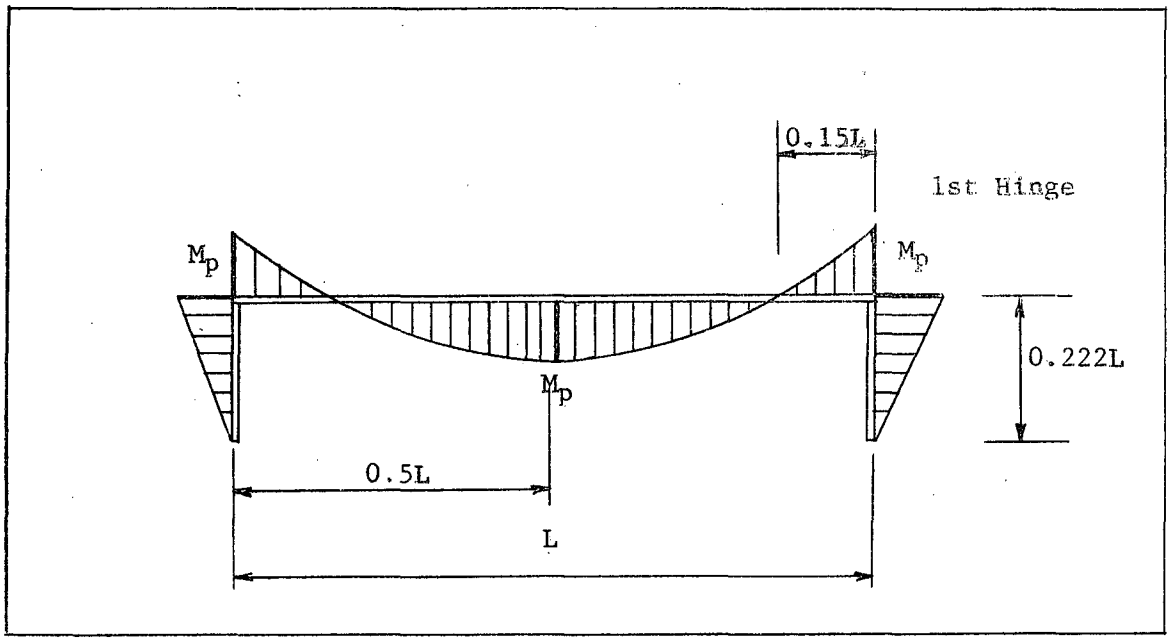

(a) Moment Diagram for Theoretical Single-Span Flat-Roofed Frame (36 WF 230)

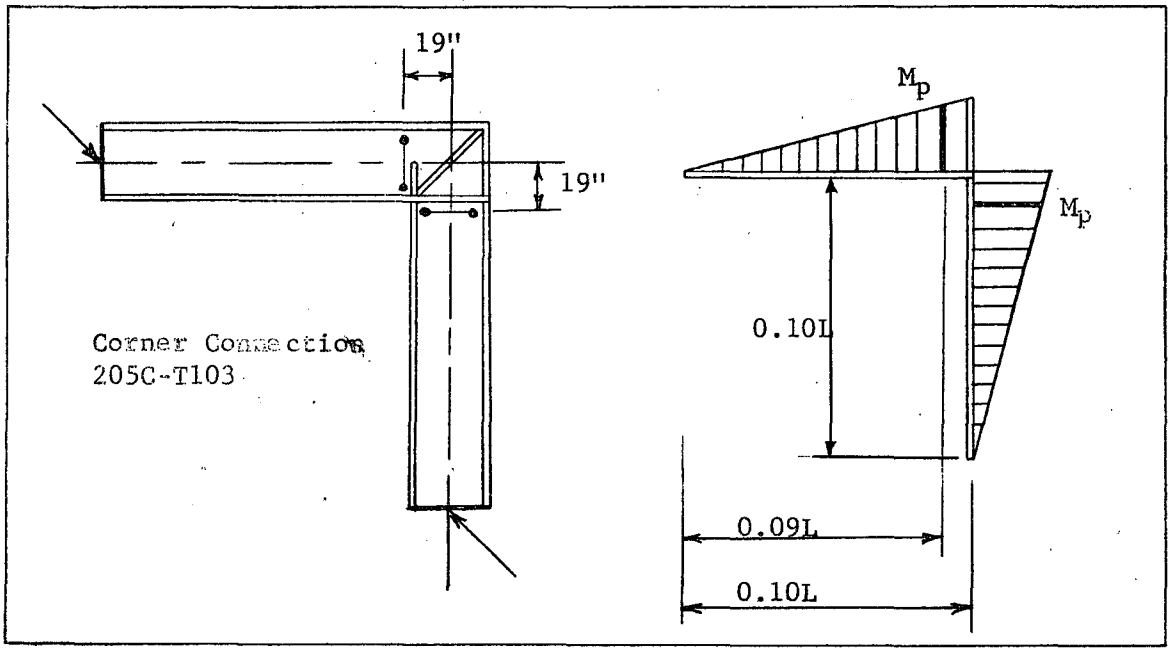

(b) Moment Diagram for Experimental Corner Connection (36WF230)

FIG 5.19 COMPARISON OF MOMENT DIAGRAM FOR THEORETICAL EXAMPLE OF SINGLE-SPAN FRAME WITH MOMENT DIAGRAM FOR EXPERIMENTAL TEST OF CORNER CONNECTION

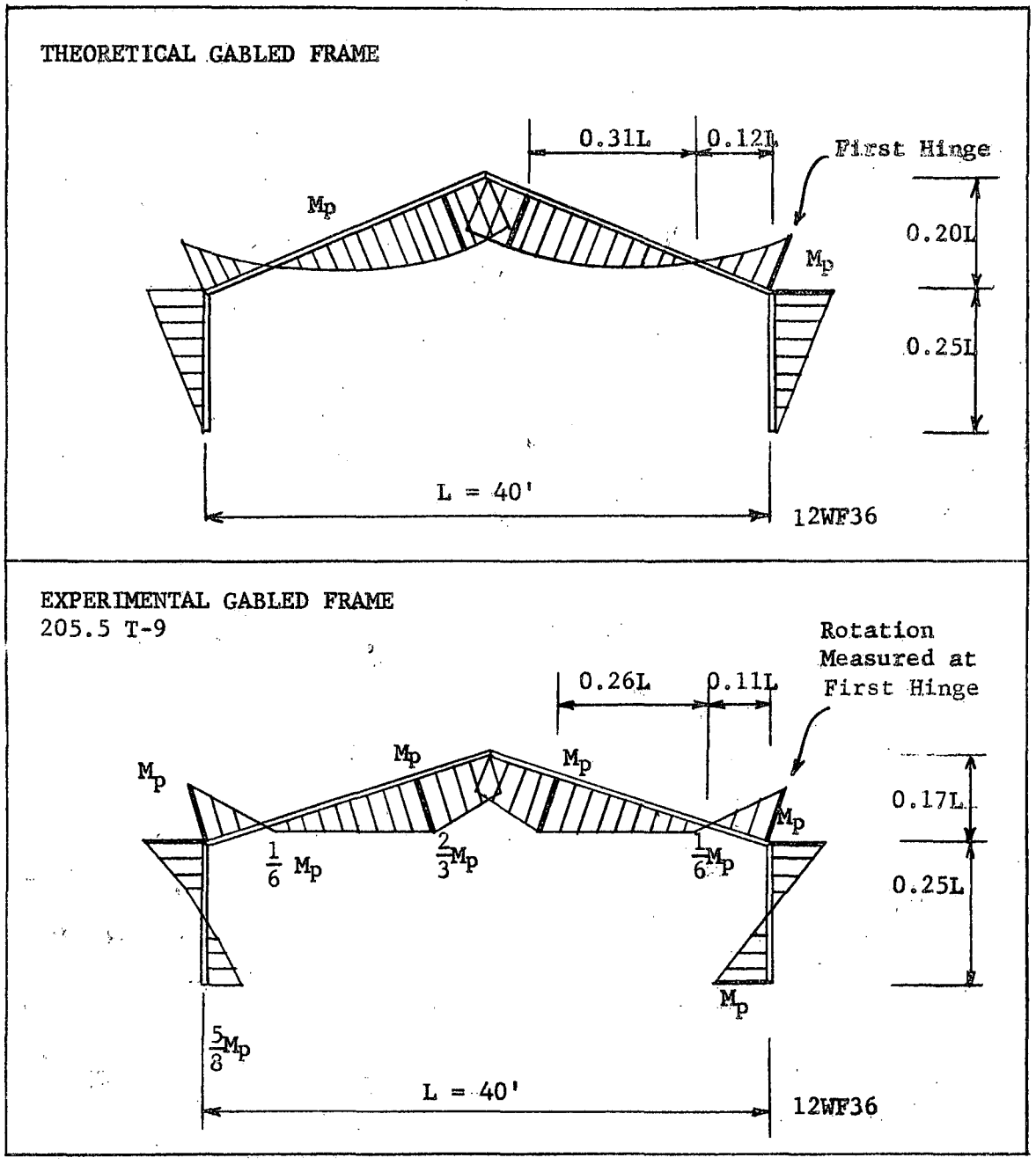

FIG 5.20 COMPARISON OF MOMENT DIAGRAM FOR THEORETICAL EXAMPLE OF GABLED FRAME WITH MOMENT DIAGRAM FOR EXPERIMENTAL TEST OF A GABLED FRAME

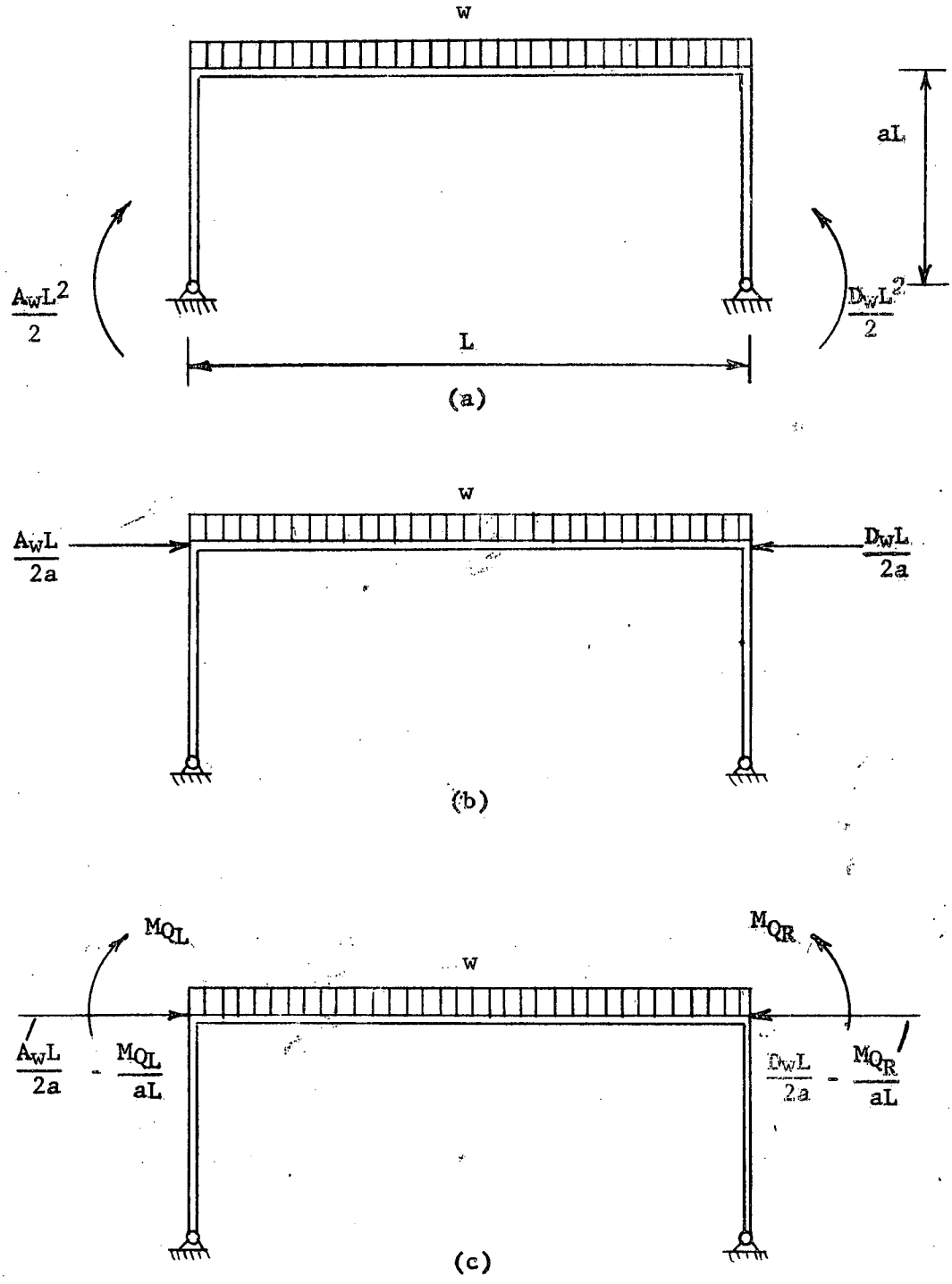

FIG 6.1 THREE EQUIVALENT LOADINGS FOR SUBASSEMBLAGES OF MULTI-SPAN FRAMES

b = 0

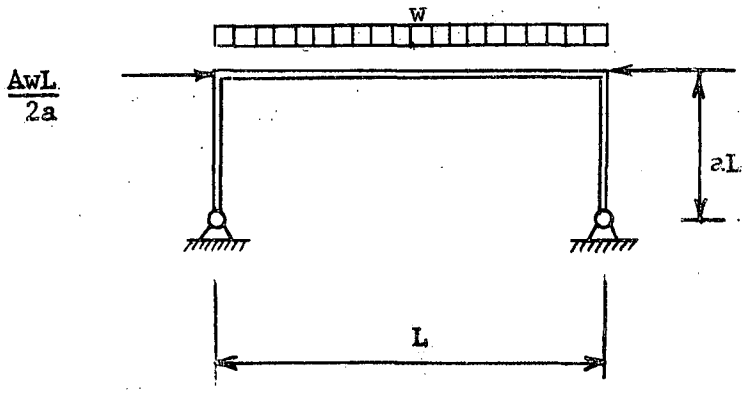

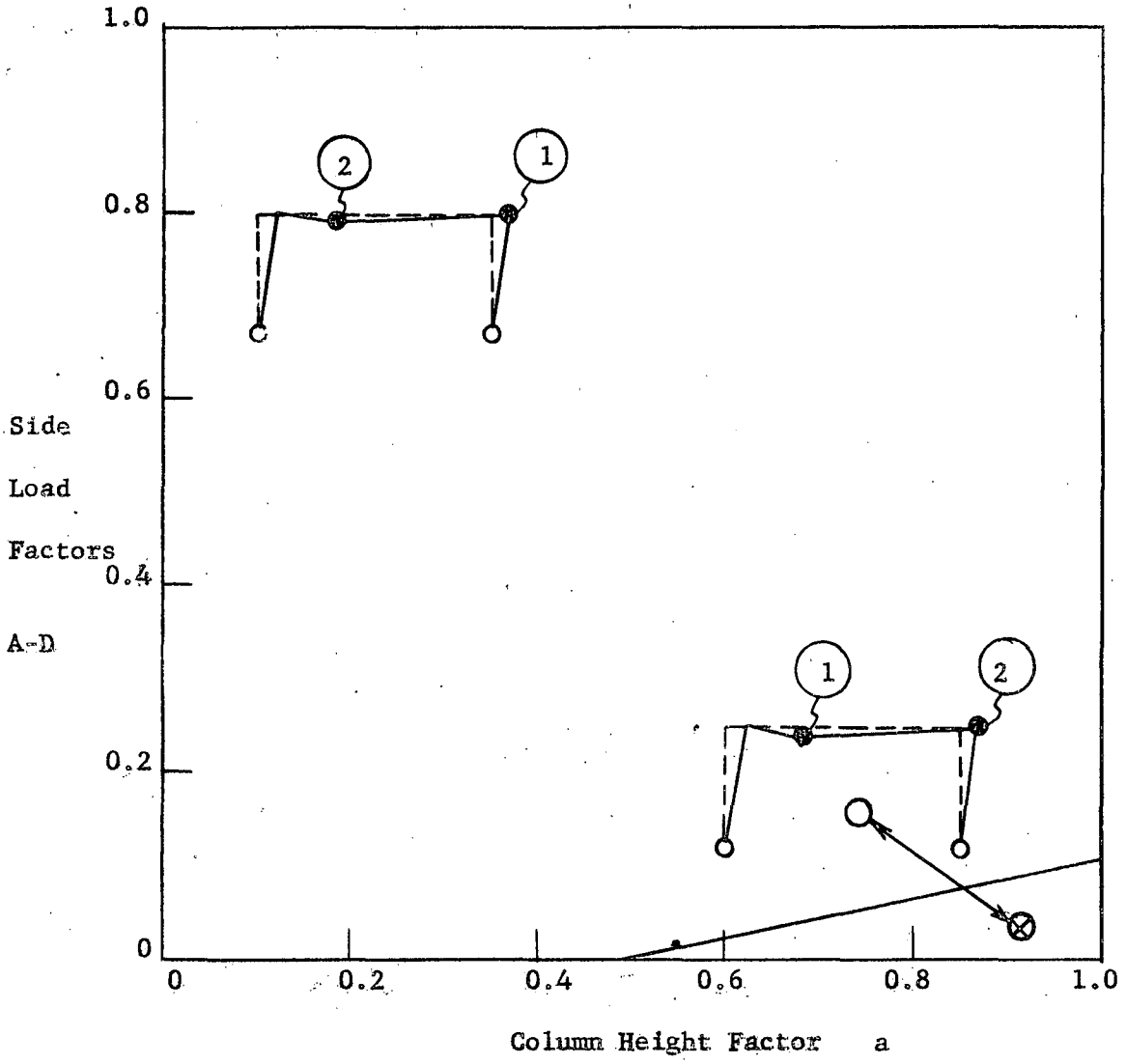

FIG 6.2 DOMAINS FOR MECHANISMS OF MULTI-SPAN FRAMES

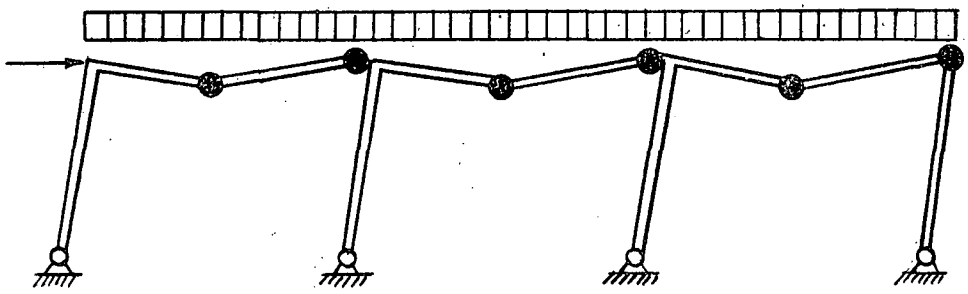

(a) Typical Mechanism for Multi-Span Frame

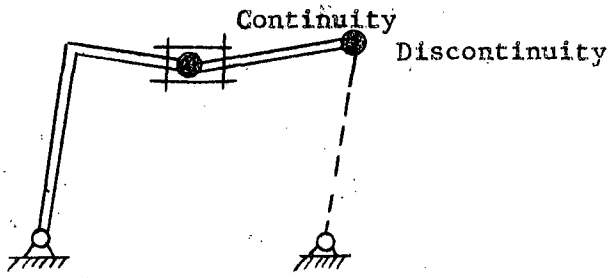

(b) Self-Supporting Subassemblage (Stable)

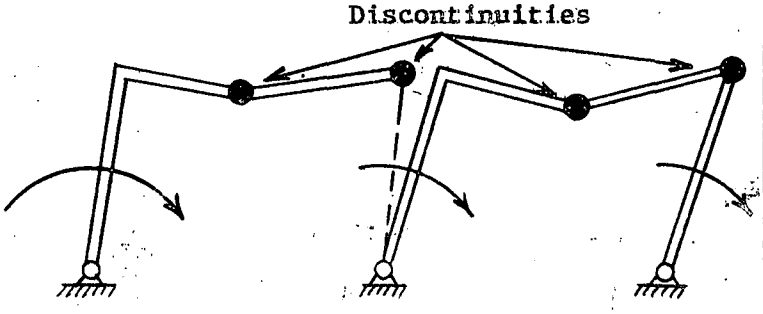

(c) Non-Self-Supporting Subassemblages (Unstable)

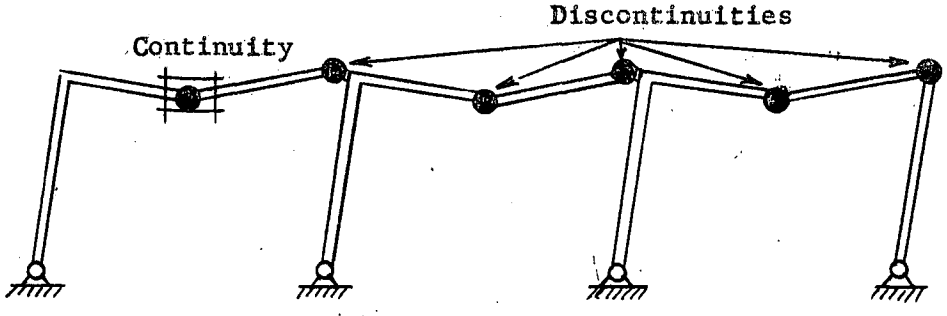

(d) Attachment to Self-Supporting Subassemblages Creates Stable Structure

FIG 6.3 SELF-SUPPORTING AND NON-SELF-SUPPORTING SUBASSEMBLAGES

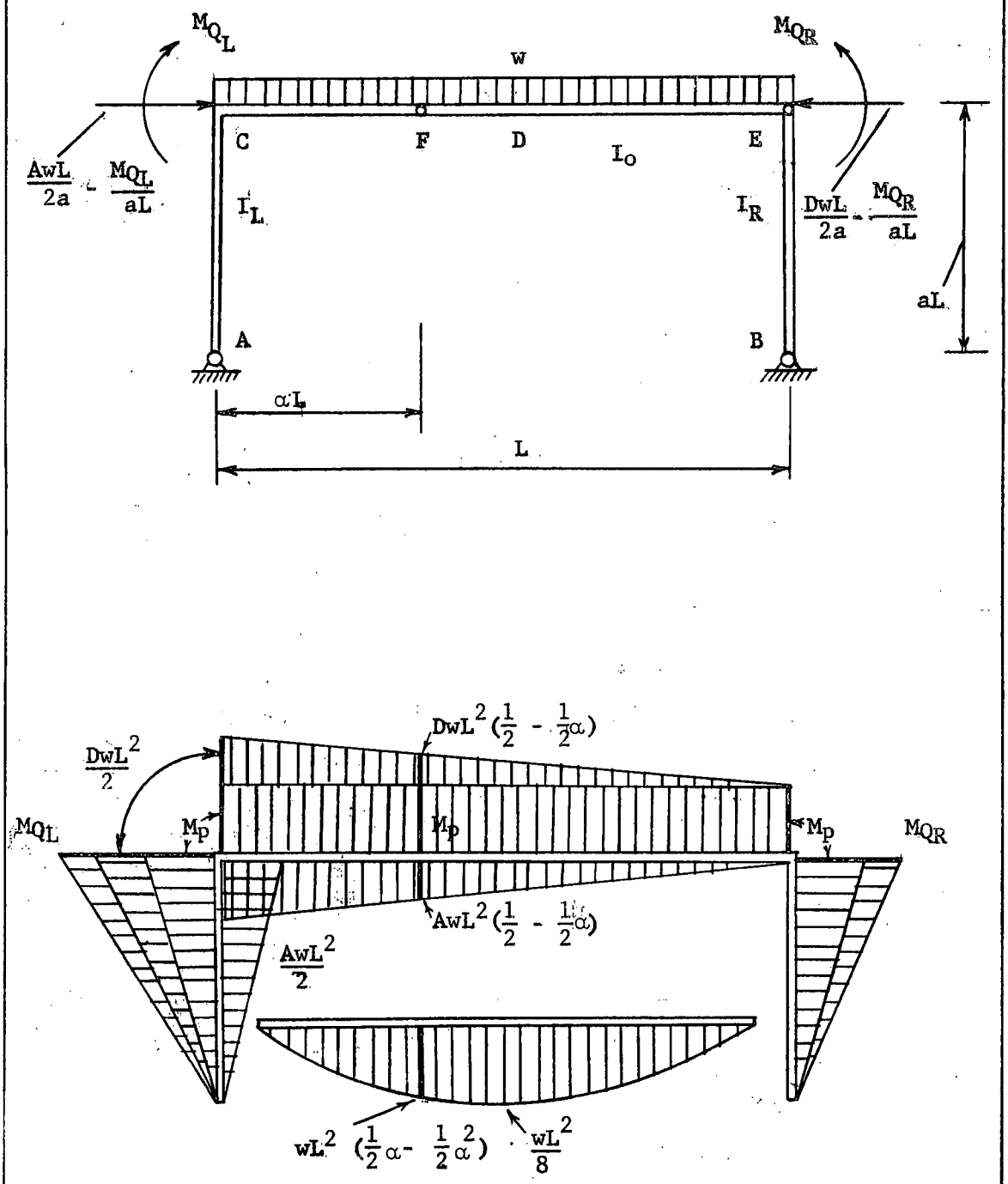

FIG 6.4 MOMENT DIAGRAM FOR FLAT-ROOFED FRAMES

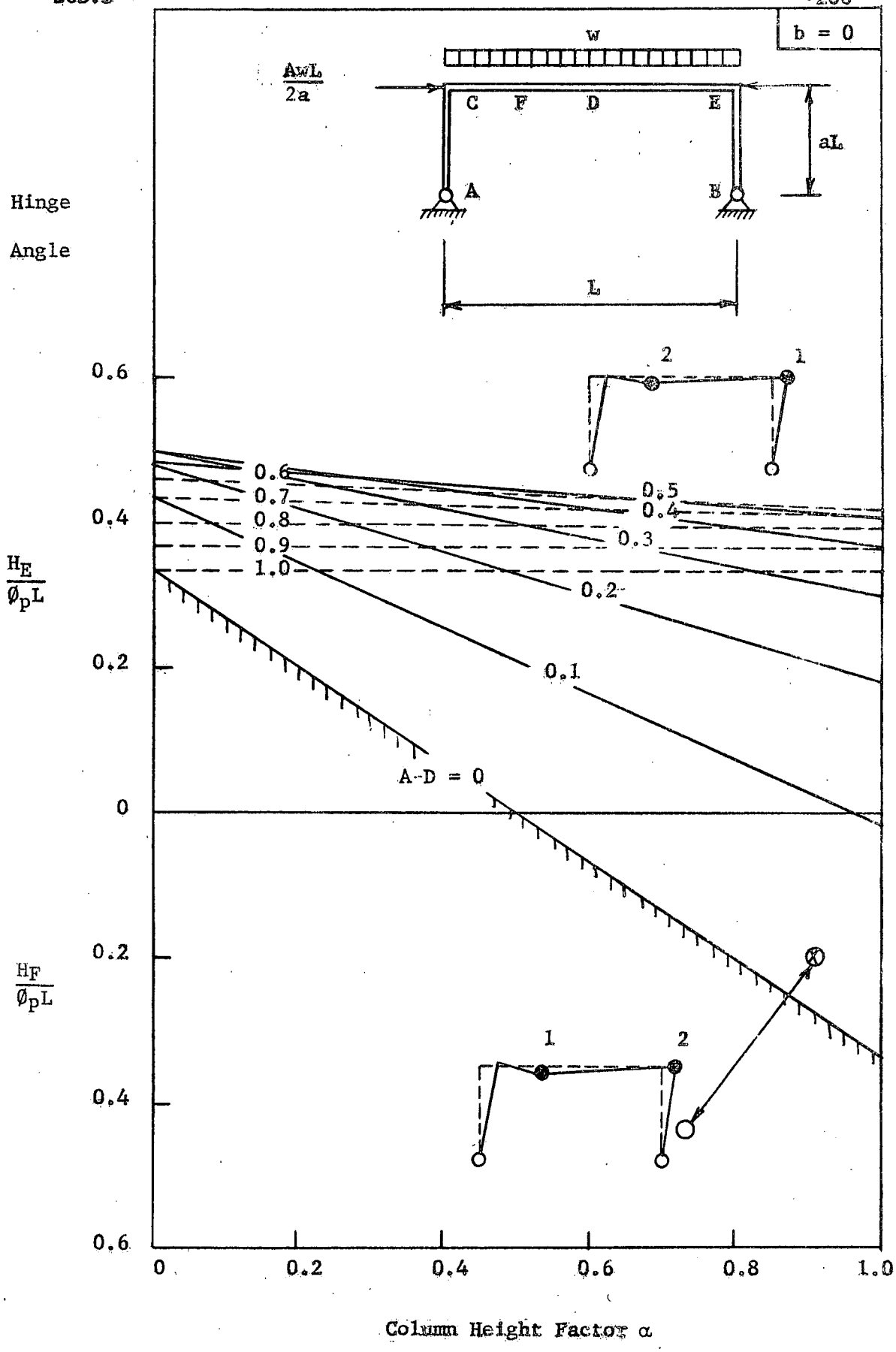

FIG 6.5 HINGE ANGLES FOR MULTI-SPAN FRAMES (b=0)

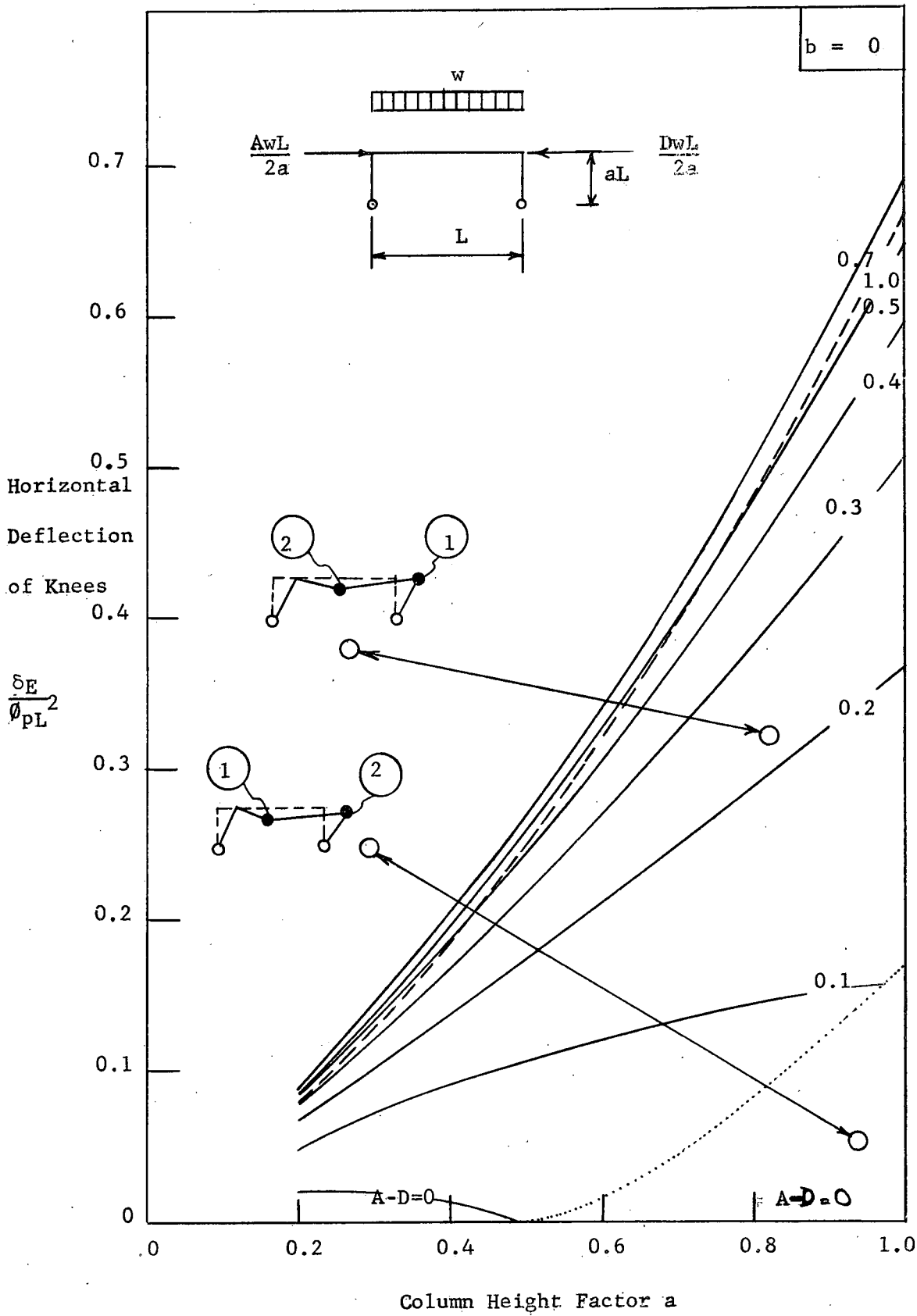

FIG 6.6 DEFLECTION OF LEE KNEE OF MULTI-SPAN FRAMES (b=0)

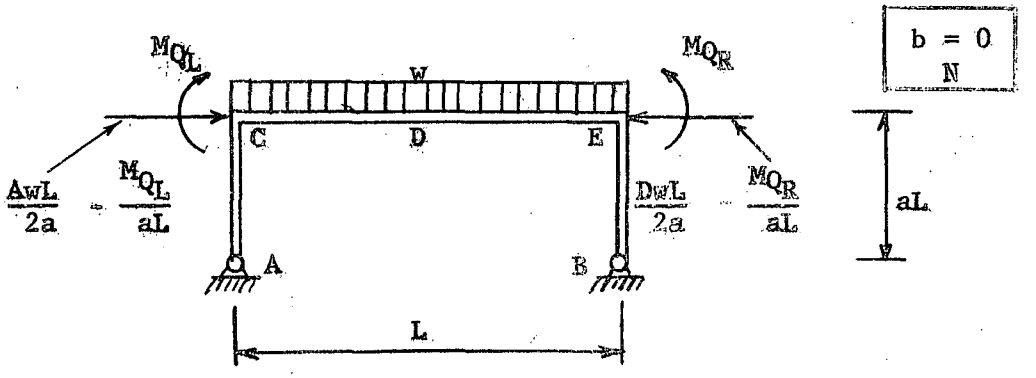

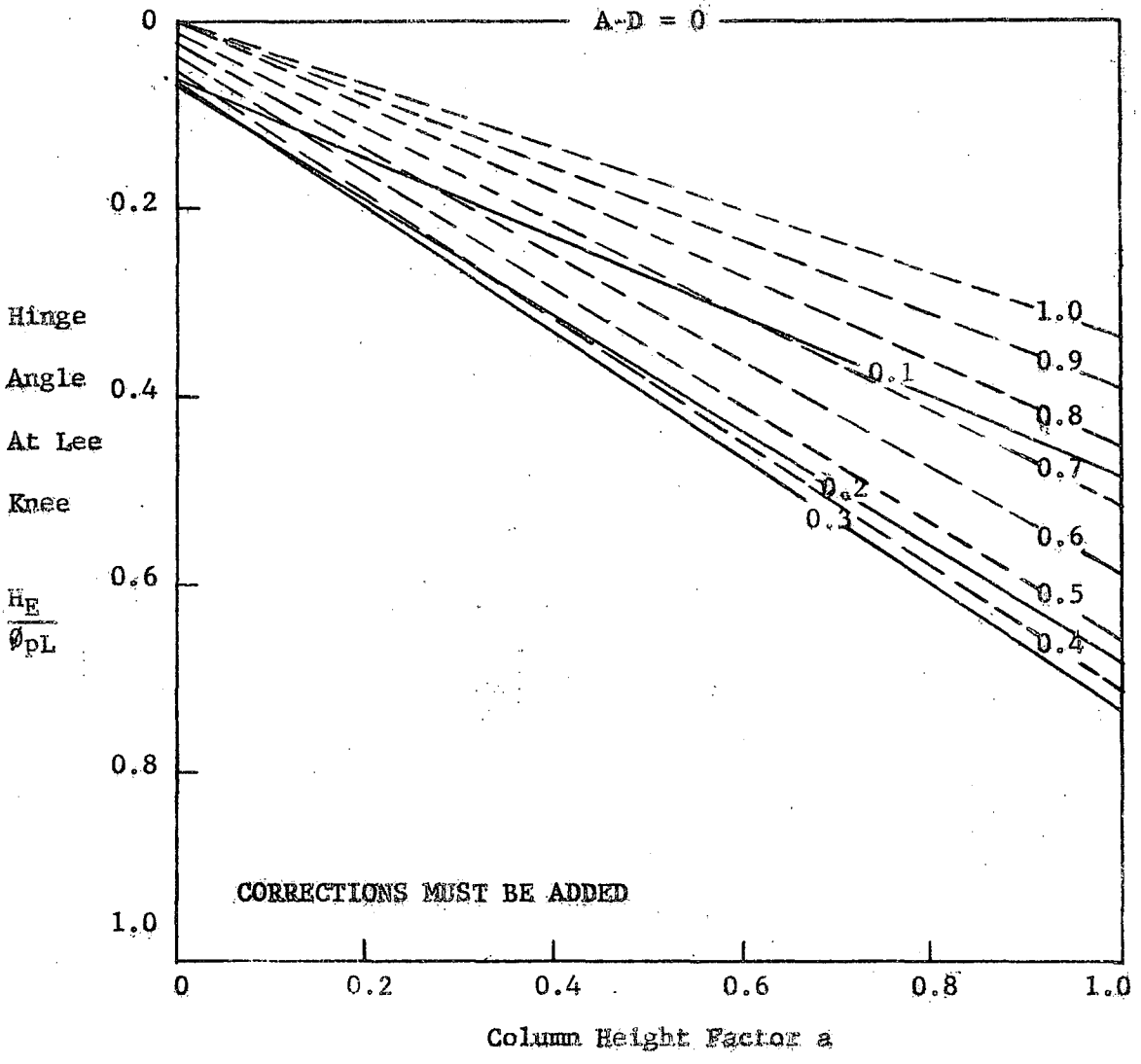

FIG 6.7 HINGE ANGLE AT LEE KNEE FOR NON-SELF-SUPPORTING SUBASSEMBLAGE (b = 0)

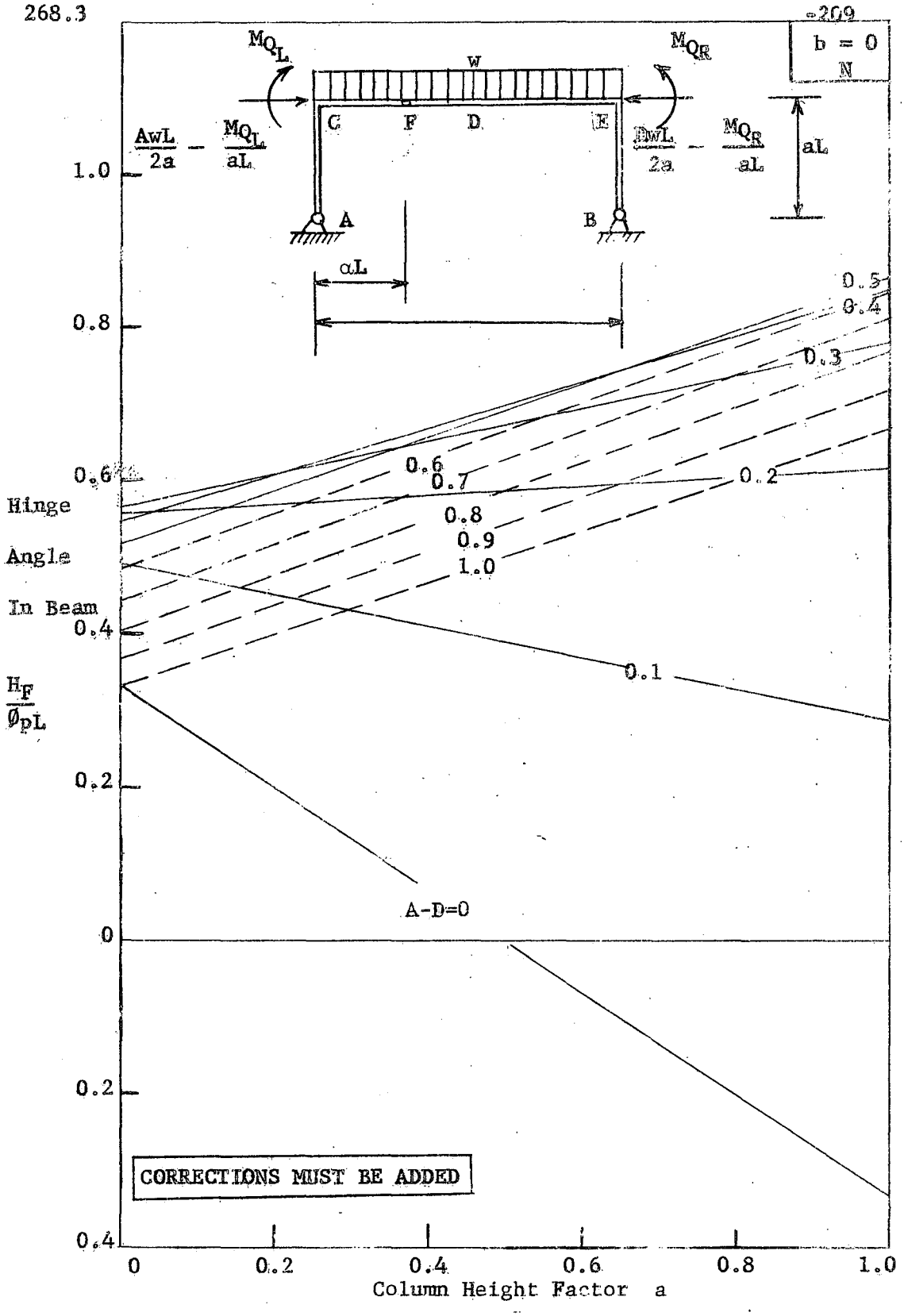

FIG 6.8 HINGE ANGLE IN BEAM AT POINT F FOR NON-SELF-SUPPORTING SUBASSEMBLAGE (b = 0)

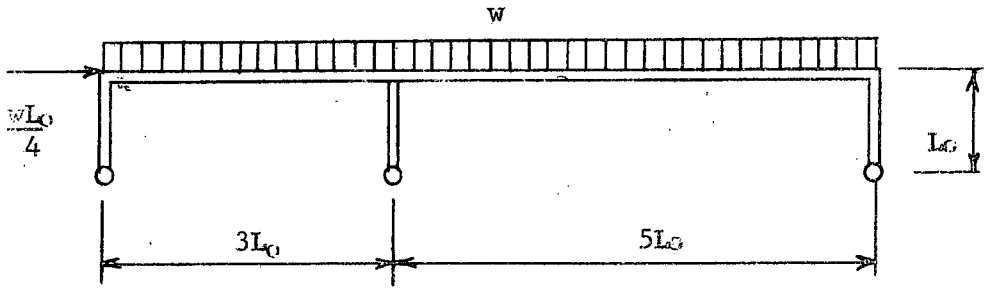

FIG 6.9 TWO-SPAN FRAME DESIGNED IN EXAMPLE

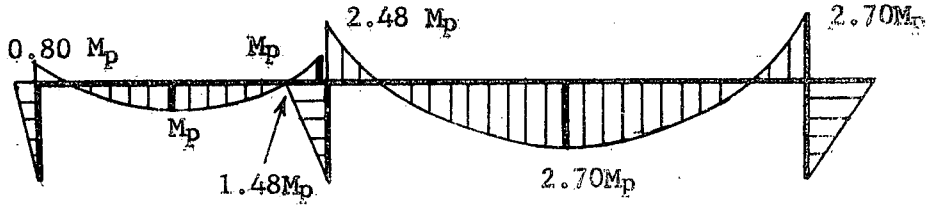

FIG 6.10 MAXIMUM LOAD MOMENT DIAGRAM FOR TWO-SPAN FRAME

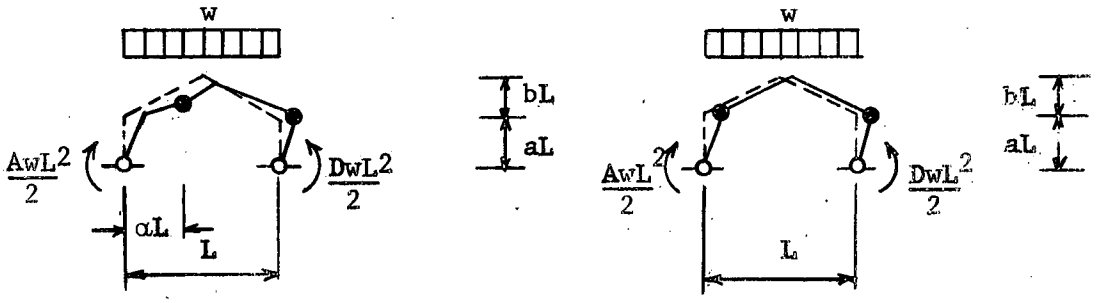

(a) General Composite Mechanism (b) Panel Mechanism

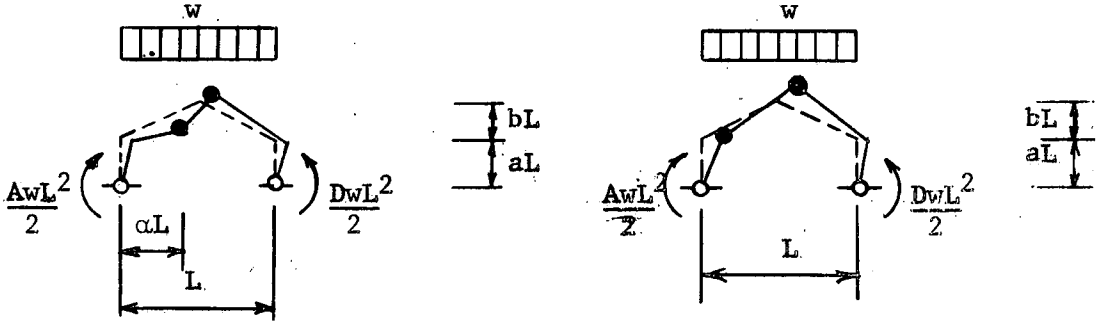

(c) Reverse Composite Mechanism (d) Reverse Gable Mechanism

FIG 7.1 POSSIBLE MECHANISMS FOR SUBASSEMBLAGE OF MULTI-SPAN GABLED FRAME

$\frac{b}{a} = 1.0$

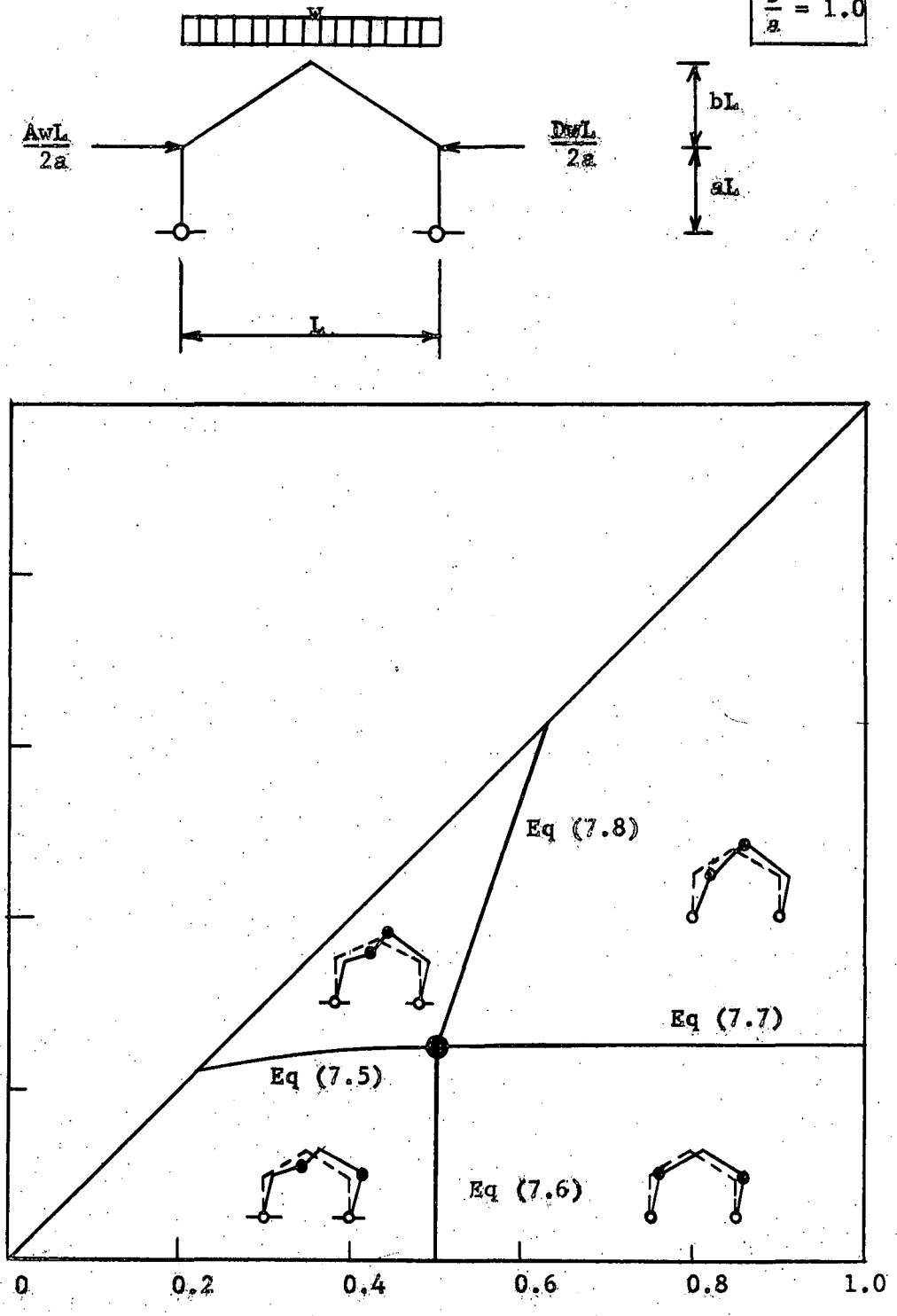

FIG 7.2 LIMITS OF MECHANISMS FOR b/a = 1.0

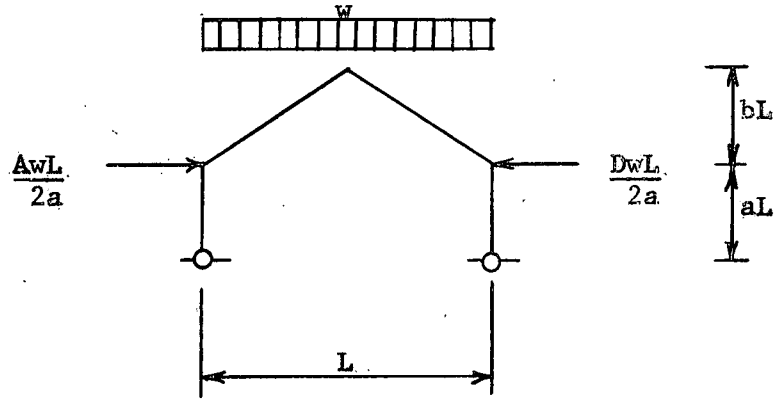

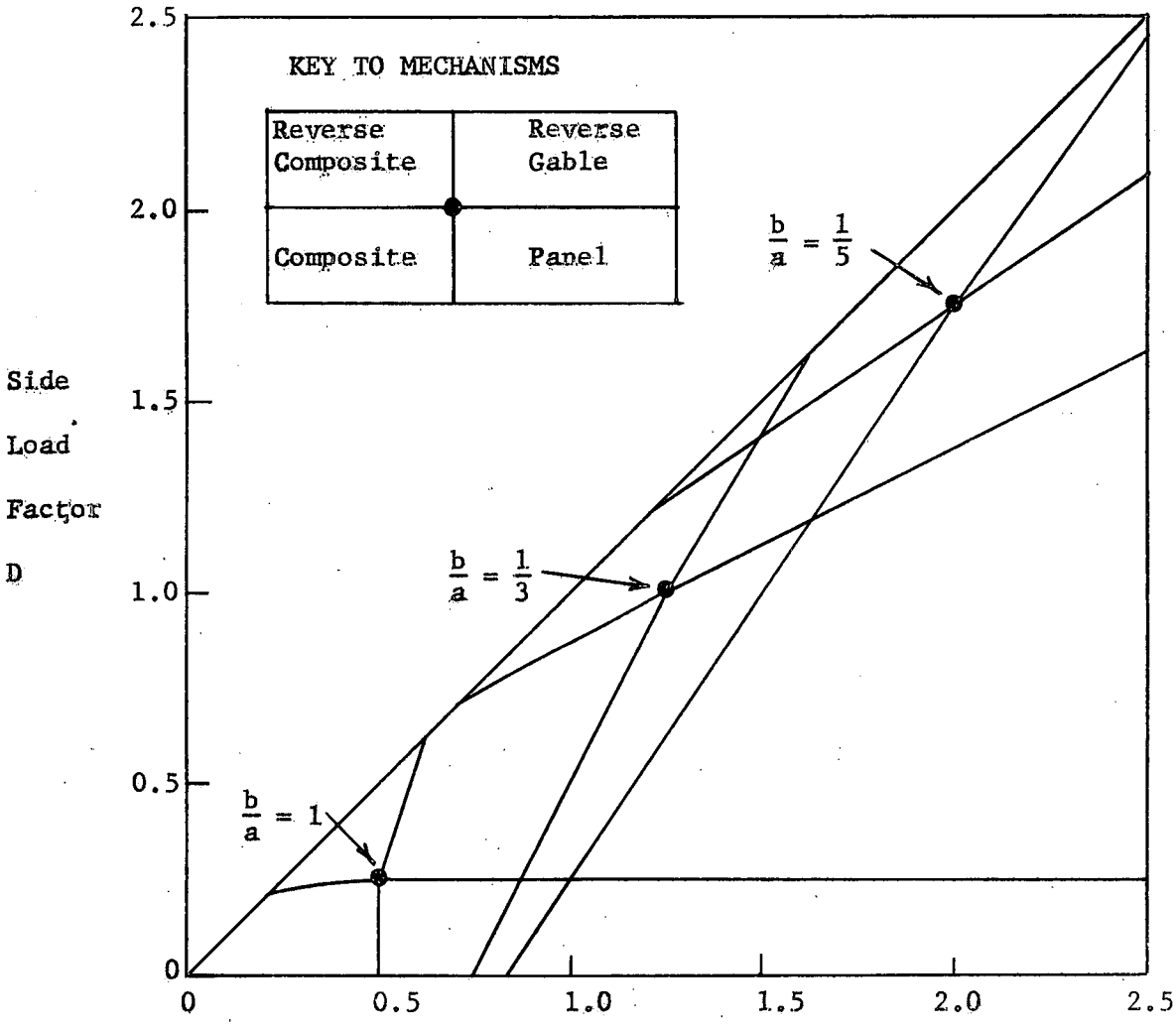

FIG 7.3 LIMITS OF MECHANISMS FOR THREE b/a VALUES

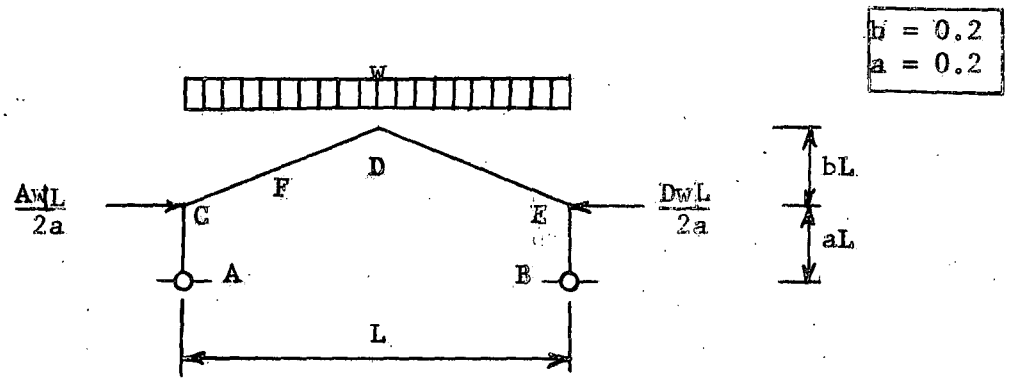

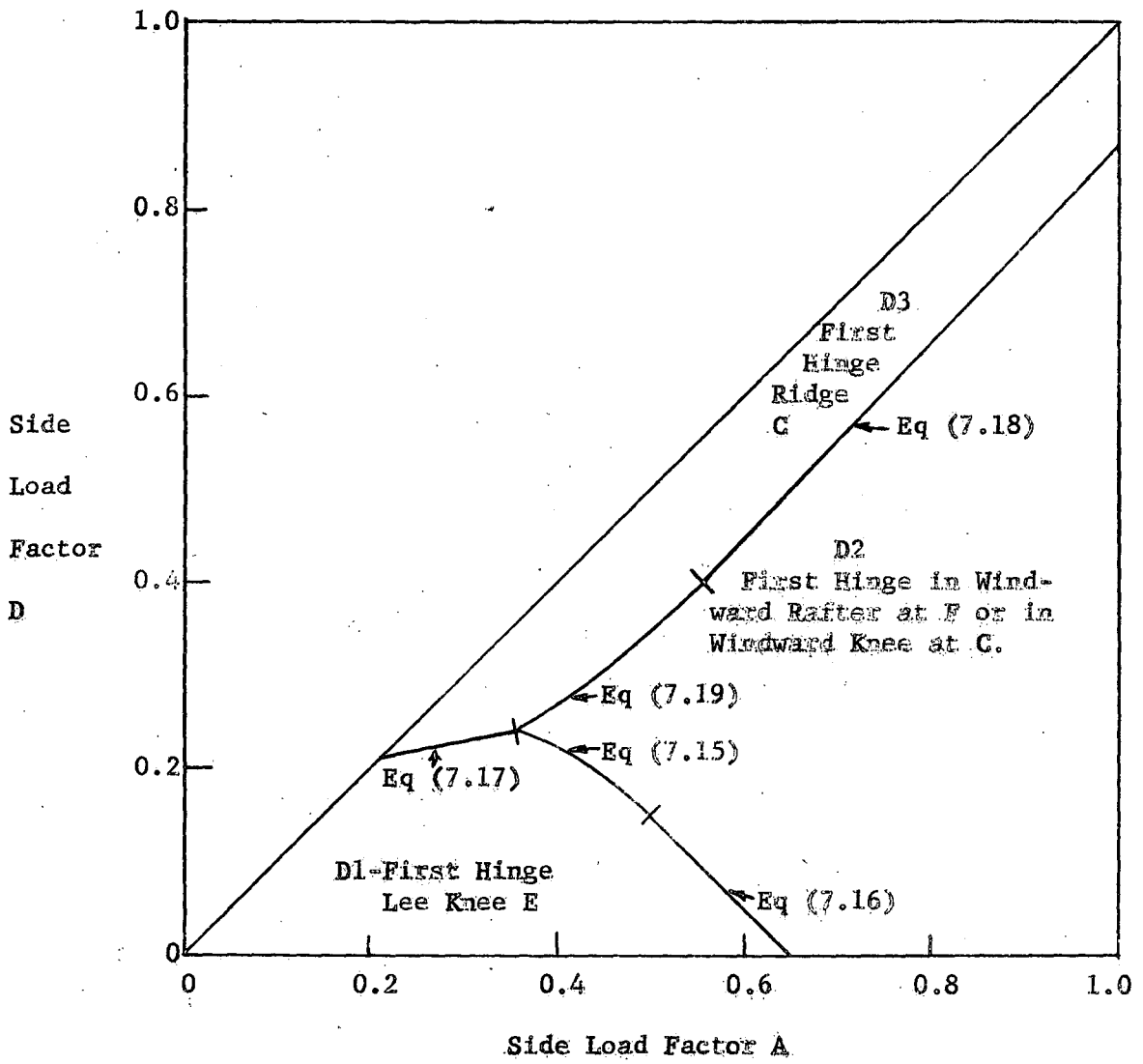

FIG 7.4 LIMITS OF FORMATION OF FIRST PLASTIC HINGE (b = 0.2 a = 0.2)

-215

b = 0.2

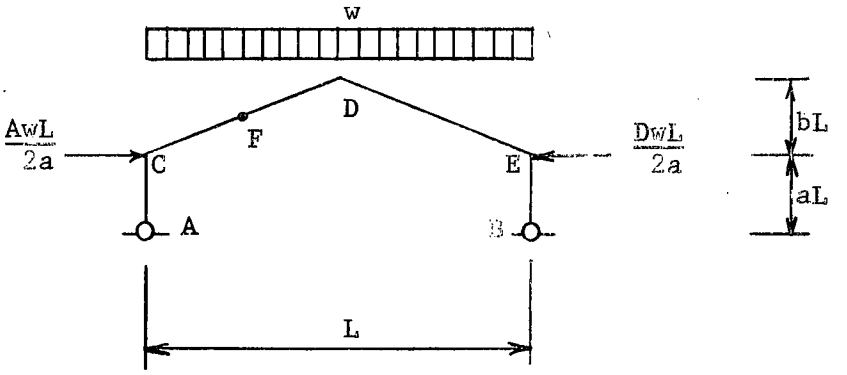

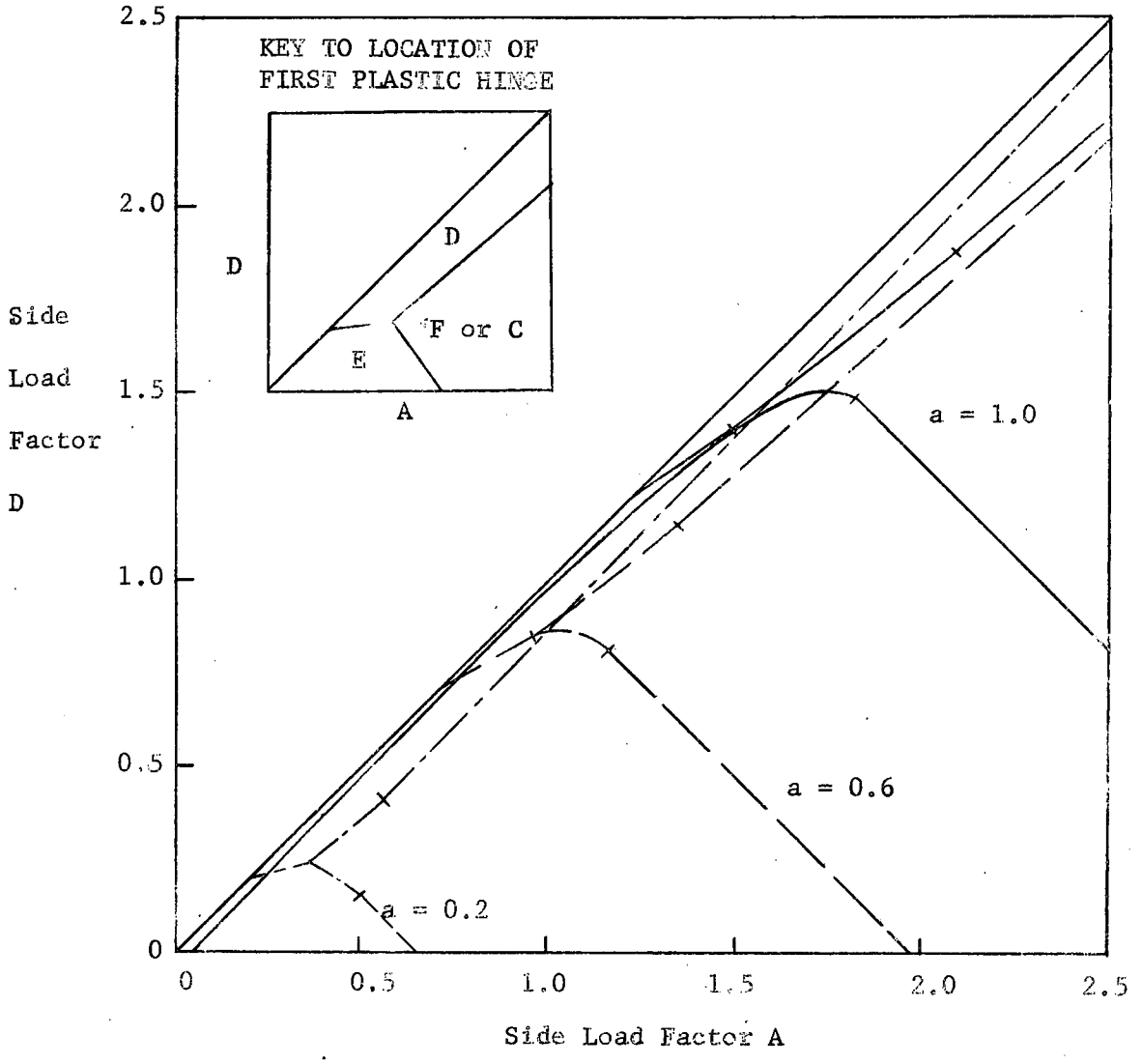

FIG 7.5 LIMITS OF FIRST PLASTIC HINGES FOR THREE COLUMN FRAMES (= 0.2)

b =	0.2
a =	0.2

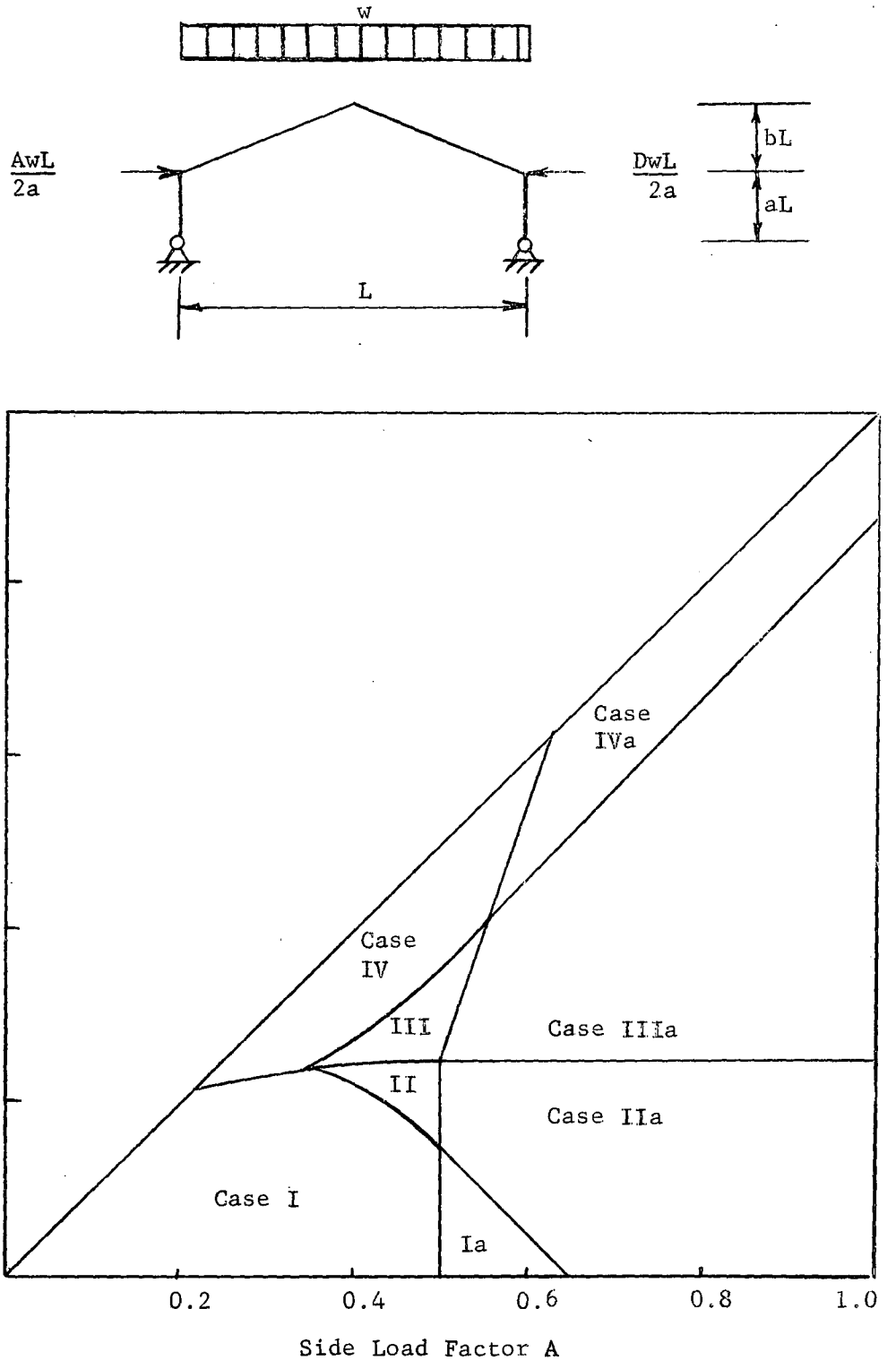

FIG 7.6 DOMAINS FOR FORMATION OF MECHANISMS IN MULTI-SPAN GABLED FRAMES (b=0.2 a=0.2)

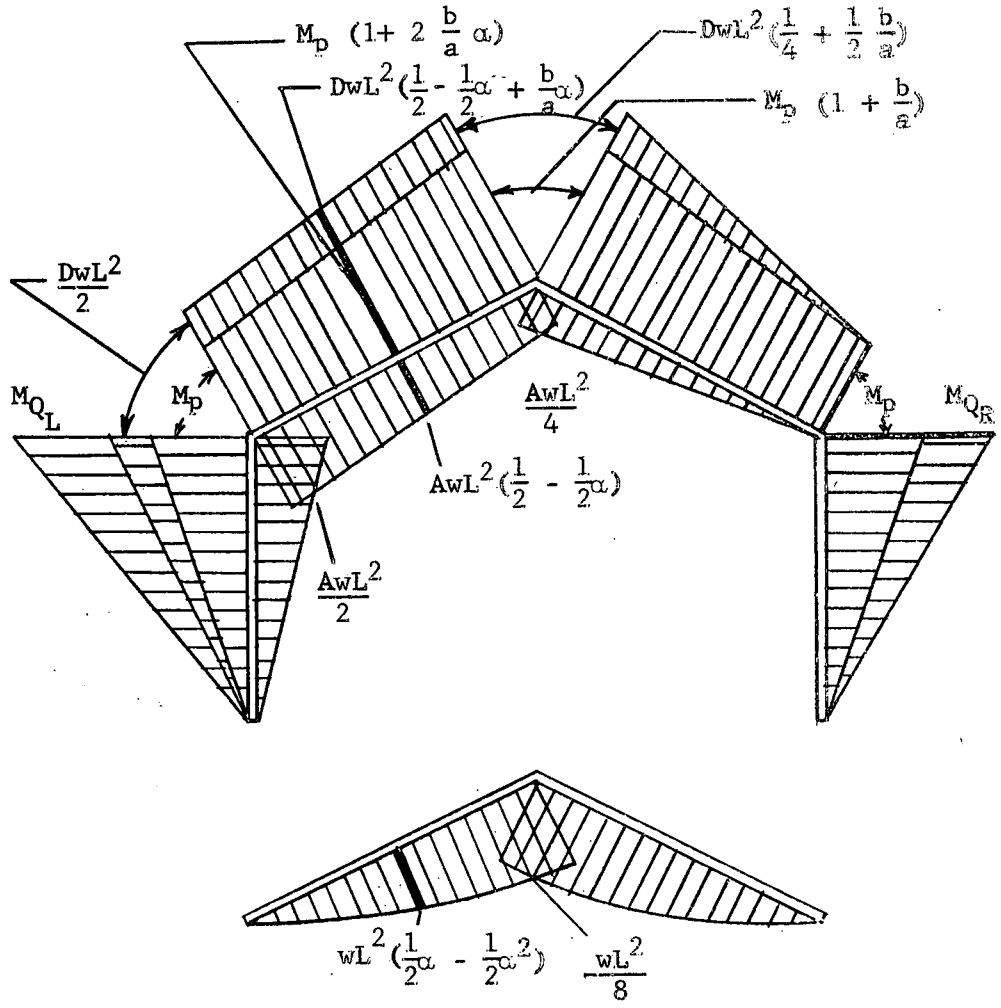

FIG 7.7 MOMENT DIAGRAM FOR CASES I & II
(MULTI-SPAN FRAMES)

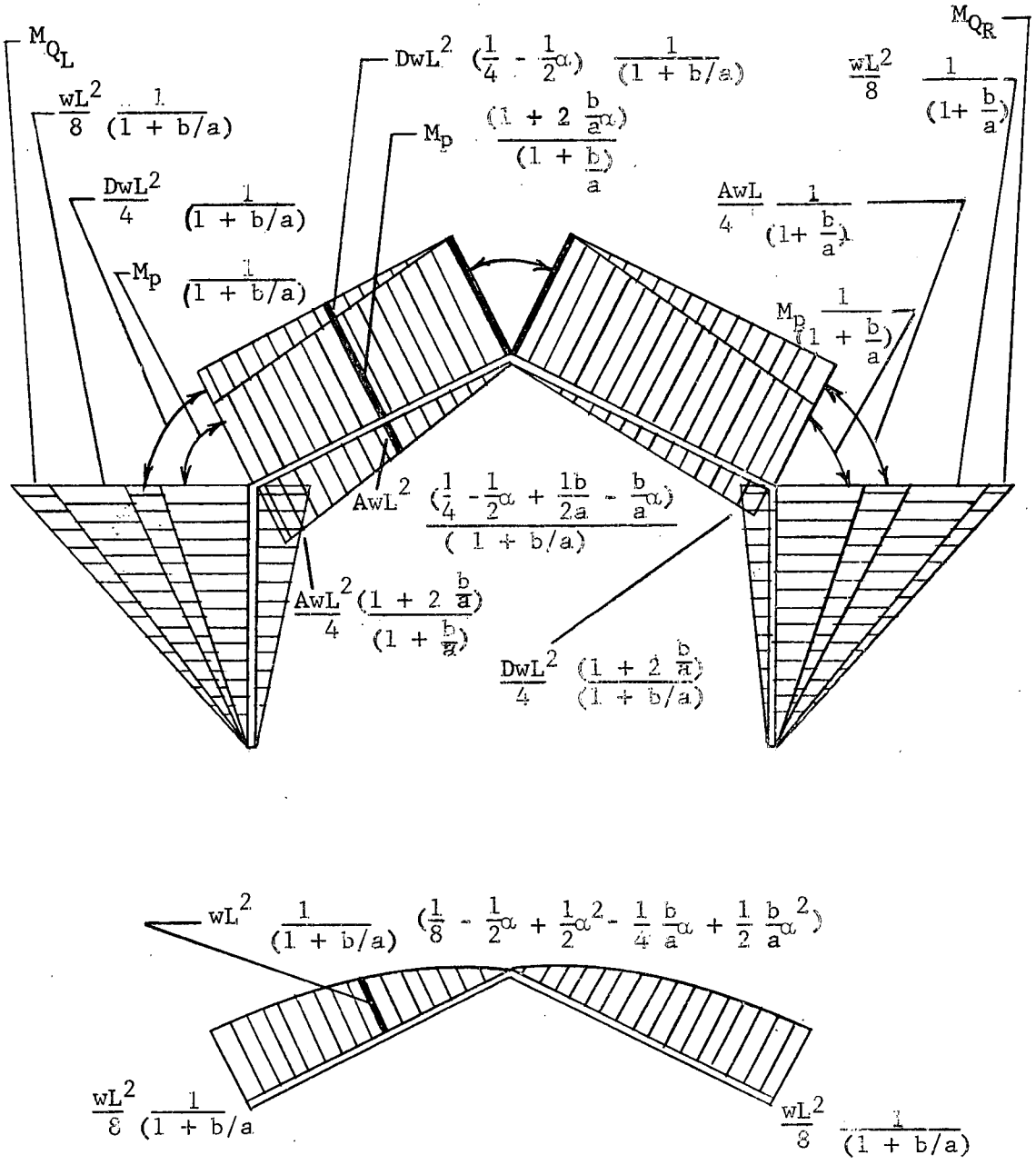

FIG 7.8 MOMENT DIAGRAM FROM CASE III & IV
(MULTI-SPAN FRAMES)

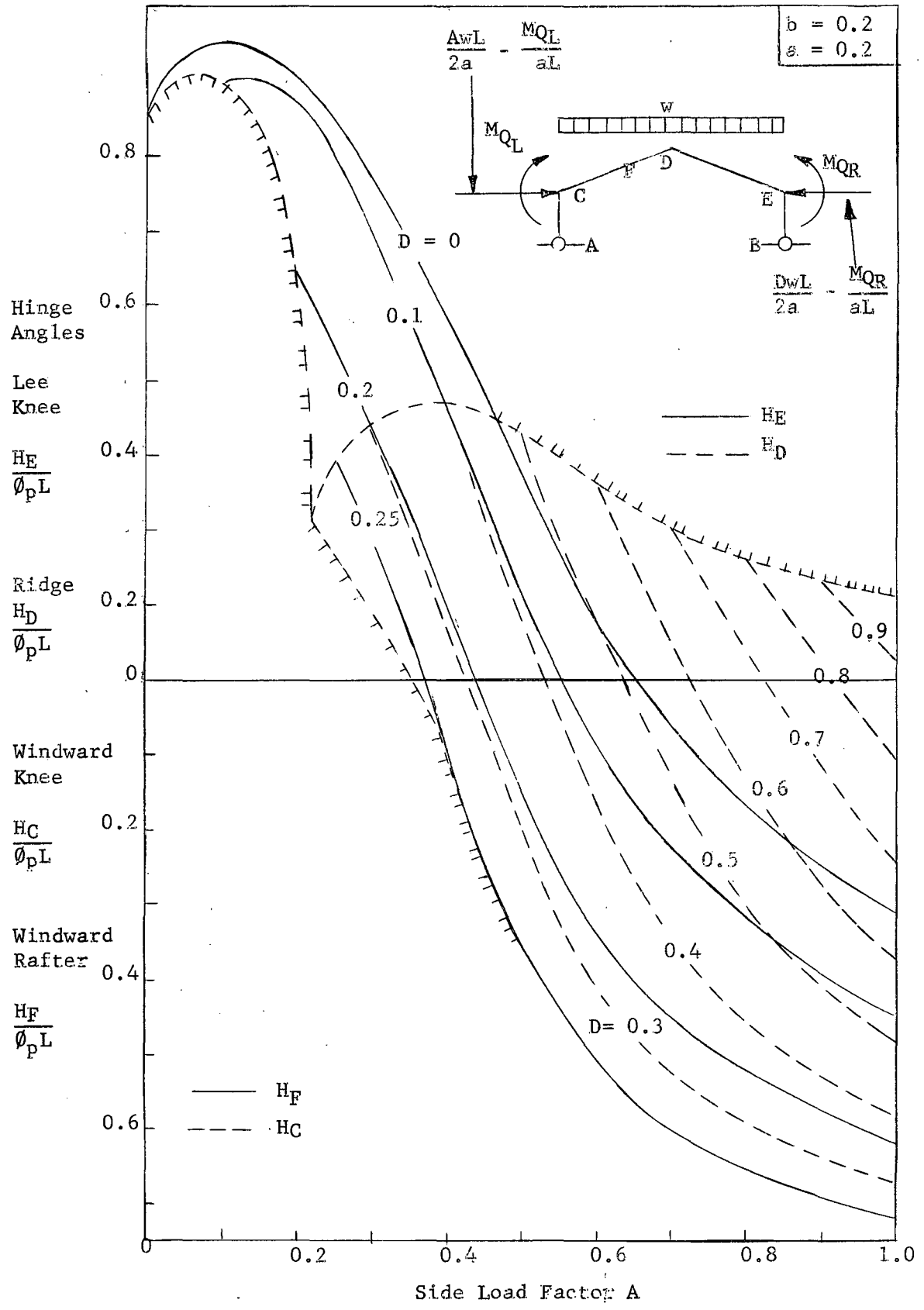

FIG 7.9 HINGE ANGLES FOR SELF-SUPPORTING SUBASSEMBLAGE

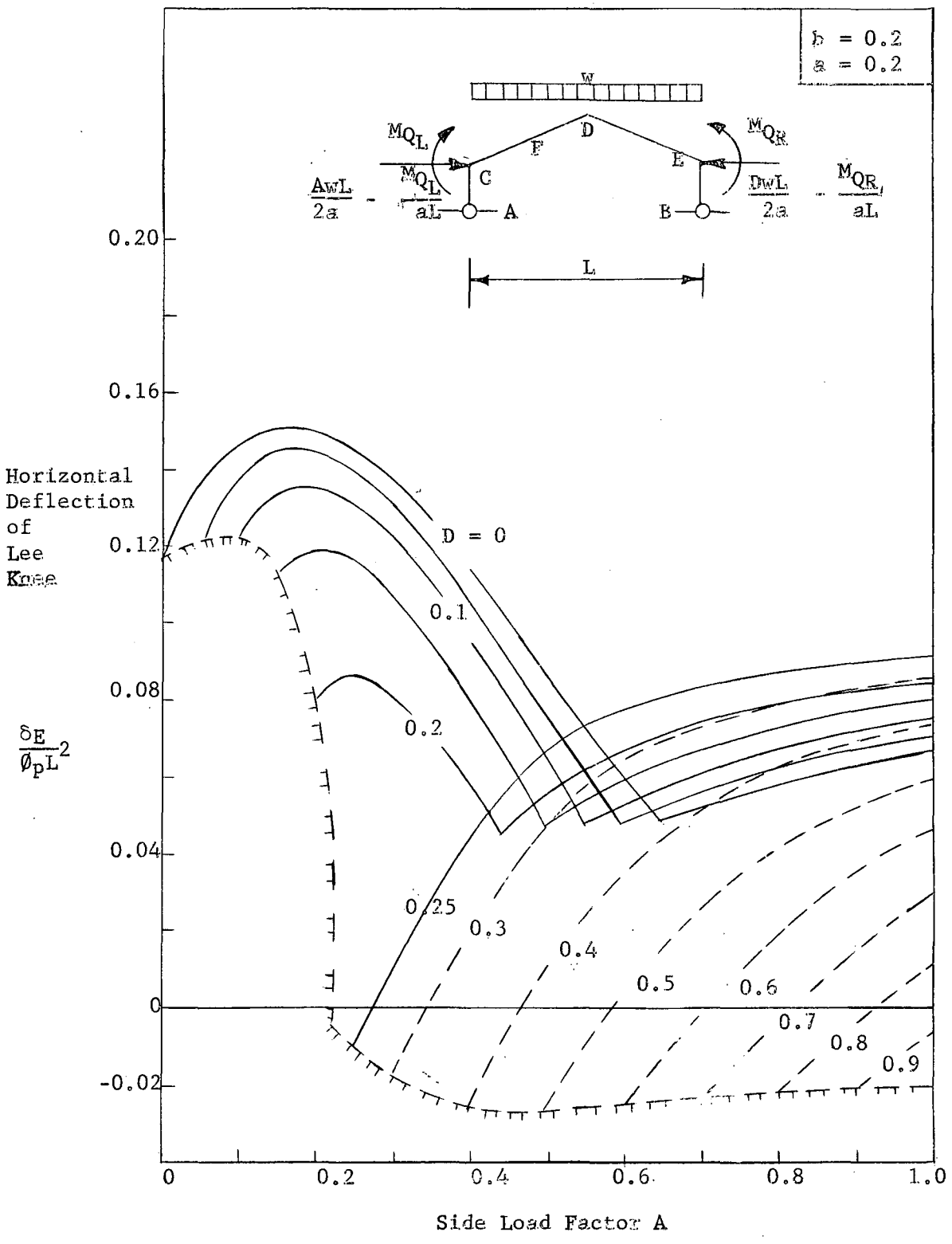

FIG 7.10 HORIZONTAL DEFLECTION OF LEE KNEE--
SELF-SUPPORTING SUBASSEMBLAGE

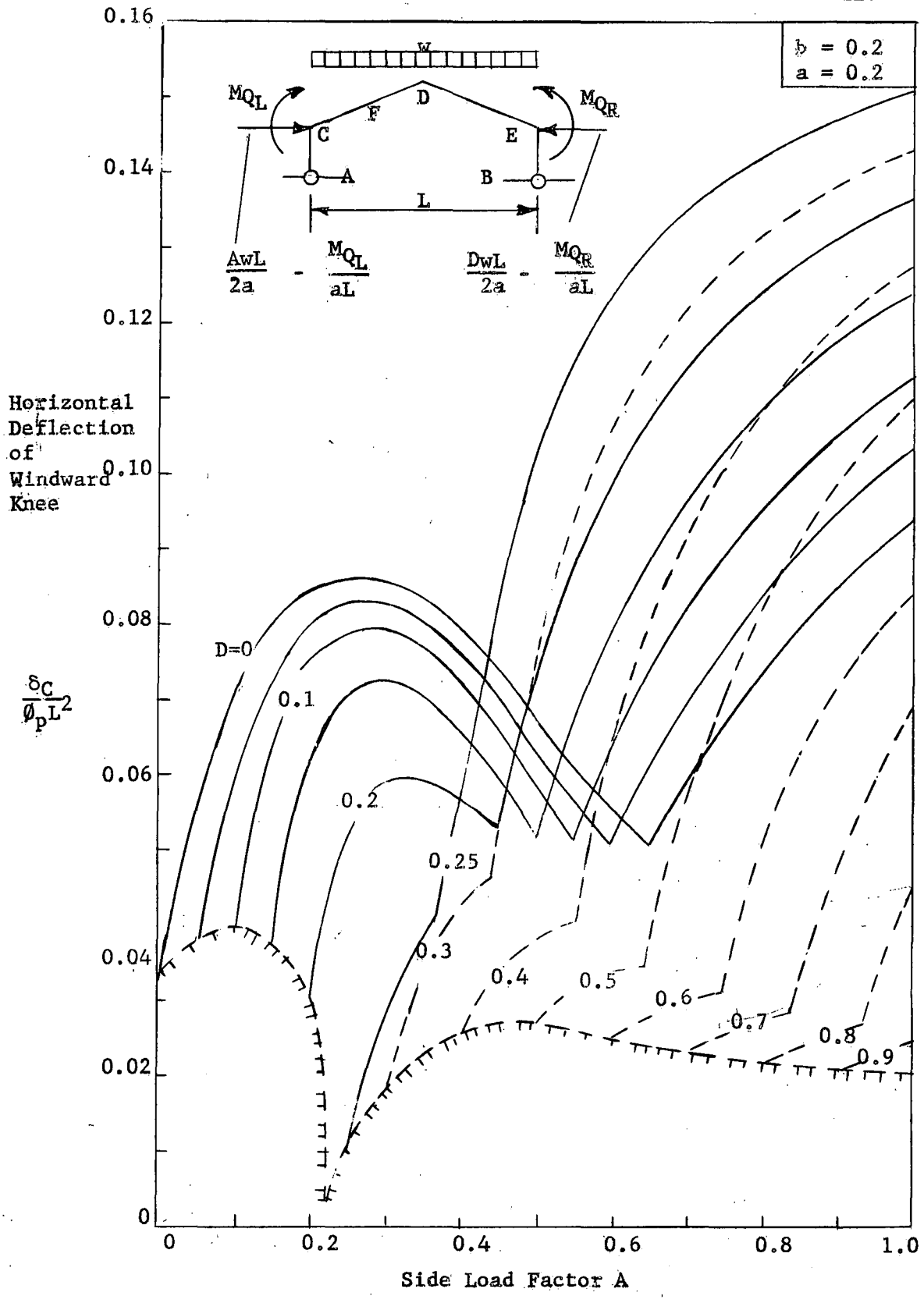

FIG 7.11 HORIZONTAL DEFLECTION OF WINDWARD KNEE--
SELF-SUPPORTING SUBASSEMBLAGE

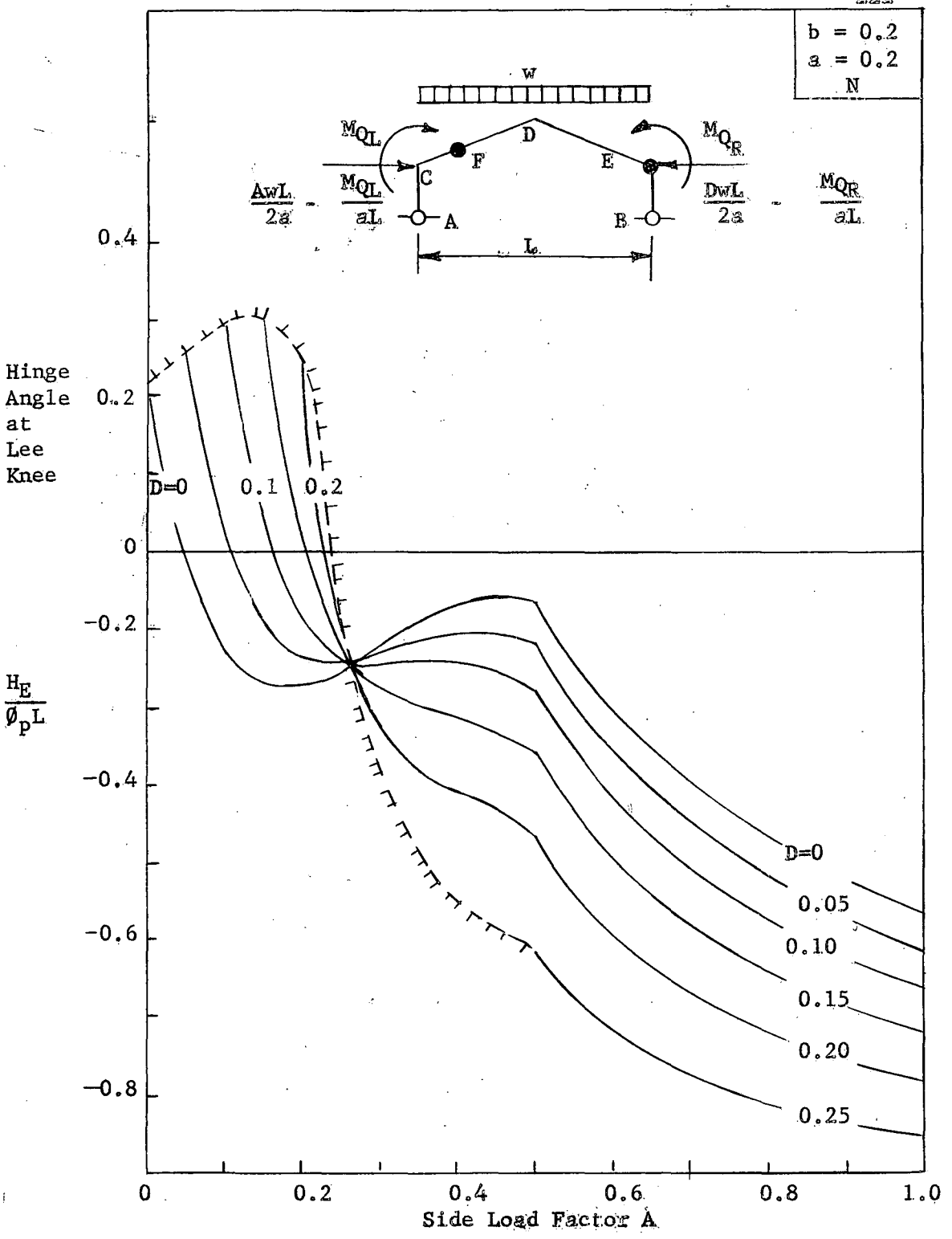

FIG 7.12 HINGE ANGLES AT LEE KNEE--
NON-SELF-SUPPORTING SUBASSEMBLAGE--
CASES I, Ia, II, IIa

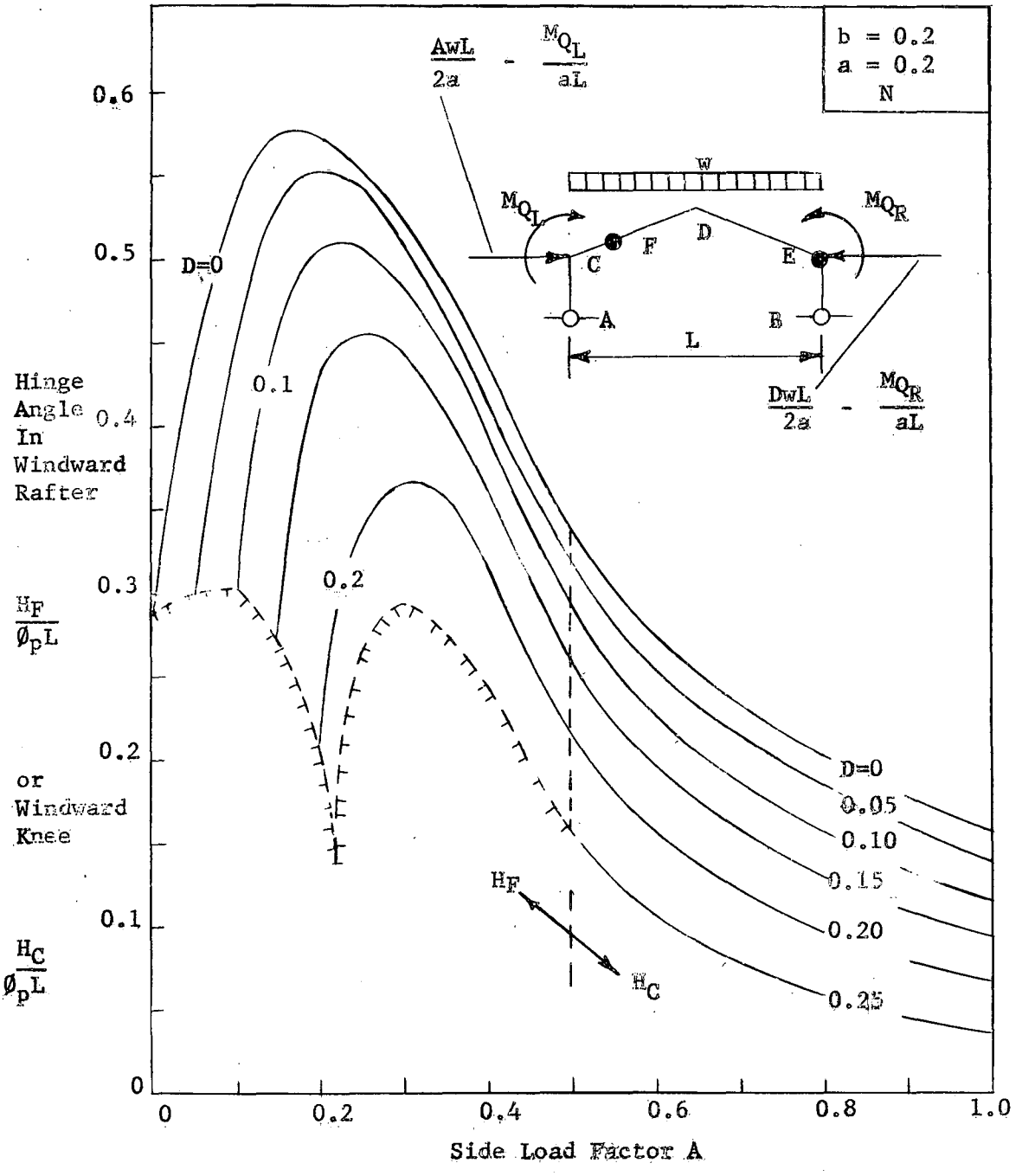

FIG 7.13 HINGE ANGLES IN WINDWARD RAFTER AND WINDWARD KNEE-- NON-SELF-SUPPORTING SUBASSEMBLAGE-- CASES I,Ia,II,IIa

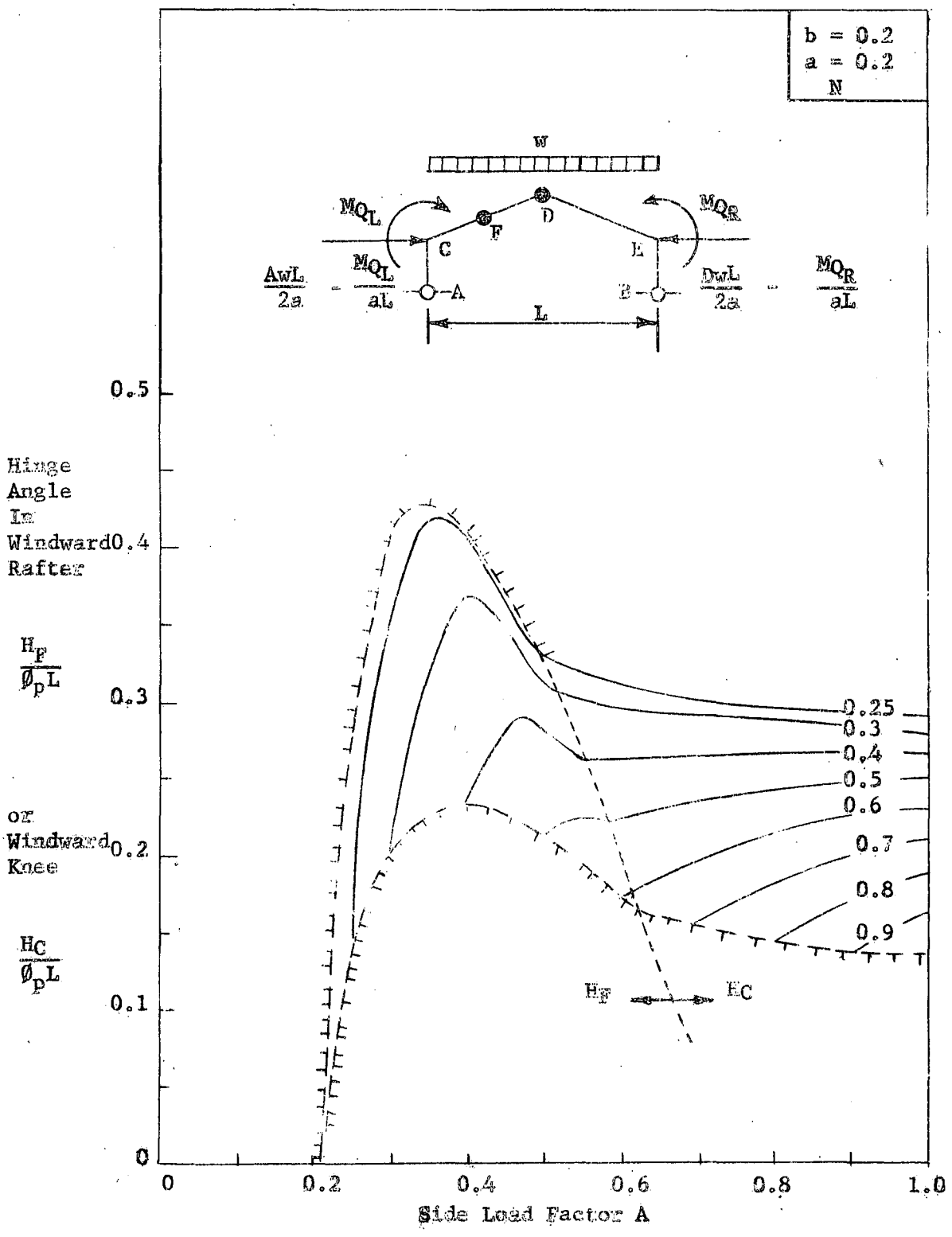

FIG 7.14 HINGE ANGLES IN WINDWARD RAFTER AND WINDWARD KNEE-- NON-SELF-SUPPORTING SUBASSEMBLAGE-- CASES III, IIIa, IV, IVa

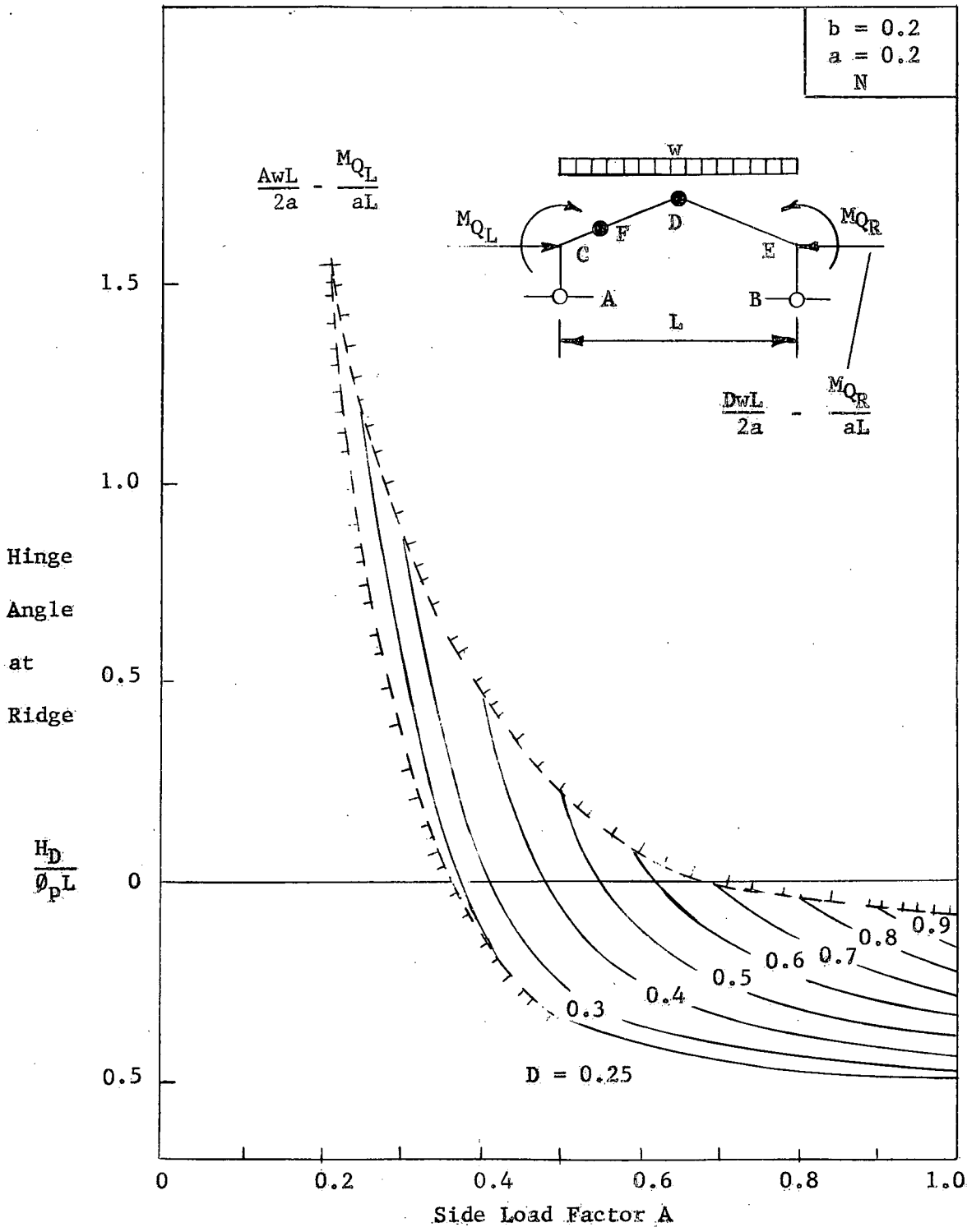

FIG 7.15 HINGE ANGLES AT RIDGE-- NON-SELF-SUPPORTING SUBASSEMBLAGE, CASES III, IIIa, IV, IVa

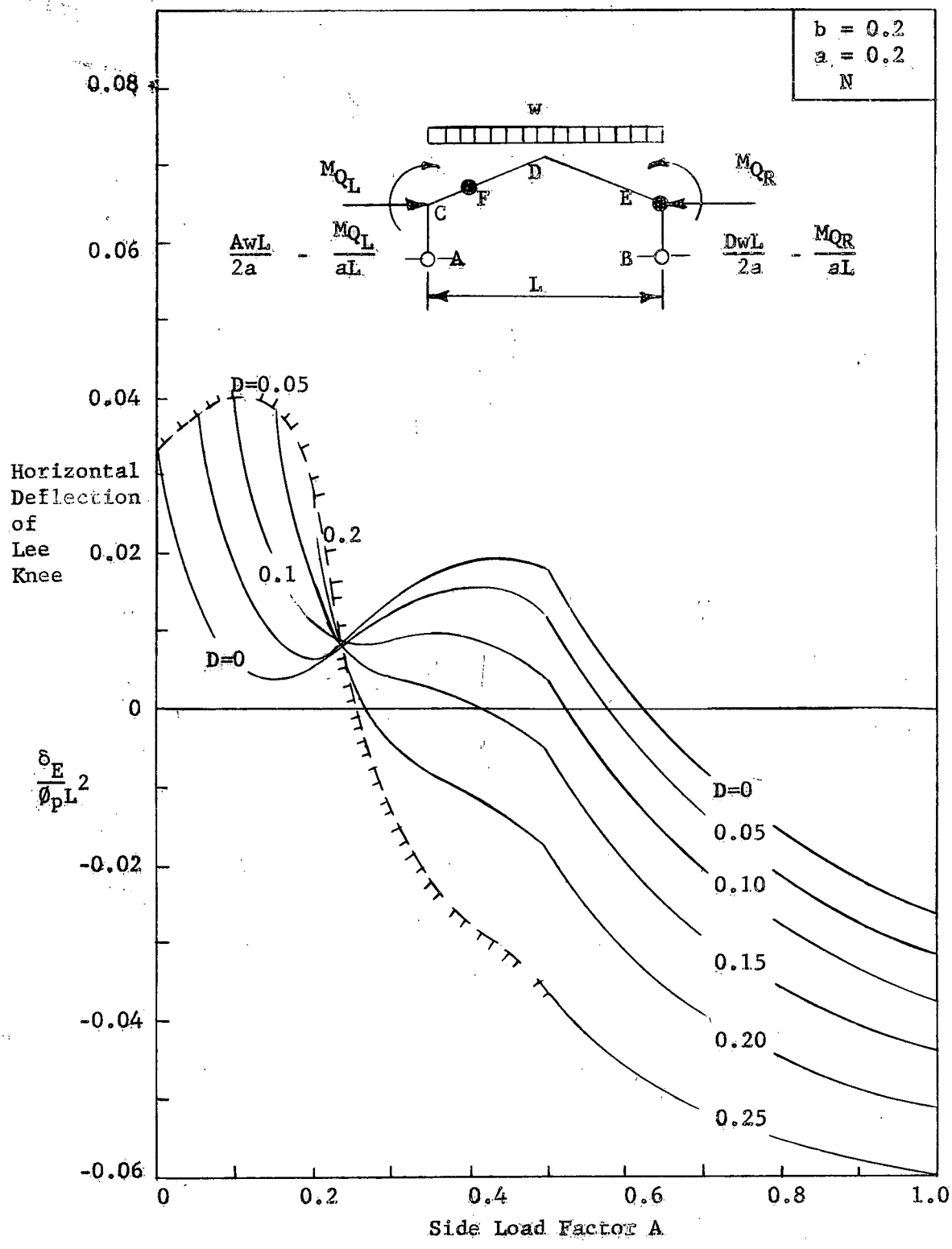

FIG 7.16 HORIZONTAL DEFLECTION OF LEE KNEE NON-SELF-SUPPORTING SUBASSEMBLAGE CASES I, Ia, II, IIa

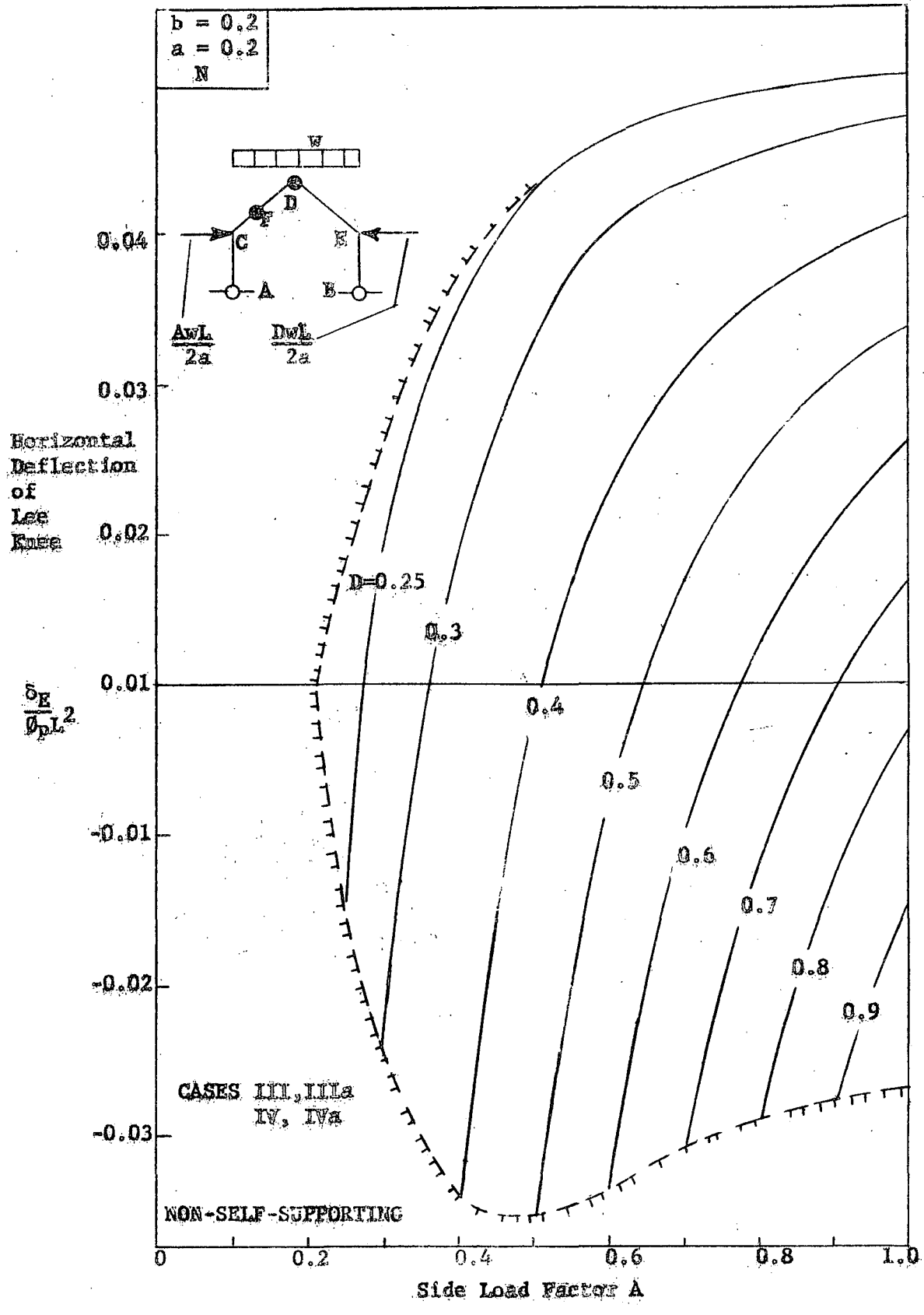

FIG 7.17 HORIZONTAL DEFLECTION OF LEE KNEE

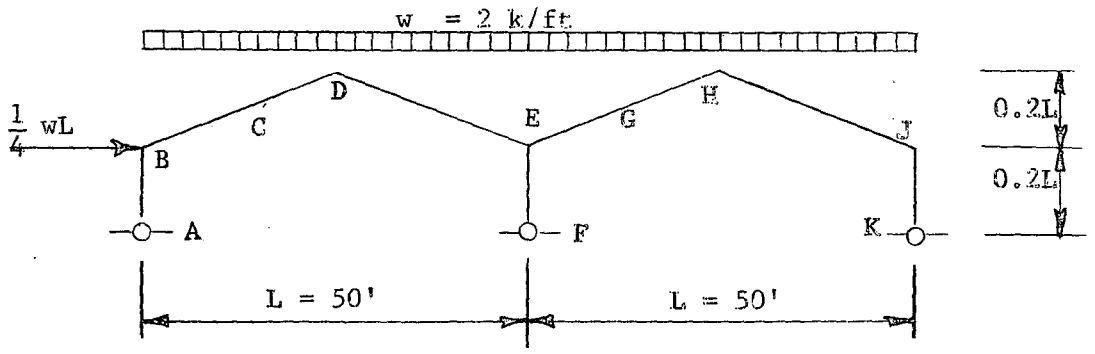

FIG 7.18 TWO-SPAN GABLED FRAME DESIGNED IN EXAMPLE

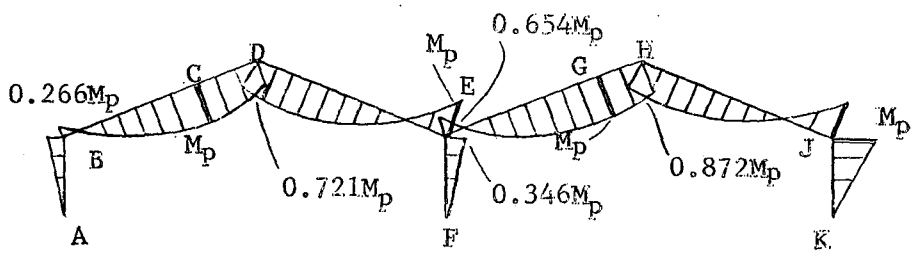

FIG 7.19 MOMENT DIAGRAM FOR TWO-SPAN GABLED FRAME DESIGNED IN EXAMPLE

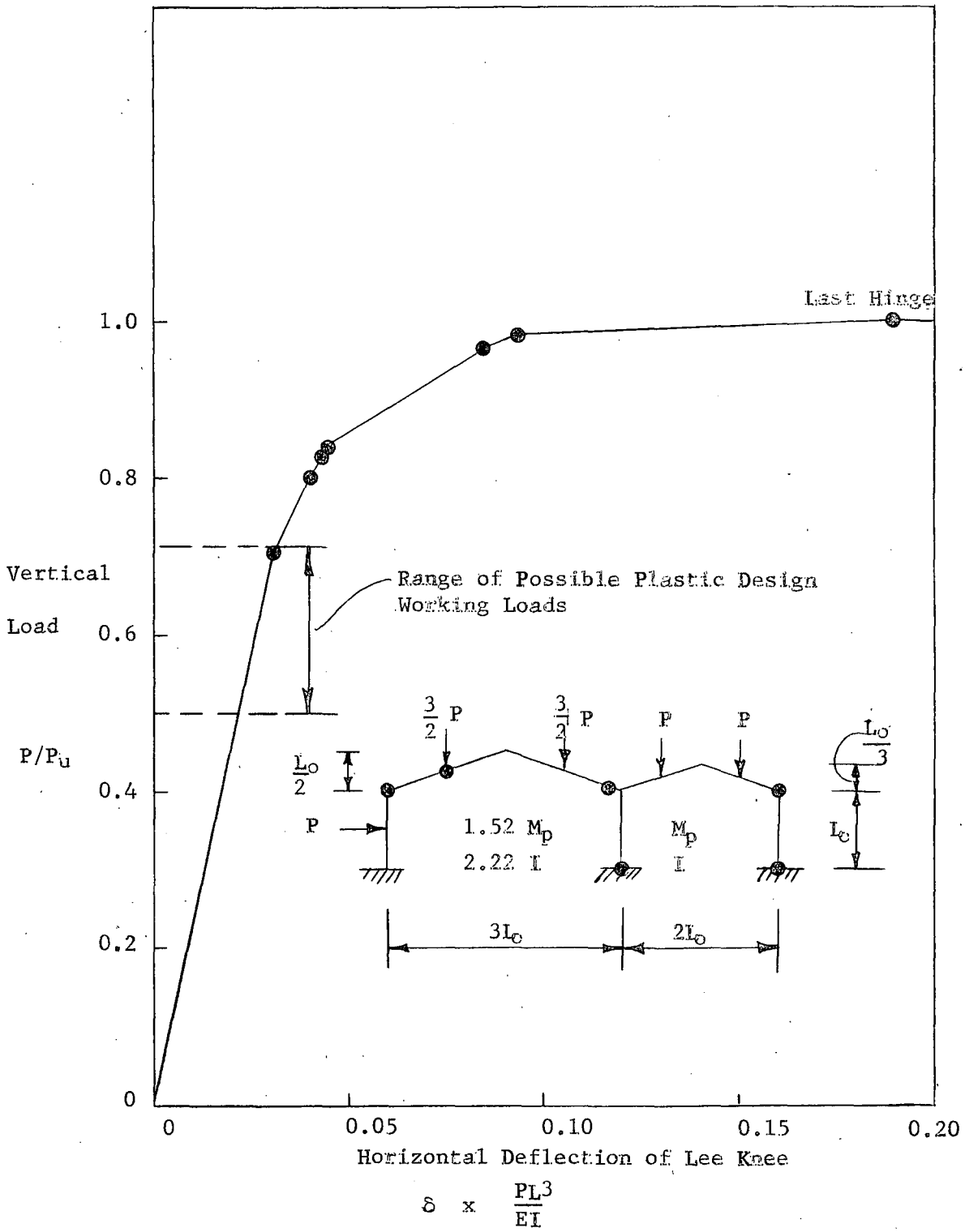

FIG 7.20 THEORETICAL LOAD-DEFLECTION CURVE FOR TWO-SPAN GABLED FRAME

268.3

V I T A

The author was born in Mineola, New York, on January 26, 1927, the first child of George and Viola Driscoll. He graduated from Port Washington Senior High School in Port Washington, New York, in 1944.

He attended Rutgers University from 1944 to 1945 as a trainee in the Army specialized Training Reserve Program. Following this, he served in the U. S. Army Air Forces in 1945 and 1946. On completion of military service he reenrolled at Rutgers University in 1947. He was awarded the B.S. in Civil Engineering with highest honors in 1950, receiving also the Theodore Frelinghuysen Vail Prize for scholarship and the Edward Fuller Brooks Memorial Prize in Civil Engineering. He was also elected to the Rutgers Chapter of Tau Beta Pi.

He joined the staff of Lehigh University in September 1950 as a Graduate Assistant in Civil Engineering. In February 1952, he was appointed Assistant Engineer of Tests in the Fritz Engineering Laboratory and continued to serve in that capacity until June 1957. He received the M.S. in Civil Engineering from Lehigh University in 1952. In November 1952, he joined the staff of the research project on Welded Continuous Frames and Their Components. He was appointed Research Instructor in Civil Engineering in July 1957.